UC San Diego

UC San Diego Electronic Theses and Dissertations

Title

The spatio-temporal dynamics of a neural network for response control

Permalink

https://escholarship.org/uc/item/0j59q1zb

Authors

Swann, Nicole Christiane
Swann, Nicole Christiane

Publication Date

2012

Peer reviewed|Thesis/dissertation

eScholarship.org Powered by the California Digital Library
University of California

UNIVERSITY OF CALIFORNIA, SAN DIEGO

The Spatio-temporal Dynamics of a Neural Network for Response Control

A dissertation submitted in partial satisfaction of the requirements for the degree Doctor of Philosophy

in

Neurosciences

by

Nicole Christiane Swann

Committee in charge:

Professor Adam Aron, Chair
Professor Anders Dale
Professor Eric Halgren
Professor Howard Poizner
Professor John Serences

2012

Copyright

Nicole Christiane Swann, 2012

All rights reserved.

The Dissertation of Nicole Christiane Swann is approved, and it is acceptable in quality and form for publication on microfilm and electronically:

_____

_____

_____

_____

_____

Chair

University of California, San Diego

2012

DEDICATION

I wish to dedicate this dissertation to my family, who supported me through some very big challenges during my time in graduate school. I can't express how grateful I am to have you in my life, and I couldn't have done it without you guys. I love you.

TABLE OF CONTENTS

SIGNATURE PAGE……iii

DEDICATION……...iv

TABLE OF CONTENTS ……...v

LIST OF FIGURES……...vi

LIST OF TABLES……ix

LIST OF ABBREVIATIONS……x

ACKNOWLEDGEMENTS……...xi

VITA……..…..……xiii

ABSTRACT….……....xiv

CHAPTER 1: Introduction……..1

CHAPTER 2: Intracranial EEG reveals a time– and frequency–specific role for the right inferior frontal gyrus and primary motor cortex in stopping initiated responses……...…37

CHAPTER 3: Deep brain stimulation of the subthalamic nucleus alters the cortical profile of response inhibition in the beta frequency band: a scalp EEG study in Parkinson's disease……....……...81

CHAPTER 4: Roles for the pre-supplementary motor area and the right inferior frontal gyrus in stopping action: electrophysiological responses and functional and structural connectivity……..……118

CHAPTER 5:Intracranial EEG reveals dissociable roles for dorsal and ventrolateral prefrontal cortex in preparing to stop action……...165

CHAPTER 6: Conclusions…...……...200

APPENDIX…….236

LIST OF FIGURES

Figure 2.1: Conditional stop signal task used in the electrocorticography experiment…….....67

Figure 2.2: Location of intracranial grids on the right hemisphere……...68

Figure 2.3: ECoG analysis procedure……...69

Figure 2.4: Correspondence between fMRI and ECoG for patient TA341……..70

Figure 2.5: Right IFG results for ECoG……71

Figure 2.6: A representative electrode from auditory cortex……72

Figure 2.7: Right primary motor cortex results for ECoG……....73

Figure 3.1: Stop signal task…….107

Figure 3.2: Behavioral results…….108

Figure 3.3: Time-frequency plots for stop trials for ON vs. OFF stimulation……109

Figure 3.4: The beta increase of ON vs. OFF is stronger over the right hemisphere than the left…….110

Figure 3.5: Time-frequency plots for stop trials. ……...111

Figure 4.1: Task and brain activations……151

Figure 4.2: Electrode locations for all electrodes in the preSMA and rIFG regions..152

Figure 4.3: Diffusion tensor imaging and cortio-cortial evoked potentials…...…….153

Figure 4.4: ECoG: Preparing to stop for preSMA and rIFG……...…154

Figure 4.5: ECoG: Outright stopping for preSMA and rIFG……..155

Figure 4.6: ECoG: Outright stopping for the wider cortical network in the gamma band…….156

Figure 5.1: Task and functional MRI……..188

Figure 5.2: DLPFC and VLPFC activity in the task cue and go cue periods…….189

Figure 5.3: The full dynamic picture of activity for a single subject during a preparing to stop trial……..190

Figure 5.4: Representative spectral plots for DLPFC and VLPFC for preparing to stop……..191

Figure 5.5: VLPFC shows consistent activity across subjects when preparing to stop……..192

Figure 5.6: VLPFC activity is time-locked to the motor response on a single trial level…….193

Figure 6.1: Network model for proactive and reactive control……...227

Supplementary Figure 2.1: The right IFG response to stopping is fairly specific within wider right lateral PFC – subject TS007 day 1……...240

Supplementary Figure 2.2: The right IFG response to stopping is fairly specific within wider right lateral PFC – subject TS007 day 2……...241

Supplementary Figure 2.3: The right IFG response to stopping is fairly specific within wider right lateral PFC – subject TS005…….242

Supplementary Figure 2.4: The right IFG response to stopping is fairly specific within wider right lateral PFC – subject TA341……..…….....243

Supplementary Figure 2.5: Auditory electrode from subject TS007 day 1……....244

Supplementary Figure 2.6: Auditory electrode from subject TS005……..……....245

Supplementary Figure 2.7: Auditory electrode from subject TA341……..……...246

Supplementary Figure 2.8: Auditory electrode from subject TA344……..……...247

Supplementary Figure 2.9: Comparison of slow and fast go trials…….248

Supplementary Figure 3.1: Time-frequency plot of go trials for ON vs. OFF stimulation……...249

Supplementary Figure 4.1: preSMA location…….250

Supplementary Figure 4.2: Locations of electrodes with non-zero CCEP or DTI values……..251

Supplementary Figure 4.3: Example CCEPs……..252

Supplementary Figure 4.4: Time-frequency responses for all preSMA electrodes for MS_Go and NS_Go trials and the difference between the two……..253

Supplementary Figure 4.5: Time-frequency responses for all rIFG electrodes for MS_Go and NS_Go trials and the difference between the two……..254

Supplementary Figure 4.6: Time-frequency responses for all preSMA electrodes MS_SS trials, MS_US trials, and the difference between the two…….255

Supplementary Figure 4.7: Time-frequency responses for all rIFG electrodes MS_SS trials, MS_US trials, and the difference between the two……...256

Supplementary Figure 4.8: Superior parietal ECoG……...257

Supplementary Figure 4.9: Temporal Parietal Junction (TPJ) ECoG……258

LIST OF TABLES

Table 2.1: Data collection parameters…….....65

Table 2.2: Behavioral data……66

Table 3.1: Demographic and Rating Scale Measures…….103

Table 3.2: Patient Clinical Characteristics……..104

Table 3.3: Stop signal task behavioral performance……..…….106

Table 4.1: Behavioral results……..149

Table 4.2: Macrostimulation results……150

Table 5.1: Behavioral Results…….187

Supplementary Table 4.1: Preparing to stop fMRI values……..236

Supplementary Table 4.2: Outright stopping fMRI values..……...237

Supplementary Table 3: CCEPs and DTI results from the whole brain reveal functional/structural connections between the preSMA and the rIFG in particular...238

LIST OF ABBREVIATIONS

DBS: deep brain stimulation

DLPFC: dorsolateral prefrontal cortex

ECoG: electrocorticography

EEG: electroencephalography

fMRI: functional magnetic resonance imaging

IFC: inferior frontal cortex

IFG: inferior frontal gyrus

rIFG: right inferior frontal gyrus

M1: primary motor area

MFG: middle frontal gyrus

MRI: magnetic resonance imaging

PD: Parkinson's Disease

preSMA: pre-supplementary motor area

SSD: stop signal delay

SSRT: stop signal reaction time

STN: subthalamic nucleus

TMS: transcranial magnetic stimulation

VLPFC: ventrolateral prefrontal cortex

ACKNOWLEDGEMENTS

All the projects described in this dissertation are of a highly collaborative nature and could not have been done without the help of many people. I would like to acknowledge Dr. Adam Aron for his encouragement and help through all my projects including the countless hours of meetings, late nights reading over my drafts, and helpful insight into interpreting my data. I would also like to thank Dr. Nitin Tandon and his lab, without whom there would be very little data in this thesis. Dr. Howard Poizner also made a substantial contribution by providing much insight, assistance, and guidance for the Parkinson's Disease portions of this dissertation. Finally, I would like to thank my committee for their helpful comments and unwavering encouragement.

Chapter 2, in full, is a reprint of material as it appears in The Journal of Neuroscience, 2009: Swann NC, Tandon N, Canolty R, Ellmore TM, McEvoy LK, Dreyer S, DiSano M, Aron AR. (2009) Intracranial EEG reveals a time- and frequency-specific role for the right inferior frontal gyrus and primary motor cortex in stopping initiated responses. The dissertation author was the primary investigator and author of this paper.

Chapter 3, in full, is a reprint of material as it appears in The Journal of Neuroscience, 2011: Swann NC, Poizner H, Houser M, Gould S, Greenhouse I, Cai W, Strunk J, George J, Aron AR. (2011) Deep brain stimulation of the subthalamic nucleus alters the cortical profile of response inhibition in the beta frequency band: a

scalp EEG study in Parkinson's disease. The dissertation author was the primary investigator and author of this paper.

Chapter 4, in full, is a reprint of material as it appears in Neuroimage, 2012: Swann NC, Cai W, Conner RC, Pieters TA, Claffey MP, George JS, Aron AR, Tandon N. (2012) Roles for the presupplementary motor area and the right inferior frontal gyrus in stopping action: electrophysiological responses and functional and structural connectivity. The dissertation author was the primary investigator and author of this paper.

Chapter 5, in full, has been submitted for publication of materials as it may appear in Cerebral Cortex, 2012: Swann NC, Tandon N, Pieters TA, Aron AR, Tandon N. (2012) Intracranial EEG reveals dissociable roles for dorsal and ventrolateral prefrontal cortex in preparing to stop action. The dissertation author was the primary investigator and author of this paper.

VITA

2003–2006	Research Assistant, University of California, Berkeley
2006	Bachelor of Arts, Molecular Cellulear Biology and Psychology, University of California, Berkeley
2012	Doctor of Philosophy, Neurosciences, University of California, San Diego

PUBLICATIONS

Hales JB, Israel SL, Swann NC, Brewer JB. (2009) Dissociation of frontal and medial temporal lobe activity in maintenance and binding of sequentially presented paired associates. Journal of Cognitive Neuroscience, 21(7): 1244-1254.

Swann NC, Tandon N, Canolty R, Ellmore TM, McEvoy LK, Dreyer S, DiSano M, Aron AR. (2009) Intracranial EEG reveals a time- and frequency-specific role for the right inferior frontal gyrus and primary motor cortex in stopping initiated responses. Journal of Neuroscience 29:12675-12685.

Swann NC, Poizner H, Houser M, Gould S, Greenhouse I, Cai W, Strunk J, George J, Aron AR. (2011) Deep brain stimulation of the subthalamic nucleus alters the cortical profile of response inhibition in the beta frequency band: a scalp EEG study in Parkinson's disease. Journal of Neuroscience 31:5721-5729.

Swann NC, Cai W, Conner RC, Pieters TA, Claffey MP, George JS, Aron AR, Tandon N. (2012) Roles for the presupplementary motor area and the right inferior frontal gyrus in stopping action: electrophysiological responses and functional and structural connectivity. Neuroimage 59:2860-2870.

ABSTRACT OF THE DISSERTATION

The Spatio-temporal Dynamics of a Neural Network for Response Control

by

Nicole Christiane Swann

Doctor of Philosophy in Neurosciences

University of California, San Diego, 2012

Professor Adam Aron, Chair

A key aspect of daily functioning is our ability to control our response tendencies. An experimentally tractable way to study such control is by focusing on how initiated movements are stopped and changed (action control). Previous research has elucidated a network of structurally connected regions critical for action control including the right inferior frontal cortex (IFG), the pre-supplementary motor area (preSMA), and the subthalamic nucleus (STN) of the basal ganglia. This thesis examines the functioning of this circuit in humans using a combination of electrocorticography (ECoG, providing both high spatial and temporal resolution) and

electroencephalography (EEG) recorded at the scalp during stimulation of the STN. Evidence is presented for a possible mechanism of neural communication between the nodes of this network involving beta frequency oscillations. Specifically, there are beta increases in both the right IFG and preSMA, functional connectivity in beta between the two when stopping is successful, and modulation of cortical beta during action control associated with changes in stimulation of the STN. The thesis also presents evidence regarding different functional contributions of separate prefrontal regions in the performance of the action control. Specifically, it is proposed that the preSMA plays a role in task configuration, by preparing the wider network for a possible need to resolve competing response tendencies, the right IFG is engaged during the actual action control, and the dorsolateral prefrontal cortex represents action control rule.

CHAPTER 1:

Introduction

The importance of Cognitive Control

How do we control ourselves? When you go to a party with the goal of refraining from having a drink because you know you have an early morning engagement the next day, what determines your success (or failure)? What causes some people to be bad at controlling themselves (to the point of pathology, such as in cases of attention deficit hyperactivity disorder (ADHD), obsessive compulsive disorder, or anger management problems), while others succeed with ease? The ability to control ourselves is an integral component of how we live our lives. The neural basis of "cognitive control' remains an area of active investigation. Cognitive control encompasses a variety of functions such as: how we maintain goals, make and adhere to plans, suppress urges to deviate from these goals, and generally stop and flexibly change actions.

Use of the Motor System as a Model

Studying the broad and complex concept of cognitive control can be a challenge in the laboratory. However, various tasks have been developed which attempt to model cognitive control within a simplified framework. One such strategy is to study how impulses are stopped or changed by using the motor system as a model. Such an approach provides an experimentally tractable model for engaging

stopping behavior in humans in the laboratory. It has the advantage of having an overt behavioral measure (i.e. movements) by which to gauge the success of control. While clearly an oversimplification, the use of the motor system as a model seems to have relevance to the broader question of cognitive control and has led to significant advances in understanding the neural substrates of this function. Both these features will be discussed in detail below.

The Stop Signal Task

One task that has been used to study cognitive control in the motor domain (response control) is the stop-signal task (Logan and Cowan, 1984). The basic version of this task involves placing the subjects in a context where they are responding as quickly as possible to go cues (with button presses for instance). Then, on a minority of trials, a second cue (stop signal) is unpredictably presented after the go cue, indicating that the subject should attempt to withhold the initiated response. The timing of the stop signal relative to the go signal (stop signal delay, SSD), is changed using various methods, including dynamic adjustment based on the subject's behavior (Aron and Poldrack, 2006). In this manner, the difficulty and prepotency of the task can be maintained for the duration of the task session, such that an active inhibitory process is necessary to successfully stop the response. Furthermore, because success in this task depends on the outcome of a 'race' between the, largely independent, 'Going' and the 'Stopping' processes (Logan and Cowan, 1984), a metric corresponding to the estimated time taken to stop can be estimated (stop signal reaction time, SSRT)(Aron

and Poldrack, 2006; Verbruggen and Logan, 2009). This is computed by modeling the probability of stopping at various delays, or by determining, using behavior-based adjustments, the SSD where the probability of stopping is close to 50%, and comparing these values to the subject's go RT (Logan and Cowan, 1984; Verbruggen and Logan, 2009).

This simple task has many advantages in terms of the feasibility of implementation in the laboratory, reliability over time of the SSRT measure (Williams et al., 1999; Congdon et al., 2012), and relative simplicity in explaining and performing the task, allowing it to be used in human patients (Aron et al., 2003b; Gauggel et al., 2004; van den Wildenberg et al., 2006; Ray et al., 2009; Mirabella et al., 2011) as well as animals (Eagle et al., 2007; Chen et al., 2010; Leventhal et al., 2012). The disadvantage of this task is that since it is based in the motor domain it may appear to have limited extensions. For instance, it is unclear if generalizations can be made to emotional control, for instance.

Despite being a motoric model for a more complicated cognitive process, it seems this task may generalize to at least some broader aspects of control, perhaps because it relies on common neural substrates. For instance, people with disorders of "control" such as ADHD, obsessive-compulsive disorder, addiction, and Parkinson's Disease all show deficits in SSRT (Oosterlaan et al., 1998; Aron et al., 2003a; Overtoom et al., 2003; Gauggel et al., 2004; Bekker et al., 2005; Monterosso et al., 2005; Menzies et al., 2007). Moreover, in ADHD, it has been shown that behavioral deficits in the stop signal task are accompanied by structural and functional deficits in

regions associated with successful inhibitory control (described below) (Rubia et al., 1999; Sowell et al., 2003). Overall, these findings imply that the stopping of action recruited during the stop signal task may have wider implications for control in real-life contexts, which may extend beyond the motor system. This generalizability may stem from a similar underlying neural circuitry used to stop action for other, more general, control processes.

Other Motoric Cognitive Control Tasks

There are three other popular tasks that measure response control, and bear similarities to the stop signal task. While, the experiments presented in this thesis all use variants of the stop signal task, these other tasks are briefly explained here, since findings from other studies using these tasks are relevant for a full understanding of the literature.

The first is the stop-change task, which is identical to the stop signal task, except that the stop signal indicates that subjects must both stop their initiated response, and make an alternative response. This task has the advantage of a trial-by-trial metric that can be indexed (stop-change RT), as opposed to the stop signal task, where success on a stop trial is determined by the absence of a response. Indeed because the stop and alternative response processes seem to be serial, or nearly serial, the RT of the alternative response (stop-change RT), can theoretically reflect trial by trial fluctuations of the stopping process (but would depend on the going process as well) (Verbruggen and Logan, 2009). Moreover, it seems that successful stop-change

trials recruit the same brain areas as successful stop trials (plus motor areas associated with the response) (Kenner et al., 2010).

The second task is the Go/NoGo task, which is similar to the stop signal task except that there is no delay between the go signal and the stop signal (essentially the SSD is zero). Therefore subjects are cued that they are not to respond without being first cued to go. Typically, Go trials are more frequent than NoGo trials and rapid responses are required, leading to a prepotency to respond, and thus, an active inhibitory process on NoGo trials. Despite these differences there is remarkable consistency in terms of neural recruitment between stop signal and Go/NoGo tasks (Garavan et al., 1999; Garavan et al., 2006; Levy and Wagner, 2011).

The third task is the switching task. Here a prepotency is built up about which response is expected by establishing a context or rule, but on a minority of trials the task-context switches so that now a different response is appropriate. Like the stop signal task this task involves the suppression of a prepotent response, and similar to the stop-change task, execution of an alternative response. However, like the Go/NoGo task, the switch signal typically does not follow the go signal, but rather appears coincident with it (Isoda and Hikosaka, 2007, 2008) or is otherwise predictable (Aron et al., 2004). The switching task also seems to recruit similar brain regions as the stop signal task (Isoda and Hikosaka, 2007, 2008; Neubert et al., 2010), although with somewhat more complexity (additional involvement of regions in keeping in mind task-set, i.e. working memory) (see Aron et al., 2004).

Brain Areas for Cognitive Control

Imaging studies have revealed activation of a variety of brain regions associated with the response control tasks described above (reviewed by Rubia et al., 2003; Aron et al., 2007a; Aron et al., 2007b; Li et al., 2008; Chikazoe, 2010; Levy and Wagner, 2011). This predominantly right-lateralized (Garavan et al., 1999) network includes the inferior frontal gyrus (IFG), the pre-supplementary motor area (preSMA), and the basal ganglia, perhaps particularly the subthalamic nucleus (STN), although the striatum has also been implicated (Vink et al., 2005; Zandbelt and Vink, 2010). Performance of this task also involves on a variety of regions which have been implicated in other cognitive functions, for instance, regions associated with working memory, such as the dorsolateral prefrontal cortex (Goldman-Rakic, 1990; Petrides, 2000; Muller and Knight, 2006), and attention like the superior parietal lobe and temporal-parietal junction (Corbetta and Shulman, 2002). Interestingly, some of these regions (specifically IFG and preSMA) have been described as 'negative motor regions' during functional mapping for neurosurgeries (Luders et al., 1988; Fried et al., 1991). Stimulation of these regions resulted in motor arrest, suggesting that it is possible that they may play a causal role in motor inhibition.

Lesion studies have further supported the necessity of at least 3 of these regions in stopping: the right IFG, preSMA, and STN. In humans, damage to the right IFG specifically (and not the left) caused slowing of SSRT (Aron et al., 2003b; Rieger et al., 2003). Damage to preSMA and neighboring regions, is also associated with impaired SSRT and other measures of inhibition, though evidence for this is less

strong (Floden and Stuss, 2006; Nachev et al., 2007). Human damage to the STN specifically, is rare, but has been shown to cause hemiballism (Postuma and Lang, 2003), a disorder characterized by uncontrolled movement of the contralateral limbs. This disorder could perhaps be described as a catastrophic failure of response control, since, apparently, voluntary control over movement is severely impaired. Furthermore, rats with lesions to this area show a decrease in stopping accuracy (Eagle et al., 2007), and modulation of STN activity in humans with Deep Brain Stimulation (DBS) electrodes implanted as a treatment for Parkinson's Disease also modulates SSRT (van den Wildenberg et al., 2006; Mirabella et al., 2011).

Transcranial Magnetic Stimulation (TMS) data also implicates these regions in stopping. Delivery of repetitive TMS at a low frequency (~1 Hz) is thought to induce a virtual lesion of the region being stimulated (i.e. a temporary disruption to the function of that region) (Chen et al., 1997). Using this method prior to performance of the stop signal task (i.e. the off-line, repetitive, low frequency, method) led to subsequently impaired task performance as indexed by lower probability of successfully stopping and/or slower SSRTs. This was the case when stimulation was delivered over both right IFG (Chambers et al., 2006; Chambers et al., 2007) and the preSMA (Chen et al., 2009). These findings establish firmly the necessity of these regions in some aspect of the stop signal task, free from the potential confound of functional reorganization in lesion studies, where patients may have had many years to recover.

Additionally, more evidence for the importance of the IFG comes from studies relating individual differences in behavioral performance of the stop task to

differences in functional and structural imaging. For instance, using a modeling approach during a response control task, Forstmann and collegues showed that individual differences in a measure of the efficacy of response control correlated with the BOLD signal in the IFG (such that better inhibition was associated with stronger BOLD activation). They also showed that both the behavioral and BOLD measures correlated with a structural measure (fractional anisotropy in the IFG) (Forstmann et al., 2008). Therefore, correspondence of individual differences in behavioral measures (related to response control) with functional and structural properties of the IFG support the importance of this region in control.

Electrophysiological Cognitive Control Findings: ERP and Single Units

In humans, electrophysiological recordings have traditionally been achieved using EEG since it is non-invasive and relatively inexpensive. EEG signals, though, are difficult to ascribe to certain brain regions because of the method's low spatial resolution. Nevertheless, several ERP studies have identified the N2 and P3 components as important for response control (reviewed by Folstein and Van Petten, 2008). Importantly the fronto-central N2 has a good temporal correspondence to typical SSRT in healthy human (~200 ms). Furthermore, increased N2 amplitude has been associated with successful inhibition during a stop signal task when compared to failed inhibitions (Schmajuk et al., 2006). Additionally, this study showed that the successful compared to failed stop N2 difference was greatest over right frontal electrodes. While strong claims cannot be made about neural sources from scalp EEG

studies, such a distribution is consistent with numerous reports suggesting that a right lateralized fronto-basal ganglia network is recruited during this task (Garavan et al., 1999; Aron et al., 2003b; Chikazoe, 2010). A similar right frontal N2 difference was observed when comparing a group of subjects with ADHD to healthy controls. Here the ADHD patients had marked reductions in N2 amplitudes, and this difference was most pronounced over right frontal electrodes (Pliszka et al., 2000). This electrophysiological difference is paralleled by numerous reports of behavioral deficits in stopping in the ADHD population (Oosterlaan et al., 1998; Aron et al., 2003a; Overtoom et al., 2003; Bekker et al., 2005).

Several electrophysiological studies in animals have been able to examine some of the regions identified as critical for response control in similar tasks, such as Go/NoGo or switching tasks. Recently two studies used both these tasks to investigate the roles of STN and preSMA using monkey electrophysiology (specifically, single-unit recordings) (Isoda and Hikosaka, 2007, 2008). Isoda and Hikosaka showed that there were neurons that responded strongly on switch trials (compared to non-switch trials), in both these regions. They also show that, on successful trials, activity in both regions was early enough to drive the switch itself (i.e. it was earlier than the time when behaviorally correct switch trials were above chance), while this was not the case for failed switch trials. Furthermore, stimulation of the preSMA (which putatively enhances its function), improved accuracy on switch trials. When the same neurons involved in switching were examined during the Go/NoGo task, in each region they were able to identify neurons sensitive to Go trials, NoGo trials, both kinds of trials

(dual), and non-specific neurons. Notably the Go, NoGo, and dual types of neurons were equally common in preSMA (Isoda and Hikosaka, 2007), while NoGo neurons dominated in the STN (Isoda and Hikosaka, 2008). The authors interpret this observation as suggesting that preSMA exerts both inhibitory and facilitatory effects, and thus plays a role in resolving response conflict. The STN, on the other hand, is primarily inhibitory, playing a role in suppressing automatic in favor of goal-directed behavior. The authors were also able to compare the timing of activity between regions (though not simultaneously), which allowed them to draw some inferences about network properties of this system. These results will be discussed further in the network section below.

Another paper also reported preSMA single unit recordings in monkeys, here using a version of the stop-signal task (Scangos and Stuphorn, 2010). Like the Isoda and Hikosaka report (2007), Scangos and Stuphorn also found preSMA neurons that displayed activity patterns consistent with a role in response control. Specifically, they observed a subset of preSMA (and SMA) neurons that responded more on trials where stopping was successful compared to failures. For some of these neurons, the time of the response was early enough (before SSRT) that it could reflect a causal role in the response control, in this case, response inhibition. However, while these results point to a possible role of preSMA in response control, other findings from this study suggest that this may not be the primary role of the preSMA. The majority of preSMA neurons responded mainly on go trials (and the authors report that the response most likely reflected a motivational signal, since its timing related more to reward than

movement initiation.) Moreover, of the neurons that did respond mainly on stop trials, most of the neurons showed the response later than the SSRT, too late, the authors argue, to be related to response control. Therefore, while preSMA may play a role in response control, it certainly has other functions as well.

Finally, another monkey neurophysiology paper by Sakagami and colleagues (2001) reported single-unit recordings from the ventrolateral prefrontal cortex (VLPFC), a possible homologue to the human IFG, during a Go/NoGo task. They found neurons that responded to both Go trials and NoGo trials ("Go-type" and "NoGo-type" neurons). However, an important feature of their data was the response was specific to NoGo trials for both neuron-types. NoGo-type neurons fired specifically to stimuli that corresponded to a NoGo trial (i.e. trials which require response inhibition). Likewise, Go-type neurons fired non-specifically on go trials, but consistently reduced their activity when a NoGo stimulus was presented. The authors interpret these results to suggest that the VLPFC in monkeys is particularly active for the cognitive process of 'response inhibition', or more generally 'response control'. This interpretation could extend to the human IFG since the VLPFC area is a good candidate for the homologous region in monkeys.

Neural Network for Cognitive Control

Much converging evidence suggests that the preSMA, IFG, and STN are all critical for cognitive control. Moreover, it has now been demonstrated in humans that these three regions are connected to one another via white matter, as revealed by

diffusion tensor imaging (Johansen-Berg et al., 2004; Ford et al., 2010; King et al., 2012). These observations are also supported by tract-tracing studies in monkeys (Inase et al., 1999; Nambu et al., 2002). Importantly, these cortical to STN connections could underlie the 'hyper-direct' pathway observed in primates which is structurally well-positioned to have a fast, non-specific inhibitory effect on the motor systems, perhaps even canceling an initiated response (Mink, 1996; Nambu et al., 2002). These results together suggest that these three regions: the preSMA, IFG, and STN may form (part of) a 'network' for cognitive control. This conclusion is further supported by the recent observation that the strength of the tract between IFG and STN as well as preSMA to STN and the striatum significantly correlates with SSRT (wherein higher fractional anisotropy was correlated with faster SSRT) (King et al., 2012). (However, another group showed a similar effect instead for the anterior cingulate-STN connection (Forstmann et al., 2012).) Therefore, components of this network seem to have a link to inhibitory behavior in particular on a subject-by-subject basis.

Having established the presence of this network, there remain questions about how it might work. How do these areas communicate? What are the individual roles of each node of the network, and are they dissociable? One way to address these questions, which has gained favor in recent years, is the technique of paired-pulse TMS. Here the first TMS coil is placed over one region, such as IFG or preSMA, and the second coil is placed over a second area, usually primary motor cortex (M1). Then two pulses are delivered, from the first and second coil in succession, with a short

delay between the two. At predetermined stimulation intensities, the first pulse should activate the first region (such as IFG or preSMA), and the second will activate M1, allowing a motor evoked potential (MEP) to be recorded with electromyography (EMG) from the targeted muscle. If the task involves an influence of the first region on the second (in a time-frame consistent with the delay between the two pulses), then the priming of the first region by the first pulse may cause a change in its influence over the second that can be indexed as a change in the MEP.

A paired-pulse TMS approach was used in two studies that examined the effects of right IFG (ventral premotor region, specifically) and preSMA separately on M1 during a switching task. The first study examined the effect of preSMA on M1 and found that it facilitated the M1 responses on switch trials, but not non-switch trials (Mars et al., 2009). A different version of the task showed the opposite effect when testing right IFG's influences on M1. Namely, a conditioning pulse over right IFG inhibited M1 on switch trials (but again, not on trials without a switch) (Buch et al., 2010). A third study was then performed to more fully examine the possible timing differences of the preSMA and IFG influences on M1. Here they showed that in the same task, preSMA exerted its excitatory effect on M1 125 ms following the switch cue, while IFG exerted its inhibitory effects 175 ms following the switch cue (and neither exerted these effects for non-switch trials) (Neubert et al., 2010). This observation established that preSMA influenced M1 prior to IFG, but not that they influenced one another. To address this, preSMA was disrupted using repetitive TMS, prior to the IFG being tested using the paired pulse technique, so that effects of

preSMA on IFG could be observed. This approach showed that disruption of preSMA abolished the inhibitory influence of IFG on M1, suggesting that preSMA plays an upstream role to IFG during switch trials (Neubert et al., 2010). The final experiment in that paper, examined correlations between the paired-pulse MEP effects and structural properties of the white matter tracts (fractional anisotropy) derived from each subject's structural MRI. They observed that for a short interval between the two pulses (6 ms), the only significant correlations were between white matter tracts connecting cortical areas. However for a longer delay (12 ms), connections to the basal ganglia (in the vicinity of STN) were also apparent. These results suggest that each of these regions exerts a direct effect on M1 over short time-scales, but also an indirect one via the basal ganglia over longer intervals (Neubert et al., 2010).

This impressive series of paired-pulse TMS studies has suggested a model of activity where preSMA influences IFG, which then influences M1 (directly or via the basal ganglia) during switching (Neubert et al., 2010). A different pattern was observed using the stop signal task with another method. Here Duann and colleagues applied Granger causality techniques to fMRI data, and found evidence for bi-directional communication between right IFG and preSMA (but mainly from IFG to preSMA), and preSMA influences on subcortical areas (Duann et al., 2009). However, there is some ambiguity about whether or not Granger causality can be applied to fMRI data, with its relatively slow time-scale compared to the underlying neural activity.

While, both these approaches have made valuable contributions, there are limitations to each. TMS only provides measurements at discrete time points, thus the effects at other times remain opaque. Functional MRI, on the other hand, samples more continuously, but on the order of seconds and may lack the temporal resolution to reliably apply causal measures, particularly for interactions that apparently occur on a very fast, millisecond, time-scale (Neubert et al., 2010). One solution to address this problem is to address these questions using methods with higher temporal resolution (and more continuous sampling). Electrophysiology can fill this void. Moreover, electrophysiology can reveal information about the type of activity, for instance the frequency band in which it occurs, which appears to have functional relevance (Siegel et al., 2012). Furthermore, electrophysiology can also inform functional connectivity (Fries, 2005). An electrophysiology approach, which could begin to address network properties of the system, was used in two of the monkey studies described earlier (Isoda and Hikosaka, 2007, 2008). Here, recordings from both preSMA and STN showed single neuron activation during switch trials in both regions. Moreover, preSMA preceded STN in terms of the time at which the switch trial activation reliably differed from non-switch trials, suggesting that perhaps preSMA may trigger the switching process in STN (Isoda and Hikosaka, 2008).

Electrophysiological responses such as those reported by Isoda and Hikosaka have the potential to elucidate the dynamics of the cognitive control network. However, such recordings have so far been scarce in humans. This is problematic since executive functions like cognitive control, may differ in humans compared to

animal models. For instance, some regions in the cognitive control network (like IFG) are not unambiguously defined in the animal model. Moreover, there is no guarantee that animals use the same strategies to perform the tasks as humans, particularly because they have been over-trained. Therefore, human studies are preferable. Moreover, because the recordings reported by Isoda and Hikosaka were not obtained simultaneously, influences of these areas on one another (functional connectivity) cannot be directly established. This thesis begins to fill these gaps.

How Might Electrophysiology Elucidate Communication Between Regions?

Recently much attention has been given to the possibility that neural communication between brain regions may be revealed by examining the electrophysiological oscillatory properties of each region (Siegel et al., 2012). These oscillatory changes are thought to primary reflect summed activity of excitatory post-synaptic potentials (i.e. input to neurons) (Logothetis et al., 2001; Lachaux et al., 2003; Ray et al., 2008b). One popular proposal for how oscillatory properties might reflect communication between distant areas is via coherence (Fries, 2005). This model suggests that if two areas are oscillating with a phase relationship that allows activity in one region to reach the other when it is more likely to be excited (in an 'up-state'), than communication will be more effective. Therefore, if two regions have a consistent phase relationship at a certain frequency, it may be that these regions are communicating, and this phase relationship at the specific frequency could be a 'fingerprint' of the communication (Siegel et al., 2012). Much research has shown

task-relevant modulations of this phase-relationship, supporting its putative role in neural communication (Womelsdorf et al., 2007; Gregoriou et al., 2009; van Elswijk et al., 2010). Importantly, modeling and other in vivo and in vitro methods have suggested that lower frequencies (3-20 Hz for instance) may be best suited for this communication since the longer period (~50-300 ms) of these lower frequencies is conducive to phase synchronization between regions over the long distances necessary for inter-regional communication (Kopell et al., 2000; Kopell et al., 2010).

An extension of this account comes from research looking at phase-amplitude coupling between frequencies (reviewed by Canolty and Knight, 2010). Here it has been demonstrated that high frequency amplitude increases (such as high gamma, ~90-130 Hz) are locked to the phase of low frequencies. The interpretation of this is that the lower frequency activity can drive the higher frequency activity. It has been proposed that high gamma activity is a good index of local neural activity (Edwards et al., 2005; Miller et al., 2007; Ray et al., 2008b; Conner et al., 2011; Scheeringa et al., 2011). Therefore, the observation that low frequency activity, suited for long-distance communication, can drive high frequency activity, reflecting local neural processing, suggests that this low frequency-high frequency relationship could explain how activation in one area (reflected in high frequency increases) can communication with a distant brain area (via low frequency activity), to then cause activations (high frequency increase) in this distant region. This motivates consideration of low and high frequency communication separately as they may have different contributions to neuronal functioning, with low frequency changes reflecting a putative index for long-

range communication (as investigated in chapters 2, 3, and 4), and high frequency communication reflecting local neural activity (investigated in chapters 4 and 5).

Pathological Oscillations in Parkinson's Disease

One observation that is interesting to consider in the context of the role of low frequencies in neural communication is the type of oscillatory activity observed in Parkinson's disease. Many studies show there is pathological over-synchronization in the beta band in the basal ganglia and in the cortex, and pathologically high beta amplitude in the basal ganglia of patients with Parkinson's Disease (Brown and Williams, 2005; Silberstein et al., 2005; Brown, 2007; Hammond et al., 2007; Jenkinson and Brown, 2011). Moreover, simultaneous recordings from the basal ganglia and the cortex reveal presumably excessive bidirectional beta coupling/synchronization between the two (Sharott et al., 2005; Lalo et al., 2008; Hirschmann et al., 2011; Litvak et al., 2011). This pathological beta activity correlates with the severity of bradykinesia and rigidity, and the improvement of these symptoms from either dopamanergic medication or deep brain stimulation also correlates with reduction of STN beta (Weinberger et al., 2006; Ray et al., 2008a; Eusebio et al., 2011). Furthermore, inducing beta in the basal ganglia, by stimulating DBS electrodes at this frequency (rather than the typically therapeutic, higher, frequencies), leads to exacerbated slowing of movements (Moro et al., 2002; Chen et al., 2007; Eusebio et al., 2008; Chen et al., 2011). To some extent, this may generalize to healthy populations since inducing beta oscillations in cortical regions of control subjects also

results in modest slowing . Overall therefore, there is evidence that pathologically high beta activity in basal ganglia and/or cortex is causally related to the movement slowing that occurs in Parkinson's disease. Together, these observations suggest that beta may be an especially salient frequency for communication between cortex and basal ganglia, and that pathologically high levels of beta may be associated with bradykinesea (slowed movement) and rigidity (perhaps generalizable to healthy populations (Pogosyan et al., 2009).)

The Role of Beta in the Stopping Network

Another approach to conceptualizing functional roles of different frequency bands is to try to ascribe a general mechanistic function to each. This approach is perhaps viable insofar as specific neural network assemblies may be recruited predominantly for certain functions. Notably, the frequency at which oscillations occur seems to depend on relative contributions of inhibitory interneuron and pyramidal cell networks (Klausberger et al., 2003; Whittington and Traub, 2003; Kopell et al., 2010). So, it is possible that specific frequencies might dominate in particular brain regions where these populations of cells are more or less common. For many years the beta band was mainly regarded as a marker for idling activity (Pogosyan et al., 2009). Recently, though, it has been ascribed a more complex functional role, mainly 'maintenance of the status quo' (Pfurtscheller et al., 1996). This account suggests that the beta band plays a role in maintaining the current cognitive or motor set, particularly in the face of distraction. For stopping then, the

beta band's role may be maintaining (or re-establishing) a static position, despite interference from an expected (or partially initiated) response.

Since the beta band seems to be a key player in cortical-basal ganglia communication and motor processes, and the response control network involves cortical-basal ganglia connections, it is possible that beta may be an efficient frequency for the communication between nodes in this network. This would also fit with the notion that beta is important for 'maintaining the status quo' described above. Further support comes from observations that link beta to response control and stopping in particular. Specifically, Go/NoGo experiments have revealed that there is increased beta for NoGo relative to Go trials recorded from both the cortex (Engel and Fries, 2010) and from the STN (Kühn et al., 2004). Similar effects are seen in the stop signal task (increases in beta for successful stop trials) again, in both the cortex (Alegre et al., 2004) and STN (Marco-Pallares et al., 2008; Ray et al., 2012). Further examination of beta during stopping in humans will be discussed using a method with high spatio-temporal resolution in humans in chapters 2 and 4, and possible communication between regions in beta will be addressed in chapters 3 and 4.

Preparing to Stop

While the study of outright stopping has proven a useful model in understanding cognitive control, cases where an external signal tells us to suppress an initiated overt movement in our daily lives are probably fairly rare. Therefore, a more ecologically valid model may be one in which we use our goals to prepare to stop

(Leventhal et al., 2012). Recently, several studies have adopted this approach of examining preparing to stop by comparing go trials where a stop signal is possible to go trials when no stop signal could occur (or when it is less likely). In addition to possibly being more relevant to real life, this approach has the advantage of potentially being better suited to delineate possible dissociable roles for different brain regions. For instance, it could be that the activity observed for reactive stopping may be entirely associated with the outright stopping itself, or it could be driven more by the implicit preparation for stopping in the simple stop signal task. Such questions are better addressed by examining preparing to stop in comparison to outright stopping, instead of outright stopping alone.

Studies which adopted this approach found that many of the same regions recruited for stopping (reactive control) including the right IFG, preSMA, and basal ganglia, are also recruited for anticipating a stop signal (proactive control) (Chikazoe et al., 2009; Jahfari et al., 2010; Zandbelt and Vink, 2010; Zandbelt et al., 2012). Moreover, when response slowing is taken as a metric for degree of preparedness for stopping, one report showed a trade-off wherein areas active for outright stopping, required less of this activation when subjects were more prepared (Aron, 2011). Also, another study revealed that the amount of IFG activity when preparing to stop scaled with the degree of response slowing (i.e. more IFG activity for 'more preparation') (Chikazoe et al., 2009). These results suggest that the network identified as crucial for outright stopping, may have mechanistic importance for preparing to stop as well.

Together, these findings raise the question of how this network may be differentially involved in preparing to stop and outright stopping. Moreover, separating activity into a preparing to stop and an outright stopping phase, and even subdividing the preparing to stop phase into early and later periods, may help to shed light on the different functional roles of each region. Several studies have addressed this question, attempting to ascribe certain functional roles to specific regions. For instance, Zandbelt and collegues recently showed that preSMA was active early on in the trial, near the time of the cue which indicated the probability of a stop signal occurring, while the right IFG's activity was closer in time to the go signal, during the response phase of the task (Jahfari et al., 2010). They interpret these findings to suggest that the preSMA plays a role in setting up the motor system for the possibility of stopping (preparing to stop), while the IFG plays a role in violation of expectation (because a stop signal did not occur). This, relatively novel account of IFG function stands in contrast to other accounts that suggest IFG is important for action control (meaning actually playing some motoric inhibitory role for stopping and/or preparing to stop) (Aron et al., 2007a; Jahfari et al., 2010; Zandbelt et al., 2012), attentional monitoring (Hampshire et al., 2010; Neubert et al., 2010; Sharp et al., 2010), or both of these possibly in dissociable sub-regions(Verbruggen and Chambers, 2010; Levy and Wagner, 2011; Chatham et al., 2012) during reactive control.

It is possible that these roles for preparing to stop, may generalize to reactive stopping as well, such that the relatively improved sensitivity by isolating activity associated with preparation to stop vs outright stopping, may be more generally

informative. The use of this approach, and possible different roles for each of these regions in proactive vs. reactive control will be discussed further in chapters 4 and 5.

Other Cognitive Functions Engaged during the Stop Task

While most of the studies discussed here have focuses on the response control component of the stop signal task, the task inherently involves other functions such as keeping in mind rules/goals (working memory), attention to the stop signal, response monitoring, violation of expectation, and more. This may be particularly evident in examinations of preparing to stop, which may rely heavily on working memory processes. Therefore, using preparing-to-stop tasks may be particularly helpful in determining if any of these cognitive functions are performed primarily by specific brain regions. For instance, dorsolateral prefrontal cortex has been consistently implicated in working memory processes (Petrides, 2000; Muller and Knight, 2006; Chikazoe, 2010), so its role in preparing to stop may be related to this function. In contrast, several roles, described above, have been ascribed to IFG (action control(Goldman-Rakic, 1990; Aron et al., 2007a; Neubert et al., 2010), attentional monitoring (Hampshire et al., 2010; Jahfari et al., 2010; Sharp et al., 2010; Boehler et al., 2011), or both(Chikazoe, 2010; Verbruggen and Chambers, 2010; Chatham et al., 2012)). Further exploration of these possibly distinct roles, particularly using preparing-to-stop tasks, would potentially be fruitful. Chapter 5 aims to approach this question.

Summary

While, it has now been well established that there is a neural network important for cognitive control, and response control in particular, two major questions remain. First, how and when do different nodes of the network become active and communicate with one another? Second, what is the functional contribution of regions within this structural/function network? In particular, proper performance of the stop signal task relies on a number of different cognitive processes, such as: motor inhibition, task configuration, attentional orienting, keeping in mind task rules/goals, etc. Which of these processes relate to nodes within the network? This thesis takes steps to address these gaps.

One strategy to shed light on these questions is to use methods that provide information about the temporal dynamics of these regions during stopping. However, in humans, many of the most popular non-invasive methods lack either sufficient temporal resolution (fMRI, PET, lesion studies), or high spatial resolution (EEG). Therefore, for most of the studies described in this thesis we turn to electrocorticography (ECoG), which are invasive recordings in epilepsy patients receiving brain surgery, where electrodes are places directly on the cortex, beneath the dura, providing both high temporal *and* high spatial resolution. To investigate subcortical contributions, we adopt a strategy of examining changes to cortical EEG recordings (from the scalp), during modulation of STN using DBS. Using these methods together, this thesis provides one of the first thorough examinations in humans of the spatial-temporal dynamics of response control and also gives insight

into how brain regions may work together as a network, each region making a unique contribution, in order to produce coordinated behavior.

References

Alegre M, Gurtubay IG, Labarga A, Iriarte J, Valencia M, Artieda J (2004) Frontal and central oscillatory changes related to different aspects of the motor process: a study in go/no-go paradigms. Exp Brain Res 159:14-22.

Aron AR (2011) From reactive to proactive and selective control: developing a richer model for stopping inappropriate responses. Biol Psychiatry 69:e55-68.

Aron AR, Poldrack RA (2006) Cortical and subcortical contributions to Stop signal response inhibition: role of the subthalamic nucleus. J Neurosci 26:2424-2433.

Aron AR, Dowson JH, Sahakian BJ, Robbins TW (2003a) Methylphenidate improves response inhibition in adults with attention-deficit/hyperactivity disorder. Biological Psychiatry 54:1465-1468.

Aron AR, Monsell S, Sahakian BJ, Robbins TW (2004) A componential analysis of task-switching deficits associated with lesions of left and right frontal cortex. Brain 127:1561-1573.

Aron AR, Fletcher PC, Bullmore ET, Sahakian BJ, Robbins TW (2003b) Stop-signal inhibition disrupted by damage to right inferior frontal gyrus in humans. Nat Neurosci 6:115-116.

Aron AR, Behrens TE, Smith S, Frank MJ, Poldrack RA (2007a) Triangulating a cognitive control network using diffusion-weighted magnetic resonance imaging (MRI) and functional MRI. J Neurosci 27:3743-3752.

Aron AR, Durston S, Eagle DM, Logan GD, Stinear CM, Stuphorn V (2007b) Converging evidence for a fronto-basal-ganglia network for inhibitory control of action and cognition. J Neurosci 27:11860-11864.

Bekker EM, Overtoom CC, Kenemans JL, Kooij JJ, De Noord I, Buitelaar JK, Verbaten MN (2005) Stopping and changing in adults with ADHD. Psychol Med 35:807-816.

Boehler CN, Appelbaum LG, Krebs RM, Chen L-C, Woldorff MG (2011) The role of stimulus salience and attentional capture across the neural hierarchy in a stop-signal task. PLoS ONE 6:e26386.

Buch ER, Mars RB, Boorman ED, Rushworth MFS (2010) A network centered on ventral premotor cortex exerts both facilitatory and inhibitory control over primary motor cortex during action reprogramming. J Neurosci 30:1395-1401.

Canolty RT, Knight RT (2010) The functional role of cross-frequency coupling. Trends in Cognitive Sciences 14:506-515.

Chambers CD, Bellgrove MA, Stokes MG, Henderson TR, Garavan H, Robertson IH, Morris AP, Mattingley JB (2006) Executive "brake failure" following deactivation of human frontal lobe. J Cogn Neurosci 18:444-455.

Chambers CD, Bellgrove MA, Gould IC, English T, Garavan H, McNaught E, Kamke M, Mattingley JB (2007) Dissociable mechanisms of cognitive control in prefrontal and premotor cortex. J Neurophysiol.

Chatham CH, Claus ED, Kim A, Curran T, Banich MT, Munakata Y (2012) Cognitive control reflects context monitoring, not motoric stopping, in response inhibition. PLoS One 7:e31546.

Chen CY, Muggleton NG, Tzeng OJ, Hung DL, Juan CH (2009) Control of prepotent responses by the superior medial frontal cortex. Neuroimage 44:537-545.

Chen R, Classen J, Gerloff C, Celnik P, Wassermann EM, Hallett M, Cohen LG (1997) Depression of motor cortex excitability by low-frequency transcranial magnetic stimulation. Neurology 48:1398-1403.

Chen X, Scangos KW, Stuphorn V (2010) Supplementary motor area exerts proactive and reactive control of arm movements. J Neurosci 30:14657-14675.

Chikazoe J (2010) Localizing performance of go/no-go tasks to prefrontal cortical subregions. Curr Opin Psychiatry.

Chikazoe J, Jimura K, Hirose S, Yamashita K-i, Miyashita Y, Konishi S (2009) Preparation to Inhibit a Response Complements Response Inhibition during Performance of a Stop-Signal Task. J Neurosci 29:15870-15877.

Congdon E, Mumford JA, Cohen JR, Galvan A, Canli T, Poldrack RA (2012) Measurement and reliability of response inhibition. Front Psychol 3:37.

Conner C, Ellmore TM, Pieters TA, Disano M, Tandon N (2011) Variability of the Relationship between Electrophysiology and BOLD-fMRI across Cortical Regions in Humans. Journal of Neuroscience in press.

Corbetta M, Shulman GL (2002) Control of goal-directed and stimulus-driven attention in the brain. Nat Rev Neurosci 3:201-215.

Duann JR, Ide JS, Luo X, Li CS (2009) Functional connectivity delineates distinct roles of the inferior frontal cortex and presupplementary motor area in stop signal inhibition. J Neurosci 29:10171-10179.

Eagle DM, Baunez C, Hutcheson DM, Lehmann O, Shah AP, Robbins TW (2007) Stop-Signal Reaction-Time Task Performance: Role of Prefrontal Cortex and Subthalamic Nucleus. Cereb Cortex.

Edwards E, Soltani M, Deouell LY, Berger MS, Knight RT (2005) High gamma activity in response to deviant auditory stimuli recorded directly from human cortex. J Neurophysiol 94:4269-4280.

Engel AK, Fries P (2010) Beta-band oscillations-signalling the status quo? Current Opinion in Neurobiology.

Eusebio A, Thevathasan W, Doyle Gaynor L, Pogosyan A, Bye E, Foltynie T, Zrinzo L, Ashkan K, Aziz T, Brown P (2011) Deep brain stimulation can suppress pathological synchronisation in parkinsonian patients. J Neurol Neurosurg Psychiatry 82:569-573.

Floden D, Stuss DT (2006) Inhibitory control is slowed in patients with right superior medial frontal damage. Journal of cognitive neuroscience 18:1843-1849.

Folstein JR, Van Petten C (2008) Influence of cognitive control and mismatch on the N2 component of the ERP: a review. Psychophysiology 45:152-170.

Ford A, McGregor KM, Case K, Crosson B, White KD (2010) Structural connectivity of Broca's area and medial frontal cortex. Neuroimage 52:1230-1237.

Forstmann BU, Jahfari S, Scholte HS, Wolfensteller U, van den Wildenberg WP, Ridderinkhof KR (2008) Function and structure of the right inferior frontal cortex predict individual differences in response inhibition: a model-based approach. J Neurosci 28:9790-9796.

Forstmann BU, Keuken MC, Jahfari S, Bazin P-L, Neumann J, Schäfer A, Anwander A, Turner R (2012) Cortico-subthalamic white matter tract strength predicts interindividual efficacy in stopping a motor response. Neuroimage 60:370-375.

Fried I, Katz A, McCarthy G, Sass KJ, Williamson P, Spencer SS, Spencer DD (1991) Functional organization of human supplementary motor cortex studied by electrical stimulation. J Neurosci 11:3656-3666.

Fries P (2005) A mechanism for cognitive dynamics: neuronal communication through neuronal coherence. Trends in Cognitive Sciences 9:474-480.

Garavan H, Ross TJ, Stein EA (1999) Right hemispheric dominance of inhibitory control: an event-related functional MRI study. Proc Natl Acad Sci U S A 96:8301-8306.

Garavan H, Hester R, Murphy K, Fassbender C, Kelly C (2006) Individual differences in the functional neuroanatomy of inhibitory control. Brain Res 1105:130-142.

Gauggel S, Rieger M, Feghoff TA (2004) Inhibition of ongoing responses in patients with Parkinson's disease. J Neurol Neurosurg Psychiatry 75:539-544.

Goldman-Rakic PS (1990) Cellular and circuit basis of working memory in prefrontal cortex of nonhuman primates. Prog Brain Res 85:325-335; discussion 335-326.

Gregoriou GG, Gotts SJ, Zhou H, Desimone R (2009) High-frequency, long-range coupling between prefrontal and visual cortex during attention. Science 324:1207-1210.

Hampshire A, Chamberlain SR, Monti MM, Duncan J, OWEN AM (2010) The role of the right inferior frontal gyrus: inhibition and attentional control. NeuroImage.

Hirschmann J, Ozkurt TE, Butz M, Homburger M, Elben S, Hartmann CJ, Vesper J, Wojtecki L, Schnitzler A (2011) Distinct oscillatory STN-cortical loops revealed by simultaneous MEG and local field potential recordings in patients with Parkinson's disease. Neuroimage 55:1159-1168.

Inase M, Tokuno H, Nambu A, Akazawa T, Takada M (1999) Corticostriatal and corticosubthalamic input zones from the presupplementary motor area in the macaque monkey: comparison with the input zones from the supplementary motor area. Brain Res 833:191-201.

Isoda M, Hikosaka O (2007) Switching from automatic to controlled action by monkey medial frontal cortex. Nat Neurosci 10:240-248.

Isoda M, Hikosaka O (2008) Role for subthalamic nucleus neurons in switching from automatic to controlled eye movement. J Neurosci 28:7209-7218.

Jahfari S, Stinear CM, Claffey M, Verbruggen F, Aron AR (2010) Responding with restraint: what are the neurocognitive mechanisms? Journal of cognitive neuroscience 22:1479-1492.

Johansen-Berg H, Behrens TE, Robson MD, Drobnjak I, Rushworth MF, Brady JM, Smith SM, Higham DJ, Matthews PM (2004) Changes in connectivity profiles define functionally distinct regions in human medial frontal cortex. Proc Natl Acad Sci U S A 101:13335-13340.

Kenner NM, Mumford JA, Hommer RE, Skup M, Leibenluft E, Poldrack RA (2010) Inhibitory motor control in response stopping and response switching. J Neurosci 30:8512-8518.

King AV, Linke J, Gass A, Hennerici MG, Tost H, Poupon C, Wessa M (2012) Microstructure of a three-way anatomical network predicts individual differences in response inhibition: A tractography study. Neuroimage 59:1949-1959.

Kopell N, Ermentrout GB, Whittington MA, Traub RD (2000) Gamma rhythms and beta rhythms have different synchronization properties. Proc Natl Acad Sci USA 97:1867-1872.

Kopell N, Kramer MA, Malerba P, Whittington MA (2010) Are different rhythms good for different functions? Front Hum Neurosci 4:187.

Lachaux JP, Rudrauf D, Kahane P (2003) Intracranial EEG and human brain mapping. J Physiol Paris 97:613-628.

Lalo E, Thobois S, Sharott A, Polo G, Mertens P, Pogosyan A, Brown P (2008) Patterns of bidirectional communication between cortex and basal ganglia during movement in patients with Parkinson disease. J Neurosci 28:3008-3016.

Leventhal DK, Gage GJ, Schmidt R, Pettibone JR, Case AC, Berke JD (2012) Basal Ganglia Beta oscillations accompany cue utilization. Neuron 73:523-536.

Levy BJ, Wagner AD (2011) Cognitive control and right ventrolateral prefrontal cortex: reflexive reorienting, motor inhibition, and action updating. Ann N Y Acad Sci 1224:40-62.

Li CS, Yan P, Sinha R, Lee TW (2008) Subcortical processes of motor response inhibition during a stop signal task. Neuroimage 41:1352-1363.

Litvak V, Jha A, Eusebio A, Oostenveld R, Foltynie T, Limousin P, Zrinzo L, Hariz MI, Friston K, Brown P (2011) Resting oscillatory cortico-subthalamic connectivity in patients with Parkinson's disease. Brain 134:359-374.

Logan GD, Cowan WB (1984) On the Ability to Inhibit Thought and Action: A Theory of an Act of Control. Psych Rev 91:295-327.

Logothetis NK, Pauls J, Augath M, Trinath T, Oeltermann A (2001) Neurophysiological investigation of the basis of the fMRI signal. Nature 412:150-157.

Luders H, Lesser RP, Dinner DS, Morris HH, Wyllie E, Godoy J (1988) Localization of cortical function: new information from extraoperative monitoring of patients with epilepsy. Epilepsia 29 Suppl 2:S56-65.

Marco-Pallares J, Camara E, Munte TF, Rodriguez-Fornells A (2008) Neural mechanisms underlying adaptive actions after slips. J Cogn Neurosci 20:1595-1610.

Mars RB, Klein MC, Neubert F-X, Olivier E, Buch ER, Boorman ED, Rushworth MFS (2009) Short-latency influence of medial frontal cortex on primary motor cortex during action selection under conflict. J Neurosci 29:6926-6931.

Menzies L, Achard S, Chamberlain SR, Fineberg N, Chen CH, del Campo N, Sahakian BJ, Robbins TW, Bullmore E (2007) Neurocognitive endophenotypes of obsessive-compulsive disorder. Brain 130:3223-3236.

Miller KJ, denNijs M, Shenoy P, Miller JW, Rao RPN, Ojemann JG (2007) Real-time functional brain mapping using electrocorticography. Neuroimage 37:504-507.

Mink JW (1996) The basal ganglia: focused selection and inhibition of competing motor programs. Prog Neurobiol 50:381-425.

Mirabella G, Iaconelli S, Romanelli P, Modugno N, Lena F, Manfredi M, Cantore G (2011) Deep Brain Stimulation of Subthalamic Nuclei Affects Arm Response Inhibition In Parkinson's Patients. Cereb Cortex.

Monterosso JR, Aron AR, Cordova X, Xu J, London ED (2005) Deficits in response inhibition associated with chronic methamphetamine abuse. Drug Alcohol Depend 79:273-277.

Muller NG, Knight RT (2006) The functional neuroanatomy of working memory: Contributions of human brain lesion studies. In: Neuroscience, pp 51-58.

Nachev P, Wydell H, O'Neill K, Husain M, Kennard C (2007) The role of the pre-supplementary motor area in the control of action. Neuroimage 36 Suppl 2:T155-163.

Nambu A, Tokuno H, Takada M (2002) Functional significance of the cortico-subthalamo-pallidal 'hyperdirect' pathway. Neurosci Res 43:111-117.

Neubert FX, Mars RB, Buch ER, Olivier E, Rushworth MF (2010) Cortical and subcortical interactions during action reprogramming and their related white matter pathways. Proc Natl Acad Sci U S A 107:13240-13245.

Oosterlaan J, Logan GD, Sergeant JA (1998) Response inhibition in AD/HD, CD, comorbid AD/HD + CD, anxious, and control children: a meta-analysis of studies with the stop task. J Child Psychol Psychiatry 39:411-425.

Overtoom CCE, Verbaten MN, Kemner C, Kenemans JL, van Engeland H, Buitelaar JK, van der Molen MW, van der Gugten J, Westenberg H, Maes RAA, Koelega HS (2003) Effects of methylphenidate, desipramine, and L-dopa on attention and inhibition in children with Attention Deficit Hyperactivity Disorder. Behavioural Brain Research 145:7-15.

Petrides M (2000) The role of the mid-dorsolateral prefrontal cortex in working memory. Exp Brain Res 133:44-54.

Pfurtscheller G, Stancak A, Jr., Neuper C (1996) Post-movement beta synchronization. A correlate of an idling motor area? Electroencephalogr Clin Neurophysiol 98:281-293.

Pliszka SR, Liotti M, Woldorff MG (2000) Inhibitory control in children with attention-deficit/hyperactivity disorder: event-related potentials identify the processing component and timing of an impaired right-frontal response-inhibition mechanism. Biol Psychiatry 48:238-246.

Pogosyan A, Gaynor LD, Eusebio A, Brown P (2009) Boosting cortical activity at Beta-band frequencies slows movement in humans. Curr Biol 19:1637-1641.

Postuma RB, Lang AE (2003) Hemiballism: revisiting a classic disorder. Lancet Neurol 2:661-668.

Ray N, Jenkinson N, Brittain J, Holland P, Joint C, Nandi D, Bain P, Yousif N, Green A, Stein J, Aziz T (2009) The role of the subthalamic nucleus in response inhibition: Evidence from deep brain stimulation for Parkinson's disease. Neuropsychologia.

Ray NJ, Brittain JS, Holland P, Joundi RA, Stein JF, Aziz TZ, Jenkinson N (2012) The role of the subthalamic nucleus in response inhibition: Evidence from local field potential recordings in the human subthalamic nucleus. Neuroimage 60:271-278.

Ray NJ, Jenkinson N, Wang S, Holland P, Brittain JS, Joint C, Stein JF, Aziz T (2008a) Local field potential beta activity in the subthalamic nucleus of patients with Parkinson's disease is associated with improvements in bradykinesia after dopamine and deep brain stimulation. Exp Neurol 213:108-113.

Ray S, Crone NE, Niebur E, Franaszczuk PJ, Hsiao SS (2008b) Neural correlates of high-gamma oscillations (60-200 Hz) in macaque local field potentials and their potential implications in electrocorticography. J Neurosci 28:11526-11536.

Rieger M, Gauggel S, Burmeister K (2003) Inhibition of ongoing responses following frontal, nonfrontal, and basal ganglia lesions. Neuropsychology 17:272-282.

Rubia K, Smith AB, Brammer MJ, Taylor E (2003) Right inferior prefrontal cortex mediates response inhibition while mesial prefrontal cortex is responsible for error detection. Neuroimage 20:351-358.

Rubia K, Overmeyer S, Taylor E, Brammer M, Williams SC, Simmons A, Bullmore ET (1999) Hypofrontality in attention deficit hyperactivity disorder during higher-order motor control: a study with functional MRI. Am J Psychiatry 156:891-896.

Sakagami M, Tsutsui K, Lauwereyns J, Koizumi M, Kobayashi S, Hikosaka O (2001) A code for behavioral inhibition on the basis of color, but not motion, in ventrolateral prefrontal cortex of macaque monkey. J Neurosci 21:4801-4808.

Scangos KW, Stuphorn V (2010) Medial frontal cortex motivates but does not control movement initiation in the countermanding task. J Neurosci 30:1968-1982.

Scheeringa R, Fries P, Petersson KM, Oostenveld R, Grothe I, Norris DG, Hagoort P, Bastiaansen MC (2011) Neuronal dynamics underlying high- and low-frequency EEG oscillations contribute independently to the human BOLD signal. Neuron 69:572-583.

Schmajuk M, Liotti M, Busse L, Woldorff MG (2006) Electrophysiological activity underlying inhibitory control processes in normal adults. Neuropsychologia 44:384-395.

Sharott A, Magill PJ, Bolam JP, Brown P (2005) Directional analysis of coherent oscillatory field potentials in the cerebral cortex and basal ganglia of the rat. The Journal of Physiology 562:951-963.

Sharp DJ, Bonnelle V, De Boissezon X, Beckmann CF, James SG, Patel MC, Mehta MA (2010) Distinct frontal systems for response inhibition, attentional capture, and error processing. Proceedings of the National Academy of Sciences:1-6.

Siegel M, Donner TH, Engel AK (2012) Spectral fingerprints of large-scale neuronal interactions. Nat Rev Neurosci 13:121-134.

Sowell ER, Thompson PM, Welcome SE, Henkenius AL, Toga AW, Peterson BS (2003) Cortical abnormalities in children and adolescents with attention-deficit hyperactivity disorder. Lancet 362:1699-1707.

van den Wildenberg WPM, van Boxtel GJM, van der Molen MW, Bosch DA, Speelman JD, Brunia CHM (2006) Stimulation of the subthalamic region facilitates the selection and inhibition of motor responses in Parkinson's disease. Journal of cognitive neuroscience 18:626-636.

van Elswijk G, Maij F, Schoffelen J-M, Overeem S, Stegeman DF, Fries P (2010) Corticospinal beta-band synchronization entails rhythmic gain modulation. J Neurosci 30:4481-4488.

Verbruggen F, Logan GD (2009) Models of response inhibition in the stop-signal and stop-change paradigms. Neurosci Biobehav Rev 33:647-661.

Verbruggen F, Chambers ARAMASCD (2010) Theta burst stimulation dissociates attention and action updating in human inferior frontal cortex. Proceedings of the National Academy of Sciences:1-38.

Vink M, Kahn RS, Raemaekers M, van den Heuvel M, Boersma M, Ramsey NF (2005) Function of striatum beyond inhibition and execution of motor responses. Hum Brain Mapp 25:336-344.

Weinberger M, Mahant N, Hutchison WD, Lozano AM, Moro E, Hodaie M, Lang AE, Dostrovsky JO (2006) Beta oscillatory activity in the subthalamic nucleus and its relation to dopaminergic response in Parkinson's disease. J Neurophysiol 96:3248-3256.

Williams BR, Ponesse JS, Schachar RJ, Logan GD, Tannock R (1999) Development of inhibitory control across the life span. Dev Psychol 35:205-213.

Womelsdorf T, Schoffelen JM, Oostenveld R, Singer W, Desimone R, Engel AK, Fries P (2007) Modulation of neuronal interactions through neuronal synchronization. Science 316:1609-1612.

Zandbelt BB, Vink M (2010) On the role of the striatum in response inhibition. PLoS One 5:e13848.

Zandbelt BB, Bloemendaal M, Neggers SFW, Kahn RS, Vink M (2012) Expectations and violations: Delineating the neural network of proactive inhibitory control. Hum Brain Mapp.

CHAPTER 2:

Intracranial EEG reveals a time– and frequency–specific role for the right inferior frontal gyrus and primary motor cortex in stopping initiated responses

ABSTRACT

Inappropriate response tendencies may be stopped via a specific fronto/basal-ganglia/primary-motor-cortical network. We sought to characterize the functional role of two regions in this putative stopping network, the right inferior frontal gyrus (IFG) and the primary motor cortex (M1), using electocorticography from subdural electrodes in four patients while they performed a stop signal task. On each trial, a motor response was initiated, and on a minority of trials a stop signal instructed the patient to try to stop the response. For each patient, there was a greater right IFG response in the beta frequency band (~16 Hz) for successful vs. unsuccessful stop trials. This finding adds to evidence for a functional network for stopping because changes in beta frequency activity have also been observed in the basal ganglia in association with behavioral stopping. In addition, the right IFG response occurred 100 - 250 ms after the stop signal – a time range consistent with a putative inhibitory control process, rather than stop signal processing or feedback regarding success. A downstream target of inhibitory control is M1. In each patient, there was alpha/beta-band desynchronization in M1 for stop trials. However, the degree of desynchronization in M1 was less for successfully than unsuccessfully stopped trials. This reduced desynchronization on successful stop trials could relate to increased

GABA inhibition in M1. Taken together with other findings, the results suggest that behavioral stopping is implemented via synchronized activity in the beta-frequency band in a right IFG/basal-ganglia network, with downstream effects on M1.

INTRODUCTION

Cognitive control is required to stop inappropriate action. One way to study this experimentally is with the stop signal task (Logan, 1994; Verbruggen and Logan, 2009). On each trial, the participant initiates a motor response, and on a minority of trials tries to stop the response when a stop signal occurs. Behaviorally, such stopping is operationalized as the time to stop the response: Stop Signal Reaction Time (SSRT). Loss of function studies show that the dorsomedial frontal cortex and the right inferior frontal gyrus (IFG) are critical regions for stopping (Aron et al., 2003; Chambers et al., 2006; Floden and Stuss, 2006; Chambers et al., 2007; Chen et al., 2008), and functional MRI affirms this (Rubia et al., 2003; Aron and Poldrack, 2006; Li et al., 2006; Aron et al., 2007; Chevrier et al., 2007; Chamberlain et al., 2008). Yet the precise functional role of these regions in behavioral stopping is still unclear.

While the right IFG may implement an inhibitory control function, it may also be important for stop signal detection, working memory, response selection, and stimulus-driven attention (Corbetta and Shulman, 2002; Hampshire et al., 2007; Mars et al., 2008; Mostofsky and Simmonds, 2008; Zandbelt et al., 2008). One way to dissociate these functions is with the high temporal resolution of electroencephalography (EEG). Studies with scalp EEG show that successfully

stopped trials are associated with a larger negativity at ~200 ms (after the stop signal) than unsuccessful stop trials or trials with no stop signal (e.g. Kok et al., 2004; Schmajuk et al., 2006; Liotti et al., 2007; Dimoska and Johnstone, 2008). This timing is consistent with a putative inhibitory function generated after the stop signal, but before SSRT typically elapses (typically around 250 ms). However, as the spatial resolution of scalp EEG is limited, it is uncertain what is the neural source of this event-related potential.

We sought to elucidate the functional role of the right IFG by harnessing the high spatio-temporal resolution of electrocorticography (ECoG). We recorded directly from the cortical surface of patients undergoing presurgical monitoring. For each patient we selected a right IFG electrode in an unbiased manner and analyzed the ECoG for stop trials. If the right IFG implements an inhibitory control function, then we predicted it would show a strong response within a time-window ranging from the stop signal to the SSRT. Moreover, the frequency band of the response was also of interest. Finding a stopping-related response in right IFG within a particular frequency band might help to characterize the information-processing function of the right IFG within the wider putative fronto-basal-ganglia network. It has been hypothesized that communication between functionally/structurally connected brain regions may occur in specific frequency-bands (Fries, 2005).

We also examined M1 – a downstream target of inhibitory control. Studies with transcranial magnetic stimulation (TMS) suggest that successful stop trials are associated with increased GABA-mediated inhibition in M1 (Sohn et al., 2002; Coxon

et al., 2006; van den Wildenberg et al., 2009) and an fMRI study showed different responses for successful and unsuccessful stop trials in this region (Aron and Poldrack, 2006). ECoG could provide convergent evidence for understanding the dynamics of M1 during behavioral stopping in terms of the timing of the neural response and the frequency band.

MATERIAL AND METHODS

Participants

Four right-handed patients (three female, mean age 32, range 20 to 47) with medically refractory epilepsy were studied with ECoG. All patients had subdural electrode arrays implanted over their right hemispheres. Two of the patients (TA341 and TA344) were also studied with functional MRI on a similar task (prior to grid placement). One patient (TA344) had a right anterior temporal lobectomy 10 years prior to this study. Another patient (TS007) had a prior bilateral depth electrode evaluation and a past history of meningitis. All patients provided written informed consent according to Institutional Review Board guidelines at the University of Texas Medical School at Houston.

The stop signal task used for ECoG

The task was highly similar to that used in an earlier study [see the study by Aron et al. (2007) for full details]. Here it is reprised in brief, with key additional information. On each trial a left- or right-pointing arrow stimulus was presented

(Figure 2.1). This was displayed on a laptop computer screen, placed on a table over the patient's bed in the epilepsy monitoring unit. Once the arrow stimulus was presented, the patient responded as fast as possible with a left or right key press (using index and middle fingers of either the left or right hand, see Table 2.1). [Note that hand use varied due to clinical exigencies, such as placement of intravenous lines. Prior research shows that the right-hemisphere basis of stop signal response inhibition is unlikely related to the hand used (Konishi et al., 1999; Chambers et al., 2006) and our results are consistent with this]. On a minority of trials (33%), an auditory stop signal (500 Hz; 400 ms duration) was played at a particular stop-signal delay (SSD) subsequent to the arrow stimulus. When the patient detected the tone, he or she was required to try to stop the initiated response, but only if the arrow was pointing in a 'critical' direction: leftward pointing for TS007 (both days of testing) and TS005; and rightward pointing for TA341 and TA344. [We note that with the exception of one auxiliary analysis, see Supplementary Figure 2.3, the data presented here focus only on trials where the arrow pointed in the critical direction. Thus, in what follows go trials are go critical, successful stop trials are successful stop critical, and unsuccessful stop trials are unsuccessful stop critical].

In each block there were 32 stop and 64 go trials (96 trials total). In every twenty-four trials, there were eight stop trials and 16 go trials, trial order was random, and the number of leftward- and rightward-pointing arrows was equal. Each trial began with a colored circular fixation ring (subtending 4.3 degrees of visual angle) appearing in the center of a white background screen. Half the circle was red (e.g. left

side) and the other half green, to help remind the patient of the critical direction. This was a constant arrangement for each patient's session. After 500 ms, a black arrow (subtending 1.9 degrees of visual angle) was displayed within the fixation ring. The fixation ring and arrow remained on the screen for up to 1 s (limited hold), after which they disappeared, and the background screen was shown for an inter-trial interval (ITI) of 1.4 seconds. When the patient responded within the limited hold window, the fixation ring and arrow disappeared, and the background was shown for the remainder of the limited hold and ITI. A stop trial was identical to a go trial, except that a tone was played at some stop signal delay after the arrow stimulus. If the response was stopped, then the arrow and fixation ring remained onscreen for the duration of the limited hold. If the subject responded, then the arrow and fixation ring disappeared, and the background screen was displayed for the remainder of the time. The SSD changed dynamically throughout the experiment, depending on the subject's behavior with respect to the critical key, to yield ~50% p(stop) [see the study by Aron et al. (2007) for precise details]. Tracking in this way is desirable to achieve a roughly equal number of successful and unsuccessful stop trials for ECoG analysis.

Before the experiment started, patients were trained to perform go and stop trials. Instructions made it clear that stopping and going were equally important and that it would not always be possible to stop. Each block was preceded by an instruction screen and was followed by feedback in the form of median-correct reaction time (RT), the number of discrimination errors on go trials, and the number of times when the patient incorrectly stopped when the arrow pointed in the noncritical

direction (where going is always appropriate.) During the course of each block, pauses were inserted every 24 trials to allow the patient to rest. We aimed to collect eight blocks (96 trials each) for each patient/session. However, fatigue made this impossible in some cases (Table 2.1).

The stop signal task used for fMRI

The task/procedure used was identical to that reported in a prior fMRI study (Aron and Poldrack, 2006). Two patients (TA341 and TA344) performed 3 blocks/scans (6 minutes each) of a standard stop signal task within the MRI magnet using their left hand to respond. The fMRI task was administered prior to subdural array placement and ECoG. Although the standard stop signal task is slightly different from the conditional stop signal task used for ECoG, both have been shown to activate the right IFG similarly (Aron and Poldrack, 2006; Aron et al., 2007). For fMRI, we used the standard task as a right IFG 'localizer' because it enabled us to attain more stop trials per unit time.

Behavioral analysis

For both ECoG and fMRI sessions we computed median correct go RT, the percentage of successful stop trials, the mean stop signal delay, the percentage of discrimination errors on go trials and the % of response omissions on go trials. In most patients the dynamic tracking of SSD allowed convergence to ~50% successful stop

trials, however this was not the case for all patients and we therefore estimated SSRT for everyone using the integration method (Verbruggen and Logan, 2009).

ECoG acquisition and filtering

Data were collected using an EEG 1100 Neurofax clinical Nihon Koden acquisition system. The number and placement of electrodes and the sampling rate were determined by clinical considerations (Table 2.1). Trial onsets for the behavioral task were sent to the ECoG data acquisition computer via transistor-transistor logic pulses. All data were referenced to a subdural electrode outside the regions of interest and then subsequently digitally re-referenced to a common average reference for analysis.

Electrode Localizations

Subdural electrodes were localized through a procedure that involved registration to preoperative structural MRI (pre-MRI) and postoperative CT scan. The pre-MRI was a high-resolution T1-weighted anatomical scan acquired on a 3T Philips scanner. From this, a cortical surface model was generated (Dale et al., 1999). Following subdural electrode implantation, a high-resolution contiguous thin-slice CT was acquired (post-CT). The post-CT was co-registered to the pre-MRI with a rigid-body transformation algorithm using a mutual information cost function (Cox, 1996). The center of individual electrodes was localized using the post-CT. The subdural electrodes are visualized with Freesurfer tools. as spherical geometric objects (Figure

2.2). To account for the possibility that non-linear deformation of the cortical surface occurs after electrode implantation (Studholme et al., 2001), we modified the pial cortical surface model to disregard fissures and sulci, creating a smoothed envelope exactly fitting the shape and size of the subject's brain. The electrodes were then re-aligned to this new surface by placing them along a surface normal to the point on the envelope closest to their location on the deformed brain surface. Our results with this method reveal highly accurate electrode localization having a mean deviation of less than 2 mm per electrode compared with electrode locations determined using intra-operative photographs.

ECoG Analysis: generating condition-specific time-frequency data

After digitally re-referencing to the common average, the data were manually inspected for inter-ictal discharges, 60 Hz noise contamination and other causes of low signal-to-noise ratio. Electrodes with contamination were excluded from analysis. Epochs that were contaminated by any spreading ictal events were excluded for all electrodes in the dataset. For one patient (TA341) there was intermittent electrical artifact, likely from hospital or recording equipment. This artifact was relatively broadband and high frequency, and we were unable to eliminate it during recording. Therefore, only low frequency data are presented for this patient (30 Hz and below). The ECoG analysis was highly similar to a published report (Canolty et al., 2007). The key steps are shown in Figure 2.3. We first summarize the overall procedure and then provide an illustrative example for a right IFG electrode. First, a fast Fourier transform

was applied to all data from a single channel, thus converting the data from the time domain into the frequency domain. The transformed signal was then multiplied by many overlapping Gaussians centered at selected frequencies of interest and with different standard deviations depending on the center frequency. These values, and the number of Gaussians used, varied for different patients, according to their sampling rates. In all cases the lowest center frequency was 2.5 Hz and the highest was less than half the sampling rate (Nyquist cut off), and always <300 Hz, the maximum high frequency cutoff of the hardware. (Note: For TA341, for whom higher frequencies were contaminated by electrical noise, the maximum frequency examined was 30 Hz.) (Note: This process is analogous to a Gabor wavelet analysis in the temporal domain, but is performed in the frequency domain for computational efficiency.) The data were then separated into different groups with each group having a different center frequency. An inverse fast Fourier transform was applied to data in each group, converting it back into the time domain. The resulting data, referred to as the analytic signal, had an equal number of time points as the original raw signal, but the signal is now separated into the different frequencies of interest. The amplitude of this analytic signal was used to calculate power, which is the dependent variable for the ECoG analysis. Next, the data were broken up with respect to events of interest (for instance the period of time around each stop signal), baseline corrected to account for pre-stimulus activity, and averaged (e.g. mean power was attained for all successful stop trials, across many frequencies, and for a specific period of time around the stop signal). Finally, the analytic power was converted to z-scores.

Taking the example of a single channel in the right IFG: The signal was filtered into many separate frequencies and the analytic signal was obtained as described above. For a single center frequency, and for each successful stop trial, data were extracted corresponding to the analytic signal from 1750 ms before the stop signal, to 1750 ms after the stop signal (-1750 to 1750, where zero is the time at which the stop signal occurred). An average ERTF (event related time-frequency) was computed by averaging the absolute value of the analytic signal (power), across all such (successful stop) trials, producing a value that corresponded to the average power for each time point. An average prestimulus baseline was obtained by averaging power values, across time, for 500 ms of the inter-trial interval (-1750ms to -1250ms relative to the stop signal). This value was then subtracted from the ERTF values. This procedure was repeated for all filtered frequencies. The entire process described thus far was also performed for unsuccessful stop trials. A similar procedure, but with 0 ms corresponding to the Go stimulus instead of the stop stimulus, was performed for M1 electrodes.

ECoG Analysis: generating condition-specific z-scores

Statistical inference used a published method (Canolty et al., 2007). This uses boostrapping to implement 10,000 runs time locked to random events, in order to derive an ensemble of average analytic signal values for each separate frequency. Each generated number was used to offset from the real event indices, to generate data which was time-locked to a random event, but was otherwise sampled in a manner

analogous to the real data (same number of trials, same relative spacing). From each of these 10,000 runs a value corresponding to the amplitude of the analytic signal was stored. This ensemble was fit to a normal distribution, and a standard deviation was derived representing the variability of the data at a particular frequency.

A z-score was obtained for each condition by dividing the ERTF values (see the prior section) for each frequency and time point by the above-derived standard deviation for each frequency. This z-score was used to determine the probability that each deviation could occur by chance (uncorrected, two tailed). The procedure of obtaining z-scores was also performed for the difference between successful stopping and unsuccessful stopping conditions. In this case, ERTF values were obtained from the subtraction of the analytic signals for the two conditions, without baseline correction.

A correction for multiple comparisons was made using the false discovery rate (FDR) method. For all 10 to 11 electrodes in each patient's right IFG region (probabilistically determined from an anatomical atlas: Eickhoff et al., 2005) we calculated the p values associated with the above-determined z-scores for each condition (successful and unsuccessful stop trials) across all time points of interest (0 to 800 ms after the stop signal for the right IFG and 0 to 1250 ms after the go signal for M1) and across all frequencies. The p values associated with all these z-scores, were then sorted in ascending order (p_1, p_2, p_3, ….p_K,…p_M), and a threshold was determined such that:

$$p_K > (K^{\star}\alpha)/M,$$

where p_K is the FDR corrected alpha value ($p<0.01$), K is the rank ordering of the p-value which corresponds to this threshold, alpha is 0.01, and M is the total number of comparisons.

ECoG Analysis: between-condition statistical comparison

In Results, we describe how a single right IFG and M1 electrode is selected for each patient for further analysis. Once this selection was performed, we tested the difference between successful and unsuccessful stop trials at this electrode in two ways. The first used the boostrapping method above (by which all results were significant $p<0.05$, but not FDR corrected). The second method used a 'masking approach' which honed in on a particular time window and frequency range of interest (rather than all possible time and frequency ranges). For the masking approach, we selected the time and frequency range in a way that should not create bias to find a difference between conditions. For each patient, for the right IFG (or M1) electrode of interest, time-frequency activity was computed for all stop trials (compared to baseline) for the period ranging from the stop signal to 1 second later. The result was corrected for multiple comparisons using FDR ($p<0.01$). This analysis, similar to that shown in Figure 2.5, reveals a strong response in the beta band in all patients. A 'mask' was derived for each patient which contained the data-points in the beta band (13 to 18 Hz) from 0 to 1 second after the stop signal which surpassed the FDR corrected threshold for all stop trials compared to the baseline. This mask was then applied to a time-frequency matrix of z-scores of the difference between successful

and unsuccessful stop trials. For each data point within the mask, we noted: a) the direction of the difference, and b) how many of these data points ('observed' values) were statistically significant ($p<.05$) using the uncorrected, two tailed method for obtaining z-scores for successful vs. unsuccessful trials. The number of observed data points was then compared with the number of data points expected to be significant by chance alone (i.e. 5% of the total number of data points examined). A chi square test compared the disparity between the number of observed and expected observations for each patient.

fMRI acquisition and analysis.

Data acquisition and analysis were the same as reported in a prior study (Aron and Poldrack, 2006) with two exceptions: a) this was a Phillips 3T Scanner at the University of Texas Medical Center, Houston, and b) functional images had the following parameters: thirty-three axial slices (3mm slice thickness, 2.75 in-plan resolution) were sampled (TE 30 ms, TR 2000 ms, flip angle, 90 degrees). Preprocessing was done with tools from the FMRIB software library (www.fmrib.ox.ac.uk/fsl) as previously described (Aron and Poldrack, 2006). Model fitting was done for each patient separately and included the following events after convolution with a canonical hemodynamic response function: go, successful stop, unsuccessful stop, and nuisance events consisting of go trials on which subjects did not respond or made errors. Events were modeled at the time of the arrow stimulus. Temporal derivatives were included as covariates of no interest to improve statistical

sensitivity. Null events were not explicitly modeled, and therefore constituted an implicit baseline. For each scan, the contrasts go-null and successful stop–go were computed. Earlier we had shown that the contrast successful – unsuccessful stop is not effective at isolating frontal stopping-related activation (Aron and Poldrack, 2006; Aron et al., 2007; Xue et al., 2008) [but see (Rubia et al., 2003; Li et al., 2006)]. A higher-level, fixed-effects, analysis was performed across the three scans for each patient. Activations were corrected for multiple comparisons at $z>2.0$, $p<0.05$ wholebrain cluster correction and overlaid on the patient's own T1 structural scan with the subdural electrode grid superimposed.

RESULTS

Behavioral results for ECoG and fMRI

Table 2.2 contains the behavioral data. For ECoG, go trial RT was fairly quick (mean = 572 ms), there was a low number of discrimination errors on go trials (mean = 2.27%), and the patients made relatively few errors of omission on trials for which a response was required (mean for go critical trials = 0.89%; mean for go non critical trials = 1.4%; mean for stop noncritical trials = 6.2%). With regard to trials on which stopping was required, the mean SSRT was 279 ms, the mean stop signal delay was 233 ms and the mean probability of stopping was 50.3%. An anomaly was the low stopping rate (24%) in patient TA344. This related to a poor choice of starting stop signal delay for this ECoG session. Overall, however, it is clear that the ECoG patients performed the task well.

For the two patients with fMRI, the behavioral scores also suggested satisfactory performance and SSRT was roughly consistent with ECoG even though this was a slightly different stopping paradigm (TA341 ECoG = 214 ms, fMRI = 278 ms; TA344 ECoG = 360 ms, fMRI = 368 ms).

Functional MRI results and correspondence with ECoG electrodes

For patient TA341 there was significantly greater activation in the pars triangularis/opercularis of the right IFG for successful stop trials compared to go trials ($p<0.05$, wholebrain corrected) (see Figure 2.4), consistent with prior results in healthy control subjects (Aron and Poldrack, 2006; Aron et al., 2007; Xue et al., 2008). Strikingly, the electrode that was closest to this showed the strongest ECoG result (in terms of z-score) for successful stop trials (Figure 2.4). The contrast of go-null also activated the right sensorimotor region, as expected ($p<0.05$, wholebrain corrected) (data not shown).

For TA344, although we obtained fMRI and ECoG for this patient, a portion of the right prefrontal region was determined to be pathological (i.e. showed ictal activity), and was subsequently resected. Therefore we do not provide right IFG fMRI and ECoG results for this patient. However, we do analyze ECoG M1 data for this patient. For fMRI, the contrast of go-null activated the right sensorimotor region, as expected ($p<0.05$, wholebrain corrected) (data not shown).

Electrode Selection

A key issue was deciding which right IFG electrode within the rather large, probabilistically determined (Eickhoff et al., 2005), anatomical region to analyze in each patient in an unbiased way. We used the following procedure: For TA341, for whom we had fMRI data, we used the electrode within the right IFG that corresponded with the maximum peak in BOLD signal for the fMRI contrast of successful stop - go trials (see Figure 2.4**).** For TS007 and TS005, where fMRI data were not available, we used the following method. For each right IFG electrode, time-frequency activity was computed for all stop trials (compared to baseline) for the period ranging from the stop signal to 1 second later. Of these, we selected as the key electrode the one with the strongest response, where this was defined as having the maximum number of points (across time and frequency band) whose absolute value surpassed the z-score threshold of 85% of the maximum z-score for all stop trials from all electrodes in the right IFG region for each patient individually. This method takes into account both the strength of the power modulation (in z-score) and also how long the modulation lasted, without creating bias towards time or frequency band (see Supplementary Figure 2.1).

The primary motor cortex electrodes were selected based on the anatomically defined hand region (as specified by a neurosurgical expert, NT). For TS007 there was only one clear candidate within the region. For TA341, there was only one electrode in the region which was not contaminated with electrical noise. For TA344, there was no electrode in the region, but we analyzed the closest neighbor.

ECoG results: right IFG

Having chosen a right IFG electrode for each patient/session (one patient was tested twice) according to the above criteria (except for TA344, who was determined to have ictal activity in this region) we present data from these electrodes for successful and unsuccessful stop trials, and the difference between them, all time-locked to the stop signal (Figure 2.5). There are a total of four sessions, because TS007 was tested twice over two days – once using the left hand, once with the right hand. We focused on the range of 0 to 30Hz to be consistent across all sessions. Within each patient's data, there is significant above-baseline activation at approximately 13-16 Hz (beta band) following the stop signal for both successful and unsuccessful stop trials (each comparison $p<0.01$, FDR corrected). Moreover, in all sessions, the power of this ~16 Hz activation was larger for successful than unsuccessful stop trials trials ($p<.05$ uncorrected). To evaluate this result further, we used the masking approach (see Methods). We derived a mask of beta-band activity between 0 and 1 second after the stop signal, from the contrast of all stop trials compared to baseline (FDR corrected $p<0.01$). We examined the z-scores at all data points within the mask for the contrast of successful and unsuccessful stop trials. A chi square test for each patient/session confirmed that the number of data points that surpassed significance (FDR < 0.05, uncorrected) was much greater than expected by chance (Chi square statistic was > 10, 000 and $p<<.01$ for each session). An important point is that the right frontal response for successful stop trials had some spatial

specificity in that the response was stronger within the right IFG region than outside it (see Supplementary Figures 2.1-4).

Notably, the difference between successful and unsuccessful stop trials emerged at ~100 ms to 250 ms after the stop signal for all sessions. This suggests that the right IFG response does not merely relate to auditory stop-signal processing itself because cortical responses to auditory stimuli are detectable in much less than 100 ms (Arezzo et al., 1975; Liegeois-Chauvel et al., 1991). We provide a useful control by analyzing ECoG data from an electrode over auditory cortex in each patient (see Supplementary Figure 2.5-8). Referring to a representative electrode for patient TS007, day 2 (Figure 2.6), note that in auditory cortex, unlike frontal cortex, the response for successful and unsuccessful stop trials was highly similar. Moreover, it was also a much earlier response than observed in prefrontal cortex (occurring at ~50 ms after the stop signal) consistent with previous findings (Pantev et al., 1991). This suggests that early sensory processing (at least) is identical in both conditions, and thus it is unlikely that the reduced right IFG response in the unsuccessful stop condition relates to differences in stop signal processing.

Another possible explanation for the difference between successful and unsuccessful stop trials in right IFG electrodes is that, according to the race model (Logan and Cowan, 1984), the go process is slower on successful than unsuccessful stop trials. This difference in the speed of going could potentially explain the difference in beta-frequency observed in the right IFG for successful compared to unsuccessful stop trials. This predicts that slow go trials will have increased beta

frequency power compared to fast go trials. To examine this possible confound, we performed a median split for each patient to examine slow go vs. fast go trials and we time-locked the ECoG analysis to the arrow onset. Note: we used go noncritical trials because go critical trials may include a proactive inhibitory control component that itself activates the right IFG (Jahfari et al., 2009). The result, across several sessions, is not consistent with a greater beta-frequency band response on slow go trials compared to fast ones (Supplementary Figure 2.9). This suggests that the greater right IFG response on successful vs. unsuccessful stop trials does not relate to the speed of going; instead we expect it relates to stopping.

ECoG results: right M1

A downstream target of inhibitory control is M1 (Stinear et al., 2009). Figure 2.7 shows the ECoG response for a right M1 electrode for the three patients in which the task was performed with the left hand (TS007 day one, TA341, and TA344). For each patient, and each event-type, time-locked to the go signal (on critical trials), there was a significant broadband alpha/beta power decrease relative to prestimulus baseline ($p<0.01$, FDR corrected). This power decrease, or 'desynchronization', denotes a pattern that lacks regular periodicity in a particular frequency range relative to baseline. Alpha/beta desynchronization has been previously observed in M1 for movement generation (Crone et al., 1998; Pfurtscheller et al., 2003; Alegre et al., 2006). Consistent with this we found significant alpha/beta desynchronization on unsuccessful stop trials ($p<0.01$, FDR corrected). Moreover, we also observed

significant alpha/beta desynchronization for successful stop trials $p<0.01$, FDR corrected), but it was diminished. This difference between successful and unsuccessful trials was significant ($p<.05$ uncorrected). Again, to evaluate this difference further, we took the masking approach (see Methods). We derived a mask of alpha and beta-band activity (8 to 30 Hz) between 0 and 1 second after the go signal, from the contrast of all stop trials compared to baseline (FDR corrected $p<0.01$). We examined the z-scores at all data points within the mask for the contrast of unsuccessful and successful stop trials. A chi square test for each patient confirmed that the number of data points that surpassed significance (FDR < 0.05, uncorrected) was much greater than expected by chance (Chi square statistic was > 10, 000 and $p<<.01$ for each patient). We note that the smaller desynchronization for successful vs unsuccessful stop trials probably does not merely reflect the fact that there was movement for unsuccessful stop trials while there was none for successful stop trials. Instead we expect it relates to the stopping of an initiated response. We note that the successful stop trials showed a desynchronization relative to a non-movement baseline. We argue that this reflects the initiated movement, which is subsequently stopped.

DISCUSSION

Much evidence implicates the right IFG, along with the dorsomedial frontal cortex, the basal ganglia and the primary motor cortex, in stop signal and Go/NoGo response inhibition (e.g. Schall et al., 2002; Rubia et al., 2003; Garavan et al., 2006; Li et al., 2006; Aron et al., 2007; Isoda and Hikosaka, 2007, 2008; Li et al., 2008;

Mostofsky and Simmonds, 2008; Chambers et al., 2009; Stinear et al., 2009). Here we sought to better characterize the functional role of the right IFG and primary motor cortex in behavioral stopping with ECoG.

For the right IFG, there was a significant above-baseline response for successful stop trials and also for unsuccessful stop trials in the beta frequency band (~16 Hz) in the range 100 to 500 ms after the stop signal, and the response on successful stop trials was stronger than unsuccessful stop trials. These findings provide novel evidence regarding the functional role of the right IFG in behavioral stopping. First, the right IFG response on stop trials began 100 to 250 ms after the stop signal. This is roughly consistent with the N200 event-related potential observed in many scalp EEG studies of stopping (e.g. Kok et al., 2004; Schmajuk et al., 2006; Liotti et al., 2007; Dimoska and Johnstone, 2008). The increase we observed between 100 and 250 ms for successful and unsuccessful trials (and the difference) is unlikely related to mere auditory processing of the stop signal because this latency is much too late to reflect a cortical response to the tone (which may occur within 13 ms in auditory cortex and not much later in frontal cortex Arezzo et al., 1975; Liegeois-Chauvel et al., 1991). Indeed, in the auditory cortex of our patients there were power modulations very soon after the stop signal that did not differ for successful vs. unsuccessful stop trials. Thus, the right IFG response is probably not related to mere stop signal detection.

Another important aspect of the stopping-related increase in right IFG power, was that it was most prominent in the beta frequency band. This is striking because

other studies show motor-related effects in the beta-frequency range when recording from the subthalamic nucleus (e.g. Kuhn et al., 2004; Kuhn et al., 2005; Klostermann et al., 2007). In particular, the study by Kuhn et al. (2004) reported beta-frequency power increases on no-go trials. This suggests that an increase in beta power could relate to behavioral response inhibition in the subthalamic nucleus, as it does in the right IFG. Other evidence shows that the subthalamic nucleus plays a role in stop signal and other kinds of response inhibition (Aron and Poldrack, 2006; van den Wildenberg et al., 2006; Chamberlain et al., 2008; Eagle et al., 2008; Isoda and Hikosaka, 2008; Ray et al., 2009) and human tractography suggests it is connected with the right IFG via a 'hyperdirect' tract (Aron et al., 2007). Furthermore, coupling between the subthalamic nucleus and other frontal regions involved in motor networks, occurs in the beta band (Lalo et al., 2008). It is thus possible that the beta-frequency response of the right IFG reflects functional communication with the subthalamic nucleus within a structurally-connected network that supports inhibitory control. This is a testable hypothesis, for example in patients undergoing simultaneous cortical and subcortical recording during task performance.

These findings in the right IFG converge with other data (reviewed in Chambers et al., 2009) to point to a stopping-related function implemented in this region. While being able to stop successfully presumably requires an inhibitory control function, it must also require working memory and forms of attention (Corbetta and Shulman, 2002; Aron and Poldrack, 2005; Hampshire et al., 2007; Mostofsky and Simmonds, 2008). We cannot rule out the possibility that it is these

attentional/mnemonic processes which relate to the right IFG response observed here rather than inhibitory control per se. Future research will need to carefully control for this possibility.

On a technical note, prior research reports alpha/beta power increases that follow decreases – and this is taken to reflect an 'idle' or suppressed state (Pfurtscheller et al., 1996). Yet here the right IFG beta power increase was not a 'rebound' of a previous power decrease. Rather, it followed the onset of the tone at 100 to 250 ms, with activity prior to the tone similar to the baseline intertrial interval. Thus, the well-known beta patterns associated with movement may not hold for areas outside the sensorimotor cortex such as the prefrontal cortex. Instead, changes in beta power outside the sensorimotor cortex could be interpreted as signaling an 'active-akinetic' process rather then a lack of movement (Brown and Williams, 2005).

A puzzling feature of our data (in common with scalp EEG findings) is that the ECoG response was greater for successful than unsuccessful stop trials, whereas some functional MRI studies have only found reliable activation of the right IFG region for the contrast of successful stopping with go trials (Aron and Poldrack, 2006; Aron et al., 2007; Xue et al., 2008) [but see (Rubia et al., 2003; Li et al., 2006)]. Indeed a well-powered fMRI meta-analysis from 101 subjects showed that the contrast of successful and unsuccessful stop trials did not activate the right IFG region (Congdon, Xue, Aron and Poldrack, unpublished observations). There are several possible reasons for this discrepancy between ECoG and fMRI data. First, according to the Race Model, whether a patient stops is determined by the speed of the go and the stop process

(Logan and Cowan, 1984). In healthy participants the success of stopping may largely relate to variability in going, rather than stopping – and this may explain why both successful and unsuccessful stop trials activate the right IFG similarly in some studies. In our patients however stopping may not always be triggered (e.g. due to fatigue) – hence a difference would emerge between successful and unsuccessful stop trials. Second, there are differences in what is measured by fMRI and ECoG. While both methods are sensitive to excitatory post-synaptic potentials, the BOLD response is more related to higher frequency bands than lowers ones such as the beta band response observed here (Logothetis et al., 2001; Mukamel et al., 2005). Third, differences in activity for successful vs. unsuccessful stop trials may occur for too short a time period to be detected with fMRI, whereas the difference between successful stop and go trials is more substantial (so it can be observed with fMRI). Finally, ECoG (but not fMRI) is sensitive to synchrony between and within regions. Thus, the difference between successful and unsuccessful stop trials may not be a difference in the firing rate of right IFG neurons, nor their input or local activity, but rather the degree of synchrony within the right IFG or between the right IFG and the basal ganglia. This could produce a different ECoG response for successful and unsuccessful stop trials, but no difference for the BOLD signal (Ray et al., 2008). Turning next to M1; there was a low frequency power decrease (desynchronization) for unsuccessful stop trials. This is consistent with prior reports of alpha/beta desynchronization for M1 associated with movement (Crone et al., 1998; Pfurtscheller et al., 2003). This is a validation of our data collection and analysis techniques and of

the assumption that non-pathologic brain regions of epilepsy patients may serve as good models. Importantly, there was less desynchronization for successful compared to unsuccessful stop trials. Notably, TMS studies have shown that successful stop trials are associated with more GABA-ergic mediated inhibition in M1 than go trials (Sohn et al., 2002; Coxon et al., 2006; van den Wildenberg et al., 2009). We thus speculate that the diminished desynchronization on successful stop trials may be due to increased GABA-ergic inhibition. Indeed, GABA agonists (benzodiazepines) have been shown to modulate beta activity in M1 (Jensen et al., 2005). This study thus contributes potentially useful information about the relationship between frequency band, behavioral control and neuromodulatory tone in primary motor cortex.

This study had limitations: (1) One of the patients we studied (TA 344) underwent a subsequent right prefrontal resection, therefore ECoG data are not presented for this person (although M1 data are), (2) The sampling rate was different across patients, and in some cases, lower than desirable (overall limiting examination of higher frequencies). Indeed our not reporting high frequency responses should not be taken to show that such ranges are not important for prefrontal function and stopping (c.f. Canolty et al., 2006), (3) fMRI was not acquired in all patients; Thus the observed correspondence between ECoG and BOLD signal in right IFG is preliminary.

In summary, we used the high spatiotemporal resolution afforded by ECoG to clarify the functional role of the right IFG in stop signal response inhibition. There was a significant above-baseline response for each of successful and unsuccessful stop

trials in the beta frequency band (~16 Hz) in the range 100 to 500 ms after the stop signal, with the response being stronger on successful than unsuccessful stop trials. The finding that right IFG activity begins around 100 to 250 ms after the stop signal suggests that it is not merely related to the detection of the signal, and the finding that it ends by approximately 500 ms suggests that it is not merely related to processing the success (or not) of stopping. Instead it likely reflects a function that is key to the behavioral stopping itself, as suggested by converging evidence from loss-of-function studies (Chambers et al., 2009). The observation that the right IFG response occurred in the beta frequency band provides novel information in support of the hypothesis that the right IFG is part of a network which includes the subthalamic nucleus of the basal ganglia (Aron et al., 2007). We also examined the downstream effects of behavioral stopping, in primary motor cortex. Making a movement on unsuccessful stop trials was associated with a strong below-baseline desynchronization, whereas successfully stopping an initiated movement was associated with a less strong desynchronization. We interpret this reduction in desynchronization on successful stop trials in the context of other studies as an increase in GABA-mediated inhibition in primary cortex (Sohn et al., 2002; Jensen et al., 2005; Coxon et al., 2006; van den Wildenberg et al., 2009). Together, these findings provide convergent evidence for a fronto/basal-ganglia/primary-cortical-motor network for stopping initiated responses, and they point to the importance of inter-regional binding by synchronized neuronal activity in the beta-frequency range for likely functional connectivity within this network.

ACKNOWLEDGEMENTS

Chapter 2, in full, is a reprint of material as it appears in The Journal of Neuroscience, 2009: Swann NC, Tandon N, Canolty R, Ellmore TM, McEvoy LK, Dreyer S, DiSano M, Aron AR. (2009) Intracranial EEG reveals a time- and frequency-specific role for the right inferior frontal gyrus and primary motor cortex in stopping initiated responses. The dissertation author was the primary investigator and author of this paper.

The authors thank John Serences for helpful comments. NS is supported by an NSF Graduate Student Fellowship. ARA is supported by an Alfred P Sloan Fellowship and NIH grant 1R01DA026452 - 01A1.

Table 2.1 Data collection parameters

	Sampling Rate (Hz)	Blocks Run	Hand Used	# successful stop trials (before artifact reject/after)	# unsuccessful stop trials (before artifact reject/after)
TS007 (day 1)	200	8	Left	85/65	43/32
TS007 (day 2)	1000	8	Right	81/69	47/41
TS005	500	4.5	Right	36/24	44/26
TA341	1000	7	Left	64/59	58/49
TA344	1000	8	Left	36/24	92/64

Table 2.2 Behavioral Data. ECoG = electrocorticography; fMRI = functional magnetic resonance imaging; RT = Reaction Time on go trials (no stop signal); Go Errors = % of Go errors; SSRT = stop signal reaction time; SSD = average stop signal delay; P(stop) = probability of stopping the response on stop trials; Omission Errors = % of trials on which the subject did not respond (shown separately for the different trial types on which responses needed to be made).

Patients	Expt.	RT (ms) *Median (Standard deviation)*	Go Errors (%)	SSRT (ms)	SSD (ms)	P(stop)	Omission Errors (%) (go critical/go noncritical/stop noncritical trials)
TS007 (day 1)	ECoG	689(178)	1.17	220	304	66.4	0.78/5.08/8.59
TS007 (day 2)	ECoG	699(225)	0.39	248	288	63.3	3.12/1.17/7.81
TS005	ECoG	494(138)	1.39	351	158	45	0/0.63/5.0
TA341	ECoG	512(134)	4.69	214	255	54	0.52/0/8.33
	fMRI	538(102)	5.2	278	358	53	NA
TA344	ECoG	466(111)	3.32	360	158	24	0/0.52/1.04
	fMRI	550(89)	2.6	368	228	49	NA

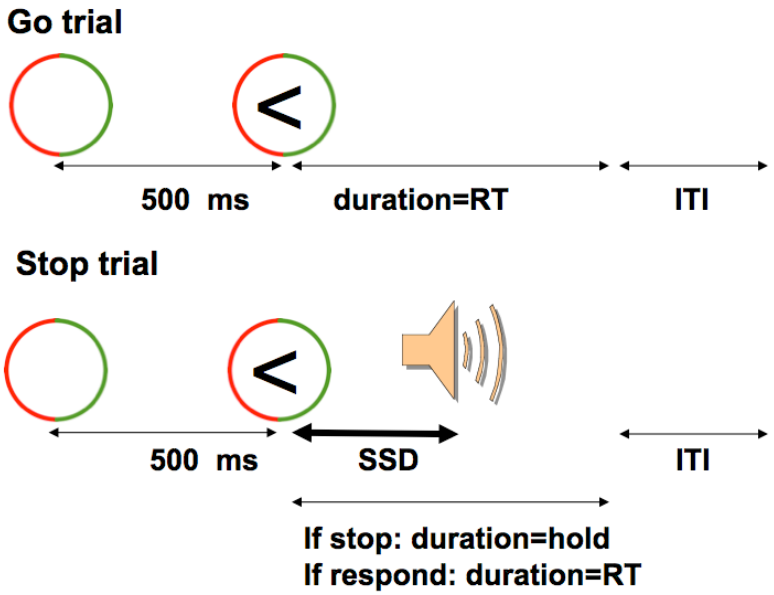


Figure 2.1: Conditional stop signal task used in the electrocorticography experiment. Each trial begins with a cue circle (in this case left half red, right half green). The cue reminds the participant that the "critical" direction (red) is the left response, and the "noncritical" direction (green) is the right response. The rules stay the same for the entire session. On Go trials, the participant has 1 second (the hold period) to press the left or right button in response to a stimulus. On a stop trial, a tone is played at some delay (stop-signal delay, SSD) after the arrow stimulus. The SSD changes dynamically throughout the experiment (increasing or decreasing by 50 ms depending on whether the participant stopped or not on prior stop trials). If the arrow stimulus is in the critical direction AND a tone occurs then the subject must try to stop, but if the arrow is in the noncritical direction AND a tone occurs then the subject must respond anyway.

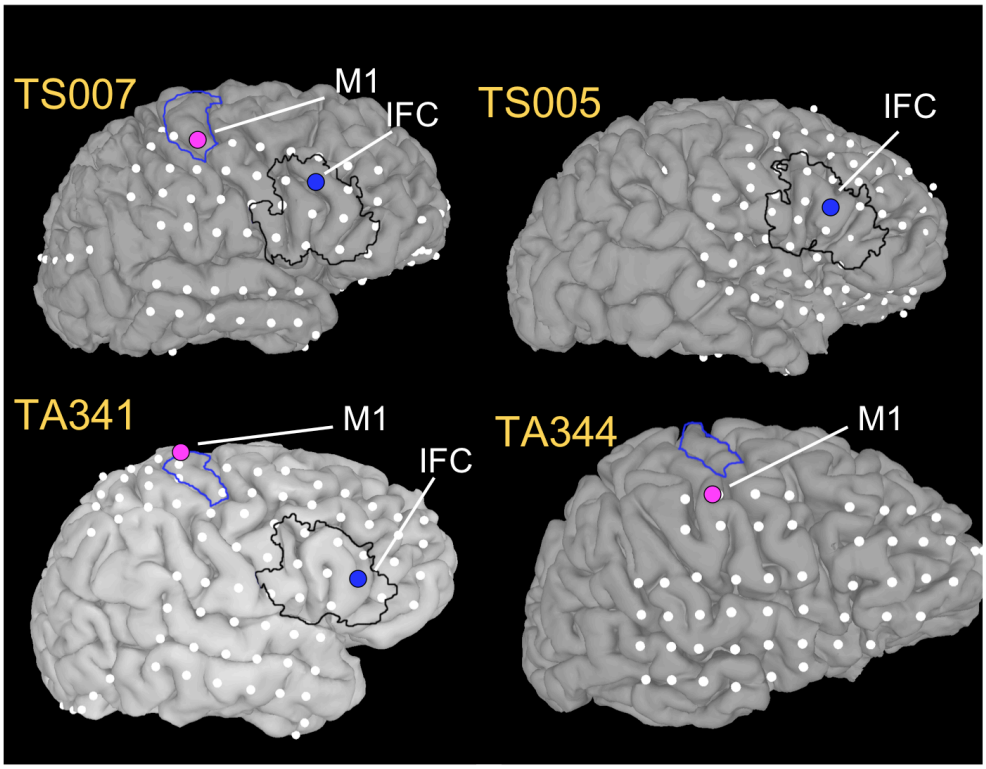


Figure 2.2: Location of intracranial grids on the right hemisphere. For each patient the ECoG grid is registered to the patient's own structural MRI. For the patients for whom we report a right IFG response, the probabilistically determined right IFG region is outlined in black (Eickhoff et al., 2005). For the patients for whom we report M1 results, the hand area of M1 is outlined in blue.

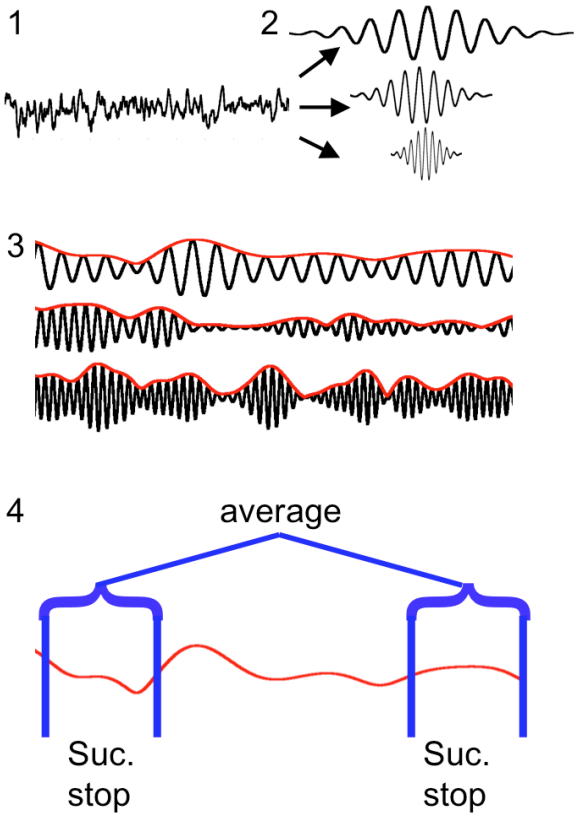


Figure 2.3: ECoG analysis procedure. 1) Raw EEG signal (after referencing to common average). 2) Filtering. The raw signal is filtered using a gabor wavelet technique into many separate frequencies (only three are shown for visualization purposes). 3) Deriving the analytic signal. Traces of the filtered signal for three representative frequencies are shown in black. The red line shows the analytic amplitude ("power"), for each of these frequencies. It is this analytic value over time for each frequency that is used for the remainder of the analysis. 4) Epoching. All events of one trial type, e.g. successful stop, are grouped together. The analytic signals across the length of the trial are averaged together at each particular frequency. The panel shows one frequency band for illustration.

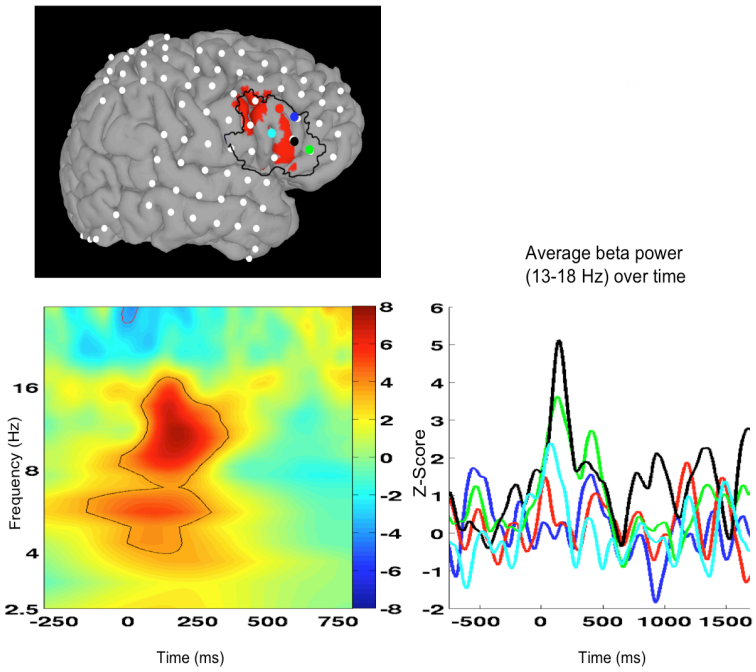


Figure 2.4: Correspondence between fMRI and ECoG for patient TA341. Functional MRI activation represents the contrast successful stop - go (red). The time frequency plot (lower left panel) shows ECoG data from one electrode (marked in black on the MRI) for successful stop trials. Zero ms is the time of the stop signal. The right panel shows beta power over time for this and several other electrodes in the region. The color of each trace corresponds to the color of the electrode shown on the structural MRI. The electrode marked in black was selected for further analysis and had both the closest spatial correspondence to right IFG fMRI activation and also the strongest response (Z ~6.) [Note, the other electrodes in the IFG were excluded from analysis because of electrical noise contamination].

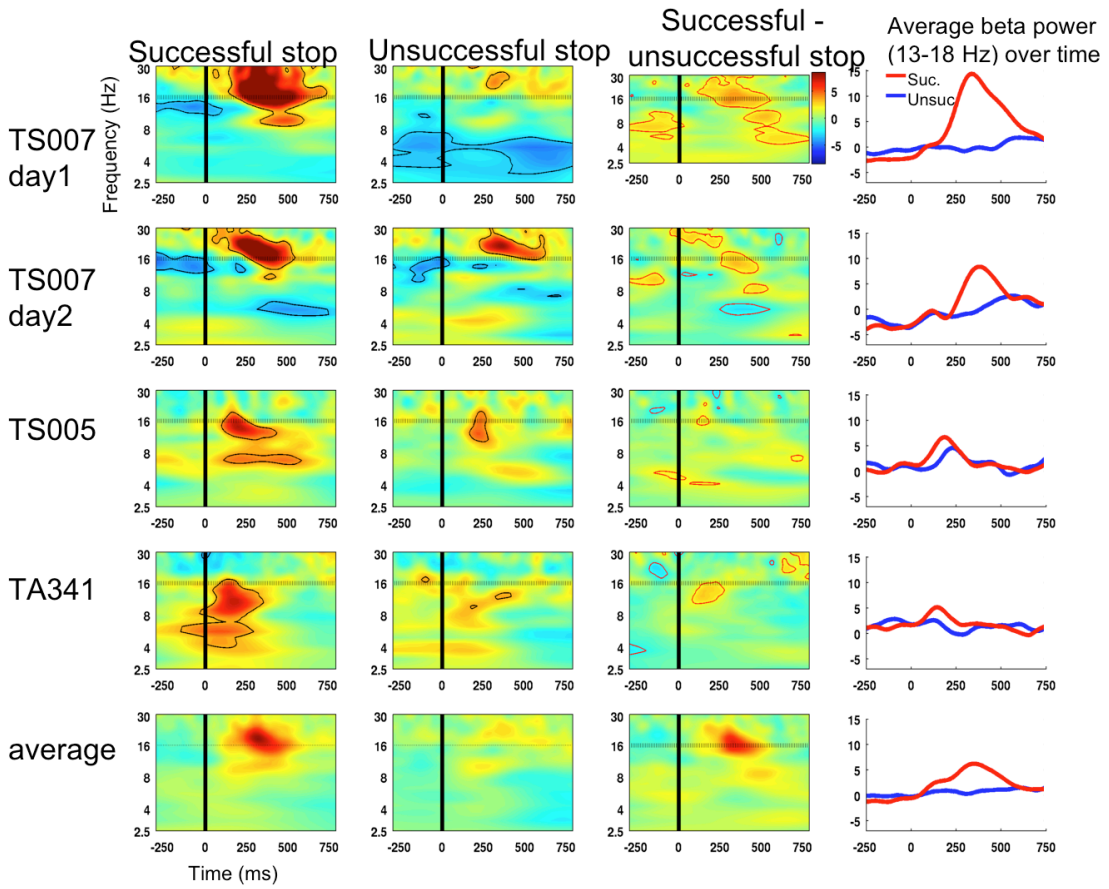


Figure 2.5: Right IFG results for ECoG. The figure shows a stronger ECoG response for successful vs. unsuccessful stop trials. Data are shown for three patients, and for one patient there were two days. Zero ms is the time of the stop signal, indicated by a thick vertical black line. The first two columns show data from each condition relative to baseline period (ITI) as a z-score. The third column shows the difference between conditions (relative to one another, not to the baseline), also as a z-score. The fourth column shows the same data with power averaged across the beta band (13-18 Hz), plotted for both conditions over time (red line indicates successful stopping, blue line indicates unsuccessful stopping). In all cases there is a beta increase (~16 Hz) that is larger for successful vs. unsuccessful stop trials. The thin black outlines in columns 1 and 2 indicate $p<.01$ FDR corrected. The thin red outlines shown in the difference column indicate $p<.05$ uncorrected. The dotted horizontal line marks 16 Hz for all patients. The bottom row of panels shows the average of z-scores across patients, obtained by averaging the average z-scores for each patient, down-sampled to 100 Hz to be comparable across patients.

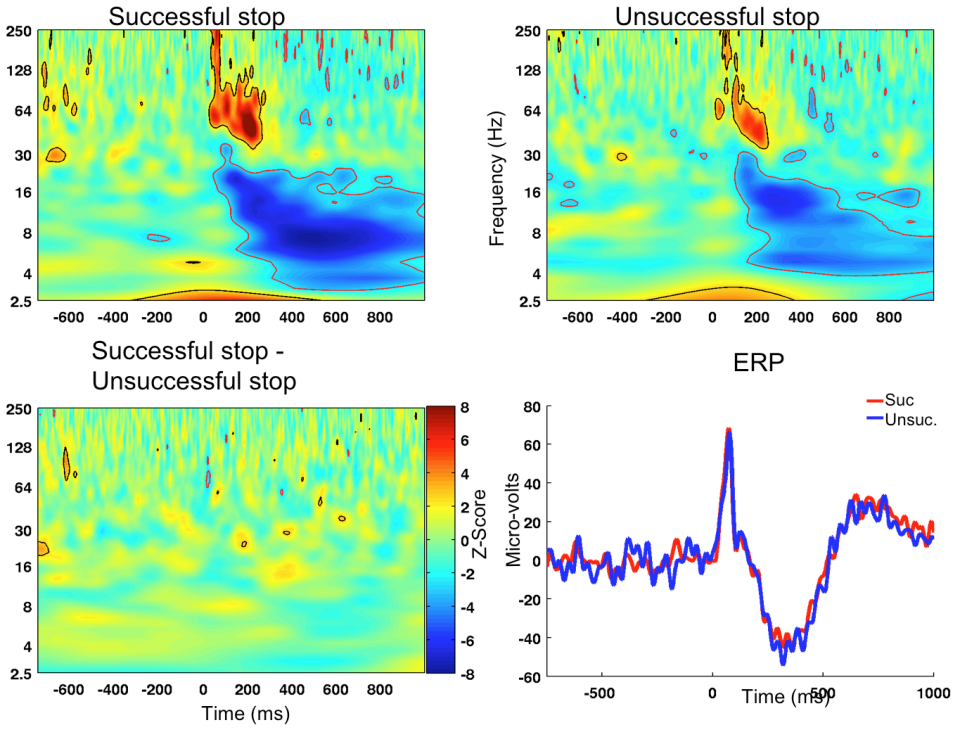


Figure 2.6: A representative electrode from auditory cortex. This shows a very different pattern of response for successful vs. unsuccessful stop trials compared to right IFG. These data are from one electrode for patient TS007 (see Supplementary Figure 2 for other patients). No substantial, statistically significant, differences are present for the contrast of these event types (see difference plot). The event-related potential (low pass filtered at 40 Hz) shows an almost exactly overlapping response between conditions, which begins very shortly after the stop signal (< 50 ms).

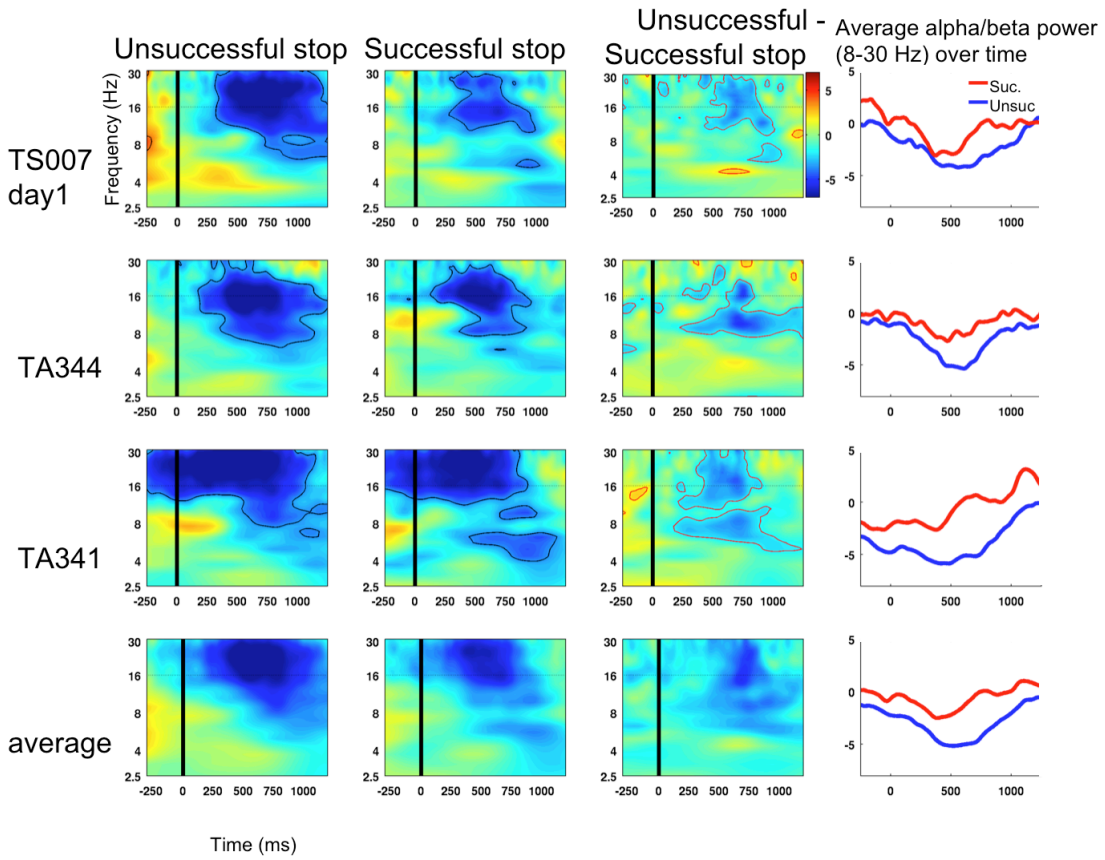


Figure 2.7: Right primary motor cortex results for ECoG. There is a different ECoG response for successful vs unsuccessful stop trials. Zero ms is the time of the go signal, indicated by a thick vertical black line. The first two columns show data from both conditions relative to baseline period (ITI) as a z-score. The third column shows the difference between conditions (relative to one another, not to the baseline), also as a z-score. The fourth column shows average alpha/beta power (8-30 Hz) over time. As for figure 5, thin black outlines indicate $p<.01$ FDR corrected, thin red outlines in the difference column indicate $p<.05$ uncorrected, dotted horizontal line marks 16 Hz for all subjects. The bottom row shows the average of z-scores across patients. Responses were made with the left hand.

REFERENCES

Alegre M, Gurtubay IG, Labarga A, Iriarte J, Malanda A, Artieda J (2003) Alpha and beta oscillatory changes during stimulus-induced movement paradigms: effect of stimulus predictability. Neuroreport 14:381-385.

Alegre M, Imirizaldu L, Valencia M, Iriarte J, Arcocha J, Artieda J (2006) Alpha and beta changes in cortical oscillatory activity in a go/no go randomly-delayed-response choice reaction time paradigm. Clin Neurophysiol 117:16-25.

Arezzo J, Pickoff A, Vaughan HG, Jr. (1975) The sources and intracerebral distribution of auditory evoked potentials in the alert rhesus monkey. Brain Res 90:57-73.

Aron AR, Poldrack RA (2005) The cognitive neuroscience of response inhibition: relevance for genetic research in attention-deficit/hyperactivity disorder. Biol Psychiatry 57:1285-1292.

Aron AR, Poldrack RA (2006) Cortical and subcortical contributions to Stop signal response inhibition: role of the subthalamic nucleus. J Neurosci 26:2424-2433.

Aron AR, Fletcher PC, Bullmore ET, Sahakian BJ, Robbins TW (2003) Stop-signal inhibition disrupted by damage to right inferior frontal gyrus in humans. Nat Neurosci 6:115-116.

Aron AR, Behrens TE, Smith S, Frank MJ, Poldrack RA (2007) Triangulating a cognitive control network using diffusion-weighted magnetic resonance imaging (MRI) and functional MRI. J Neurosci 27:3743-3752.

Bekker EM, Kenemans JL, Hoeksma MR, Talsma D, Verbaten MN (2005) The pure electrophysiology of stopping. Int J Psychophysiol 55:191-198.

Brown P, Williams D (2005) Basal ganglia local field potential activity: character and functional significance in the human. Clin Neurophysiol 116:2510-2519.

Canolty RT, Edwards E, Dalal SS, Soltani M, Nagarajan SS, Kirsch HE, Berger MS, Barbaro NM, Knight RT (2006) High gamma power is phase-locked to theta oscillations in human neocortex. Science 313:1626-1628.

Canolty RT, Soltani M, Dalal SS, Edwards E, Dronkers NF, Nagarajan SS, Kirsch HE, Barbaro NM, Knight RT (2007) Spatiotemporal dynamics of word processing in the human brain. Front Neurosci 1:185-196.

Chamberlain SR, Hampshire A, Muller U, Rubia K, Campo ND, Craig K, Regenthal R, Suckling J, Roiser JP, Grant JE, Bullmore ET, Robbins TW, Sahakian BJ (2008) Atomoxetine Modulates Right Inferior Frontal Activation During Inhibitory Control: A Pharmacological Functional Magnetic Resonance Imaging Study. Biol Psychiatry.

Chambers CD, Garavan H, Bellgrove MA (2009) Insights into the neural basis of response inhibition from cognitive and clinical neuroscience. Neurosci Biobehav Rev 33:631-646.

Chambers CD, Bellgrove MA, Stokes MG, Henderson TR, Garavan H, Robertson IH, Morris AP, Mattingley JB (2006) Executive "brake failure" following deactivation of human frontal lobe. J Cogn Neurosci 18:444-455.

Chambers CD, Bellgrove MA, Gould IC, English T, Garavan H, McNaught E, Kamke M, Mattingley JB (2007) Dissociable mechanisms of cognitive control in prefrontal and premotor cortex. J Neurophysiol 98:3638-3647.

Chevrier AD, Noseworthy MD, Schachar R (2007) Dissociation of response inhibition and performance monitoring in the stop signal task using event-related fMRI. Hum Brain Mapp 28:1347-1358.

Corbetta M, Shulman GL (2002) Control of goal-directed and stimulus-driven attention in the brain. Nat Rev Neurosci 3:201-215.

Cox RW (1996) AFNI: software for analysis and visualization of functional magnetic resonance neuroimages. Comput Biomed Res 29:162-173.

Coxon JP, Stinear CM, Byblow WD (2006) Intracortical inhibition during volitional inhibition of prepared action. J Neurophysiol 95:3371-3383.

Crone NE, Miglioretti DL, Gordon B, Lesser RP (1998) Functional mapping of human sensorimotor cortex with electrocorticographic spectral analysis. II. Event-related synchronization in the gamma band. Brain 121 (Pt 12):2301-2315.

Dale AM, Fischl B, Sereno MI (1999) Cortical surface-based analysis. I. Segmentation and surface reconstruction. Neuroimage 9:179-194.

Dimoska A, Johnstone SJ (2008) Effects of varying stop-signal probability on ERPs in the stop-signal task: do they reflect variations in inhibitory processing or simply novelty effects? Biol Psychol 77:324-336.

Dimoska A, Johnstone SJ, Barry RJ (2006) The auditory-evoked N2 and P3 components in the stop-signal task: indices of inhibition, response-conflict or error-detection? Brain Cogn 62:98-112.

Eagle DM, Baunez C, Hutcheson DM, Lehmann O, Shah AP, Robbins TW (2008) Stop-signal reaction-time task performance: role of prefrontal cortex and subthalamic nucleus. Cereb Cortex 18:178-188.

Eickhoff SB, Stephan KE, Mohlberg H, Grefkes C, Fink GR, Amunts K, Zilles K (2005) A new SPM toolbox for combining probabilistic cytoarchitectonic maps and functional imaging data. Neuroimage 25:1325-1335.

Fries P (2005) A mechanism for cognitive dynamics: neuronal communication through neuronal coherence. Trends Cogn Sci 9:474-480.

Garavan H, Hester R, Murphy K, Fassbender C, Kelly C (2006) Individual differences in the functional neuroanatomy of inhibitory control. Brain Res 1105:130-142.

Hampshire A, Duncan J, Owen AM (2007) Selective tuning of the blood oxygenation level-dependent response during simple target detection dissociates human frontoparietal subregions. J Neurosci 27:6219-6223.

Isoda M, Hikosaka O (2007) Switching from automatic to controlled action by monkey medial frontal cortex. Nat Neurosci 10:240-248.

Isoda M, Hikosaka O (2008) Role for subthalamic nucleus neurons in switching from automatic to controlled eye movement. J Neurosci 28:7209-7218.

Jahfari S, Stinear CM, Claffey M, Verbruggen F, Aron AR (2009) Responding with Restraint: What Are the Neurocognitive Mechanisms? J Cogn Neurosci.

Jensen O, Goel P, Kopell N, Pohja M, Hari R, Ermentrout B (2005) On the human sensorimotor-cortex beta rhythm: sources and modeling. Neuroimage 26:347-355.

Klostermann F, Nikulin VV, Kuhn AA, Marzinzik F, Wahl M, Pogosyan A, Kupsch A, Schneider GH, Brown P, Curio G (2007) Task-related differential dynamics of EEG alpha- and beta-band synchronization in cortico-basal motor structures. Eur J Neurosci 25:1604-1615.

Knyazev GG, Levin EA, Savostyanov AN (2008) A failure to stop and attention fluctuations: an evoked oscillations study of the stop-signal paradigm. Clin Neurophysiol 119:556-567.

Kok A, Ramautar JR, De Ruiter MB, Band GP, Ridderinkhof KR (2004) ERP components associated with successful and unsuccessful stopping in a stop-signal task. Psychophysiology 41:9-20.

Konishi S, Nakajima K, Uchida I, Kameyama M, Nakahara K, Sekihara K, Miyashita Y (1998) Transient activation of inferior prefrontal cortex during cognitive set shifting. Nat Neurosci 1:80-84.

Kuhn AA, Trottenberg T, Kivi A, Kupsch A, Schneider GH, Brown P (2005) The relationship between local field potential and neuronal discharge in the subthalamic nucleus of patients with Parkinson's disease. Exp Neurol 194:212-220.

Kuhn AA, Williams D, Kupsch A, Limousin P, Hariz M, Schneider GH, Yarrow K, Brown P (2004) Event-related beta desynchronization in human subthalamic nucleus correlates with motor performance. Brain 127:735-746.

Lalo E, Thobois S, Sharott A, Polo G, Mertens P, Pogosyan A, Brown P (2008) Patterns of bidirectional communication between cortex and basal ganglia during movement in patients with Parkinson disease. J Neurosci 28:3008-3016.

Li CS, Huang C, Constable RT, Sinha R (2006) Imaging response inhibition in a stop-signal task: neural correlates independent of signal monitoring and post-response processing. J Neurosci 26:186-192.

Li CS, Yan P, Sinha R, Lee TW (2008) Subcortical processes of motor response inhibition during a stop signal task. Neuroimage 41:1352-1363.

Liegeois-Chauvel C, Musolino A, Chauvel P (1991) Localization of the primary auditory area in man. Brain 114 (Pt 1A):139-151.

Liotti M, Pliszka SR, Perez R, 3rd, Luus B, Glahn D, Semrud-Clikeman M (2007) Electrophysiological correlates of response inhibition in children and adolescents with ADHD: influence of gender, age, and previous treatment history. Psychophysiology 44:936-948.

Logan G (1994) On the ability to inhibit thought and action: A users' guide to the stop signal paradigm. In: Inhibitory processes in attention, memory and language. San Diego: Academic Press.

Logan GD, Cowan WB (1984) On the Ability to Inhibit Thought and Action: A Theory of an Act of Control. Psych Rev 91:295-327.

Logothetis NK, Pauls J, Augath M, Trinath T, Oeltermann A (2001) Neurophysiological investigation of the basis of the fMRI signal. Nature 412:150-157.

Mars RB, Coles MG, Hulstijn W, Toni I (2008) Delay-related cerebral activity and motor preparation. Cortex 44:507-520.

Mostofsky SH, Simmonds DJ (2008) Response inhibition and response selection: two sides of the same coin. J Cogn Neurosci 20:751-761.

Mukamel R, Gelbard H, Arieli A, Hasson U, Fried I, Malach R (2005) Coupling between neuronal firing, field potentials, and FMRI in human auditory cortex. Science 309:951-954.

Naito E, Matsumura M (1994) Movement-related potentials associated with motor inhibition as determined by use of a stop signal paradigm in humans. Brain Res Cogn Brain Res 2:139-146.

Pantev C, Makeig S, Hoke M, Galambos R, Hampson S, Gallen C (1991) Human auditory evoked gamma-band magnetic fields. Proc Natl Acad Sci U S A 88:8996-9000.

Pfurtscheller G, Stancak A, Jr., Neuper C (1996) Event-related synchronization (ERS) in the alpha band--an electrophysiological correlate of cortical idling: a review. Int J Psychophysiol 24:39-46.

Pfurtscheller G, Graimann B, Huggins JE, Levine SP, Schuh LA (2003) Spatiotemporal patterns of beta desynchronization and gamma synchronization in corticographic data during self-paced movement. Clin Neurophysiol 114:1226-1236.

Ray NJ, Jenkinson N, Brittain J, Holland P, Joint C, Nandi D, Bain GP, Yousif N, Green A, Stein JS, Aziz TZ (2009) The role of the subthalamic nucleus in response inhibition: Evidence from deep brain stimulation for Parkinson's disease. Neuropsychologia.

Ray S, Crone NE, Niebur E, Franaszczuk PJ, Hsiao SS (2008) Neural correlates of high-gamma oscillations (60-200 Hz) in macaque local field potentials and their potential implications in electrocorticography. J Neurosci 28:11526-11536.

Rubia K, Smith AB, Brammer MJ, Taylor E (2003) Right inferior prefrontal cortex mediates response inhibition while mesial prefrontal cortex is responsible for error detection. Neuroimage 20:351-358.

Schall JD, Stuphorn V, Brown JW (2002) Monitoring and control of action by the frontal lobes. Neuron 36:309-322.

Schmajuk M, Liotti M, Busse L, Woldorff MG (2006) Electrophysiological activity underlying inhibitory control processes in normal adults. Neuropsychologia 44:384-395.

Sohn YH, Wiltz K, Hallett M (2002) Effect of volitional inhibition on cortical inhibitory mechanisms. J Neurophysiol 88:333-338.

Stinear CM, Coxon JP, Byblow WD (2009) Primary motor cortex and movement prevention: where Stop meets Go. Neurosci Biobehav Rev 33:662-673.

Studholme C, Novotny E, Zubal IG, Duncan JS (2001) Estimating tissue deformation between functional images induced by intracranial electrode implantation using anatomical MRI. Neuroimage 13:561-576.

van den Wildenberg W, Burle B, Vidal F (2008) Mechanism and Dynamics of Cortical Motor Inhibition. Journal of Cognitive Neuroscience.

van den Wildenberg WP, van Boxtel GJ, van der Molen MW, Bosch DA, Speelman JD, Brunia CH (2006) Stimulation of the subthalamic region facilitates the selection and inhibition of motor responses in Parkinson's disease. J Cogn Neurosci 18:626-636.

Verbruggen F, Logan GD (2009) Models of response inhibition in the stop-signal and stop-change paradigms. Neurosci Biobehav Rev 33:647-661.

Xue G, Aron AR, Poldrack RA (2008) Common neural substrates for inhibition of spoken and manual responses. Cereb Cortex 18:1923-1932.

Zandbelt B, Van Buuren M, Gladwin TE, Hoogendam R, Kahn S, Vink M (2008) Brain regions involved in response inhibition are also activated during anticipation of inhibition. In: Society for Neuroscience. Washington DC.

CHAPTER 3:

Deep brain stimulation of the subthalamic nucleus alters the cortical profile of response inhibition in the beta frequency band: a scalp EEG study in Parkinson's disease

ABSTRACT

Stopping an initiated response could be implemented by a fronto-basal-ganglia circuit, including the right inferior frontal cortex (rIFC) and the subthalamic nucleus (STN). Intracranial recording studies in humans reveal an increase in beta-band power (~16-20 Hz) within the rIFC and STN when a response is stopped. This suggests that the beta-band could be important for communication in this network. If this is the case, then altering one region should affect the electrophysiological response at the other. We addressed this hypothesis by recording scalp EEG during a stop task while modulating STN activity with deep brain stimulation. We studied 15 human patients with Parkinson's Disease and 15 matched healthy control subjects. Behaviorally, patients OFF stimulation were slower than controls to stop their response. Moreover, stopping speed was improved for ON compared to OFF stimulation. For scalp EEG, there was greater beta power, around the time of stopping, for patients ON compared to OFF stimulation. This effect was stronger over the right compared to left frontal cortex, consistent with the putative right-lateralization of the stopping network. Thus, deep brain stimulation of the STN improved behavioral stopping performance and increased the beta-band response over the right frontal cortex. These results

complement other evidence for a structurally-connected, functional, circuit between right frontal cortex and the basal ganglia. The results also suggest that deep brain stimulation of the STN may improve task performance by increasing the fidelity of information transfer within a fronto-basal ganglia circuit.

INTRODUCTION

Imagine you are about to step into the street. Suddenly a car runs a light. Immediately, you stop your impending movement to avoid being struck. Experimentally, stopping action can be measured with tasks such as the stop signal and Go/NoGo. Converging evidence, from lesion, fMRI, and TMS studies, points to a specific brain system for stopping, including the right inferior frontal cortex (rIFC), the pre-supplementary motor area, and the subthalamic nucleus (STN) (reviewed by: Aron et al., 2007b; Chambers et al., 2009; Chikazoe, 2010) (and see recent studies by Isoda and Hikosaka, 2008; Neubert et al., 2010). Moreover, these regions are connected via white matter tracts (Inase et al., 1999; Johansen-Berg et al., 2004; Aron et al., 2007a; Ford et al., 2010; Forstmann et al.).

Recent evidence provides clues about the nature of neural communication within this network. One study recorded intracranial EEG from the rIFC during a stop signal task and found enhancement in the beta frequency band (~16hz) for successful vs. failed stop trials (Swann et al., 2009) (also see Marco-Pallares et al., 2008). Another study recorded local field potentials from the STN in patients and reported an enhancement in the beta band for NoGo compared to Go trials (Kühn et al., 2004).

These studies suggest that the putative structurally-connected, functional network for stopping could operate in the beta band. Here we tested this idea by recording scalp EEG while modulating STN activity using deep brain stimulation (DBS) in Parkinson's Disease (PD) patients.

Each patient performed a stop signal task, with STN stimulation either ON or OFF. Matched healthy controls were also studied. The stop signal task was used because of the aforementioned evidence relating it to a prefrontal-STN circuit and to the beta band, because it provides a sensitive and stable behavioral measure of stopping performance – the stop signal reaction time (SSRT) – and because the task has already been used in PD. Patients off medication have worse stopping performance (longer SSRT) than controls (Gauggel et al., 2004), while patients ON STN stimulation have faster SSRT than OFF (van den Wildenberg et al., 2006) (but see Ray et al., 2009). We thus predicted that SSRT would be longer for patients OFF STN stimulation than for healthy controls, and that SSRT would be improved with stimulation ON.

We performed time-frequency analyses of the EEG data. Based on prior intracranial and scalp EEG studies (Marco-Pallares et al., 2008; Swann et al., 2009), we predicted that stopping would be associated with an enhancement in the beta band for frontal electrodes, and we predicted, especially, that this beta enhancement would be different for ON versus OFF DBS. Thus, we aimed to show that STN stimulation modulates task-related beta band activity as measured at the scalp. Such a finding would provide evidence for the hypothesis that beta band information transfer

underlies the putative fronto-STN network for stopping. We also performed standard event-related potential analyses. We predicted differences in the N2/P3 complex for OFF vs. controls and for OFF vs. ON. This was based on prior studies with this task which have shown differences in these components for successful vs. failed stop trials (Pliszka et al., 2000; Kok et al., 2004; Ramautar et al., 2006; Schmajuk et al., 2006; Liotti et al., 2007) (reviewed by Folstein and Van Petten, 2008).

METHODS

Participants and Demographics

We studied 15 patients with Parkinson's disease (PD) who had bilaterally implanted stimulating electrodes in the STN, and 15 matched controls. Two patients were excluded from analysis because mean RT was too long (> 1 sec) and because of too-frequent omissions on go trials (one patient had only 57% correct go trials for a session and the other patient had only 45% correct go trials). One control subject was excluded due to excessive head movement artifacts in the EEG, which were uncorrectable in subsequent processing. Therefore, the data presented are from 13 patients and 14 controls.

The PD patients were clinically evaluated by a trained movement disorders specialist (MH) and were found to have moderate PD (stages II to III of the Hoehn and Yahr scale (Hoehn and Yahr, 1967)). All patients had clinically typical PD and were responsive to STN DBS in our study, see below (mean Unified Parkinson's Disease Rating Scale, UPDRS (Goetz et al., 1995), score of 36.8 for ON and 50.8 for OFF

stimulation ($t(12)=9.63$, $p<0.001$)). The patients and controls were well-matched on age, gender, and handedness, as well as on the Mini-Mental Status Exam (a screen for dementia) and the North American Reading Test (a test of IQ) (all p's>.05, see Table 3.1). Although the patients did score higher on the Beck Depression Inventory ($t(25) = 2.76$, $p=0.011$) compared to controls, the mean score of 8.9 in PD patients reflects a mild, non-clinically relevant, level of depression that is typical for PD status.

The patients took their anti-parkinsonian medication as normal (see Table 3.2 for medications and dosages, DBS stimulation settings, individual patient UPDRS scores, and other clinical details). However, doses of such medications were markedly reduced from the levels used prior to STN DBS surgery. All participants were free from significant upper limb or trunk arthritis or pain, and were without any significant neurological or psychiatric disease, except for Parkinson's disease in the PD patients.

The patients were recruited from the Scripps Clinic in La Jolla, California and the control participants were recruited from the local community. All participants provided written informed consent according to an Institutional Review Board Protocol of the University of California, San Diego.

Procedure

Each patient and control visited the laboratory once. The patients completed two EEG sessions – one ON their prescribed bilateral stimulation settings and one with the stimulator turned OFF bilaterally. The order of stimulation sessions was counterbalanced across patients. When patients were ON stimulation first the

procedure was as follows: informed consent was provided, followed by completion of rating scales (Mini-Mental Status Exam, North American Adult Reading test, Beck and handedness test), UPDRS #1, EEG setup and task explanation, EEG session #1, stimulator switched OFF, one hour break, EEG session #2, UPDRS #2, and stimulator returned to ON position. When patients were OFF stimulation first the procedure was: informed consent was provided, followed by completion of rating scales, UPDRS #1 [patients were in the ON state as usual], stimulator turned OFF, EEG setup and task explanation, UPDRS #2, EEG session #1, stimulator switched ON, one hour break, and EEG session #2. Regardless of which session was first, we ensured that at least an hour elapsed after the stimulator was turned OFF, prior to both the OFF UPDRS and OFF EEG session, to ensure that the majority of the stimulator effects had expired (Temperli et al., 2003).

For controls the visit involved consenting, rating scales, and one session of EEG.

The stop signal task

Stimuli were presented on a 22 inch monitor placed 25 inches from the participant. Two button boxes, one for each hand, were used for response collection. The button boxes were placed in a vertical position allowing a lateral movement of the index finger. This movement engages the first dorsal interosseus muscle, which is optimal for electromyography.

Each trial began with a white fixation cross centered on a black background. After 500 ms, a white square appeared, equiprobably to either the right or the left of the cross (Go Signal). Subjects responded accordingly using a button press with either their left or right hand within a limited hold time of 1.5 seconds. On a minority of trials (33%) the white square turned red (Stop Signal, SS) after a variable delay (Figure 3.1A). This stop signal delay (SSD) between the Go Signal and the Stop Signal was varied using a dynamic tracking (staircase) procedure. The delay was made smaller when the subject failed to stop, and longer with success (50 ms intervals) to achieve a 50% stopping rate and to keep the task challenging at all times. The SSD values were selected from 4 independently moving staircases (2 for each response direction) (for details see Aron and Poldrack, 2006). There were 5 blocks of 96 trials each. The patients performed two sessions (ON and OFF), and controls performed one session.

EEG recordings

EEG data were recorded using a 64+8 channel Biosemi ActiveTwo system (Biosemi Instrumentation, Amsterdam, The Netherlands) sampled at 512 Hz. Extra electrodes were placed on both mastoids, below and lateral to the right eye, and over the first dorsal interosseous muscles of each hand (one on belly and one on tendon) to record electromyography. For the analyses that follow, the button presses were sufficient and the electromyography is not further discussed.

Behavioral Analysis

The following measures were calculated: Go RT (average reaction time on correct go trials); failed stop RT (reaction time on stop trials where the participant failed to stop); percent go discrimination errors (percentage of go trials where participants responded with the wrong button box); percent go omission errors (%) (percentage of go trials where no response was made); probability of stopping overall (percentage of stop trials where stopping was successful); probability of stopping after convergence (probability of stopping after the SSD staircases had reached convergence, i.e. p(stop)~50%); overall SSD (average stop signal delay over all staircases for the whole experiment); convergence SSD (average stop signal delay over all staircases after the point where convergence was reached); and SSRT (stop signal reaction time).

SSRT was calculated using the convergence method (Logan et al., 1997; Verbruggen and Logan, 2009a). For each subject, SSRT is calculated as mean Go RT minus grand average SSD (Figure 3.1B). The grand average SSD is the average of SSD values in each of four staircases after convergence to a stopping rate of approximately 50%. SSRT was also computed using the integration method (Verbruggen and Logan, 2009b). However, results did not differ between these two methods, so only the convergence results are reported. Paired t-tests were used to compare ON vs. OFF stimulation. Unpaired t-tests were used to compare controls vs. ON and controls vs. OFF.

EEG preprocessing

The data were preprocessed using a combination of EEGlab (Delorme and Makeig, 2004) (http://www.sccn.ucsd.edu/eeglab) and custom Matlab scripts. The data were first re-referenced to the mastoids (right and left). Next, the mean of each channel (over the whole data set) was removed and an additional 0.05 Hz high pass filter was applied to reduce low frequency drift. The DBS artifact was very high frequency (usually 130-180 Hz) so most of the artifact could be removed using low pass filtering. Accordingly, a 50 Hz low pass filter was applied to all data (ON stimulation, OFF stimulation, and controls). The filtering steps in both cases used the EEGlab 'eegfilt' function, a two-way FIR filter. Eye movement and blink artifacts were removed using independent component analysis (Jung et al., 2000). Components that corresponded to eye blinks/movements were identified using a published technique that compares favorably with other artifact rejection techniques, even for patient populations (Jung et al., 2000). For each subject/session we identified at least one component that corresponded to ocular artifacts. Visual inspection confirmed both that the correct component was selected for each individual and that no detected residual blinks remained in the data.

EEG analysis

ERP and time-frequency analysis were performed with custom Matlab scripts. For each of these methods we focused on data from a right frontal 'region of interest'. This was defined as a group of three right frontal electrodes (F6, F8, FC6) based on a

previous scalp EEG study which showed right-lateralized stopping-related responses with the same task (Schmajuk et al., 2006). Here we analyzed all stop trials together, i.e. including both successful and failed stop trials. Our rationale was to increase statistical power. Note that the prerogative to test patients on the same day in two EEG sessions (ON vs. OFF stimulation) meant that the length of each session had to be restricted (5 blocks of 96 trials, with 33% of these being stop trials). This is the lower bound of trial numbers needed for EEG analysis (Luck, 2005). Hence, averaging over both successful and failed stop trials was important.

ERP analysis involved the following steps: further low pass filtering at 30 Hz; averaging across trials; aligning stop trials to the onset of the stop signal; subtraction, from the stop trials, of an average prestimulus baseline (-200 to 0 ms relative to the stop signal); averaging of the resulting ERP across the three channels in the right frontal electrode cluster (F6, F8, FC6); and comparison of the ERPs for the three different conditions (ON, OFF, and controls).

Time frequency analysis involved the following steps: raw data were filtered into individual frequencies using a wavelet method; data were epoched and averaged relative to the stop signal; an inter-trial interval baseline was removed; an optional z-scoring procedure was performed (see below); data were averaged across three channels in the right frontal electrode cluster; averages were taken across subjects; and finally t-tests were performed to compare conditions. These steps are now discussed in more detail.

First, a previously published method was used to filter each subject's raw EEG signal into 32 separate frequencies between 2 and 32 Hz (Canolty et al., 2007; Swann et al., 2009) In brief, first a Fast Fourier Transform was performed on the whole data set. This output was then multiplied by 32 Gaussians centered at the selected frequencies. The standard deviation of each Gaussian varied depending on the selected center frequency (to allow for higher temporal resolution in the higher frequencies). An inverse Fourier transform was then applied to the filtered data to produce analytic signal values. This technique is analogous to a Gabor wavelet transform performed in the frequency domain for computational efficacy, and yields an analytic amplitude signal for each of the 32 specified frequencies (Canolty et al., 2007). The absolute value of this number represents the amplitude of the signal, or 'power'. Second, data were extracted for stop trials, aligned so that time zero was the stop signal, and averaged across trials for each frequency individually. Third, an average baseline for each frequency (corresponding to -1500 to -1000 ms relative to the stop signal, falling in the inter-trial interval) was subtracted from the trial data. Fourth, data were averaged across the three channels in the right frontal electrode cluster. Fifth, data were averaged across subjects separately for the three conditions: ON stimulation, OFF stimulation, and controls. Finally, a point-by-point paired t-test was performed across subjects to test the idea that beta power around the time of stopping might differ for ON compared to OFF stimulation. An unpaired t-test was performed for both ON and OFF compared to controls. One sample t-tests compared to zero were used to examine stop trials compared to baseline for each group separately.

An auxiliary analysis was also performed to see if the results differed if the data were normalized prior to averaging across subjects. For this step, done after baseline correction, but before averaging across channels (between steps three and four), z-scores were derived from the averaged epoched data, using a permutation method (Canolty et al., 2007; Swann et al., 2009). These z-scored values were then used for the remainder of the calculations. This method did not produce substantially different results, so only the non-z-scored results are reported.

RESULTS

Behavioral Results

SSRT was significantly longer for PD OFF stimulation compared to healthy controls ($t(25) = 2.8$, $p<0.01$) (Figure 3.2A), consistent with an earlier study (Gauggel et al., 2004). SSRT was significantly speeded when patients were ON compared to OFF stimulation ($t(12) = 2.4$, $p<0.05$), similar to previous results (van den Wildenberg et al., 2006). SSRT was longer for ON vs. controls, but this was not a significant difference ($t(25)=1.6$, $p=0.12$) (see Figure 3.2A). Similar results obtained even for non-parametric, Wilcoxon, tests.

A scatter plot of SSRT for ON versus OFF stimulation showed two interesting features (Figure 3.2B). First, there was a significant correlation across subjects (Pearson's $r = 0.74$, $p<0.01$). This illustrates that SSRT estimation was highly reliable. Second, it was apparent that every patient, except one, showed an improvement of SSRT with stimulation. Thus the ON vs. OFF effect was highly robust.

Strikingly, these between-group SSRT differences were evident even while Go RT was not different ($t(12)=0.93$, $p = 0.37$) (Figures 3.2C,D) and nor was any other measure (all p's >0.05) (Table 3.3). Thus, the effect of stimulation was specific to the stopping process.

We performed several auxiliary analyses. SSRT did not differ depending on which hand was stopped ($p>0.1$ for all left vs. right hand comparisons for each of ON stimulation, OFF stimulation and control groups). Moreover, the slower SSRT for ON vs. OFF was unlikely due to fatigue: in an ANOVA with the factors of session order (i.e. ON then OFF vs. OFF then ON) and STN DBS status (i.e. ON vs. OFF) there was no interaction ($F(1,11) = 2.3$, $p = 0.16$).

EEG – Time Frequency Results

ON vs OFF stimulation was compared to examine the predicted stopping-related beta difference (Marco-Pallares et al., 2008; Swann et al., 2009). Importantly, there was significantly greater beta power around the time of stopping for ON compared to OFF ($t(12)> 3.05$, $p<0.01$)(Figure 3.3A) [A similar result was obtained with a Wilcoxon test]. Because it is possible that this result relates to the use of different baselines for ON vs. OFF, we also performed the analysis on data that did not have the baseline removed. A similar beta power difference (in the same direction) was found – therefore baseline differences did not drive this key effect (Figure 3.3B). Differences between controls and patients were examined, but were not significant,

probably because of reduced power for the between-group as opposed to within-group comparison.

To examine the spatial specificity of the ON vs. OFF difference, we performed the same analysis for a left frontal electrode cluster (F5, F7, FC7). There was no significant difference for ON vs. OFF for beta power ($p>0.05$) (Figure 3.4A-C). However, other differences seen in the right frontal analysis (e.g. an early theta effect) were still apparent. This suggests that it is specifically the beta effect that was right lateralized. A paired t-test showed that the right hemisphere electrode cluster had significantly greater beta power for the ON vs OFF comparison around the time of stopping compared to the left hemisphere ($t(12)>2.18$, $p<0.05$, See Figure 3.4D).

To further examine the specificity of this effect to the right frontal cortex, we also examined a frontal midline electrode cluster (Fz, F1, F2), and two parietal clusters, in the left and right hemispheres (P5, P7, CP5 and P6, P8, CP6 respectively). In these three clusters there was also a beta difference between ON and OFF (potentially due to volume conduction), but for each cluster the beta effect was smaller than for the right frontal cluster, and this was a significant difference when comparing right frontal and left parietal clusters ($t(12)>2.18$, $p<0.05$). Overall, while we are mindful that strong conclusions about cortical sources cannot be made from scalp recordings, our results suggest the beta effect is largest over the right hemisphere and perhaps especially over the right frontal region (c.f. Swann et al., 2009). Note that while it was specifically beta changes that were observed for stopping when comparing ON vs OFF, the ON vs. OFF comparison for go trials did not show such a

specific effect. Instead there were general power differences across many frequencies (See Supplementary Figure 3.1).

Each condition (ON stimulation, OFF stimulation, and controls) was separately examined relative to baseline to see what drove the observed difference between ON and OFF, and to address the prediction of increased beta power soon after the stop signal (Marco-Pallares et al., 2008; Swann et al., 2009). For controls, there was a beta increase above baseline starting around 200 ms after the stop signal, a time consistent with this group's SSRT (Figure 3.5C). This effect was small, not quite reaching significance with the point-by-point test. A similar pattern was observed for patients ON stimulation (at a slightly longer latency, perhaps reflecting prolonged SSRT) (see Figure 3.5A). However no such pattern was observed for patients OFF stimulation (see Figure 3.5B).

In order to visualize how the beta increase might be related to SSRT, beta power was averaged over 15-17 Hz (Swann et al., 2009), and plotted over time, with a prestimulus baseline of -500 to 0 relative to the stop signal (Figure 3.5D). Notably, the beta power increase began before SSRT. Moreover, the controls had the earliest beta peak and the shortest SSRT, whereas both were delayed for patients ON stimulation. OFF stimulation patients exhibited disorganized beta activity with no clear peak.

EEG – Event Related Potentials

ERPs were calculated for each group (patients ON stimulation, OFF stimulation and controls) to examine changes in the N2/P3 complex associated with

response inhibition (Ramautar et al., 2006; Schmajuk et al., 2006; Liotti et al., 2007; Folstein and Van Petten, 2008). While ERPs for these components were present, the comparison between conditions was not easily made because the patients had overall reduced amplitude of all ERPs compared to controls (i.e. for all components, not merely stopping-related ones). Comparisons of ON to OFF stimulation did not reveal significant differences for the N2/P3 complex. This probably relates to the low trial numbers. Consequently, we do not further discuss ERPs and instead focus on the time-frequency results. Note that it is not unusual to have different findings for ERP compared to time-frequency analysis since ERPs reflect only phase-locked activity and primarily the very low frequencies, while time-frequency analyses capture non-phase locked activity as well as higher frequencies (such as beta).

DISCUSSION

Consistent with prior reports, we show that PD patients OFF stimulation were worse at stopping motor responses than healthy controls and that this deficit was ameliorated by STN DBS. The EEG showed an increase in beta-band power for ON vs. OFF stimulation, which was greater over the right frontal region than the left. These results support the hypothesis that stopping a motor response involves communication within a fronto-basal-ganglia circuit in the beta frequency band.

Our behavioral finding that SSRT is affected by STN DBS supports imaging studies in humans (Aron and Poldrack, 2006; Aron et al., 2007b; Li et al., 2008), lesion studies in rodents (Eagle et al., 2007) and neurophysiological recordings in

primates (Isoda and Hikosaka, 2008) all pointing to STN as a key node for stopping. The improvement in stopping for ON vs. OFF STN DBS agrees with one prior STN DBS study (van den Wildenberg et al., 2006), but not with another (Ray et al., 2009). (However, the latter study employed all unilaterally implanted patients – which may account for the difference). Thus, our findings affirm that bilateral STN stimulation, at treatment-prescribed settings, shortens SSRT to levels near healthy age-matched controls. These behavioral findings set the stage for a comparison of EEG beta power.

Critically, we observed a greater beta response for stop trials for ON vs. OFF stimulation over the right frontal electrode cluster but not over the left frontal cluster. Moreover, the right frontal effect was significantly greater than the left frontal one, consistent with a putative right-lateralized network for inhibitory control (Garavan et al., 1999; Konishi et al., 1999; Aron et al., 2003; Rieger et al., 2003; Rubia et al., 2003; Garavan et al., 2006; Chikazoe, 2010). These results support our hypothesis of a structurally-connected functional network between frontal cortex and STN, that operates in the beta-band (Kühn et al., 2004; Swann et al., 2009). The results also speak to the therapeutic mechanism by which STN DBS may restore behavioral control. We speculate that STN DBS reduces the pathologically high beta synchrony between the basal ganglia and cortex so that task-related communication is facilitated. The reasoning is as follows. In untreated PD, there is pathologically high resting beta activity (reviewed by Brown and Williams, 2005; Brown, 2007; Hammond et al., 2007; Garcia-Munoz et al., 2010). This activity is associated with bradykinesia and rigidity (Kühn et al., 2006; Kühn et al., 2009), and is reduced by dopamine

replacement therapy and STN DBS (Kühn et al., 2006; Wingeier et al., 2006; Kühn et al., 2008). Thus, STN DBS may improve symptoms by reducing the basal ganglia's pathologically high resting beta synchrony (Kühn et al., 2008; Garcia-Munoz et al., 2010). By contrast, we show that ON vs. OFF STN DBS leads to *increased* cortical beta activity during task performance. Thus, the distinction between resting activity and task activity is key. If STN DBS leads to normal levels of background or resting beta oscillatory activity then this could 'free up' neurons to allow a resumption of task-related beta coupling, as may be needed for stopping (Garcia-Munoz et al., 2010). Thus STN DBS may have its behavioral benefit by improving the fidelity of information transfer in cortico-basal-ganglia circuits (Brown, 2007).

Our hypothesis was that the beta increase relates to implementation of the stopping process via cortical-STN communication. If so, the beta increase should occur before the end of the stopping process, i.e. before SSRT. Although the beta increase clearly began before SSRT had elapsed (Figure 3.5D), the peak beta difference tended to fall after the average SSRT, later than expected. Several considerations bear on this. First, assuming the beta increase reflects cortical-STN communication via long-distance coupling, then it is not clear that this communication should abruptly terminate after stopping is implemented. Indeed, an intracranial EEG study showed a beta increase soon after the stop signal, which was maintained for a few hundred milliseconds, such that it peaked shortly after SSRT (Swann et al., 2009). If this sustained pattern occurred in the current study, then one would expect the observed pattern of an initial increase in beta after the stop signal with the peak

occurring after SSRT (See Figure 3.5A). Second, SSRT is a single estimate that is derived for each individual, yet, on a trial-by-trial basis, the speed of stopping doubtless varies. Thus variability in the time at which stopping happens for an individual subject could produce some 'spread' in the beta response. Third, there is variability in SSRT between individuals, further increasing spread of the beta response. Fourth, time-frequency analysis introduces some temporal imprecision (the standard deviation for 16 Hz is 67 ms). Notwithstanding these considerations it is clearly the case that the increase begins before SSRT elapses.

A paradoxical aspect of the current findings is that STN DBS improves stopping (and see van den Wildenberg et al., 2006) while, in rare cases, STN DBS leads to the opposite of good stopping, i.e. impulsive behavior such as hypomania and hypersexuality (Kulisevsky et al., 2002; Appleby et al., 2007). However, these rare cases may result from inadvertent stimulation of the ventral (limbic) territory of the STN (Mallet et al., 2007), or of adjacent structures or fibers of passage. If this is the case, it explains why such symptoms are rare and why they were not observed in our patients, since typical therapeutic stimulation sites are in the dorsal (sensorimotor) territory of the STN (reviewed by Kuncel and Grill, 2004).

There were several limitations to this study. First, some effects (e.g. ERPs and within-condition comparisons of stop versus baseline) were weak. This likely relates to the small trial number. EEG studies normally involve several hundred trials for averaging. Yet we needed to keep the trial number relatively low in order to keep the length short enough for PD patients to perform both ON and OFF sessions on the

same day without fatigue. (The same-day sessions were important to reduce variability.) Notwithstanding the low trial number, there were clear-cut behavioral differences and EEG differences for ON vs. OFF. A second limitation that flows from the first is that we could not compare successful and failed stop trials as prior studies have done (Ramautar et al., 2006; Schmajuk et al., 2006; Marco-Pallares et al., 2008). Instead, because of low trial number we grouped together all stop trials. Although comparisons of successful and failed stopping would be interesting, the fact that we analyzed all stop trials together does not impugn our finding that beta-band activity was greater for ON vs. OFF stimulation. Third, we did not include an OFF medication condition – instead the patients were tested on their normal medications. Since PD medications have been shown to alter beta activity in the STN (Kühn et al., 2006), it would also be interesting to examine beta activity during stopping in patients who are OFF medication. Fourth, because we recorded scalp EEG, we cannot make specific claims about which cortical area(s) underlie the beta increase, except to say they are evidently stronger in the right hemisphere than the left. Fifth, our study falls short of tightly linking the beta power increase to SSRT or the success/failure of stopping. However, other studies *have* demonstrated this relationship. Greater beta power for successful compared to failed stopping has been reported for scalp EEG (Marco-Pallares et al., 2008) and for intracranial EEG from the rIFC specifically (Swann et al. 2009). We note that, even considering these studies, it is unclear which precise cognitive function relates to the beta increase. It is likely that rIFC is important for both attentional detection (Hampshire et al., 2010; Sharp et al., 2010) and

implementing inhibitory control (Aron et al., 2004; Neubert et al., 2010), and these functions may be dissociable to different IFC subregions (Chikazoe, 2010; Verbruggen et al., 2010). While it is possible that attentional detection could involve coupling with the basal ganglia in the beta-band, the evidence is stronger that the beta-band is important for motor function, such as inhibitory control. For example, entraining beta synchronizations in motor cortex leads to slowed movement (Pogosyan et al., 2009), and performing NoGo trials leads to increased beta activity in the STN (Kühn et al., 2004). Future work is required to investigate whether the increase in cortical beta relates to attentional detection, inhibitory control or both. However, our contribution here is to show that behavioral stopping has its counterpart in an increase in beta-band amplitude from right frontal electrodes, and that this is modulated by STN DBS.

In summary, we have shown that STN stimulation improves stopping behaviorally and modulates scalp recorded beta activity at a time consistent with the stopping process. Taken together with earlier results (Marco-Pallares et al., 2008; Swann et al., 2009), these findings support the hypothesis that there is a structurally-connected functional network between the cortex and STN that operates in the beta-band. In addition these results provide insight into the mechanism by which STN stimulation improves action control. Specifically, they suggest that the therapy works by increasing the fidelity of information transfer in cortico-basal ganglia networks during task performance.

ACKNOWLEDGEMENTS

Chapter 3, in full, is a reprint of material as it appears in The Journal of Neuroscience, 2011: Swann NC, Poizner H, Houser M, Gould S, Greenhouse I, Cai W, Strunk J, George J, Aron AR. (2011) Deep brain stimulation of the subthalamic nucleus alters the cortical profile of response inhibition in the beta frequency band: a scalp EEG study in Parkinson's disease. The dissertation author was the primary investigator and author of this paper.

Thanks to David Petersen for discussion and help with artifact rejection. We gratefully acknowledge funding from the Alfred P. Sloan Foundation, National Institutes of Health (NIH) Grant R01-DA026452-01A1, and NARSAD to A.R.A. (PI), NSF Graduate Student Research Fellowship, and NIH (UCSD Institute of Neural Computation training grant) to N.S, and NIH grant #2 R01 NS036449 and ONR MURI Award No.: N00014-10-1-0072 to H.P.

Table 3.1: Demographic and Rating Scale Measures. UPDRS = The Unified Parkinson's Disease Rating Scale; MMSE = Mini-Mental Status Exam; NAART = North American Adult Reading Test; Beck = Beck Depression Inventory.

	PD Patients - Mean(SD)	Controls - Mean(SD)
Age(years)	64.4(6.8)	66.4(8.0)
Sex	12 males/1 female	11 males/3 females
Handedness	13 right/0 left/0 ambidex.	12 right/1 left/1 ambidex.
MMSE	29.2(.6)	29.6(.6)
NAART	41.1(10.3)	46.4(7.1)
Beck*	8.9(6.9)	3.4(2.7)
UPDRS**	50.8(7.5)-OFF Stim. 36.8(6.9)-ON Stim.	N/A

*$t(25) = 2.76$, $p=.011$

**$t(12) = 9.63$, $p<<.0001$ for ON stimulation vs OFF stimulation; higher values reflect more impaired performance. Maximum score is 108.

Table 3.2: Patient Clinical Characteristics. UPDRS = Unified Parkinson's Disease Rating Scale; qd = once a day; bid = twice a day; tid = three times a day; qid = four times a day; hs = at bedtime.

Patient ID	Age/ Gender /Hand-edness	Disease Duration (years)	Years since surgery	Medications	Left treatment setting (contact #, voltage, pulse width/Hz)	Right treatment setting (contact #, voltage, pulse width/Hz)	UPDRS (OFF /ON)
ST01	60/M/ R	15	4	1) Comtan 200 mg bid 2) Sinemet 25/100 half 5x/day 3) Requip 2 mg 5x/day 4) Azilect 1 mg 5) Clonazepam .5 mg	Case+1-, 2.4, 60/185	Case+5-, 3.3, 60/185	63/44
ST02	68/M/ R	14	2	1) Sinemet 25/100, ½ qid 2) Stalevo 150 mg, ½ qid 3) Requip XL 8 mg 1.5 tabs 4) Azilect 1mg	Case+1-, 3.1, 60/185	Case+5-, 2.9, 60/185	42/31
ST03	58/F/R	8	0.33	1) Sinemet CR 25/100 tid 2) Xanax 0.5 mg up to tid 3) Artane 1mg bid	Case+1-, 0.6, 60/130	Case+5-, 3.0, 150/130	54/33
ST04	73/M/ R	6	0.6	1) Sinemet 25/100 bid	Case+2-, 2.5, 90/160	Case+5-, 1.7, 90/160	57/42
ST05	61/M/ R	11	0.67	1) Stalevo 100mg bid 2) Mirapex 1mg qd	Case+1-, 0.8, 90/130	Case+4-, 2.1, 90/130	42/30
ST06	53/M/ R	15	2	1) Sinemet 50mg tid	Case+1-, 2.5, 60/185	Case+5-, 2.4, 60/185	47/35
ST07	72/M/ R	4	0.6	1) Azilect 1mg 2) Parcopa 100mg tid	Case+0-, 1.0,60/180	Case+(5,4)-, 2.1, 90/180	56/34

Table 3.2: Patient Clinical Characteristics, continued.

Patient ID	Age/ Gender /Hand-edness	Disease Duration (years)	Years since surgery	Medications	Left treatment setting (contact #, voltage, pulse width/Hz)	Right treatment setting (contact #, voltage, pulse width/Hz)	UPDRS (OFF /ON)
ST08	73/M/ R	12	3	1) Sinemet 100mg tid 2) Sinemet 100mg hs 3) Amantadine 100mg bid 4) Requip 4mg tid 5) Clonazepam 1mg	Case+1-, 2.6, 60/160	Case+5-, 2.6, 60/160	49/45
ST09	69/M/ R	11	1	1) Stalevo 100mg qid 2) Eldepryl 5mg bid 3) Requip XL8 bid 4) Requip 1mg	3+1-, 2.9, 60/80	7+(5,6)-, 2.5, 60/80	58/40
ST10	66/M/ R	5	0.75	1) Stalevo 100mg tid 2) Requip XL 8mg 3) Azilect 0.5 mg	Case+1-, 2.6, 60/130	Case+4-, 1.5, 60/130	37/21
ST11	60/M/ R	10	0.75	1) Sinemet 25/100 bid 2) Mirapex 0.5mg bid 3) Azilect 1mg	Case+1-, 3.3, 90/160	7+5-, 3.5, 90/160	53/40
ST12	68/M/ R	18	2	1) Namenda 10mg bid 2) Sinemet 25/100 tid 3) Mirapex 1.5mg tid 4) Comtan 200mg tid 5) Exelon 9.5mg	Case+1-, 2.5, 60/185	Case+5-, 2.5, 60/185	48/41
ST13	56/M/ R	10	0.28	1) Requip 8mg qd 2) Azilect 1mg 3) Stalevo 50mg tid	3+2-, 2.4, 60/160	7+5-, 2.2, 60/160	55/43

Table 3.3: Stop signal task behavioral performance. Go RT = mean correct go reaction time; Failed stop RT = mean reaction time on failed stop trials; Go Discrimination error = percent discrimination errors on go trials; Go omission error = percent omission errors on go trials; Prob. Stop overall = probability of stopping on stop trials overall; Prob. Stop after convergence = probability of stopping on stop trials after convergence; Overall SSD = mean stop signal delay overall; Convergence SSD = stop signal delay after convergence; SSRT = stop signal reaction time.

	Controls	Patients – ON Stim.	Patients – OFF Stim.
Go RT (ms)	606(143)	624(144)	650(166)
Failed Stop RT (ms)	522(127)	550(127)	554(137)
Go Discrimination error (%)	0.3(0.5)	2.5(4.1)	1.9(2.9)
Go Omission error (%)	0.6(1.1)	3.4(7.3)	2.8(5.6)
Prob. Stop overall (%)	54.5(4.8)	53.8(3.9)	54.2(6.1)
Prob. Stop after converge (%)	51.2(6.4)	50.5(2.6)	51.1(3.7)
Overall SSD (ms)	330(127)	322(135)	313(137)
Convergence SSD	350(145)	341(155)	338(180)
SSRT*	256(39)	283(51)	311(62)

*ON vs OFF: $t(12)= 2.4$, $p =0.033$, controls vs ON: $t(25) = 1.6$, $p=0.12$, controls vs OFF: $t(25)=2.8$, $p=0.009$

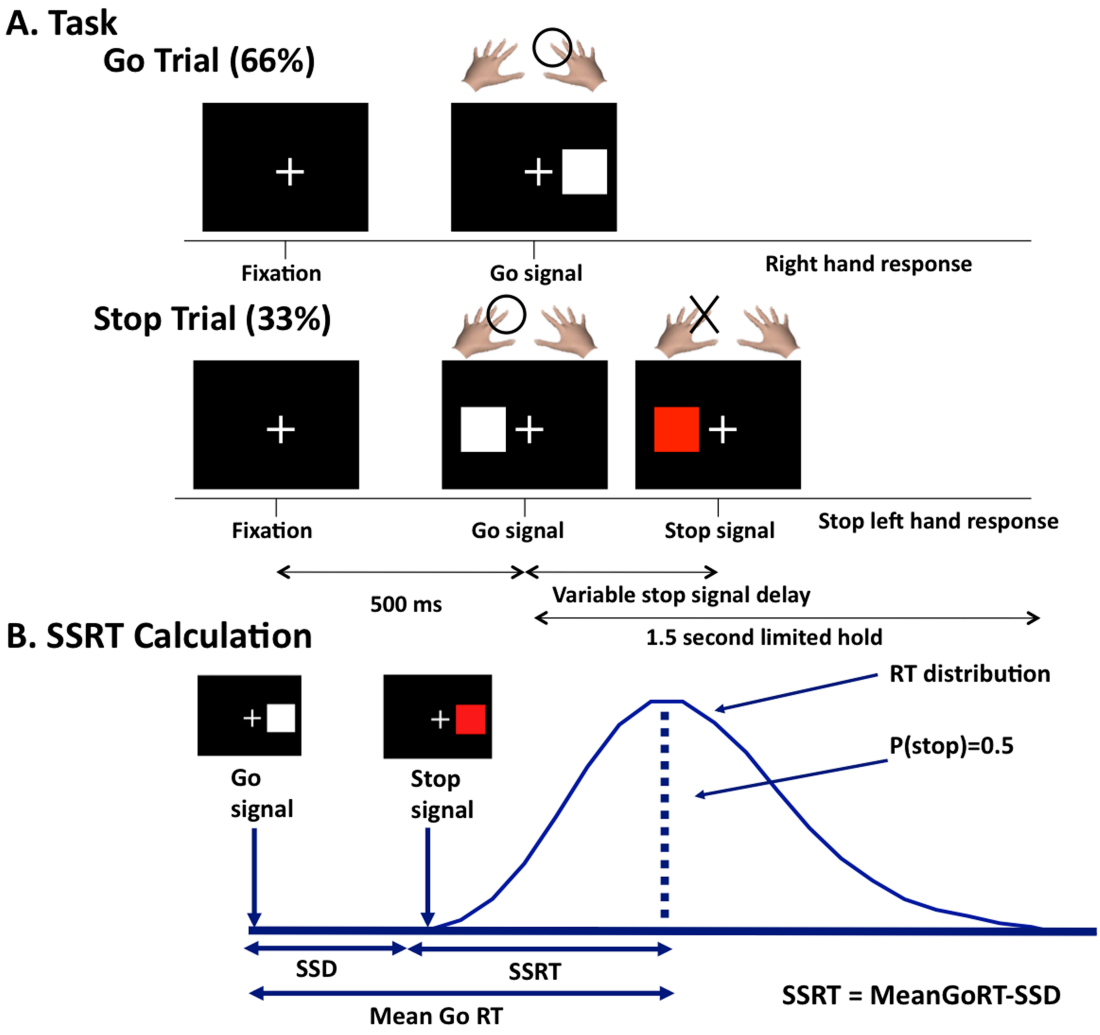


Figure 3.1: Stop Signal Task. A. Each trial began with a fixation cross, followed 500 ms later by the appearance of a white square (Go signal). The square appeared to either the left or the right of the fixation cross requiring a response from the corresponding hand. Stop trials were identical to go trials, except they were less likely (33% of trials) and the white square turned red after a variable delay (stop signal delay). B. Schematic illustrating the way in which SSRT is calculated. The Stop Signal Delay (SSD) is varied dynamically to yield a probability of stopping, p(stop) of ~0.5. Assuming the Go and Stop processes race each other independently, this 50% point will correspond to the mean of the Go distribution. SSRT can then be calculated as MeanGoRT-SSD.

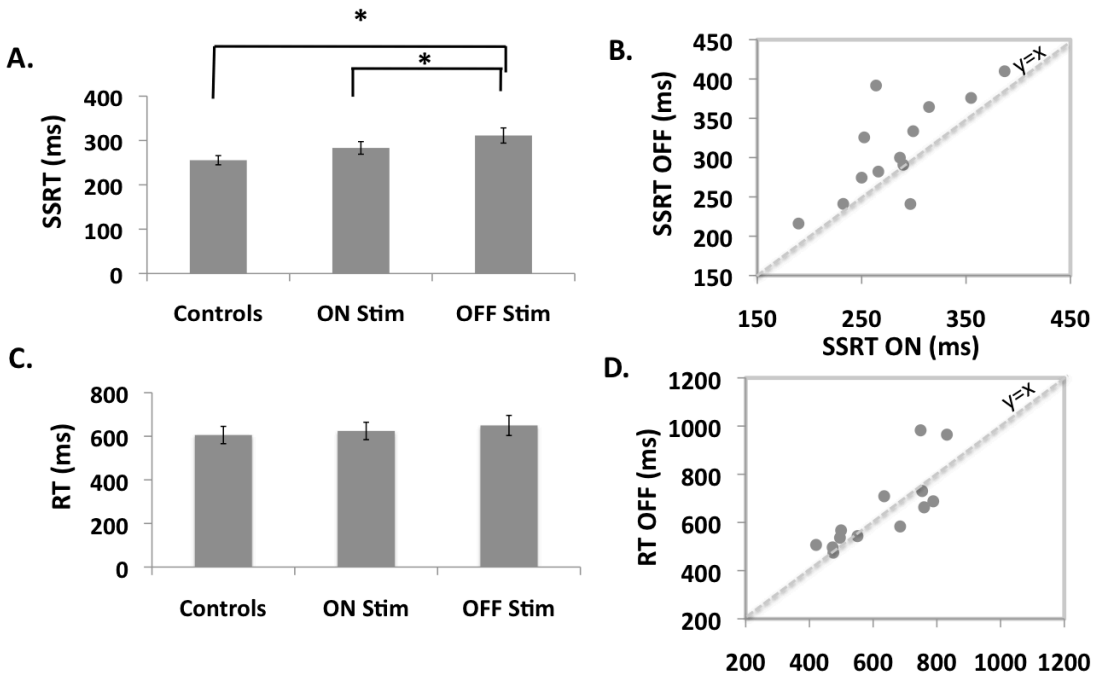


Figure 3.2: Behavioral Results. A. Stop Signal Reaction Times (SSRTs) was significantly longer for patients OFF stimulation compared to ON stimulation and for patients OFF stimulation compared to controls (both $p<0.05$). B. SSRTs for individual patients. SSRT estimation was reliable since there was a strong correlation ($r = 0.74$, $p<0.01$). The speeding of SSRT for ON versus OFF stimulation was also robust since every patient bar one improves. C. Go RT was not different. D. Go RT for individual patients. There was a strong correlation between ON and OFF ($r = .81$, $p<0.01$), however STN DBS did not affect Go RT consistently.

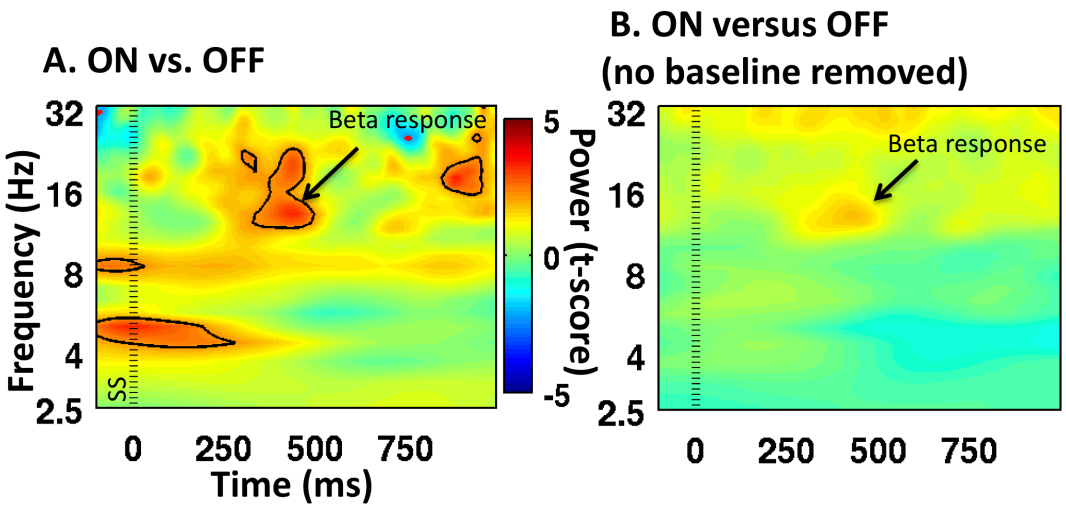


Figure 3.3: Time-frequency plots for stop trials for ON vs. OFF stimulation. A. Significantly greater beta power (~16 Hz) for patients ON compared to OFF stimulation. Both conditions are first normalized to their own baselines prior to subtraction. B. The effect in panel A is still visible even when the comparison is made between ON vs. OFF without first applying a baseline correction. Power is expressed with color as a t-score. Zero ms was the time of the stop signal (SS, indicated with the standard dotted line). Power changes that are significant at $p<0.05$ are encircled with either a black line (for ON > OFF) or a red line (for OFF > ON).

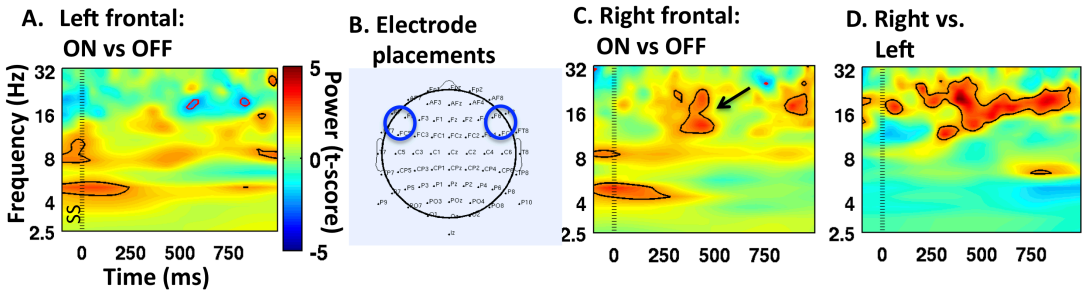


Figure 3.4: The beta increase of ON vs. OFF is stronger over the right hemisphere than the left. A. Time-frequency plot of stop trials ON vs. OFF for a left frontal ROI. The beta difference around the time of SSRT is not significant. B. Left and right frontal ROIs. The left electrode cluster includes F5,F7,FC5 and the right one includes F6, F8, FC6. C. The plot is the same comparison as Figure 3.4A, but with data from a right frontal ROI. Note the significant beta difference around the time of stopping. Power is expressed in color as a t-score. Zero ms was the time of the stop signal (SS, indicated with the standard dotted line). Power changes significant at $p<0.05$ are encircled with either a black line (for ON > OFF) or a red line (for OFF > ON.) Note that this figure is identical to Figure 3.3A. D. Time frequency plot comparing the ON vs. OFF stimulation effects for stop trials in the right frontal ROI vs the left frontal ROI. Power differences are expressed in color as a t-score. Power differences significant at $p<0.05$ are encircled in black (for right > left) or red (left > right). The beta power around the time of stopping is significantly greater in the right frontal ROI.

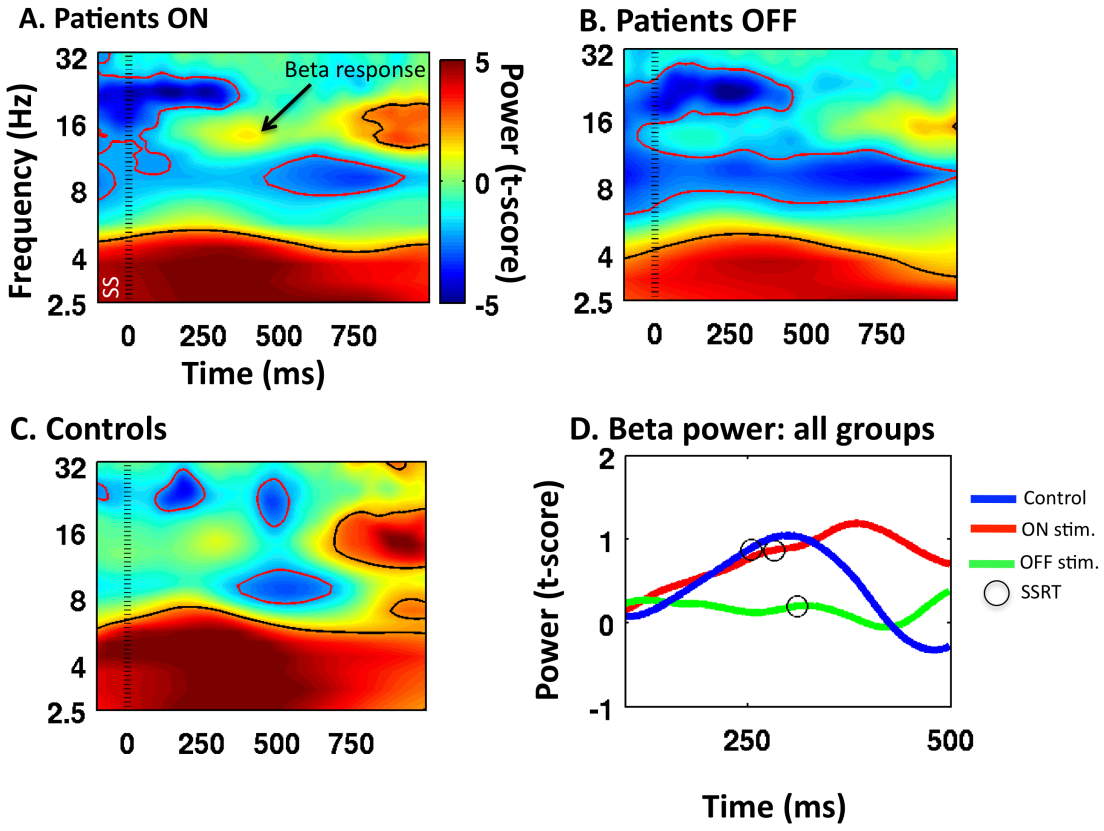


Figure 3.5: Time-frequency plots for stop trials. Power expressed with color as a t-score is plotted for patients ON stimulation (A), OFF stimulation (B), and controls (C). Note the predicted response in the beta band for controls and patients ON stimulation. Zero ms was the time of the stop signal (SS, indicated with the standard dotted line). Power changes that are significant at $p<0.05$ are encircled with either a black line (for increases above baseline) or a red line (for decreases below baseline). D. Average beta power from 15-17 Hz using a prestimulus baseline (-500 to 0). For controls there is an increase in beta power before SSRT elapses. Patients ON stimulation show a slightly later increase consistent with a longer SSRT. There is no discernable beta increase for patients OFF stimulation

REFERENCES

Aron AR, Poldrack RA (2006) Cortical and subcortical contributions to Stop signal response inhibition: role of the subthalamic nucleus. J Neurosci 26:2424-2433.

Aron AR, Robbins TW, Poldrack RA (2004) Inhibition and the right inferior frontal cortex. Trends Cogn Sci 8:170-177.

Aron AR, Fletcher PC, Bullmore ET, Sahakian BJ, Robbins TW (2003) Stop-signal inhibition disrupted by damage to right inferior frontal gyrus in humans. Nat Neurosci 6:115-116.

Aron AR, Behrens TE, Smith S, Frank MJ, Poldrack RA (2007a) Triangulating a cognitive control network using diffusion-weighted magnetic resonance imaging (MRI) and functional MRI. J Neurosci 27:3743-3752.

Aron AR, Durston S, Eagle DM, Logan GD, Stinear CM, Stuphorn V (2007b) Converging evidence for a fronto-basal-ganglia network for inhibitory control of action and cognition. J Neurosci 27:11860-11864.

Brown P (2007) Abnormal oscillatory synchronisation in the motor system leads to impaired movement. Curr Opin Neurobiol 17:656-664.

Canolty RT, Soltani M, Dalal SS, Edwards E, Dronkers NF, Nagarajan SS, Kirsch HE, Barbaro NM, Knight RT (2007) Spatiotemporal dynamics of word processing in the human brain. Front Neurosci 1:185-196.

Chambers CD, Garavan H, Bellgrove MA (2009) Insights into the neural basis of response inhibition from cognitive and clinical neuroscience. Neurosci Biobehav Rev.

Chikazoe J (2010) Localizing performance of go/no-go tasks to prefrontal cortical subregions. Curr Opin Psychiatry.

Delorme A, Makeig S (2004) EEGLAB: an open source toolbox for analysis of single-trial EEG dynamics including independent component analysis. J Neurosci Methods 134:9-21.

Eagle DM, Baunez C, Hutcheson DM, Lehmann O, Shah AP, Robbins TW (2007) Stop-Signal Reaction-Time Task Performance: Role of Prefrontal Cortex and Subthalamic Nucleus. Cereb Cortex.

Folstein JR, Van Petten C (2008) Influence of cognitive control and mismatch on the N2 component of the ERP: a review. Psychophysiology 45:152-170.

Ford A, McGregor KM, Case K, Crosson B, White KD (2010) Structural connectivity of Broca's area and medial frontal cortex. Neuroimage 52:1230-1237.

Forstmann BU, Anwander A, Schafer A, Neumann J, Brown S, Wagenmakers EJ, Bogacz R, Turner R (2010) Cortico-striatal connections predict control over speed and accuracy in perceptual decision making. Proc Natl Acad Sci U S A 107:15916-15920.

Garavan H, Ross TJ, Stein EA (1999) Right hemispheric dominance of inhibitory control: an event-related functional MRI study. Proc Natl Acad Sci U S A 96:8301-8306.

Garavan H, Hester R, Murphy K, Fassbender C, Kelly C (2006) Individual differences in the functional neuroanatomy of inhibitory control. Brain Res 1105:130-142.

Garcia-Munoz M, Carrillo-Reid L, Arbuthnott GW (2010) Functional anatomy: dynamic States in Basal Ganglia circuits. Front Neuroanat 4:144.

Gauggel S, Rieger M, Feghoff TA (2004) Inhibition of ongoing responses in patients with Parkinson's disease. J Neurol Neurosurg Psychiatry 75:539-544.

Goetz CG, Stebbins GT, Chmura TA, Fahn S, Klawans HL, Marsden CD (1995) Teaching tape for the motor section of the unified Parkinson's disease rating scale. Mov Disord 10:263-266.

Hampshire A, Chamberlain SR, Monti MM, Duncan J, Owen AM (2010) The role of the right inferior frontal gyrus: inhibition and attentional control. NeuroImage.

Hoehn MM, Yahr MD (1967) Parkinsonism: onset, progression and mortality. Neurology 17:427-442.

Inase M, Tokuno H, Nambu A, Akazawa T, Takada M (1999) Corticostriatal and corticosubthalamic input zones from the presupplementary motor area in the macaque monkey: comparison with the input zones from the supplementary motor area. Brain Res 833:191-201.

Isoda M, Hikosaka O (2008) Role for subthalamic nucleus neurons in switching from automatic to controlled eye movement. J Neurosci 28:7209-7218.

Johansen-Berg H, Behrens TE, Robson MD, Drobnjak I, Rushworth MF, Brady JM, Smith SM, Higham DJ, Matthews PM (2004) Changes in connectivity profiles define functionally distinct regions in human medial frontal cortex. Proc Natl Acad Sci U S A 101:13335-13340.

Jung TP, Makeig S, Westerfield M, Townsend J, Courchesne E, Sejnowski TJ (2000) Removal of eye activity artifacts from visual event-related potentials in normal and clinical subjects. Clin Neurophysiol 111:1745-1758.

Kok A, Ramautar JR, De Ruiter MB, Band GP, Ridderinkhof KR (2004) ERP components associated with successful and unsuccessful stopping in a stop-signal task. Psychophysiology 41:9-20.

Konishi S, Nakajima K, Uchida I, Kikyo H, Kameyama M, Miyashita Y (1999) Common inhibitory mechanism in human inferior prefrontal cortex revealed by event-related functional MRI. Brain 122 (Pt 5):981-991.

Kühn AA, Kupsch A, Schneider G-H, Brown P (2006) Reduction in subthalamic 8-35 Hz oscillatory activity correlates with clinical improvement in Parkinson's disease. Eur J Neurosci 23:1956-1960.

Kuncel AM, Grill WM (2004) Selection of stimulus parameters for deep brain stimulation. Clin Neurophysiol 115:2431-2441.

Li CS, Yan P, Sinha R, Lee TW (2008) Subcortical processes of motor response inhibition during a stop signal task. Neuroimage 41:1352-1363.

Liotti M, Pliszka SR, Perez R, 3rd, Luus B, Glahn D, Semrud-Clikeman M (2007) Electrophysiological correlates of response inhibition in children and

adolescents with ADHD: influence of gender, age, and previous treatment history. Psychophysiology 44:936-948.

Logan GD, Schachar RJ, Tannock R (1997) Impulsivity and inhibitory control. Psychological Science 8:60-64.

Luck SJ (2005) An Introduction to the Event-Related Potential Technique: MIT Press.

Mallet L, Schupbach M, N'Diaye K, Remy P, Bardinet E, Czernecki V, Welter ML, Pelissolo A, Ruberg M, Agid Y, Yelnik J (2007) Stimulation of subterritories of the subthalamic nucleus reveals its role in the integration of the emotional and motor aspects of behavior. Proc Natl Acad Sci U S A 104:10661-10666.

Marco-Pallares J, Camara E, Munte TF, Rodriguez-Fornells A (2008) Neural mechanisms underlying adaptive actions after slips. J Cogn Neurosci 20:1595-1610.

Neubert FX, Mars RB, Buch ER, Olivier E, Rushworth MF (2010) Cortical and subcortical interactions during action reprogramming and their related white matter pathways. Proc Natl Acad Sci U S A 107:13240-13245.

Pliszka SR, Liotti M, Woldorff MG (2000) Inhibitory control in children with attention-deficit/hyperactivity disorder: event-related potentials identify the processing component and timing of an impaired right-frontal response-inhibition mechanism. Biol Psychiatry 48:238-246.

Pogosyan A, Gaynor LD, Eusebio A, Brown P (2009) Boosting cortical activity at Beta-band frequencies slows movement in humans. Curr Biol 19:1637-1641.

Ramautar JR, Kok A, Ridderinkhof KR (2006) Effects of stop-signal modality on the N2/P3 complex elicited in the stop-signal paradigm. Biol Psychol 72:96-109.

Ray N, Jenkinson N, Brittain J, Holland P, Joint C, Nandi D, Bain P, Yousif N, Green A, Stein J, Aziz T (2009) The role of the subthalamic nucleus in response inhibition: Evidence from deep brain stimulation for Parkinson's disease. Neuropsychologia.

Rieger M, Gauggel S, Burmeister K (2003) Inhibition of ongoing responses following frontal, nonfrontal, and basal ganglia lesions. Neuropsychology 17:272-282.

Rubia K, Smith AB, Brammer MJ, Taylor E (2003) Right inferior prefrontal cortex mediates response inhibition while mesial prefrontal cortex is responsible for error detection. Neuroimage 20:351-358.

Schmajuk M, Liotti M, Busse L, Woldorff MG (2006) Electrophysiological activity underlying inhibitory control processes in normal adults. Neuropsychologia 44:384-395.

Sharp DJ, Bonnelle V, De Boissezon X, Beckmann CF, James SG, Patel MC, Mehta MA (2010) Distinct frontal systems for response inhibition, attentional capture, and error processing. Proceedings of the National Academy of Sciences:1-6.

Swann N, Tandon N, Canolty R, Ellmore TM, McEvoy LK, Dreyer S, DiSano M, Aron AR (2009) Intracranial EEG reveals a time- and frequency-specific role for the right inferior frontal gyrus and primary motor cortex in stopping initiated responses. J Neurosci 29:12675-12685.

Temperli P, Ghika J, Villemure J-G, Burkhard PR, Bogousslavsky J, Vingerhoets FJG (2003) How do parkinsonian signs return after discontinuation of subthalamic DBS? Neurology 60:78-81.

van den Wildenberg WPM, van Boxtel GJM, van der Molen MW, Bosch DA, Speelman JD, Brunia CHM (2006) Stimulation of the subthalamic region facilitates the selection and inhibition of motor responses in Parkinson's disease. Journal of cognitive neuroscience 18:626-636.

Verbruggen F, Logan GD (2009a) Models of response inhibition in the stop-signal and stop-change paradigms. Neurosci Biobehav Rev 33:647-661.

Verbruggen F, Logan GD (2009b) Proactive adjustments of response strategies in the stop-signal paradigm. J Exp Psychol Hum Percept Perform 35:835-854.

Verbruggen F, Aron AR, Stevens MA, Chambers CD (2010) Theta burst stimulation dissociates attention and action updating in human inferior frontal cortex. Proc Natl Acad Sci U S A 107:13966-13971.

CHAPTER 4:

Roles for the pre-supplementary motor area and the right inferior frontal gyrus in stopping action: electrophysiological responses and functional and structural connectivity

ABSTRACT

Both the pre-supplementary motor area (preSMA) and the right inferior frontal gyrus (rIFG) are important for stopping action outright. These regions are also engaged when preparing to stop. We aimed to elucidate the roles of these regions by harnessing the high spatio-temporal resolution of electrocorticography (ECoG), and by using a task that engages both preparing to stop and stopping outright. First, we validated the task using fMRI in 16 healthy control participants to confirm that both the preSMA and the rIFG were active. Next, we studied a rare patient with intracranial grid coverage of both these regions, using macrostimulation, diffusion tractography, cortico-cortical evoked potentials (CCEPs) and task-based ECoG. Macrostimulation of the preSMA induced behavioral motor arrest. Diffusion tractography revealed a structural connection between the preSMA and rIFG. CCEP analysis showed that stimulation of the preSMA evoked strong potentials within 30 ms in rIFG. During the task, when preparing to stop, there was increased high gamma amplitude (~70-250 Hz) in both regions, with preSMA preceding rIFG by ~750 ms. For outright stopping there was also a high gamma amplitude increase in both regions, again with preSMA

preceding rIFG. Further, at the time of stopping, there was an increase in beta band activity (~16 Hz) in both regions, with significantly stronger long-range coherence for successful vs. unsuccessful stop trials. The results complement earlier reports of a structural/functional action control network between the preSMA and rIFG. They go further by revealing between-region timing differences in the high gamma band when preparing to stop and stopping outright. They also reveal strong between-region coherence in the beta band when stopping is successful. Implications for theories of action control are discussed.

INTRODUCTION

Lesion studies and Transcranial Magnetic Stimulation show that stopping an initiated response depends on the integrity of the right inferior frontal gyrus (rIFG) as well as the presupplementary motor area (preSMA) (reviewed by Nachev et al., 2008; Chambers et al., 2009; Aron, 2010; Chikazoe, 2010; Levy and Wagner, 2011). Additionally, diffusion tensor imaging (DTI) tractography shows that the IFG and the preSMA are structurally connected to one another, and to the basal ganglia, comprising a putative network for action control (Johansen-Berg et al., 2004; Aron et al., 2007; Ford et al., 2010; Forstmann et al., 2010). Electrophysiological studies have begun to characterize the neural communication within this putative network, pointing to increased activity in the beta frequency band during successful stopping (Marco-Pallares et al., 2008; Swann et al., 2009; Swann et al., 2011).

Yet, while the preSMA and the rIFG are key nodes of this putative network, their relative functional roles in stopping are still unclear. For instance, it has been suggested that they could both be important for inhibitory control, or one could be important in monitoring for the stop signal and/or detecting conflict and another for implementing inhibitory control (Mostofsky and Simmonds, 2008; Duann et al., 2009; Hampshire et al., 2010; Sharp et al., 2010). Notably, recent fMRI studies show that both regions are active when *preparing* to stop, as well as during outright stopping (Chikazoe et al., 2009a; Jahfari et al., 2009; Verbruggen et al., 2010; Zandbelt and Vink, 2010). This raises the additional possibility that one or both regions are involved in setting up the stopping network in advance so that inhibitory control can subsequently be triggered when the stop signal is detected. While we refer to this as 'preparing to stop' we note that it could also be described as increased response caution, favoring accuracy over speed, or proactive inhibitory control. If the preSMA is important for setting up the stopping network, i.e. a task configuration role (Vink et al., 2005) then it should be active soon after a cue that instructs the participant that stopping is likely, and before the rIFG; whereas if the rIFG is important for this function then the reverse timing relation should be observed. Testing this with fMRI is difficult because of the poor temporal resolution. Instead, we studied a single, rare, patient who had electrocorticography (ECoG) electrodes implanted over both the preSMA and the rIFG.

We designed a new task to engage both preparing to stop and outright stopping (Figure 4.1). Each trial began with a cue "Maybe Stop" or "No Stop" which was

followed by a Go stimulus and then, on Maybe Stop trials alone, this was sometimes followed by a stop signal. By comparing Maybe Stop and No Stop trials we could examine the preparing-to-stop process; while by comparing Maybe Stop successful stop vs. unsuccessful stop trials (or Maybe Stop successful stop compared to Maybe Stop go trials or baseline) we could examine outright stopping. We used fMRI in healthy young participants to confirm that this task activated the preSMA and rIFG as expected.

In the patient we performed macrostimulation and DTI, and we collected cortico-cortical evoked potentials (CCEP) and task-related ECoG. First, macrostimulation was applied systematically to different electrode contacts in dorsal-medial frontal cortex while the patient performed vocal or manual movements. We aimed to confirm prior reports that macrostimulation of anterior SMA (preSMA) induces motor arrest (Fried et al., 1991; Rushworth et al., 2004). Second, DTI was used to verify the connection between the preSMA and the rIFG that has been established in normative populations (Luders et al., 1988; Johansen-Berg et al., 2004; Aron et al., 2007; Forstmann et al., 2010). Third, we evaluated task-independent functional connectivity between the preSMA and the rIFG using CCEPs (Matsumoto et al., 2004; Ford et al., 2010). By stimulating different dorsomedial contacts (in a pair-wise fashion) we could ‘map’ the spatial and temporal responses in the right lateral frontal cortex. We were interested in determining whether CCEPs from specific preSMA electrodes elicited short-latency responses within specific rIFG electrodes. Finally, we recorded ECoG while the patient performed the Maybe Stop/No Stop task.

For preparing to stop (time-locked to the cue) we anticipated high gamma amplitude changes in both rIFG and preSMA since fMRI studies of preparing-to-stop have shown BOLD signal increases in both these regions (Matsumoto et al., 2007; Chikazoe et al., 2009a; Jahfari et al., 2009; Zandbelt and Vink, 2010), and high gamma increases are associated with the BOLD signal (Logothetis et al., 2001; Vink et al., 2005; Scheeringa et al., 2011). Our observations go beyond previous reports by identifying *when* these regions are involved in preparing to stop, which could help differentiate their roles.

For outright stopping (time-locked to the stop signal) we aimed to examine both high gamma and beta band activity. High gamma activity was anticipated in both regions since they show BOLD signal increases for stopping, and, as described earlier, high gamma increases are associated with the BOLD signal (Logothetis et al., 2001; Conner et al., 2011; Scheeringa et al., 2011). We also expected an increase in beta band amplitude over rIFG for successful vs. unsuccessful stop trials based on our earlier report (Conner et al., 2011). We also predicted that there would be beta band increases in the preSMA, given the evidence for involvement of this region in response control and its structural connectivity to rIFG. Further, we planned to examine beta band coherence between the preSMA and the rIFG. Coherence is a measure of functional connectivity thought to reflect communication between brain areas (Swann et al., 2009). If beta band coherence between the preSMA and the rIFG is important for successful stopping then it should be stronger on successful than unsuccessful stop trials.

METHODS

Experiment 1: fMRI in healthy adults

Participants

Sixteen young adults (8 female, 18-28 years old) were recruited from the local community. All participants provided written consent in accordance with the Internal Review Board of the University of California at San Diego. They received monetary compensation.

Task

An event-related Maybe Stop (MS) / No Stop (NS) task was used (see Figure 4.1A). On each trial, a cue was presented in the center of the screen for 1 sec. The cue was either the words “Maybe Stop” (red on a black background) or “No Stop” (green on a black background) equiprobably. A go signal (white arrow) followed the cue. Participants made right index or left index finger presses in response to rightward and leftward pointing arrows as quickly as possible. In the MS condition, a beep (stop signal) followed the go signal, on 50% of trials, with a variable delay. Participants were instructed to withhold responses when the stop signal occurred. In order to achieve 50% stopping accuracy, the stop signal delay was dynamically changed based on behavior (for full details of the procedure see Fries, 2005). The initial stop signal delay was 150 ms. The response window was 1 second and the inter-trial-interval was jittered between 1.5-5 seconds. Five participants performed two blocks of the task and

10 participants performed one block of the task (because of limited scanning time). Each block included 20 MS_Go trials, 20 MS_Stop trials and 40 NS_Go trials. Participants were practiced on the task initially before entering the scanner and were encouraged to respond quickly on go trials and to do their best to stop their response on stop trials.

MRI data collection

MRI data were acquired with a 3T GE SIGNA HDX scanner with an eight channel head coil at the UCSD Center for functional MRI. A high-resolution T1 3D FSPGR scan was acquired for the purpose of registration (slice thickness, 1 mm; TR, 7.8 seconds; TE, 3 seconds; matrix, 192 x 192; FOV, 256; 172 sagittal slices, voxel size 1.3 x 1.3 x 1 mm^3). Each functional scan comprised 180 T2*-weighted echo planar images (slice thickness, 4 mm; TR, 2 seconds; TE, 30 ms; flip angle, 90^o; matrix, 64x64; FOV, 200; 32 axial slices, voxel size 3.1 x 3.1 x 4 mm^3).

Behavioral Analysis

We calculated mean RT and accuracy for each of MS_Go and NS_Go trials; the average stop signal delay (after staircase convergence); and stop signal reaction time (SSRT) (for details see Aron and Poldrack, 2006).

Functional MRI data preprocessing and analysis

MRI data were processed using the FSL software library (www.fmrib.ox.ac.uk/fsl). The functional series were aligned to compensate for small head movements. A two-step registration procedure was applied whereby the EPI images were first registered to the participant's own T1 image, then normalized to the MNI152 template using 12-parameter affine registration. All data were spatially smoothed with a Gaussian kernel of 5 mm at full-width half-maximum and were high-pass filtered at 66 s.

Five regressors were defined for each scan for each participant: NS_Go (correct NS go trials), MS_Go (correct MS go trials), MS_SS (MS successful stop trials), MS_US (MS unsuccessful stop trials), and Others (i.e. incorrect go trials or omissions on go trials). The regressors were modeled at the onset of the Go stimulus, and they were convolved with a canonical hemodynamic response function. For each participant and each scan, we generated the two main contrasts of interest: i.e. MS_Go vs. NS_Go (preparing to stop) and, i.e. MS_SS vs. MS_Go (outright stopping).

Functional MRI data processing was carried out using FEAT (FMRI Expert Analysis Tool) version 5.98. Higher-level analysis was performed by first doing fixed-effects across scans for each participant (for the participants who had two scans), followed by a random-effects analysis across all participants for each of the two contrasts. Higher-level analysis was carried out using FLAME (FMRIB's Local Analysis of Mixed Effects) stage 1 (Beckmann et al., 2003; Aron and Poldrack, 2006; Woolrich, 2008). Activations were corrected for multiple comparisons at $z>2.3$, $p<0.05$ whole-brain cluster corrected.

Experiment 2: Case study

Participant

The participant was a 27 year old, right-handed, male undergoing evaluation for possible resective surgery to treat medically intractable epilepsy. He was enrolled into the study after providing informed consent according to a protocol at the University of Texas at Houston Medical School's committee for protection of human participants. We note that the locus of his epileptic activity was subsequently determined to *not* include either the preSMA or the IFG. Besides the epilepsy, this patient was judged to be neurologically normal. Formal neuropsychological testing revealed a verbal IQ of 106 and a performance IQ of 118.

Subdural electrode placement and localization

The electrode localization methodology and recording strategies used were similar to those previously described (Woolrich et al., 2004; Swann et al., 2009; Khursheed et al., 2011). Briefly, subdural electrodes spaced 1 cm apart were implanted (Tertel et al., 2010). A post-operative CT scan was co-registered with pre-implantation MRI. Subdural electrodes were localized on the CT scan, projected onto a cortical surface model generated in FreeSurfer (Tandon, 2008), and visualized with SUMA software as spheres (Dale et al., 1999). These locations were verified using intra-operative photographs. Electrodes were then given anatomical labels, in semi-automated fashion, using a FreeSurfer parcellation scheme.

Macrostimulation procedure

Macrostimulation was carried out to localize functional zones prior to resection for epilepsy. A balanced faradic current was delivered at 50 Hz using a S88 Grass stimulator that generates trains of biphasic rectangular waves (Grass technologies, West Warwick, Rhode Island). The duration of each wave was 500 μs, and these were delivered in trains of 3-5 second duration via two contacts located on the cortical surface during performance of simple motor or verbal tasks described below. Current strength ranged from 1 – 10 mA, determined by overt phenomenology or the induction of after discharges in the concurrent ECoG (Saad et al., 2003). To assess the impact on motor function, the patient was asked to open and close his hands rapidly (as if making a symbol for a flashing light) and articulation was assessed by asking him to recite the letters of the alphabet and to read from a card held about 20 inches in front of him.

DTI acquisition and analysis

DTI was acquired on a 3T whole-body MR scanner (Philips Medical Systems, Bothell WA) equipped with an eight channel SENSE head coil. One B0 (non-diffusion weighted) image volume and diffusion weighted images were collected with the Philips 32-directions diffusion encoding scheme (high angular resolution) with the "gradient overplus" option. Seventy axial slices were acquired with 1.75 mm pixels, 2 mm slice thickness, and a maximum b-value of 800 s/mm^2. Individual diffusion-weighted images volumes were realigned to the participant's skull-stripped anatomical

MRI, and a single-model diffusion tensor was computed. Deterministic fiber tracking was performed with DTIQuery using the streamline tracking algorithm (STT) with optimal parameters (Sherbondy et al., 2005; Tandon, 2008): path step size (in millimeters)=1.0, seed point spacing (in millimeters)=2.0, FA termination threshold=0.15, angle termination threshold (in degrees)=45, min pathway length (in millimeters)=5.0, and max pathway length (in millimeters)=300.0, and Euler's Method for STT numerical integration. We placed 1 cm wide cuboids (with minimal overlap) over each of the dorsomedial electrodes as seeds for the deterministic generation of tracts to remote regions. All connections to the opposite hemisphere were eliminated.

CCEP acquisition and analysis

Adjoining electrode pairs in the inter-hemispheric electrode array were stimulated in bipolar fashion using single pulses (10 mA, 500 μs, 1 Hz for 50 seconds – total of 50 pulses for each pair), delivered by a Grass Stimulator. Concurrent ECoG was performed at 1000 Hz. All channels were referenced to an average of all intracranial electrodes except the stimulating electrodes, and electrodes within 2 cm from the site of stimulation, which served to eliminate effects of the stimulation artifact. The 50 epochs were time-locked, averaged and displayed as traces of the mean +/- 3 SEM. These tracings were compared to a baseline artifact-free ECoG trace (>60 sec long) acquired separately during the same recording session with the patient awake and at rest. Channels with significant ($p<0.001$) shifts from baseline with a maximum peak >150mV were identified for subsequent analysis using a t-test. We

only included responses of latency >10 ms (to exclude stimulus artifact) and <30 ms (to eliminate indirect connections), and with amplitude <200 mV (to exclude direct current spread). The peak amplitude and time to peak for the CCEPs were computed for each recording channel. To depict the CCEPs graphically, spheroids whose size and color were dependent on the amplitude and latency of the CCEP, were generated and overlaid onto the cortical surface.

ECoG paradigm, data acquisition and analysis

The patient performed the MS/NS task described in Experiment 1 with four differences. First, the response window was slightly longer: 1.5 seconds instead of 1 second to allow for slower responses from the patient if necessary. Second, the inter-trial interval was randomly varied from 1 to 1.4 second (in intervals of 100 ms) (instead of the longer ITI necessary for fMRI). Third, the patient was asked to respond using his left hand (index or middle finger), so we could sample ECoG from right primary motor cortex. (Note that this change is unlikely to change the results related to the stopping network since its right-laterality seems to be independent of hand used (Akers et al., 2005; Chambers et al., 2006; Swann et al., 2009).) Fourth, the patient completed 7 blocks (96 trials each) of the task (since more trials are necessary for ECoG compared to fMRI).

Data were collected using an EEG 1100 Neurofax clinical Nihon Koden acquisition system recorded at 1000 Hz sampling rate. Trial onsets for the behavioral task were sent to the ECoG data acquisition computer via transistor–transistor logic

pulses. Behavioral responses were recorded via button responses made with the patient's left hand, on a keyboard. All data were digitally re-referenced to a common average. This excluded channels with artifact or frequent ictal activity.

The ECoG analysis was nearly identical to our previous report (Konishi et al., 1998). In brief, the data were filtered into 128 frequencies ranging from 2.5 to 250 Hz using a Gabor wavelet procedure. The filtered data were then epoched according to events of interest and averaged across trials. Analysis was time-locked to either the MS/NS cue or the stop signal. Note that for the MS/NS go comparison, the NS_Go trials were twice as frequent as MS_Go, so we randomly sub-sampled NS_Go trials to balance trial numbers. Omitting this step did not change the results. A baseline correction with a baseline period of 500 ms in the middle of the inter-trial interval was applied. Finally, the analytic amplitude for conditions relative to baseline were converted to z-scores using a permutation-based method with event indices randomly offset. To calculate z-scores for between condition comparisons (i.e. MS_Go compared to NS_Go or MS_SS to MS_US), a permutation-based, label-swapping, method was used. Where indicated, a "false discovery rate" (FDR) correction was applied to correct for multiple comparisons. For a given electrode, values for all time-points, frequencies, and conditions were considered for calculation of the FDR-corrected threshold. For further details see previous reports (Swann et al., 2009).

In addition, because of previous research highlighting low frequency activity and its potential role in the network properties of these regions during stopping (Canolty et al., 2007; Swann et al., 2009), an additional analysis was conducted to closely

examine low-frequency amplitude changes for rIFG and preSMA, as well as low-frequency coherence between these two regions for stop trials (time-locked to the stop signal). The amplitude changes were calculated in the same manner as described above except here with a prestimulus baseline of -500 to 0 ms relative to the stop signal, to more clearly visualize the instantaneous, task-related amplitude changes. Coherence is a measure of event-related amplitude and phase, which is thought to reflect functional connectivity, especially at low frequencies (Swann et al., 2011). It was computed using the corresponding auto-spectra and cross-spectra and ensemble averaging across trials as shown below.

$$Coh(t,f) = \frac{|W_{xy}(t,f)|}{\sqrt{W_{xx}(t,f)}\sqrt{W_{yy}(t,f)}} \text{ where } W_{xy}(t,f) = \frac{1}{N}\sum_{k=1}^{N} W_x(t,f).W_y*(t,f)$$

Here x and y refer to data from 2 channels. N is the number of trials and $W_x(t,f)$ is the complex analytic signal (dependant on time (t) and frequency (f)) obtained from filtering. Significance was calculated using procedures analogous to the event-related amplitude differences. For conditions relative to baseline z-scores were derived from a distribution created using 10000 iterations of mean coherence values time-locked to random events. Between conditions (MS_SS vs MS_US) z-scores were calculated using a permutation method where a distribution of differences was created using the label swapping procedure.

RESULTS

Experiment 1: fMRI study in healthy adults

Behavioral data

RT for MS_Go trials was 533 ms and for NS_Go trials was 404 ms and this was a significant difference, $t(15)=5.86$, $p<0.001$, Table 4.1. This shows that participants were using the MS cue to prepare to stop (c.f.Fries, 2005). SSRT was estimated at 182 ± 50 ms. However, because of limited stop trials for some subjects (who only performed one block of the task), SSD values did not always have time to dynamically adjust to a 50% probability of stopping. Thus SSRT may not have been estimated very accurately for some subjects.

Functional MRI

Preparing to stop

The contrast of MS_Go vs. NS_Go revealed significant activation of the preSMA and the rIFG, as well as other regions of prefrontal cortex and the parietal and temporal lobe in both hemispheres ($z>2.3$, $p<0.05$ whole-brain corrected, see Figure 4.1B, see Supplementary Table 4.1 for full details). Because reaction times differed for these two conditions the effect of RT variance on the brain activation was also examined by including an additional regressor of RT. Significant activations in the preSMA and the rIFG in the contrast of MS_Go versus NS_Go were still observed ($z>2.3$, $p<0.05$, cluster corrected*).* These results are similar to other studies using tasks that examine preparing to stop (Chikazoe et al., 2009a; Jahfari et al., 2009). No significant activation was found for the contrast of NS_Go vs. MS_Go.

Outright Stopping

The contrast of MS_SS vs. MS_Go revealed significant activation of a predominantly right hemisphere network including the rIFG, parietal cortex, auditory cortex and other regions ($z>2.3$, $p<0.05$ whole-brain corrected, see Figure 4.1C and Supplementary Table 4.2 for full details). The activation pattern was consistent with prior studies of standard stop signal and Go/NoGo tasks (Konishi et al., 1998; Garavan et al., 1999; Rubia et al., 2003; Vink et al., 2005; Aron and Poldrack, 2006; Aron et al., 2007; Chevrier et al., 2007; Leung and Cai, 2007; Cai and Leung, 2009; Zandbelt and Vink, 2010). However, whereas those studies showed preSMA activation during outright stopping, here it was not detected, even when using a small volume correction for the anatomically defined preSMA region, and even with a lower threshold ($z=1.6$). A difference between the current task and those studies was that here outright stopping occurred in the context of preparing to stop. However, another study that examined preparing to stop*, did* show preSMA activation for outright stopping (Chikazoe et al. 2009). In that study, though, there was a 25% chance of a stop signal given a cue that stopping may occur, whereas here the probability was 50%. Thus, participants might have been in a greater state of stopping readiness in this paradigm, even on MS_Go trials, which could reduce the MS_SS vs. MS_Go difference, at least for preSMA. Another possibility is that we may have been under-powered, perhaps due to low-trial numbers, to see preSMA activation, especially if it is a subtle effect. Regardless, the current results establish for this particular behavioral paradigm that both the preSMA

and the rIFG are activated when preparing to stop, and, that consistent with prior studies, the rIFG is activated for stopping outright.

Experiment 2: Case study

Behavior

Mean RT was 618 ms for MS_Go trials and 491 ms for NS_Go trials and this was a significant difference, $t(334) = 6.38$, $p<.001$, Table 4.1. The average SSD was 379 ms and SSRT was 239 ms. These values are comparable with the healthy adults in Experiment 1 and indicate that the patient performed the task well.

Macrostimulation results

Macrostimulation was carried out for all the dorsomedial frontal electrodes (entire inter-hemispheric grid, IH 1-20, see Figure 4.2) in a pair-wise bipolar fashion (e.g. inter-hemispheric electrodes (IH) 11 and 12). We found that stimulation at electrodes IH 1, 2, 3, 11, and 12 produced 'motor arrest' (Table 4.2). Electrodes 11 and 12 in particular were the only pair to show a *bilateral* cessation of movement. These findings are consistent with previous macrostimulation studies that identified the anterior SMA along with the rIFG as "negative motor regions" (Xue et al., 2008; Kenner et al., 2010). Given that stimulation at contacts 3,4 and 12,13 led to other effects, the electrodes that can be most clearly characterized as belonging to the pre-SMA were electrodes IH 1,2, and 11, with IH11 showing the most complete (bilateral) response characteristic of the anterior SMA/preSMA region (Luders et al., 1988; Fried

et al., 1991). All of these electrodes were within the posterior preSMA, as localized by FreeSurfer parcellation (see Figure 4.2 for locations)(Fried et al., 1991). Therefore, we focus on electrode IH11 for further analyses (talaraich coordinates: 0, 12, 51, see Supplementary Figure 4.1).

DTI

Deterministic tractography using cuboid seeds placed on electrode locations corresponding to the pre-SMA (i.e. IH 1, 2 and 11, 12) (Luders et al., 1988), revealed independent projections from the preSMA to the lateral prefrontal cortex, the midbrain, the medial prefrontal cortex and the medial parietal lobe. Strikingly, the connection to the lateral prefrontal cortex was specifically to the IFG. Moreover, the electrodes that corresponded to this connection most closely were IH11 (IH = inter-hemispheric) and LF16/15 (LF = lateral frontal) (Figure 4.3A and see Supplementary Table 4.3 for additional tract information and Supplementary Figure 4.2 for additional electrode locations). Although a white matter connection between the preSMA and the rIFG has previously been revealed by probabilistic tractography (Picard and Strick, 2003; Johansen-Berg et al., 2004; Aron et al., 2007) the current finding provides greater spatial specificity, and links structure and function in the same patient. Electrode IH11 was a contact at which macrostimulation induced motor arrest, and, as we show below, LF16 is the IFG electrode with both the clearest evoked potentials (when IH11 is stimulated) and the strongest ECoG responses during task performance.

CCEPs

Low frequency stimulation of the inter-hemispheric electrodes (IH 1-20) was carried out with concurrent high frequency sampling (1000 Hz) of the entire intracranial array to examine the (functional) electro-physiologic projections from preSMA. We were particularly interested in the connections to the lateral frontal cortex. To identify 'direct' connections, we restricted ourselves to evoked changes occurring within the first 30 ms (Ford et al., 2010; Forstmann et al., 2010). These direct CCEPs were found to occur in the immediate neighborhood of the stimulating electrodes (presumably mediated by U fibers) but also remotely, in the lateral frontal lobe. The frontal lobe responses were centered in the posterior inferior frontal gyrus (LF 9, 10, 15, 16), in the lateral premotor cortex (LF 3) and in the middle frontal gyrus (LF1) (See Figure 4.3B and Supplementary Figure 4.3 for an example CCEP trace). No other brain regions showed such large, rapid responses (i.e. greater than 100 μV, within 30 ms). (For full details on the CCEP values for all channels, including those outside the lateral frontal regions, see Supplementary Table 4.3 and Supplementary Figure 4.2 for additional electrode locations). These findings provide functional connectivity evidence to corroborate the structural connection between the preSMA and the IFG. Importantly, the locations of the CCEPs in the lateral frontal cortex were remarkably spatially specific and corresponded well with the tract termination in rIFG revealed by the DTI (i.e. LF16/15 see above) and with the ECoG results during task performance (LF16 see below).

ECoG

In Supplementary Figures 4.4-7 we show results from all electrodes in the anatomically defined preSMA and rIFG regions, however, in light of the above DTI and CCEP results, here we focus specifically on IH11 (preSMA) and LF16 (rIFG).

Preparing to stop: preSMA and rIFG

For the preSMA, time-locked to the MS or NS cue, there was an increase in high gamma band activity for both MS and NS trials (~70-250 Hz) relative to baseline (the inter-trial interval) **(**Figure 4.4). This increase began (defined as the point where the high gamma power first became significantly greater than baseline) after the MS or NS cue and approximately 500 ms *before* the Go stimulus (arrow) was presented ($p<0.05$ FDR corrected). The high gamma amplitude increase was much larger for MS_Go than NS_Go ($p<0.05$ FDR corrected), although this difference did not reach significance until after the Go stimulus.

For the rIFG, time-locked to the MS or NS cue, there was again an increase in high gamma band activity for each trial type. However, the above-baseline increase began about 250 ms *after* the Go cue, and the MS-NS difference did not emerge until about 500 ms later, around the time of movement onset ($p<0.05$ FDR corrected).

Thus, there was an increase in high gamma amplitude, more so for MS_Go than NS_Go trials, in both the preSMA and the rIFG, with the preSMA response began between the cue and the go stimulus and *preceding* the rIFG response. We note that high gamma band activity likely indicates local neuronal activity in each region

(Crone et al., 1998; Logothetis et al., 2001; Matsumoto et al., 2004; Edwards et al., 2005; Matsumoto et al., 2007; Miller et al., 2007a; Miller et al., 2007b; Ray et al., 2008). This provides complementary evidence to the fMRI findings in Experiment 1 of preSMA and rIFG activity for preparing to stop. However, it goes further by providing information about the relative timing of engagement of these regions. The significance of preSMA activity preceding rIFG when preparing to stop will be discussed below in relation to theories of action control.

Outright Stopping: preSMA and rIFG

While the high gamma band frequency points to neural activity *within* a region, lower frequencies may be important for long-distance communication *between* regions (Womelsdorf et al., 2007; Conner et al., 2011; Scheeringa et al., 2011). Prior research has implicated the beta band (13-30 Hz) as a candidate for communication in a putative prefrontal cortex/basal-ganglia network for action control (Kühn et al., 2004; Swann et al., 2011; Swann et al., 2009). Our earlier ECoG study specifically reported increases in the beta band in the rIFG when responses were stopped (Fries, 2005). Here we aimed to (1) replicate this finding in a new patient (and with a new task), (2) examine if beta amplitude also increases in the preSMA when stopping occurs and (3) determine if there is coherence between the rIFG and the preSMA during stopping in the beta band. Because we had this specific a-priori hypothesis, based on these previous studies, we did not apply a FDR correction for these results.

Time-locked to the stop signal, beta amplitude increases (~16 Hz) were indeed observed in both preSMA and rIFG beginning shortly after the stop signal (each region $p<0.01$, uncorrected, see Figure 4.5), compared to a pre-stimulus baseline (-500 to 0 ms relative to the stop signal). The beta response in rIFG was greater for MS_SS compared to MS_US trials ($p<0.05$, uncorrected, see Figure 4.5). Although this is similar to prior results (van Elswijk et al., 2010) it is a more subtle effect, perhaps because of the increased expectation of stopping in this paradigm relative to the standard stopping paradigm (here p(stop|MS cue) was 50%, whereas p(stop) in the standard paradigm is usually ~25-33%). Unlike the rIFG, the comparison of MS_SS vs. MS_US was not significant for the preSMA. Also evident in Figure 4.5 are differences in other frequency bands implicated in cognitive control, such as theta (Marco-Pallares et al., 2008; Cavanagh et al., 2009; Swann et al., 2009). Such findings are candidates for future exploration, however, because this was a relatively weak effect for which we did not have an a-priori hypothesis, we do not discuss it further here.

Thus, the response in the rIFG replicates our earlier results (Luu et al., 2004), and also shows a similar increase in beta band activity for the preSMA following the stop signal (and before SSRT), though there was not a significant difference for successful and unsuccessful stop trials for this region. [Note that there were also high gamma amplitude increases for outright stopping for both regions – these results are shown in the section below].

We examined task-related coherence between the preSMA and rIFG for MS_SS and MS_US trials. There was a significant increase in coherence in the beta band after the stop signal, but before SSRT elapsed, for MS_SS trials ($p<0.01$, uncorrected, see Figure 4.5), but not for MS_US trials. The difference in coherence between MS_SS and MS_US trials in the beta band was also significant ($p<0.01$, uncorrected, see Figure 4.5). Examination of phase lag can theoretically inform the directionality of the interaction, but in this case, the phase delay was near zero, suggesting overall network synchrony or that both regions may be driven by a third, unmeasured, region(s) (potentially the subthalamic nucleus) (Trujillo and Allen, 2007).

Taken together, these observations provide further evidence that the preSMA and the rIFG make up a structurally and physiologically connected circuit that is engaged in a task-related fashion.

Outright Stopping: the wider cortical network

To provide a fuller picture of the relative timing of preSMA and the rIFG, as well as other regions of putative interest for stopping such as the temporo-parietal junction (Swann et al., 2009), the superior parietal region (Swann et al., 2011), the auditory cortex, the middle frontal gyrus, and M1 (Corbetta and Shulman, 2002) we examined high gamma activity for all electrodes in the right lateral cortex and the dorsomedial region. We focused on the period of 150 ms before the stop signal to 250 ms after it. Average high gamma (100 Hz) amplitude expressed as a z-score was calculated for MS_SS trials compared to baseline (the inter-trial interval) for each 50

ms time window. Significant responses ($p<0.01$, FDR corrected) are shown in Figure 4.6.

The middle frontal gyrus showed sustained activity across the trial. This could reflect working memory for the stopping rule (Corbetta and Shulman, 2002; Olesen et al., 2004; Muller and Knight, 2006; Swann et al., 2009). The intra-parietal sulcus/superior parietal lobe was active *early* in the trial, prior to stop signal onset, perhaps related to a putative role in top-down attention (Petrides, 2000)(See Supplementary Figure 4.8 for more detail and examination of this region during preparing to stop). In the more ventral region of the temporo-parietal junction there was, by contrast, activity following the stop signal, in line with its hypothesized role in bottom-up driven attention (Goldman-Rakic, 1990) (See Supplementary Figure 4.9 for more detail and examination of this region during preparing to stop). Finally, both the (right) primary motor and primary auditory areas were active as would be expected with a task involving left hand responses and an auditory stop signal.

This analysis provides a map of the disseminated components of the stopping network and also complements the earlier results with the preSMA and rIFG (see Figure 4.5**).** The preSMA was significantly active as far back as 150 to 100 ms *before* the stop signal, with very strong activation occurring 50 to 0 ms prior to the stop signal and maintained past the estimated point at which SSRT elapses. By contrast, the rIFG was weakly active 100 to 50 ms before the stop signal, but did not become strongly active until about 50 to 100 ms *after* the stop signal, peaking between 100 and 150 ms, and then maintaining activation past the estimated SSRT.

DISCUSSION

We aimed to clarify the roles of the preSMA and the rIFG in action control. We designed a novel prepare-to-stop and outright-stop task, validated it with fMRI in healthy controls, and then examined ECoG during this task for a single rare patient with subdural coverage of the preSMA and rIFG. In healthy young controls fMRI showed that both the preSMA and the rIFG were more active for MS_Go compared to NS_Go trials – i.e. in preparation for stopping. By contrast, the rIFG alone was significantly active when comparing MS_SS and MS_Go trials – i.e. for outright stopping. We used the same behavioral paradigm in a single rare patient with intracranial grid coverage of both regions. In addition to task-related ECoG this patient was evaluated using several other methods. First, macrostimulation in the dorsomedial grid showed that only stimulation of the preSMA induced motor arrest. This method pointed especially to preSMA contact IH11. Second, deterministic tractography revealed that contact IH11 in particular had a projection to the rIFG region, with the correspondence closest to electrode LF16/15. Third, low intensity stimulation combined with simultaneous recording from all contacts showed that stimulation at IH11/12 induced CCEPs within 30 ms in rIFG, with LF16 showing one of the strongest responses. Together these results point to a structurally and functionally connected circuit between the preSMA and rIFG, and they specifically identify IH11 and LF16 as electrodes of interest for task-related ECoG. Examining these electrodes for preparing to stop showed high gamma amplitude increases with preSMA's activity

preceding that of rIFG. For outright stopping high gamma amplitude changes were again detected and again these changes occurred earlier for preSMA compared to rIFG. Furthermore, beta amplitude increases were also observed following the stop signal with greater coherence between the two regions when stopping was successful compared to when it was unsuccessful.

Preparing to stop and stopping outright: implications for theories of action control

For preparing to stop the ECoG results were mainly consistent with the fMRI results in healthy controls. There was an increase in high gamma activity, the frequency most closely associated with the BOLD signal (Logothetis et al., 2001; Corbetta and Shulman, 2002), for MS_Go vs. NS_Go trials in both the preSMA and the rIFG. Importantly, for MS_Go trials the preSMA response occurred even before the Go stimulus while the rIFG response began only after the Go stimulus – thus the preSMA preceded the rIFG. This timing difference speaks to different possible roles for each of these regions during action control. Since the preSMA was active early on and temporally nonspecifically, we speculate that it translates the stopping rule into the action system, and prepares other nodes in the 'network' to perform action control (Scheeringa et al., 2011). Within this network the rIFG may implement the action control by 'putting the brakes' on behavior (Conner et al., 2011). Such an account is in line with its observed activation around the response time. Thus rIFG may play an inhibitory control role in slowing down response emission on a MS trial, and stopping

the response outright on stop trials, perhaps via connections with the STN (Rushworth et al., 2004; Jahfari et al., 2009). This interpretation of relative roles for preSMA and IFG fits a recent TMS study of action control on switch trials (Swann et al., 2009). While their task differs from our own, it likely contains an 'outright stopping' component as the ongoing action is canceled in favor of an alternative one. The results showed that preSMA was engaged 125 ms after a switch signal while the rIFG was engaged at 175 ms. Further, disruption of preSMA with rTMS affected the functional connectivity between the rIFG and M1. These results, like our own, are consistent with the possibility that the preSMA plays a general task-configuration role by mediating rIFG function in action control.

A contrasting account argues that the rIFG is important for attentional monitoring/detection (Swann et al., 2011) while the preSMA implements inhibitory control (Hampshire et al., 2010; Neubert et al., 2010; Sharp et al., 2010). It is possible that the early preSMA engagement reflects 'setting up the inhibitory control' (the gamma response) and that rIFG monitors for the stop signal (gamma response) and detects it (beta response) and then conveys this information to the preSMA (coherent beta activity) which implements inhibitory control (beta response). However, the timing of action control in Neubert et al (2010) speaks against this account, and we also note that TMS (Duann et al., 2009) and fMRI studies (Mostofsky and Simmonds, 2008; Sharp et al., 2010; Verbruggen et al., 2010) suggest that the rIFG plays an inhibitory control role in addition to an attentional one. Indeed, the presence of beta

amplitude increases around the time of stopping in both regions argues against an attentional orienting role alone for the rIFG.

The coincident beta activity and coherence in both regions also suggests a third possibility: that inhibitory control is not implemented by the rIFG or the preSMA, but, rather, by the network as a whole including the basal ganglia (Kühn et al., 2004; Swann et al., 2011; Swann et al., 2009). Recently we reported that experimentally-induced modulation of the basal ganglia (specifically the subthalamic nucleus) alters the cortical signature of stopping in the beta band (Chikazoe et al., 2009b). This suggests that the beta band is important for long-distance communication between frontal cortex and the basal ganglia when stopping is needed, a notion supported by other observations of cortical-basal ganglia phase relationships in the beta band (Boehler et al., 2010; Cai and Leung, 2011). The current results are compatible with this 'wider network' view because there was coherent activity in the beta band for the preSMA and the rIFG, more so on successful stop trials, without clear phase-lag differences.

A fourth possibility, also related to the wider network account, is that stopping is implemented by the basal ganglia, perhaps specifically the subthalamic nucleus, and this drives strong synchronization of beta activity within an overall connected preSMA/IFG/STN network – i.e. the apparent coherence between the preSMA and rIFG may not reflect direct communication so much as the influence of a third (potentially subcortical) source. Clearly further research is required to tease apart these different theories of action control in relation to the different 'nodes' in this network.

The limitations of a single patient

As the ECoG study was based on a single, rare, patient (with both dorsomedial and right lateral coverage), we are mindful that it is important to replicate these findings using ECoG, MEG or other approaches and also to show that activity at the observed times is causally important for behavior (e.g. using disruptive techniques such as TMS). Nevertheless, the results in the patient show strong cross method consistency. There were tight relationships for the preSMA/rIFG network with macrostimulation, CCEP, DTI and ECoG – something that would difficult to establish in a group study without all these methodologies. They are also consistent with the fMRI study in the 16 healthy participants performing the same task. Taken together, the results provide further evidence for a structurally and functionally connected network between the preSMA and the rIFG. They also go further than extant reports in providing key information about the relative timing of preSMA and rIFG when preparing to stop, and also about the coherence between these regions when outright stopping is required.

Summary and Conclusions

We show that macrostimulation of a particular locus in the preSMA induced motor arrest; that lower intensity stimulation at this locus led to evoked responses at a specific locus in the rIFG within 30 ms, and that both of these loci were connected by white matter. Further, we showed, in the same patient, that these nodes of the

structural/functional network were also specifically engaged during task performance. The response at the preSMA preceded the rIFG when preparing to stop. This is consistent with the theory that that the preSMA plays a task-configuration function (e.g. to prepare the brain's network to stop) while the rIFG is important for monitoring for the environmental need to stop and/or implementing inhibitory control. When the stop signal occurred both the preSMA and the rIFG showed responses in the beta band – a good candidate for inter-regional communication, and there was strong coherence between these regions. We speculate that the different activity patterns in high frequency (gamma) vs. lower frequency (beta) could reflect differences in recruitment of individual regions and network properties, with higher frequencies being associated with local neural activity and lower ones with long distance communication (Crone et al., 1998; Fries, 2005; Sharott et al., 2005; Fogelson et al., 2006; Ray et al., 2008; Swann et al., 2011). These results for outright stopping suggest that either these two regions work together to achieve inhibitory control, or that inhibitory control is implemented via another node, such as the basal ganglia, with subsequent synchronization of the overall connected network. While the current results cannot clearly adjudicate between these different theories of action control, they provide novel information about the relative timing of recruitment of the preSMA and the rIFG and functional connectivity between them.

ACKNOWLEDGEMENTS

Funding is gratefully received from NIH grant DA026452 to A.R.A (PI) and N.T. (co-PI). N.S is supported by an NSF Graduate Student Fellowship and a NIH training grant via the Institute for Neural Computation at UCSD. NT is also supported by a Clinical and Translational Award KL2 RR0224149 from the National Center for Research Resources.

Chapter 4, in full, is a reprint of material as it appears in Neuroimage, 2012: Swann NC, Cai W, Conner RC, Pieters TA, Claffey MP, George JS, Aron AR, Tandon N. (2012) Roles for the presupplementary motor area and the right inferior frontal gyrus in stopping action: electrophysiological responses and functional and structural connectivity. The dissertation author was the primary investigator and author of this paper.

Table 4.1: Behavioral results. MS = Maybe Stop; NS = No Stop; ACC = Accuracy; SSD = stop signal delay; SSRT = Stop signal reaction time.

	Exp 1 fMRI: Mean (SD)	Exp 2 ECoG: Mean (SD)
NS_Go ACC (%)	98.6 (1.8)	94 (N/A)
NS_Go RT (ms)	404 (42)	491 (138)
MS_Go ACC (%)	98.1 (3.6)	93 (N/A)
MS_Go RT (ms)	533 (91)	618 (225)
MS_Stop ACC (%)	69.9 (9.1)	49 (N/A)
MS_Stop SSD (ms)	281 (80)	379 (84)
MS_Stop SSRT (ms)	182 (50)	239 (N/A)

Table 4.2: Macrostimulation results. The patient was tested at (i) rest (ii) while performing rapid hand closure and opening (such as making a signal for a flashing light) (iii) reading aloud and reciting the English alphabet. Channels shown in bold correspond to the anatomically defined preSMA. Current is in milliamperes, IH = interhemispheric electrodes (see Figure 4.2 for locations)

Electrode Pairs	**Current**	**Behavioral effects**
IH 1-2	**3**	**Cessation of coordinated movement & articulation**
IH 2-3	**4**	**Cessation of coordinated movement & articulation**
IH 3-4	5	Left leg flexion
IH 4-5, 5-6, 6-7, 7-8	10	No change
IH 8-9, 9-10	8	Visual hallucination: a pulsating phosphene in left inferior quadrant
IH 11-12	**8**	**Cessation of coordinated movement (bilaterally) & articulation**
IH 12-13	3	Left leg flexion
IH 13-14	4	Left arm and leg flexion and adduction
IH 14-15	4	Left arm abduction
IH 15-16	4	Left head versive movement, followed by whole body version
IH 16-17, 17-18, 18-19, 19-20	10	No change

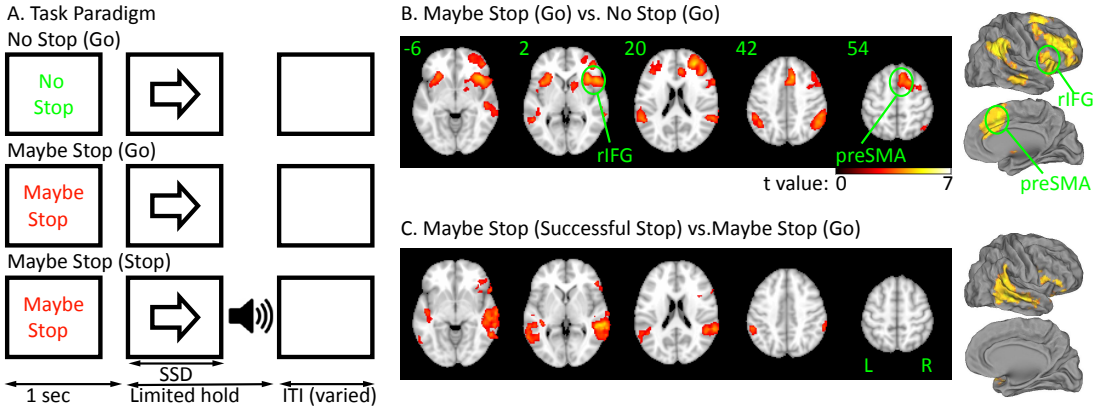


Figure 4.1: A. Task. Each trial began with a cue ("Maybe Stop" or "No Stop"). Then, a left or right arrow (go signal) followed. Participants were instructed to quickly respond. On half the "Maybe Stop" trials, a beep (stop signal) was presented shortly after the go signal. Participants were instructed to try to inhibit their response when the beep was presented. B. Brain activation for preparing to stop. The contrast is MS_Go vs. NS_Go ($z>2.3$, $p<0.05$ cluster corrected); C. Brain activation for outright stopping. The contrast is MS_SS vs. MS_Go ($z>2.3$, $p<0.05$ cluster corrected).

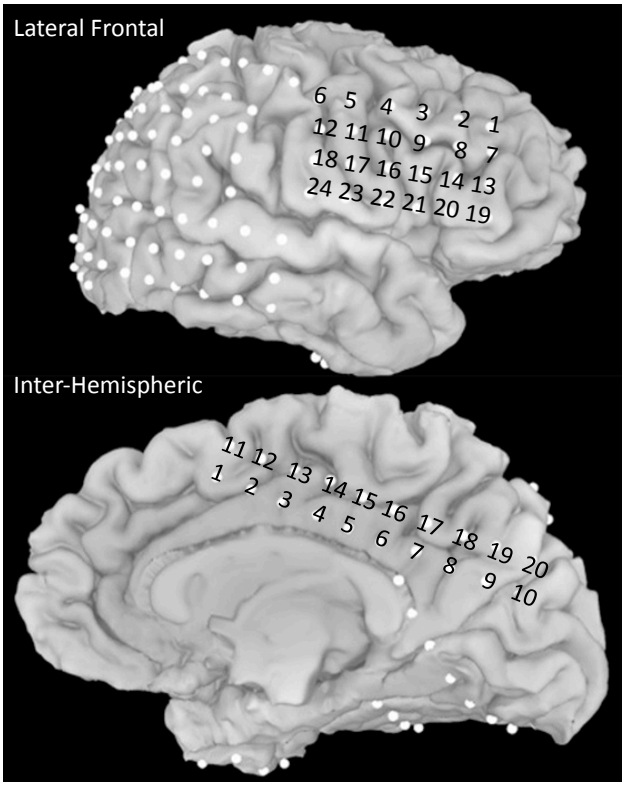


Figure 4.2: Electrode locations for all electrodes in the preSMA and rIFG regions. IH = interhemispheric, LF = lateral frontal.

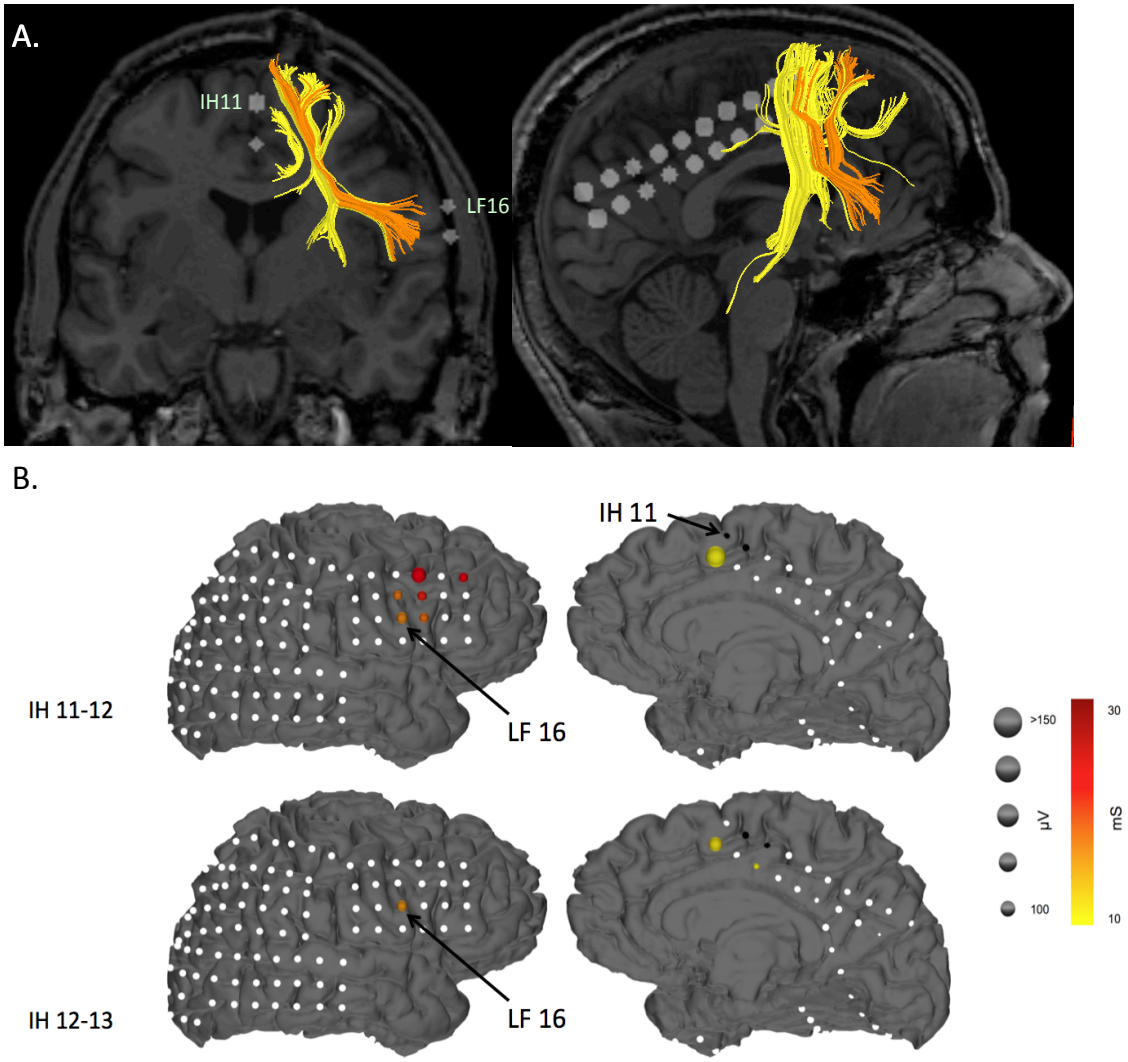


Figure 4.3: A. Diffusion Tensor Imaging. Ipsilateral tracts between the preSMA and the right lateral frontal cortex are shown (only fibers with a mean FA value of greater than 4 and a length > 20 mm were displayed). Note that IH11 (preSMA) specifically connects to LF16 (rIFG). B. Cortico-cortical Evoked Potentials. Evoked potentials occurring within 30 ms following stimulation of the IH electrodes overlying pre-SMA. Responses to 50 epochs were averaged and are diagrammatically represented for each stimulating pair. Stimulating electrodes are black, electrodes with no CCEPs are white. CCEP magnitude (peak) is represented by the size and the time to peak of the CCEP is represented by the color of the spheroids placed at site of the electrodes. Distinct and spatially specific responses were noted in rIFG and MFG with pre-SMA stimulation.

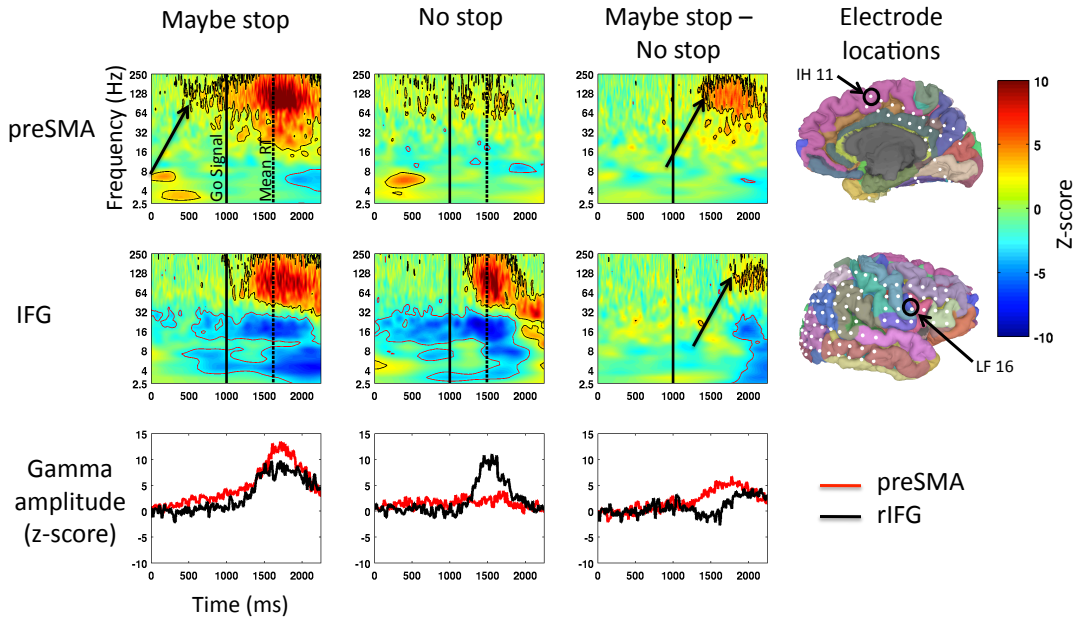


Figure 4.4: ECoG: Preparing to stop for preSMA and rIFG. Gamma amplitude increases in preSMA precede those in rIFG. Zero ms is the time of the MS/NS cue and 1000 ms is the time of the go signal (indicated by the solid black line). The dotted line indicates mean RT. Z-scored amplitude is expressed in color. All results significant at $p<0.05$, FDR corrected are outlined (black indicates significance in positive direction, red indicates negative direction). Average amplitude for gamma (90-130 Hz) is shown plotted over time in the bottom row.

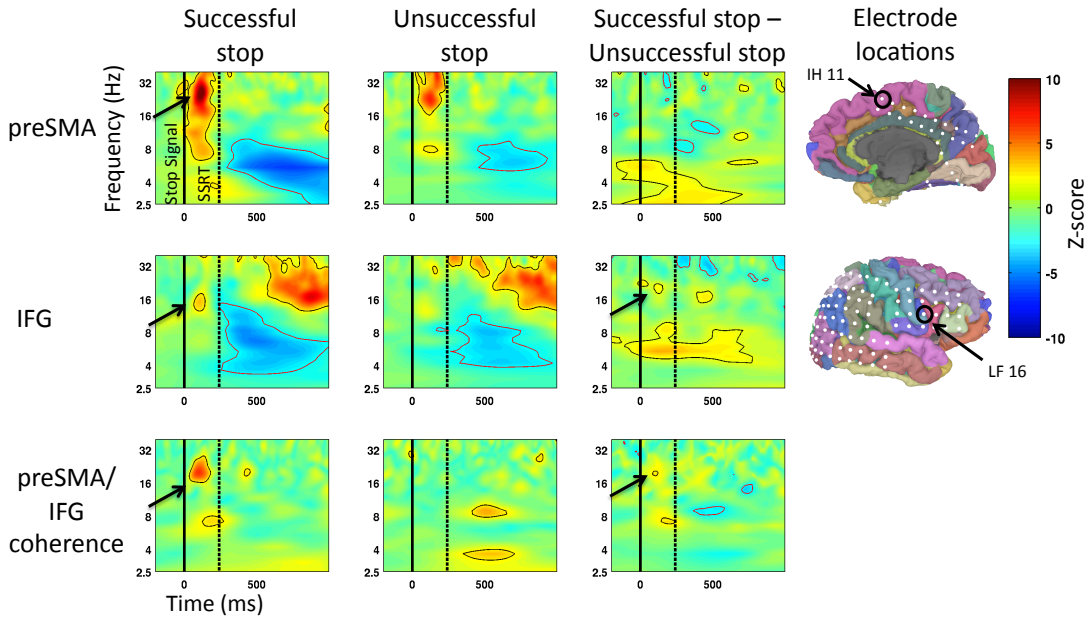


Figure 4.5: ECoG: Outright stopping for preSMA and rIFG. There are beta amplitude increases in both regions following the stop signal. Additionally, coherence between the two is greater for successful compared to unsuccessful stopping. Zero ms is the time of the stop signal (indicated by the solid black line). The dotted line indicates SSRT. For the top 2 rows, Z-scored amplitude is expressed in color. All results that are significant ($p<0.01$, uncorrected, for the conditions relative to baseline and $p<0.05$ uncorrected for the difference) are outlined (black indicates significance in positive direction, red indicates negative direction). For the bottom row Z-scored coherence values are expressed in color. All results that are significant ($p<0.01$, uncorrected) are outlined (black indicates significance in positive direction, red indicates negative direction).

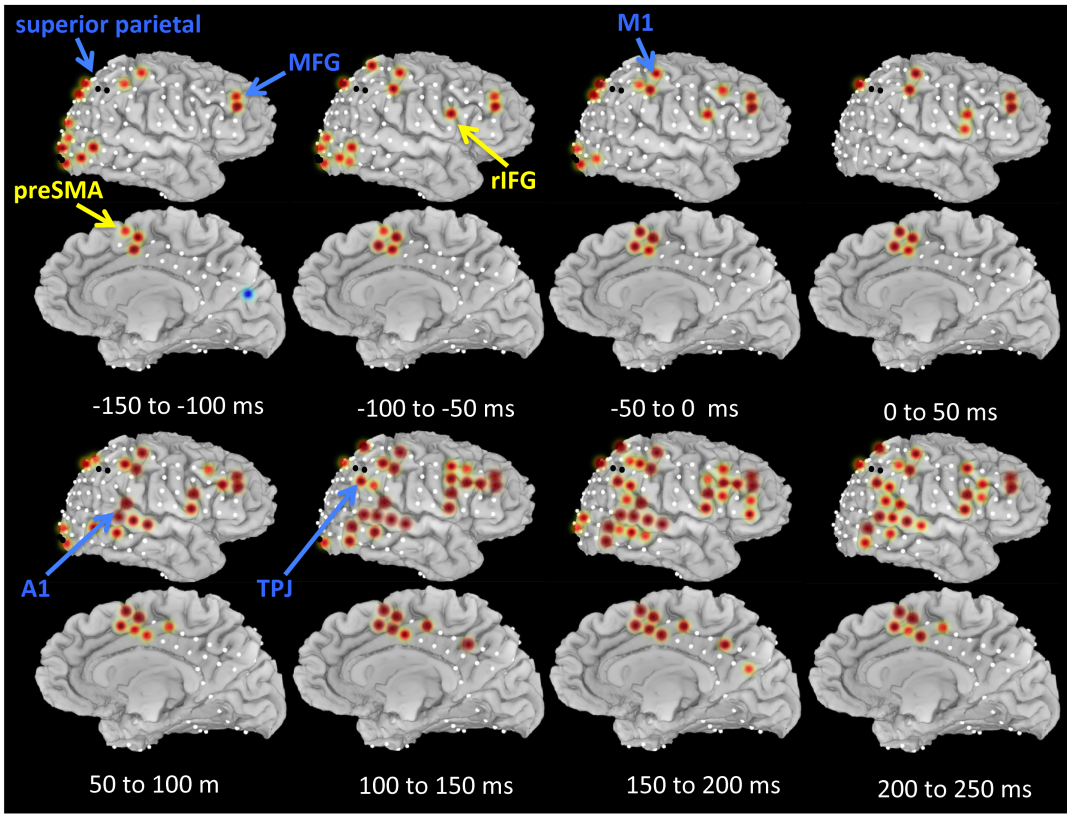


Figure 4.6: ECoG: Outright stopping for the wider cortical network in the gamma band. Average high gamma (100 Hz) amplitudes (z-scored) are shown in color (red for increases relative to baseline, blue for decreases) for sequential 50 ms windows with 0 ms corresponding to the stop signal. Only values significant at $p<0.01$ FDR corrected are shown. Electrodes for which no data were available are indicated with a black circle.

REFERENCES

Akers D, Sherbondy A, Mackenzie R, Dougherty R, Wandell B (2005) Exploring connectivity of the brain's white matter with dynamic queries. IEEE Trans Vis Comput Graph 11:419-430.

Aron AR (2010) From reactive to proactive and selective control: developing a richer model for stopping inappropriate responses. Biol Psychiatry 69:e55-68.

Aron AR, Poldrack RA (2006) Cortical and subcortical contributions to Stop signal response inhibition: role of the subthalamic nucleus. J Neurosci 26:2424-2433.

Aron AR, Behrens TE, Smith S, Frank MJ, Poldrack RA (2007) Triangulating a cognitive control network using diffusion-weighted magnetic resonance imaging (MRI) and functional MRI. J Neurosci 27:3743-3752.

Beckmann CF, Jenkinson M, Smith SM (2003) General multilevel linear modeling for group analysis in FMRI. Neuroimage 20:1052-1063.

Boehler CN, Appelbaum LG, Krebs RM, Hopf JM, Woldorff MG (2010) Pinning down response inhibition in the brain--conjunction analyses of the Stop-signal task. Neuroimage 52:1621-1632.

Cai W, Leung HC (2009) Cortical activity during manual response inhibition guided by color and orientation cues. Brain Res 1261:20-28.

Cai W, Leung HC (2011) Rule-guided executive control of response inhibition: functional topography of the inferior frontal cortex. PLoS One 6:e20840.

Canolty R, Soltani M, Dalal S, Edwards E, Dronkers N, Nagarajan S, Kirsch H, Barbaro N, Knight RT (2007) Spatiotemporal dynamics of word processing in the human brain. Front Neurosci 1.

Cavanagh JF, Cohen MX, Allen JJ (2009) Prelude to and resolution of an error: EEG phase synchrony reveals cognitive control dynamics during action monitoring. J Neurosci 29:98-105.

Chambers CD, Garavan H, Bellgrove MA (2009) Insights into the neural basis of response inhibition from cognitive and clinical neuroscience. Neurosci Biobehav Rev.

Chambers CD, Bellgrove MA, Stokes MG, Henderson TR, Garavan H, Robertson IH, Morris AP, Mattingley JB (2006) Executive "brake failure" following deactivation of human frontal lobe. J Cogn Neurosci 18:444-455.

Chevrier AD, Noseworthy MD, Schachar R (2007) Dissociation of response inhibition and performance monitoring in the stop signal task using event-related fMRI. Hum Brain Mapp 28:1347-1358.

Chikazoe J (2010) Localizing performance of go/no-go tasks to prefrontal cortical subregions. Curr Opin Psychiatry.

Chikazoe J, Jimura K, Hirose S, Yamashita K-i, Miyashita Y, Konishi S (2009a) Preparation to Inhibit a Response Complements Response Inhibition during Performance of a Stop-Signal Task. J Neurosci 29:15870-15877.

Chikazoe J, Jimura K, Asari T, Yamashita K, Morimoto H, Hirose S, Miyashita Y, Konishi S (2009b) Functional dissociation in right inferior frontal cortex during performance of go/no-go task. Cereb Cortex 19:146-152.

Conner C, Ellmore TM, Pieters TA, Disano M, Tandon N (2011) Variability of the Relationship between Electrophysiology and BOLD-fMRI across Cortical Regions in Humans. Journal of Neuroscience in press.

Corbetta M, Shulman GL (2002) Control of goal-directed and stimulus-driven attention in the brain. Nat Rev Neurosci 3:201-215.

Crone NE, Miglioretti DL, Gordon B, Lesser RP (1998) Functional mapping of human sensorimotor cortex with electrocorticographic spectral analysis. II. Event-related synchronization in the gamma band. Brain 121 (Pt 12):2301-2315.

Dale AM, Fischl B, Sereno MI (1999) Cortical surface-based analysis. I. Segmentation and surface reconstruction. Neuroimage 9:179-194.

Duann JR, Ide JS, Luo X, Li CS (2009) Functional connectivity delineates distinct roles of the inferior frontal cortex and presupplementary motor area in stop signal inhibition. J Neurosci 29:10171-10179.

Edwards E, Soltani M, Deouell LY, Berger MS, Knight RT (2005) High gamma activity in response to deviant auditory stimuli recorded directly from human cortex. J Neurophysiol 94:4269-4280.

Fogelson N, Williams D, Tijssen M, van Bruggen G, Speelman H, Brown P (2006) Different functional loops between cerebral cortex and the subthalmic area in Parkinson's disease. Cereb Cortex 16:64-75.

Ford A, McGregor KM, Case K, Crosson B, White KD (2010) Structural connectivity of Broca's area and medial frontal cortex. Neuroimage 52:1230-1237.

Forstmann BU, Anwander A, Schafer A, Neumann J, Brown S, Wagenmakers EJ, Bogacz R, Turner R (2010) Cortico-striatal connections predict control over speed and accuracy in perceptual decision making. Proc Natl Acad Sci U S A 107:15916-15920.

Fried I, Katz A, McCarthy G, Sass KJ, Williamson P, Spencer SS, Spencer DD (1991) Functional organization of human supplementary motor cortex studied by electrical stimulation. J Neurosci 11:3656-3666.

Fries P (2005) A mechanism for cognitive dynamics: neuronal communication through neuronal coherence. Trends in Cognitive Sciences 9:474-480.

Garavan H, Ross TJ, Stein EA (1999) Right hemispheric dominance of inhibitory control: an event-related functional MRI study. Proc Natl Acad Sci U S A 96:8301-8306.

Goldman-Rakic PS (1990) Cellular and circuit basis of working memory in prefrontal cortex of nonhuman primates. Prog Brain Res 85:325-335; discussion 335-326.

Hampshire A, Chamberlain SR, Monti MM, Duncan J, OWEN AM (2010) The role of the right inferior frontal gyrus: inhibition and attentional control. NeuroImage.

Jahfari S, Stinear CM, Claffey M, Verbruggen F, Aron AR (2009) Responding with Restraint: What Are the Neurocognitive Mechanisms? J Cogn Neurosci.

Johansen-Berg H, Behrens TE, Robson MD, Drobnjak I, Rushworth MF, Brady JM, Smith SM, Higham DJ, Matthews PM (2004) Changes in connectivity profiles define functionally distinct regions in human medial frontal cortex. Proc Natl Acad Sci U S A 101:13335-13340.

Kenner NM, Mumford JA, Hommer RE, Skup M, Leibenluft E, Poldrack RA (2010) Inhibitory motor control in response stopping and response switching. J Neurosci 30:8512-8518.

Khursheed F, Tandon N, Tertel K, Pieters TA, Disano MA, Ellmore TM (2011) Frequency-specific electrocorticographic correlates of working memory delay period fMRI activity. Neuroimage 56:1773-1782.

Konishi S, Nakajima K, Uchida I, Kameyama M, Nakahara K, Sekihara K, Miyashita Y (1998) Transient activation of inferior prefrontal cortex during cognitive set shifting. Nat Neurosci 1:80-84.

Leung HC, Cai W (2007) Common and differential ventrolateral prefrontal activity during inhibition of hand and eye movements. J Neurosci 27:9893-9900.

Levy BJ, Wagner AD (2011) Cognitive control and right ventrolateral prefrontal cortex: reflexive reorienting, motor inhibition, and action updating. Ann N Y Acad Sci 1224:40-62.

Logothetis NK, Pauls J, Augath M, Trinath T, Oeltermann A (2001) Neurophysiological investigation of the basis of the fMRI signal. Nature 412:150-157.

Luders H, Lesser RP, Dinner DS, Morris HH, Wyllie E, Godoy J (1988) Localization of cortical function: new information from extraoperative monitoring of patients with epilepsy. Epilepsia 29 Suppl 2:S56-65.

Luu P, Tucker DM, Makeig S (2004) Frontal midline theta and the error-related negativity: neurophysiological mechanisms of action regulation. Clin Neurophysiol 115:1821-1835.

Marco-Pallares J, Camara E, Munte TF, Rodriguez-Fornells A (2008) Neural mechanisms underlying adaptive actions after slips. J Cogn Neurosci 20:1595-1610.

Matsumoto R, Nair DR, LaPresto E, Bingaman W, Shibasaki H, Luders HO (2007) Functional connectivity in human cortical motor system: a cortico-cortical evoked potential study. Brain 130:181-197.

Matsumoto R, Nair DR, LaPresto E, Najm I, Bingaman W, Shibasaki H, Luders HO (2004) Functional connectivity in the human language system: a cortico-cortical evoked potential study. Brain 127:2316-2330.

Miller KJ, denNijs M, Shenoy P, Miller JW, Rao RPN, Ojemann JG (2007a) Real-time functional brain mapping using electrocorticography. Neuroimage 37:504-507.

Miller KJ, Leuthardt EC, Schalk G, Rao RPN, Anderson NR, Moran DW, Miller JW, Ojemann JG (2007b) Spectral changes in cortical surface potentials during motor movement. J Neurosci 27:2424-2432.

Mostofsky SH, Simmonds DJ (2008) Response Inhibition and Response Selection: Two Sides of the Same Coin. J Cogn Neurosci.

Muller NG, Knight RT (2006) The functional neuroanatomy of working memory: Contributions of human brain lesion studies. In: Neuroscience, pp 51-58.

Nachev P, Kennard C, Husain M (2008) Functional role of the supplementary and pre-supplementary motor areas. Nat Rev Neurosci 9:856-869.

Neubert FX, Mars RB, Buch ER, Olivier E, Rushworth MF (2010) Cortical and subcortical interactions during action reprogramming and their related white matter pathways. Proc Natl Acad Sci U S A 107:13240-13245.

Olesen PJ, Westerberg H, Klingberg T (2004) Increased prefrontal and parietal activity after training of working memory. Nat Neurosci 7:75-79.

Petrides M (2000) The role of the mid-dorsolateral prefrontal cortex in working memory. Exp Brain Res 133:44-54.

Picard N, Strick PL (2003) Activation of the supplementary motor area (SMA) during performance of visually guided movements. Cereb Cortex 13:977-986.

Ray S, Crone NE, Niebur E, Franaszczuk PJ, Hsiao SS (2008) Neural correlates of high-gamma oscillations (60-200 Hz) in macaque local field potentials and their potential implications in electrocorticography. J Neurosci 28:11526-11536.

Rubia K, Smith AB, Brammer MJ, Taylor E (2003) Right inferior prefrontal cortex mediates response inhibition while mesial prefrontal cortex is responsible for error detection. Neuroimage 20:351-358.

Rushworth MF, Walton ME, Kennerley SW, Bannerman DM (2004) Action sets and decisions in the medial frontal cortex. Trends Cogn Sci 8:410-417.

Saad ZS, Ropella KM, DeYoe EA, Bandettini PA (2003) The spatial extent of the BOLD response. Neuroimage 19:132-144.

Scheeringa R, Fries P, Petersson KM, Oostenveld R, Grothe I, Norris DG, Hagoort P, Bastiaansen MC (2011) Neuronal dynamics underlying high- and low-frequency EEG oscillations contribute independently to the human BOLD signal. Neuron 69:572-583.

Sharott A, Magill PJ, Bolam JP, Brown P (2005) Directional analysis of coherent oscillatory field potentials in the cerebral cortex and basal ganglia of the rat. The Journal of Physiology 562:951-963.

Sharp DJ, Bonnelle V, De Boissezon X, Beckmann CF, James SG, Patel MC, Mehta MA (2010) Distinct frontal systems for response inhibition, attentional capture, and error processing. Proceedings of the National Academy of Sciences:1-6.

Sherbondy A, Akers D, Mackenzie R, Dougherty R, Wandell B (2005) Exploring connectivity of the brain's white matter with dynamic queries. IEEE Trans Vis Comput Graph 11:419-430.

Swann N, Tandon N, Canolty R, Ellmore TM, McEvoy LK, Dreyer S, DiSano M, Aron AR (2009) Intracranial EEG reveals a time- and frequency-specific role for the right inferior frontal gyrus and primary motor cortex in stopping initiated responses. J Neurosci 29:12675-12685.

Swann N, Poizner H, Houser M, Gould S, Greenhouse I, Cai W, Strunk J, George J, Aron AR (2011) Deep brain stimulation of the subthalamic nucleus alters the cortical profile of response inhibition in the beta frequency band: a scalp EEG study in Parkinson's disease. J Neurosci 31:5721-5729.

Tandon N (2008) Cortical Mapping by Electrical Stimulation of Subdural Electrodes: Language areas. In: Textbook of Epilepsy Surgery (Luders HO, ed), pp 1001-1015. New York: Informa HealthCare.

Tertel K, Tandon N, Ellmore TM (2010) Probing brain connectivity by combined analysis of diffusion MRI tractography and electrocorticography. Comput Biol Med.

Trujillo LT, Allen JJ (2007) Theta EEG dynamics of the error-related negativity. Clin Neurophysiol 118:645-668.

van Elswijk G, Maij F, Schoffelen J-M, Overeem S, Stegeman DF, Fries P (2010) Corticospinal beta-band synchronization entails rhythmic gain modulation. J Neurosci 30:4481-4488.

Verbruggen F, Aron AR, Stevens MA, Chambers CD (2010) Theta burst stimulation dissociates attention and action updating in human inferior frontal cortex. Proc Natl Acad Sci U S A 107:13966-13971.

Vink M, Kahn RS, Raemaekers M, van den Heuvel M, Boersma M, Ramsey NF (2005) Function of striatum beyond inhibition and execution of motor responses. Hum Brain Mapp 25:336-344.

Womelsdorf T, Schoffelen JM, Oostenveld R, Singer W, Desimone R, Engel AK, Fries P (2007) Modulation of neuronal interactions through neuronal synchronization. Science 316:1609-1612.

Woolrich M (2008) Robust group analysis using outlier inference. Neuroimage 41:286-301.

Woolrich MW, Behrens TE, Beckmann CF, Jenkinson M, Smith SM (2004) Multilevel linear modelling for FMRI group analysis using Bayesian inference. Neuroimage 21:1732-1747.

Xue G, Aron AR, Poldrack RA (2008) Common neural substrates for inhibition of spoken and manual responses. Cereb Cortex 18:1923-1932.

Zandbelt BB, Vink M (2010) On the role of the striatum in response inhibition. PLoS One 5:e13848.

CHAPTER 5:

Intracranial EEG reveals dissociable roles for dorsal and ventrolateral prefrontal cortex in preparing to stop action

ABSTRACT

Preparing to stop an inappropriate action requires keeping in mind the task goal and using this to influence the action control system. We tested the hypothesis that different sub-regions of prefrontal cortex make dissociable contributions to preparing-to-stop, with dorsolateral prefrontal cortex (DLPFC) representing the task goal and ventrolateral prefrontal cortex (VLPFC) implementing action control. Five human subjects were studied using electrocorticography recorded from subdural grids over right lateral frontal cortex. On each trial, a task cue instructed the subject whether stopping might be needed or not (Maybe Stop or No Stop), followed by a go cue, and on some Maybe Stop trials, a subsequent stop signal. We focused on go trials alone, comparing Maybe Stop with No Stop. In the DLPFC, most subjects had an increase in high gamma activity around the task cue, although sometimes later. By contrast in the VLPFC, in all subjects, there was activity after the go cue, especially time-locked to the motor response on Maybe Stop trials, related to behavioral slowing, and significantly later than the DLPFC activity. These results suggest that DLPFC and VLPFC have dissociable roles, with the DLPFC representing the task goal and the VLPFC implementing action control.

INTRODUCTION

Much evidence shows that stopping an action outright (i.e. completely, and to an external signal) implicates a right hemisphere fronto-basal-ganglia network. This includes the

ventrolateral prefrontal cortex (VLPFC), the pre-supplementary motor area (preSMA) and the basal ganglia (reviewed by Aron et al., 2007b; Nachev et al., 2008; Chambers et al., 2009; Chikazoe, 2010; Levy and Wagner, 2011). However, everyday life not only requires us to stop outright but also to prepare to stop. Here we investigate the neural correlates of preparing to stop using the high spatio-temporal resolution of electrocorticography (ECoG).

Studies with fMRI have recently investigated this issue by designing tasks where preparing to stop can be separated from outright stopping. These studies show preparing to stop recruits some of the same prefrontal regions as outright stopping, including the preSMA and the right VLPFC (specifically the inferior frontal gyrus), and in addition, the dorsolateral prefrontal cortex (DLPFC) (Chikazoe et al., 2009b; Jahfari et al., 2010; Vink et al., 2005; Zandbelt et al., 2012; Zandbelt and Vink, 2010). The DLPFC finding is consistent with a role for representing goals in working memory (Goldman-Rakic, 1990; Petrides, 2000; Olesen et al., 2004; Muller and Knight, 2006) – in this case, the stopping task goal. This motivates the hypothesis that the DLPFC and VLPFC play dissociable roles in preparing to stop. Specifically, the DLPFC may represent the task goal while the VLPFC may implement action control –

by which we mean an active, although partial, suppression of the motor response (i.e. braking). A key aspect of this prediction is that the DLPFC and VLPFC activity should be temporally dissociable, with the DLPFC activity occurring early, around the time of a task goal cue (task cue) and the VLPFC activity occurring later, around the time when stopping is anticipated or perhaps around the time of the motor response itself. To test these predictions, we recorded ECoG in five subjects, each with electrode coverage of both DLPFC and VLPFC, while they performed a preparing-to-stop task.

On each trial, a stopping task cue was presented ("Maybe Stop" (MS) or "No Stop" (NS)), followed by a Go cue, and then, on the MS trials alone, a stop signal occurred half the time (Figure 5.1A). In a previous fMRI study with this task in healthy controls, we reported that the contrast of MS Go trials vs. NS Go trials activated the DLPFC bilaterally and the VLPFC in the right hemisphere, as well as the preSMA (Figure 5.1B). The preSMA is part of the stopping network, having functional and structural connectivity with the VLPFC and the subthalamic nucleus of the basal ganglia (Forstmann et al., 2010; Neubert et al., 2010; Swann et al., 2012), and all three of these regions show similar electrophysiological responses for outright stopping (Swann et al., 2009; Leventhal et al., 2012; Ray et al., 2012; Swann et al., 2012). However, in the current study, we focused uniquely on the DLPFC and VLPFC (where we had coverage in all subjects), to test the hypothesis about their distinct functional roles in preparing to stop. Notably, we examined Go trials only, to evaluate the neural correlates of preparing to stop, in a context in which there was always a

motor response. Specifically, we analyzed MS Go trials, NS Go trials, and the difference between them. We were interested especially in high gamma activity (~90-130 Hz) because of its association with local neural activity and the BOLD signal (Ray et al., 2008; Conner et al., 2011; Scheeringa et al., 2011).

Behaviorally, we expected that action control would be manifest as slower RT for MS Go vs. NS Go trials (the 'response delay effect', RDE, c.f. Chikazoe et al., 2009b; Jahfari et al., 2010; Swann et al., 2012; Zandbelt et al., 2012; Zandbelt and Vink, 2010). With ECoG we focused on two main aspects. First we tested the relative timing of activity in DLPFC vs. VLPFC. We expected increased gamma activity in the DLPFC around the time of the task cue and increased gamma activity in the VLPFC following the go cue. This would support dissociable roles for these regions. Second, we more closely examined the VLPFC to better understand its role in preparing to stop. Whereas fMRI shows increase activity in VLPFC for MS Go compared to NS Go, it is unclear when this difference occurs in time. We expected that ECoG, with its higher temporal resolution, would clarify this issue, and thus provide novel information about the functional role of right VLPFC.

METHODS

Participants

ECoG was recorded in 7 subjects with pharmacologically resistant epilepsy who underwent surgery for resection of seizure foci. All subjects provided informed consent under the auspices of the Internal Review Board at University of Texas at

Houston. Data from 2 subjects are not included in this report because of poor task performance (>30% omissions on Go trials). Thus the analysis focuses on 5 subjects (3 female, mean age 34 years, SD 9.8). All had right lateral frontal coverage that included the DLPFC and VLPFC and none of them had any evidence for right frontal abnormalities or underwent subsequent resection of these regions. One of these subjects (s2) was included in a previous report (Swann et al., 2012). However, here we focus on other aspects of this subject's data and also on the 4 additional subjects.

Task

We used a Maybe Stop (MS)/No Stop (NS) task, (Swann et al., 2012) (Figure 5.1A). Each trial began with a task cue presented for one second. The task cue was either "Maybe Stop" (red text on a black background) or "No Stop" (green text on a black background). Each cue was equally likely to occur. The task cue was followed by a go cue (white arrow), pointing to either the right or the left, to which subjects were instructed to respond with a button press. On half the MS trials an auditory beep followed the go cue, instructing the subjects to attempt to stop the motor response. In 3 subjects (s2, s4, and s5), the delay between the go cue and the stop signal (stop signal delay, SSD) was dynamically adjusted (for full details see Aron and Poldrack, 2006), with an initial delay set to 150 ms; while for the other 2 subjects (s1 and s3), SSDs were randomly selected from 3 individually-determined fixed values spaced 100 ms apart based on an initial training session. This procedural difference is not important for the current results. After the Go cue, there was a 1.5 second response window

followed by a jittered inter-trial interval (1-1.4 seconds). All subjects responded with their left hand (so that primary motor cortical responses could be recorded from the right lateral grids). The subjects performed either 6 or 7 blocks of the experiment, with 96 trials per block.

Behavioral Analysis

For each subject we calculated mean RT for MS and NS go trials (with RTs less than 100 ms excluded), the difference between the two (the response delay effect, RDE), the average stop signal delay (SSD), the percentage discrimination and omission errors on go trials, the percentage of successful stop trials and the RT for failed stop trials. We also estimated stop signal reaction time (SSRT) for each subject. For the subjects whose SSDs were determined using the "tracking" method (s2, s4, s5), SSRT was estimated with the "convergence method" (Logan et al., 1997); for the other two subjects SSRT was estimated with the "integration method" (Verbruggen and Logan, 2009). This procedural difference is not important for the current results.

Electrode Localization

Electrode localization procedures were the same as our previous reports (Swann et al., 2009; Swann et al., 2012). In brief, a CT scan was obtained after electrode implantation, and the scan was co-registered to a pre-implantation MRI scan. These electrodes were then projected onto a cortical surface model generated in

FreeSurfer (Dale et al., 1999). SUMA software was used to visualize the electrodes as spheres (Saad et al., 2003). Locations were verified with intra-operative photos.

ECoG acquisition and analysis

This was similar to our previous reports (Swann et al., 2009; Swann et al., 2012). Data were acquired with an EEG 1100 Neurofax clinical Nihon Koden acquisition system sampled at 1000 Hz. Trial onsets were sent to the EEG acquisition computer with transistor-transistor logic pulses.

The ECoG data were first digitally re-referenced to the common average, excluding channels with frequent artifacts or ictal contamination. Manual inspection was used to identify and exclude trials with either ictal activity that spread across channels or other sources of noise. Channels identified as seizure onset channels were also excluded from the entire analysis.

Analysis proceeded as follows. First, the data were filtered with Gabor wavelets into separate analytic amplitudes at 128 different center frequencies (ranging from 2.5-250 Hz) (see Canolty et al., 2007). Second, analytic amplitudes for each frequency were aligned to the task cue (for the main analysis), averaged across trials, and compared to an average baseline of 500 ms in the center of the inter-trial interval (-750 ms to -250 ms prior to trial start). Third, the average analytic amplitude values were converted to z-scores using a permutation technique where a standard deviation of the data was derived for each frequency from a distribution generated by repeating the above procedure 10,000 times, time-locking to random points in time (see Canolty

et al., 2007). For calculations of between-condition differences (MS Go vs NS Go) average analytic amplitude values for differences were directly subtracted (without a baseline correction applied), and z-scores were derived from an analogous permutation method as above, but now using 5,000 iterations of a label swapping procedure. Fourth, multiple comparisons were corrected using the false discovery rate method. Fifth, while some results show the full time-frequency spectrum, others are specifically focused on high gamma activity (~90-130 Hz). This is the frequency band that has been most closely linked to local neuronal activity, and to the BOLD signal (Ray et al., 2008; Conner et al., 2011; Scheeringa et al., 2011). For these analyses data were extracted from this frequency band (center frequency: 110Hz) and statistics were performed for this band separately.

RESULTS

Behavior

All five subjects performed well, having less than 3% discrimination errors on Go trials (i.e. errors where the incorrect button was pressed) and 10% or less omission errors on Go trials (see Table 5.1). The speed of stopping (SSRT) was in a typical range for ECoG subjects (Swann et al., 2009). Three of the five subjects (s1, s2, and s3) showed a significant response delay effect (RDE), with MS RT being significantly longer than NS RT, as in healthy participants (Chikazoe et al., 2009a; Jahfari et al., 2010; Swann et al., 2012). However, the other two subjects (s4 and s5) showed no significant RDE, perhaps because they had difficulty keeping this additional rule in

mind. Instead, they might have treated the task like a standard stopping task and thus anticipated stopping on *all* trials regardless whether they were in an MS or NS condition (such that a task goal and action control strategies were maintained for all trials, instead of for MS Go trials only). As these two subjects *did* perform the task well otherwise (i.e. their stopping behavior was typical), they are included in the ECoG analysis, and in fact the absence of the RDE is an informative control condition when examining their activity compared to the other subjects.

ECoG

Prefrontal activity when preparing to stop

Our hypothesis was that DLPFC represents the task goal (i.e. 'this is (or is not) a trial on which stopping may be needed') and that VLPFC implements action control, by which we mean an active, although partial, suppression of the motor response (i.e. braking). This predicts that DLPFC activity should occur in the task cue period, while VLPFC activity should occur later, perhaps following the go cue or around the time of the motor response.

To test this hypothesized difference for DLPFC and VLPFC we proceeded as follows: We identified electrodes with significant high gamma amplitude increases for either MS Go trials vs. baseline *or* for NS Go vs. baseline for at least 50 ms, to exclude spurious events ($p<0.05$, FDR corrected, for all electrodes and all time-points). Then, for each of these electrodes, we examined if MS Go activity was greater than NS Go, for at least 50 ms ($p<0.05$, FDR corrected for all electrodes and time-points

examined). The above steps were done separately for the two trial periods: i) the task cue period (defined as 1 second following the task cue) and ii) the go cue period (defined as 1 second following the go cue).

During the task cue period, for MS Go vs. baseline, three out of five subjects (s1, s3 and s5), exhibited significantly increased high gamma band activity in the prefrontal cortex, mainly in the DLPFC, i.e. in the middle frontal gyrus, or in and around the inferior frontal sulcus (Figure 5.2A). (Note, s2 also had DLPFC activity but it did not pass the corrected significance threshold for this particular analysis, but see Figure 5.3). However, for MS Go vs. NS Go there were no significant effects in prefrontal regions for any subject.

During the go cue period, for MS Go vs. baseline, each of the 5 subjects had significant activity in the VLPFC, i.e. in the ventral inferior frontal gyrus or in and around the precentral sulcus (Figure 5.2B). Additionally, for MS Go vs. NS Go there was activity in the VLPFC in three out of five subjects (s1, s2 and s3), and notably *all* of these subjects had significant slowing (the RDE), whereas the two subjects who did not have a significant difference in activity (s4 and s5) had an RDE close to zero. This supports the notion that the MS vs. NS activity difference in the VLPFC could relate to the behavioral slowing effect. We speculate that subjects without an RDE were perhaps exercising proactive control on <u>all</u> trials, and thus showed no difference between the two trial-types in VLPFC, but still exhibited above-baseline activity in these regions for both trial types, and see below for more on this.

For a more complete picture of the temporal dynamics of activity we also examined high gamma amplitudes for the full time course (amplitude averaged over 100 ms for each time-bin, and converted to a z-score, $p<0.05$ FDR corrected for all electrodes and time-bins), see Figure 5.3 for representative subject s2. Note that the DLPFC shows bursts of activity ~300 after the MS cue and ~200 ms after the go cue, while the VLPFC shows activity mainly after the go cue, peaking around the time of the motor response. There is also activity in occipital cortex around the time of the visual stimulus and in the precentral gyrus around the time of the motor response, providing validation of the ECoG processing stream and of the electrode localization method.

Activity in the DLPFC precedes the VLPFC

The comparison of task cue and go cue periods (Figure 5.2A vs. 5.2B) suggests a timing difference in DLPFC and VLPFC. We formally tested this as follows: A) For each subject, for the period of 500 ms before the task cue and 1 second after the go cue (i.e. a 2500 ms window), electrodes were identified in DLPFC and VLPFC which showed significant activity for MS Go vs. baseline ($p<0.05$, FDR corrected for all electrodes within each ROI and all time-points). (Note that for s4 there was no DLPFC electrode in either time window that surpassed the FDR corrected threshold, so for this analysis, for s4 alone, the threshold was lowered to $p<0.01$, uncorrected to select a DLPFC electrode.) B) For all of these electrodes, we found the time point (relative to the MS cue) where the high gamma amplitude first became significantly greater than

baseline (for subjects with more than one significant DLPFC or VLPFC electrode the onsets for all electrodes in each ROI were averaged). C) We performed a paired t-test across the 5 subjects on the latency values for DLPFC vs. VLPFC. The main result was that the DLPFC was active before the VLPFC ($p=0.0136$, $t=4.2$, $df = 4$), and this was true in each subject (Figure 5.2C). (Note that because there were no differences in average amplitude or standard deviation between the DLPFC and VLPFC ($p\sim0.9$ for each), it is unlikely that the difference in onset times is an artifact of different signal-to-noise properties of the two regions.)

We also examined the DLPFC/VLPFC timing difference using a second method. We performed a single trial analysis for MS Go trials for all the DLPFC and VLPFC channels that had significantly above baseline high gamma activity. The dependent variable for each trial, in DLPFC or VLPFC, was the time of maximum high gamma amplitude. DLPFC showed a relatively narrow peak after the MS cue and another broader and slightly smaller one after the Go cue (Figure 5.2C). Thus the DLPFC responds similarly to both the task cue and the go cue. The VLPFC, by contrast, had its largest peak after the go cue around the time of the response. This single trial analysis supports the above impressions (Figures 5.2A,B) that the DLPFC is active after both the task cue and the go cue while the VLPFC is active primarily after the go cue.

To give a more comprehensive picture, spectral plots are shown from an electrode from each region for one representative subject (s3) (Figure 5.4A). For this subject the DLPFC had significant high gamma activity shortly after the task cue, and

did not differentiate between MS Go vs NS Go. By contrast, the VLPFC was active only after the go cue, and significantly more for MS Go compared to NS Go ($p<0.05$, FDR corrected for all frequencies, time-points, and conditions). For comparison, we also show VLPFC activity from s4, who failed to show an RDE (Figure 5.4B). Note that the MS Go activity pattern for this subject was very similar to s3. However, s4, did not show a significant difference between MS Go and NS Go, and likewise had no behavioral difference either (no RDE).

The role of the VLPFC in preparing to stop

These different temporal activation patterns for DLPFC vs. VLPFC suggest different roles in preparing to stop action. In the current task, DLPFC could perhaps encode, maintain, rehearse or retrieve the stopping rule. The VLPFC, by contrast, is primarily active later in the go phase around the time of the response, consistent with a role in either action control (Aron et al., 2003; Chambers et al., 2006; Aron et al., 2007b; Chambers et al., 2007; Jahfari et al., 2010; Neubert et al., 2010), attentional monitoring for the stop signal (Chao et al., 2009; Duann et al., 2009; Hampshire et al., 2010; Sharp et al., 2010; Boehler et al., 2011; Chatham et al., 2012), both of these, although perhaps in dissociable sub-regions (Chikazoe et al., 2009b; Chikazoe, 2010; Verbruggen et al., 2010; Levy and Wagner, 2011), as well as other possible accounts such as a violation of expectancies about stopping (Zandbelt et al., 2012). We speculated that if the VLPFC is important for action control, i.e. as a brake, than its

activity might relate to the time of the motor response (especially in the 'executive' setting of MS Go trials).

To investigate this, we plotted spectral data for MS Go trials from a VLPFC electrode for each subject time-locked to the MS cue (Figure 5.5, left column) and to the reaction time (Figure 5.5, middle column). For s1-3, the electrode is the one that showed the MS Go greater than NS Go difference (see Figure 5.2B). (Note that s2 and s3 had two neighboring electrodes with this difference. While all showed a similar pattern, we show results from the one that was more clearly within the VLPFC for each subject). For subjects s4 and s5, no electrodes had an MS Go vs. NS Go difference, therefore we show the VLPFC electrode with an MS Go vs. baseline difference (shown in Figure 5.2B). For all subjects the VLPFC activity was roughly centered around the time of the motor response, usually starting well before, and continuing well after. These results point to a relationship between the VLPFC and the motor response (especially on MS Go trials). While this is consistent with a role for the VLPFC in action control, the fact that the activity was spread across time could also be consistent with other accounts, such as attentional monitoring for the stop signal. If this is the case, than its engagement should be most prominent around the time of the expected stop signal (i.e. the stop signal delay, SSD) rather than the time of the motor response. To test this, we conducted a single trial analysis sorted by either RT, or a proxy for expected SSD (based on the SSD from the last stop trial). For s2 and s5, the VLPFC electrode shown in Figure 5.5 had high gamma activity that corresponded more strongly with RT than with the time of expected SSD (Figure 5.6).

For the other three subjects the single trial analysis did not reveal any clear patterns when sorted by either variable.

DISCUSSION

We recorded ECoG from right lateral grids in 5 subjects while they performed the Maybe Stop/No Stop task. The analysis mainly focused on high gamma activity in the task cue period and following the go cue. In most subjects, there was DLPFC activity around the task cue and/or around the go cue. By contrast, in all subjects, there was activity in the VLPFC after the go cue, especially around the time of the motor response on Maybe Stop trials, and significantly later than the DLPFC activity. For the VLPFC, the activity on Maybe Stop trials was more closely time-locked to the motor response than it was to the anticipated time of the stop signal, and it was greater, relative to No Stop trials, in subjects who slowed down in anticipation of stopping compared to those who did not. These results suggest that the DLPFC and VLPFC play dissociable roles, with the DLPFC representing the task goal and the VLPFC implementing action control, perhaps specifically by 'braking' the initiated motor response when stopping is anticipated. This speaks to current theories of action control as well as the debate about the functional specialization of the prefrontal cortex.

Functional role of the DLPFC

Preparing to stop a response requires having a stopping task goal and also using this information to control the response tendency. A strong candidate region for

representing the stopping goal is the DLPFC , based on much evidence implicating it in working memory (Goldman-Rakic, 1990; Fuster, 1997; Petrides, 2000; Olesen et al., 2004; Muller and Knight, 2006). Consistent with this, functional MRI shows greater activity in DLPFC for preparing to stop (Chikazoe et al., 2009b; Jahfari et al., 2010; Swann et al., 2012; Zandbelt et al., 2012; Zandbelt and Vink, 2010), although in most studies it was not possible to establish when this difference occurred, i.e. during the task cue or go cue phase (but see Zandbelt et al., 2012). Here we used ECoG to show that DLPFC was active for MS Go versus baseline, and moreover, we could elucidate the timing. We found that DLPFC activity was not tightly linked to the time of the response/action control, but instead to the task cue and/or the go cue. It thus appears that the DLPFC encodes the task goal following the task cue and then shows a reactivation following the go cue, perhaps reflecting task goal retrieval.

The fact that significant DLPFC activity was observed around the go cue and not the task cue for some subjects could reflect a statistical thresholding issue and/or stronger reactivation or retrieval of the stopping rule as the response period draws near (i.e. when that information is most temporally pertinent). Notably, activity in the DLPFC preceded VLPFC in all subjects, which speaks to different functional roles for these regions.

Functional role of the VLPFC

Activity in the VLPFC had several features: 1) it occurred after the go cue and more specifically around the time of the response, 2) it was later than activity in the

DLPFC for all subjects, 3) it was greater for MS Go than NS Go for the three subjects who showed a behavioral RDE and not for the two who did not, 4) in two subjects, activity was more tightly related to RT than the expected SSD on a single-trial level. This pattern of data provides novel information about the temporal activations of the right VLPFC in preparing to stop, and speaks to a debate about the functional role of the right VLPFC in cognitive control. Whereas the right VLPFC is critical for the outright stopping of action (Aron et al., 2003; Chambers et al., 2006; Chambers et al., 2007; Verbruggen et al., 2010), its underlying functional role could reflect the active suppression of a response (entirely or partially), i.e. "action control" (Aron et al., 2007a; Jahfari et al., 2010), attentional monitoring (Hampshire et al., 2010; Sharp et al., 2010; Chatham et al., 2012), violation of a stopping expectancy (Zandbelt et al., 2012), or some combination of these (Chambers et al., 2009; Boehler et al., 2010; Chikazoe, 2010; Aron, 2011; Levy and Wagner, 2011).

The action control account proposes that there is slowing on MS Go trials because of partial suppression of the emitted response, and that VLPFC implements this. This is analogous to a brake that is applied as movement occurs. This predicts VLPFC activity around the time of the motor response. By contrast, the attentional monitoring account proposes that the VLPFC is monitoring for the stop signal, which predicts earlier activity, around the time of SSD. Yet, we show that the VLPFC activity in all subjects is centered around the motor response, and in two subjects, the single trial analysis clearly showed that this activity was much more tightly locked to

RT than the estimated SSD. Thus, the results are more compatible with the action control account.

While attentional monitoring is implicit in the stop signal paradigm, since one could not stop unless one detected a signal to stop, and while it is possible that VLPFC plays a role in such attentional monitoring (Corbetta and Shulman, 2002), the current data argue that VLPFC's role is not merely one of attentional monitoring. Instead, there is likely a sector that implements action control.

It is unclear how these results speak to the violation of stopping expectancy account. Based on fMRI, Zandbelt at al. (2012) proposed that VLPFC activity on go trials, in which stopping was not needed, although it was expected, reflected a violation of stopping this expectancy. Such an interpretation would be consistent with our results, provided that it is the motor response that instantaneously triggers the realization that the stop signal did not occur.

In any event, other data argue for a role for VLPFC in action control. For example, two studies using paired-pulse Transcranial Magnetic Stimulation, with one coil on right VLPFC and the other on M1, showed that VLPFC had a suppressive effect on the M1 for two kinds of response control task (Buch et al., 2010; Neubert et al., 2010).

Thus, the VLPFC activity may reflect action control that is applied as the response is being made (i.e. braking). More specifically, the right VLPFC, which is critical for stopping outright at the behavioral level, and putatively plays a role in implementing inhibitory control by projecting to the preSMA and the basal ganglia to

cancel motor output (Aron et al., 2007b), may also be recruited proactively, when stopping is anticipated. Accordingly, the proactive recruitment of the VLPFC might have the consequence that if a response is initiated it also dampened/slowed. Future studies could bolster this interpretation by, for example, using paired-pulse TMS to reveal if right VLPFC has inhibitory effects over the motor system when preparing to stop, or using electrical stimulation during task performance.

Limitations

First, the data are from epilepsy subjects and may not generalize well to the healthy population. However, some of the findings clearly were consistent across all or most of the five subjects. Further, the findings corresponded well with extant fMRI studies of preparing to stop (Chikazoe et al., 2009b; Jahfari et al., 2010; Swann et al., 2012; Zandbelt et al., 2012; Zandbelt and Vink, 2010). Further, all subjects had epileptic foci outside of the reported regions. Second, the sample size, while acceptable by the standard of ECoG studies, is small, particularly for examining differences between individuals (i.e. whether or not behavioral slowing, the RDE, was present). Further, an important result, that single-trial gamma activity in the right VLPFC tracked RT more tightly than expected SSD, could only be established in two subjects (probably because single-trial analyses are noisy, particularly in prefrontal regions). This limits the strength of the conclusion that can be drawn. Third, for two of the subjects there was no slowing down (RDE) for MS vs. NS Go trials, running against a common observation in normative populations (Chikazoe et al., 2009b;

Jahfari et al., 2010; Swann et al., 2012; Zandbelt et al., 2012; Zandbelt and Vink, 2010). We suggest they were preparing to stop on every trial, and so were not differentially sensitive to the MS vs. NS cues. However, their stopping and other task performance was otherwise satisfactory, and the absence of an RDE along with a null ECoG difference for MS Go vs NS Go, provided a nice control. Fourth, some of the electrodes with similar functional properties were in different locations across subjects with reference to gyral/sulcal landmarks. Yet it well established that there is high variability in the gyrification and cytoarchitecture of prefrontal regions (Amunts et al., 1999).

Conclusions and Implications

Our results speak to a long-standing debate about the functional specialization of the prefrontal cortex. Whereas some have argued that the primary functional role of the prefrontal cortex is working memory (with different sectors processing different kinds of information) (Goldman-Rakic, 1996), others have argued that different sectors perform different functions such as working memory, attention, inhibitory control, etc. (Fuster, 1997). The current results argue for functional specialization, with DLPFC implementing working memory for the task goal, and VLPFC implementing action control.

Within VLPFC, we more specifically observed that the activity was around the time of the motor response, rather than around the time of the estimated stop signal. This, along with other results (Buch et al., 2010; Jahfari et al., 2010; Neubert et al.,

2010) speaks in favor of a role for right VLPFC in actively braking response tendencies. This action control mechanism over response tendencies, implemented via the right VLPFC, could operate in concert with the basal ganglia and/or the primary motor cortex (Vink et al., 2005; Jahfari et al., 2010; Zandbelt and Vink, 2010).

This interpretation suggests that the task goal (represented in DLPFC) must convey information to the VLPFC. However, communication between these regions may not be direct. One possibility is that the preSMA may mediate communication between the two. This account is supported by ECoG data from our previous report where the preSMA was active between the early DLPFC activity and the later VLPFC activity in one unique subject with subdural coverage in all these areas (Swann et al., 2012). This observed timing pattern is consistent with a paired-pulse TMS study using a response control task which showed preSMA's influence on primary motor cortex preceded VLPFC, and that VLPFC's influence on primary motor cortex depended on preSMA (Neubert et al., 2010). It is possible that the preSMA plays a role in task configuration (Rushworth et al., 2004), one aspect of which is translating the working memory rule into the action system. Thus, the preSMA may mediate the putative transfer of information from DLPFC to VLPFC when preparing to stop. Clearly, future research is required to develop a richer understanding of the functional roles and neural communication of different regions within this overall putative response control network.

In conclusion, the current data provide a more mechanistic understanding of human self-control. They point to a dissociation between the task goal and the

implementation of action control in different sectors of prefrontal cortex, and they provide insight into why people respond more cautiously when they might have to stop.

ACKNOWLEDGEMENTS

Chapter 5, in full, has been submitted for publication of materials as it may appear in Cerebral Cortex, 2012: Swann NC, Tandon N, Pieters TA, Aron AR, Tandon N. (2012) Intracranial EEG reveals dissociable roles for dorsal and ventrolateral prefrontal cortex in preparing to stop action. The dissertation author was the primary investigator and author of this paper.

Funding is gratefully received from NIH grant DA026452 to A.R.A. N.S was supported by an NSF Graduate Student Fellowship, an NIMH training grant via the Institute for Neural Computation at UCSD, and an NSF GK-12 fellowship. N.T is supported by a Clinical and Translational Award KL2 RR0224149 from the National Center for Research Resources. Thanks to John Serences for his helpful comments on the manuscript.

Table 5.1. Behavioral Results: MS = Maybe Stop Go RT; NS = No Stop Go RT; RDE = Response Delay effect (mean MS RT – mean NS RT); Disc. Errors = percentage discrimination errors; Omissions errors = percentage omission errors; Failed Stop RT = mean RT on failed stop trials; SSRT = stop signal reaction time; Percent stop= percentage of stop trials with successful stopping.

Subjects	Mean MS RT (SD) ms	Mean NS RT (SD) ms	RDE ms	Disc. Errors (%)	Omission Errors (%)	Failed stop RT (SD) ms	SSRT	Percent inhibit (%)
S1*	700(168)	552(125)	148	1.0	10	603(114)	271	56
S2*	618(225)	491(138)	127	1.7	3.5	540(172)	239	49
S3*	735(168)	535(136)	200	2.2	2.4	653(121)	124	71
S4	861(325)	831(313)	30	1.6	0	645(160)	219	49
S5	598(140)	596(139)	2	.2	.8	524(163)	469	39

*significant response delay effect (MS RT sig greater than NS RT)

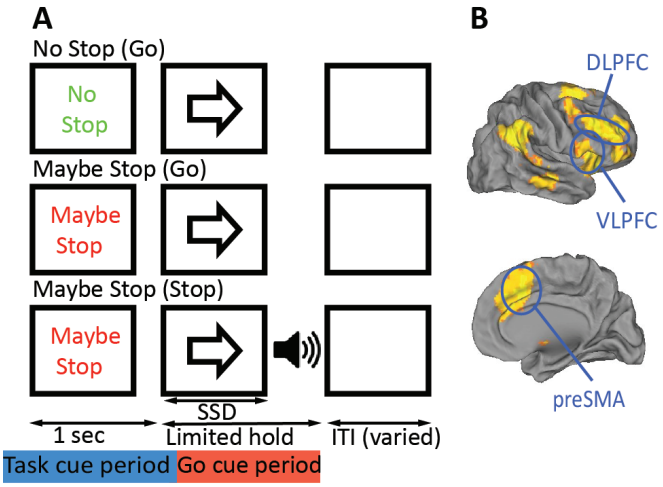


Figure 5.1: A. Task. Each trial begins with a task cue, either "No Stop" (NS) or "Maybe Stop" (MS), followed by an arrow pointing left or right. Subjects were instructed to respond with a button press to the arrows as quickly as possible. On half of the MS trials an auditory beep followed the arrow and indicated that subjects should attempt to stop the initiated response. The task cue phase (blue) and go cue phase (red) are marked to indicate each phase of the task for reference in subsequent figures. B. Functional MRI activation for MS Go trials compared to NS Go showing activation of preSMA, right VLPFC, and DLPFC. ($z>2.3$, $p<0.05$, cluster corrected) in 16 healthy subjects (Permission pending from (Swann et al., 2012)).

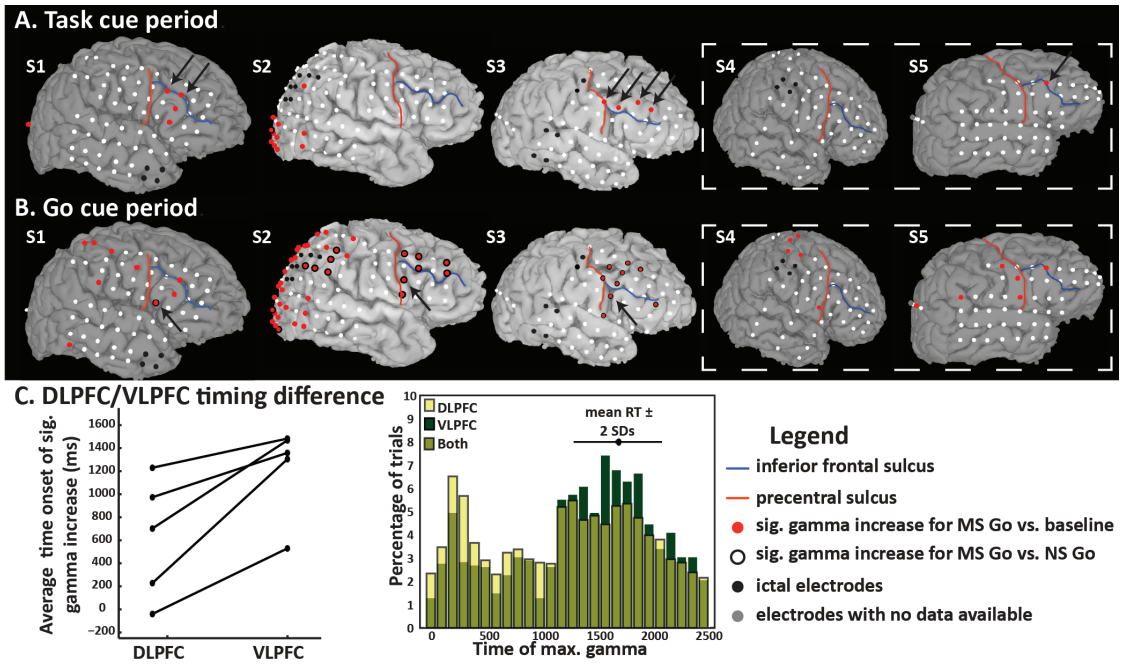


Figure 5.2: A-B. DLPFC and VLPFC activity in the task cue and go cue periods. A. The task cue period (i.e. one second following the MS cue). For most subjects, there is activity in and above the inferior frontal sulcus (i.e. DLPFC) for MS Go vs. baseline, but not for the comparison of MS Go vs NS Go. B. The go cue period (i.e. one second following the go signal). In all subjects, there is activity in and around the precentral suclus (i.e. VLPFC) and there are also differences between MS Go and NS Go for the 3 subjects who had significant behavioral slowing (RDE). Red electrodes denote significantly greater high gamma amplitude (110 Hz) for MS Go vs. baseline and black circles denote significant MS Go vs NS Go trials ($p<0.05$, FDR corrected). The dotted rectangles denote the two subjects who did not slow down in preparation for stopping. C. DLPFC precedes VLPFC. Left panel: For all subjects the time of significant gamma in DLPFC occurred earlier than VLPFC. Zero ms is the time of the "Maybe Stop" cue and 1000 ms is the time of the go signal. Right panel: Pooling across the channels in the left panel, a single trial analysis reveals that DLPFC activity increases after both the task cue and the go cue, while VLPFC mainly increases after the go cue and after DLPFC. Zero ms is the time of the MS cue and 1000 ms is the time of the go signal.

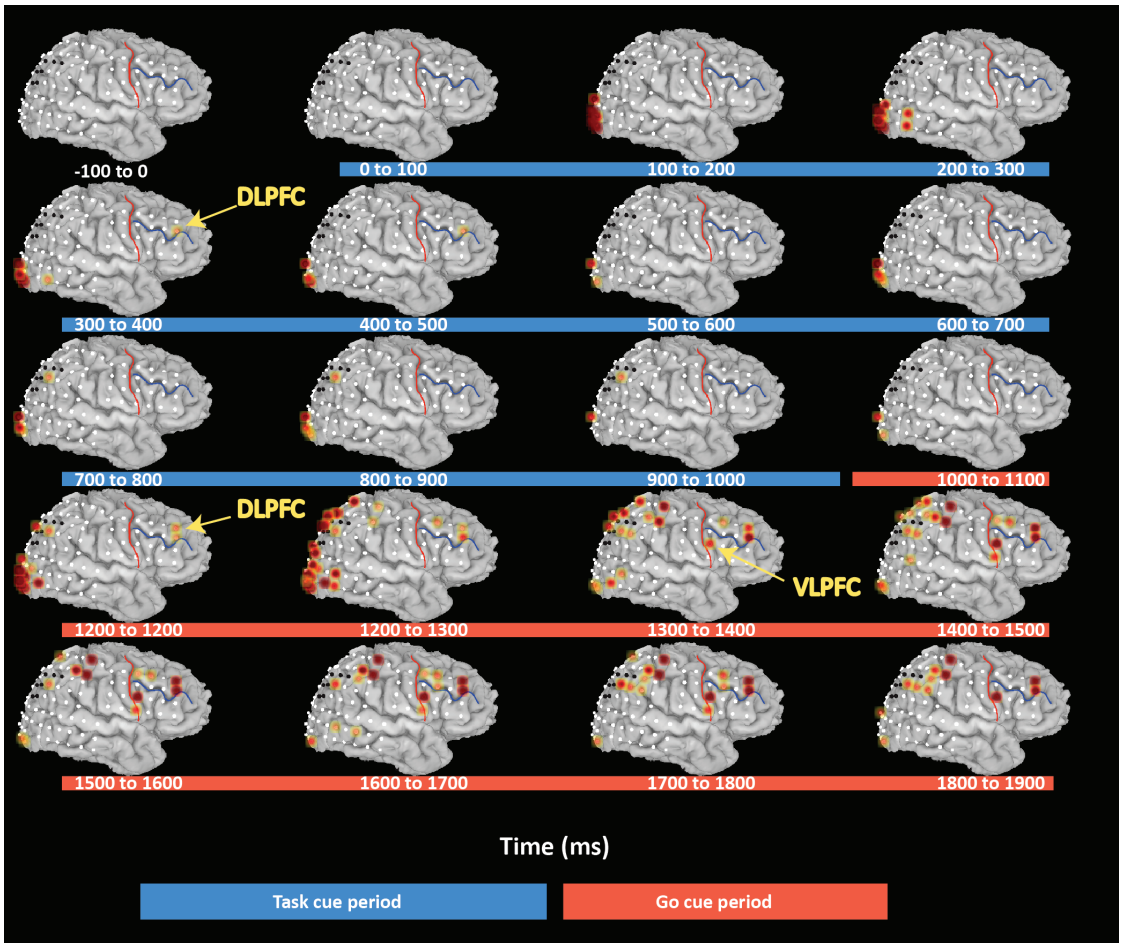


Figure 5.3: The full dynamic picture of activity for a single subject during a preparing to stop trial. DLPFC was active after both the MS cue and the go cue, and VLPFC was active later, most strongly around the time of the motor response. For subject s2, the active electrodes denote those with significant high gamma activity (z-scores) for MS Go vs baseline for each time bin ($p<0.05$, FDR corrected). The MS cue occurred at 0 ms, the go cue occurred at 1000 ms, and for this subject average RT was 618 ms (1618 ms relative to the MS cue).

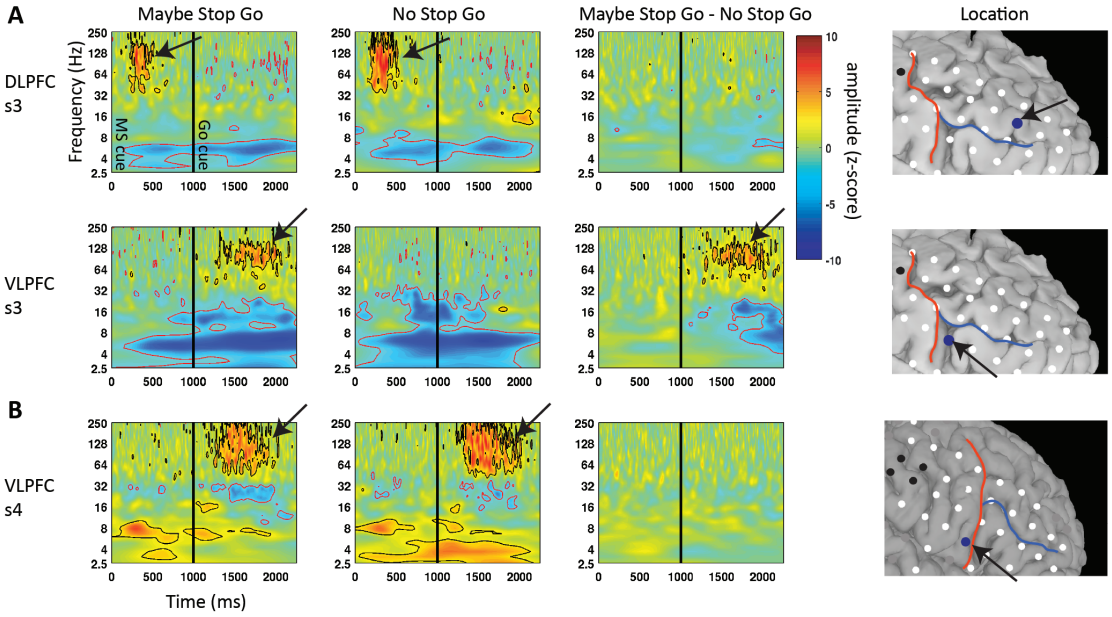


Figure 5.4: Representative spectral plots for DLPFC and VLPFC for preparing to stop. A. For s3 high gamma amplitude increases are visible for both DLPFC and VLPFC, with DLPFC preceding VLPFC. Note that only VLPFC shows a significant difference for MS Go compared to NS Go ($p<0.05$, FDR corrected). B. For a subject that did not show behavioral slowing (s4), the high gamma increases relative to baseline are still present (and are similar in time to s3), but there is no difference for MS Go vs. NS Go. Zero ms is the time of the task cue, 1000 ms is the time of the go signal. Amplitude is expressed in color as a z-score. Significant values ($p<0.05$, FDR corrected) are outlined (black indicates positive differences, red indicates negative differences). Electrode locations are indicated in blue for each subject and region.

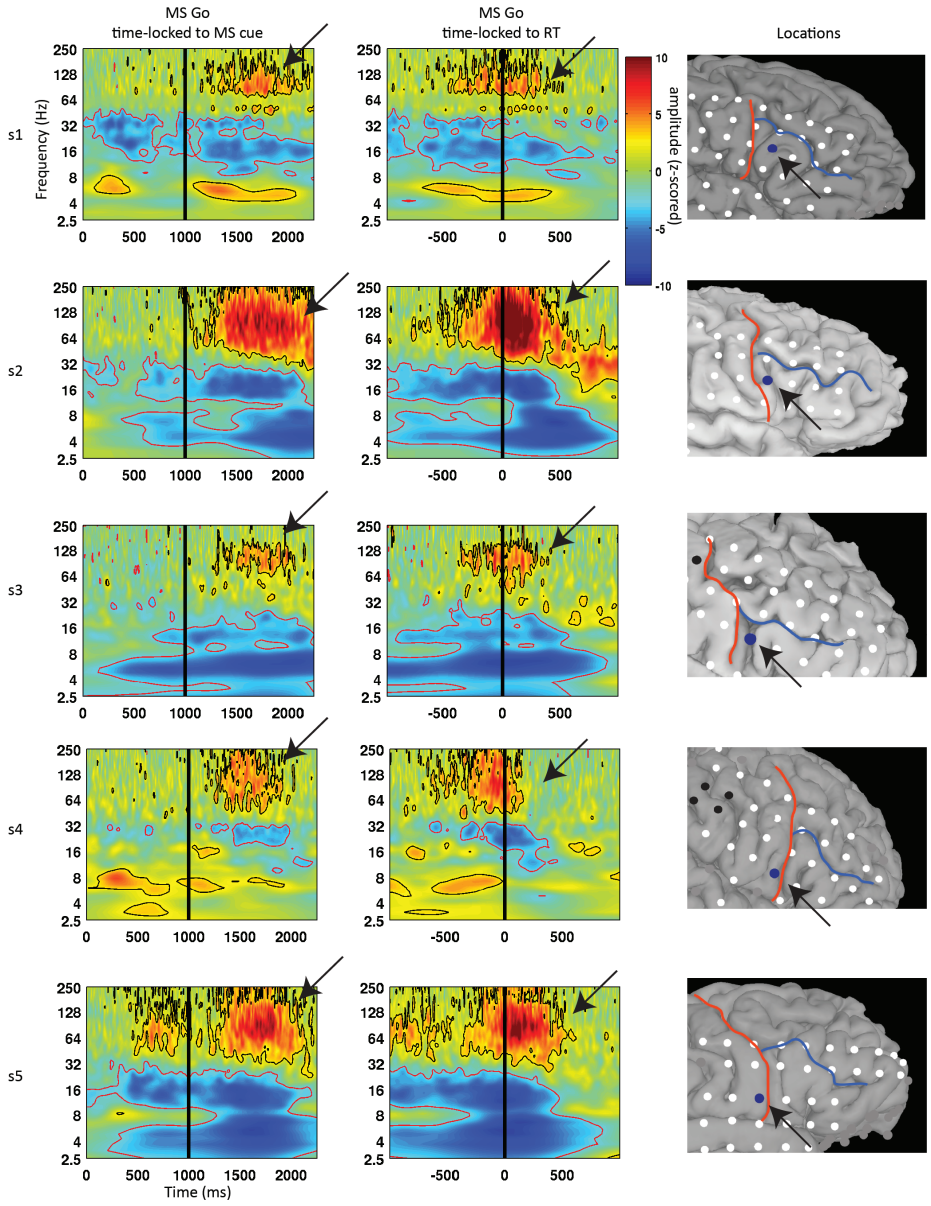


Figure 5.5: VLPFC shows consistent activity across subjects when preparing to stop. Spectral plots for MS Go vs. baseline are shown for a VLPFC electrode from each subject time-locked to both the MS cue (left column), and the RT (middle column). For each subject the high gamma activity centers around the motor response. Zero ms is the time of the task cue and 1000 ms is the time of the go signal for the left column. Zero ms is the time of the RT for the middle column. Amplitude is expressed in color as a z-score. Significant values ($p<0.05$, FDR corrected) are outlined (black indicates positive differences, red indicates negative differences). Electrode locations are indicated in blue for each subject.

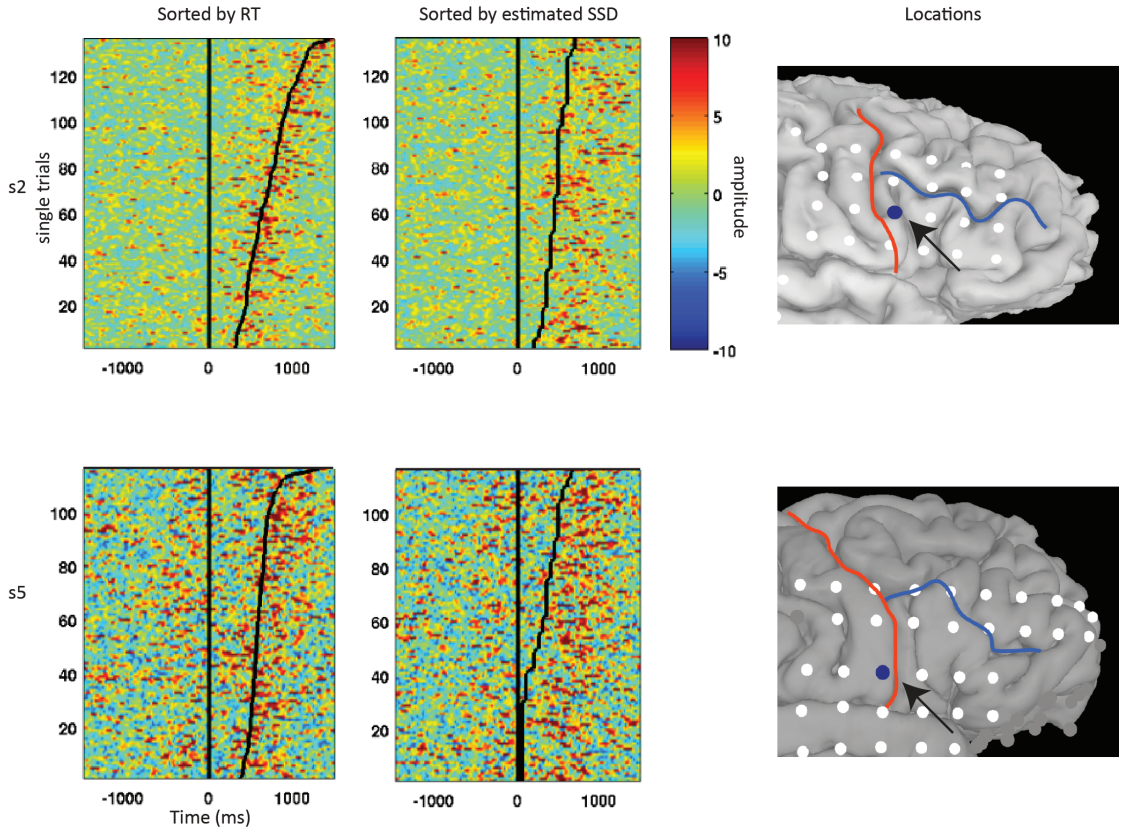


Figure 5.6. VLPFC activity is time-locked to the motor response on a single trial level. In two subjects (s2 and s5), the VLPFC response on MS Go vs baseline relates to the motor response more than the expected stop signal. The left column shows single trial high gamma amplitude (110 Hz) plotted for all MS Go trials aligned to go cue (0 ms), and sorted by RT. The middle column shows the same data sorted by the expected stop signal delay. The dark line indicates RT (left column) or expected stop signal delay (middle column) for each trial. Raw amplitude relative to baseline is shown in color. Electrode locations are indicated in blue for each subject.

REFERENCES

Amunts K, Schleicher A, Burgel U, Mohlberg H, Uylings HB, Zilles K (1999) Broca's region revisited: cytoarchitecture and intersubject variability. J Comp Neurol 412:319-341.

Aron AR (2011) From reactive to proactive and selective control: developing a richer model for stopping inappropriate responses. Biol Psychiatry 69:e55-68.

Aron AR, Poldrack RA (2006) Cortical and subcortical contributions to Stop signal response inhibition: role of the subthalamic nucleus. J Neurosci 26:2424-2433.

Aron AR, Fletcher PC, Bullmore ET, Sahakian BJ, Robbins TW (2003) Stop-signal inhibition disrupted by damage to right inferior frontal gyrus in humans. Nat Neurosci 6:115-116.

Aron AR, Behrens TE, Smith S, Frank MJ, Poldrack RA (2007a) Triangulating a cognitive control network using diffusion-weighted magnetic resonance imaging (MRI) and functional MRI. J Neurosci 27:3743-3752.

Aron AR, Durston S, Eagle DM, Logan GD, Stinear CM, Stuphorn V (2007b) Converging evidence for a fronto-basal-ganglia network for inhibitory control of action and cognition. J Neurosci 27:11860-11864.

Boehler CN, Appelbaum LG, Krebs RM, Hopf JM, Woldorff MG (2010) Pinning down response inhibition in the brain--conjunction analyses of the Stop-signal task. Neuroimage 52:1621-1632.

Boehler CN, Appelbaum LG, Krebs RM, Chen LC, Woldorff MG (2011) The role of stimulus salience and attentional capture across the neural hierarchy in a stop-signal task. PLoS One 6:e26386.

Buch ER, Mars RB, Boorman ED, Rushworth MFS (2010) A network centered on ventral premotor cortex exerts both facilitatory and inhibitory control over primary motor cortex during action reprogramming. J Neurosci 30:1395-1401.

Canolty R, Soltani M, Dalal S, Edwards E, Dronkers N, Nagarajan S, Kirsch H, Barbaro N, Knight RT (2007) Spatiotemporal dynamics of word processing in the human brain. Front Neurosci 1.

Chambers CD, Garavan H, Bellgrove MA (2009) Insights into the neural basis of response inhibition from cognitive and clinical neuroscience. Neurosci Biobehav Rev.

Chambers CD, Bellgrove MA, Stokes MG, Henderson TR, Garavan H, Robertson IH, Morris AP, Mattingley JB (2006) Executive "brake failure" following deactivation of human frontal lobe. J Cogn Neurosci 18:444-455.

Chambers CD, Bellgrove MA, Gould IC, English T, Garavan H, McNaught E, Kamke M, Mattingley JB (2007) Dissociable mechanisms of cognitive control in prefrontal and premotor cortex. J Neurophysiol.

Chao HH, Luo X, Chang JL, Li CS (2009) Activation of the pre-supplementary motor area but not inferior prefrontal cortex in association with short stop signal reaction time--an intra-subject analysis. BMC Neurosci 10:75.

Chatham CH, Claus ED, Kim A, Curran T, Banich MT, Munakata Y (2012) Cognitive control reflects context monitoring, not motoric stopping, in response inhibition. PLoS One 7:e31546.

Chikazoe J (2010) Localizing performance of go/no-go tasks to prefrontal cortical subregions. Curr Opin Psychiatry.

Chikazoe J, Jimura K, Hirose S, Yamashita K, Miyashita Y, Konishi S (2009a) Preparation to Inhibit a Response Complements Response Inhibition during Performance of a Stop-Signal Task. J Neurosci 29:15870-15877.

Chikazoe J, Jimura K, Asari T, Yamashita K, Morimoto H, Hirose S, Miyashita Y, Konishi S (2009b) Functional dissociation in right inferior frontal cortex during performance of go/no-go task. Cereb Cortex 19:146-152.

Conner C, Ellmore TM, Pieters TA, Disano M, Tandon N (2011) Variability of the Relationship between Electrophysiology and BOLD-fMRI across Cortical Regions in Humans. Journal of Neuroscience in press.

Corbetta M, Shulman GL (2002) Control of goal-directed and stimulus-driven attention in the brain. Nat Rev Neurosci 3:201-215.

Dale AM, Fischl B, Sereno MI (1999) Cortical surface-based analysis. I. Segmentation and surface reconstruction. Neuroimage 9:179-194.

Duann JR, Ide JS, Luo X, Li CS (2009) Functional connectivity delineates distinct roles of the inferior frontal cortex and presupplementary motor area in stop signal inhibition. J Neurosci 29:10171-10179.

Forstmann BU, Anwander A, Schafer A, Neumann J, Brown S, Wagenmakers EJ, Bogacz R, Turner R (2010) Cortico-striatal connections predict control over speed and accuracy in perceptual decision making. Proc Natl Acad Sci U S A 107:15916-15920.

Fuster JM (1997) The prefrontal cortex : anatomy, physiology, and neuropsychology of the frontal lobe, 3rd Edition. Philadelphia: Lippincott-Raven.

Goldman-Rakic PS (1990) Cellular and circuit basis of working memory in prefrontal cortex of nonhuman primates. Prog Brain Res 85:325-335; discussion 335-326.

Goldman-Rakic PS (1996) The prefrontal landscape: implications of functional architecture for understanding human mentation and the central executive. Philos Trans R Soc Lond B Biol Sci 351:1445-1453.

Hampshire A, Chamberlain SR, Monti MM, Duncan J, OWEN AM (2010) The role of the right inferior frontal gyrus: inhibition and attentional control. NeuroImage.

Jahfari S, Stinear CM, Claffey M, Verbruggen F, Aron AR (2010) Responding with restraint: what are the neurocognitive mechanisms? Journal of cognitive neuroscience 22:1479-1492.

Leventhal DK, Gage GJ, Schmidt R, Pettibone JR, Case AC, Berke JD (2012) Basal Ganglia Beta oscillations accompany cue utilization. Neuron 73:523-536.

Levy BJ, Wagner AD (2011) Cognitive control and right ventrolateral prefrontal cortex: reflexive reorienting, motor inhibition, and action updating. Ann N Y Acad Sci 1224:40-62.

Logan GD, Schachar RJ, Tannock R (1997) Impulsivity and inhibitory control. Psychological Science 8:60-64.

Muller NG, Knight RT (2006) The functional neuroanatomy of working memory: Contributions of human brain lesion studies. In: Neuroscience, pp 51-58.

Nachev P, Kennard C, Husain M (2008) Functional role of the supplementary and pre-supplementary motor areas. Nat Rev Neurosci 9:856-869.

Neubert FX, Mars RB, Buch ER, Olivier E, Rushworth MF (2010) Cortical and subcortical interactions during action reprogramming and their related white matter pathways. Proc Natl Acad Sci U S A 107:13240-13245.

Olesen PJ, Westerberg H, Klingberg T (2004) Increased prefrontal and parietal activity after training of working memory. Nat Neurosci 7:75-79.

Petrides M (2000) The role of the mid-dorsolateral prefrontal cortex in working memory. Exp Brain Res 133:44-54.

Ray NJ, Brittain JS, Holland P, Joundi RA, Stein JF, Aziz TZ, Jenkinson N (2012) The role of the subthalamic nucleus in response inhibition: Evidence from local field potential recordings in the human subthalamic nucleus. Neuroimage 60:271-278.

Ray S, Crone NE, Niebur E, Franaszczuk PJ, Hsiao SS (2008) Neural correlates of high-gamma oscillations (60-200 Hz) in macaque local field potentials and their potential implications in electrocorticography. J Neurosci 28:11526-11536.

Rushworth MF, Walton ME, Kennerley SW, Bannerman DM (2004) Action sets and decisions in the medial frontal cortex. Trends Cogn Sci 8:410-417.

Saad ZS, Ropella KM, DeYoe EA, Bandettini PA (2003) The spatial extent of the BOLD response. Neuroimage 19:132-144.

Scheeringa R, Fries P, Petersson KM, Oostenveld R, Grothe I, Norris DG, Hagoort P, Bastiaansen MC (2011) Neuronal dynamics underlying high- and low-frequency EEG oscillations contribute independently to the human BOLD signal. Neuron 69:572-583.

Sharp DJ, Bonnelle V, De Boissezon X, Beckmann CF, James SG, Patel MC, Mehta MA (2010) Distinct frontal systems for response inhibition, attentional capture, and error processing. Proceedings of the National Academy of Sciences:1-6.

Swann N, Tandon N, Canolty R, Ellmore TM, McEvoy LK, Dreyer S, DiSano M, Aron AR (2009) Intracranial EEG reveals a time- and frequency-specific role for the right inferior frontal gyrus and primary motor cortex in stopping initiated responses. J Neurosci 29:12675-12685.

Swann NC, Cai W, Conner CR, Pieters TA, Claffey MP, George JS, Aron AR, Tandon N (2012) Roles for the pre-supplementary motor area and the right inferior frontal gyrus in stopping action: Electrophysiological responses and functional and structural connectivity. Neuroimage 59:2860-2870.

Verbruggen F, Logan GD (2009) Models of response inhibition in the stop-signal and stop-change paradigms. Neurosci Biobehav Rev 33:647-661.

Verbruggen F, Aron AR, Stevens MA, Chambers CD (2010) Theta burst stimulation dissociates attention and action updating in human inferior frontal cortex. Proc Natl Acad Sci U S A 107:13966-13971.

Vink M, Kahn RS, Raemaekers M, van den Heuvel M, Boersma M, Ramsey NF (2005) Function of striatum beyond inhibition and execution of motor responses. Hum Brain Mapp 25:336-344.

Zandbelt BB, Vink M (2010) On the role of the striatum in response inhibition. PLoS One 5:e13848.

Zandbelt BB, Bloemendaal M, Neggers SFW, Kahn RS, Vink M (2012) Expectations and violations: Delineating the neural network of proactive inhibitory control. Hum Brain Mapp.

Chapter 6:

Conclusion

Much evidence points to the importance of a network of brain regions for response control. However, many questions remain. This thesis considers two of them. First, how and when do the different nodes of the network become active and communicate with one another? Second, what is the functional contribution of the nodes/regions within this structural/function network? In four empirical chapters, this thesis provides some preliminary answers to these questions.

Chapter 2 presented one of the first studies to look at response control (specifically stopping action) in humans using a method with high spatio-temporal resolution (i.e. electrocorticography, ECoG). It demonstrated in three patients that in right IFG there was a beta amplitude increase following the stop signal for successful stopping which were greater than that for unsuccessful stopping (Swann et al., 2009). The timing of this increase aligned well with typical stop signal reaction times (SSRT), so it is consistent with a role in action control (specifically inhibitory control). This contrasted with a reduced alpha/beta desynchronization in primary motor electrodes for stopping compared with going, consistent with previous studies showing similar desynchronizations for going (Pfurtscheller, 1981; Pfurtscheller et al., 2003), and perhaps consistent with increased GABA-ergic inhibition in M1 when stopping occurs (see Jensen et al., 2005; Coxon et al., 2006).

Interestingly, beta is a frequency that has been suggested to be well suited for long distance communication between brain regions (Kopell et al., 2000; Fries, 2005; Kopell et al., 2010). Moreover, beta may be particularly prominent in communication between cortical and basal ganglia structures (Sharott et al., 2005; Fogelson et al., 2006; Lalo et al., 2008; Hirschmann et al., 2011; Litvak et al., 2011). This is pertinent because response control is thought to rely on a network involving cortex (IFG, preSMA) and basal ganglia (particularly the STN) and these regions are structurally connected to one another (Johansen-Berg et al., 2004; Aron et al., 2007; Forstmann et al., 2008; Forstmann et al., 2012; King et al., 2012). Here, the demonstration that right IFG showed a beta amplitude increase, and that this was larger for successful compared to failed stopping, suggests that this activity pattern could be consistent with communication between IFG and the STN in the beta frequency band, and that when communication is successful, as reflected by beta amplitude increases, behavioral success during stopping is more likely. This hypothesis fits well with two recent studies that demonstrated beta increases at similar times to those observed in chapter 2, associated with successful stopping in STN recordings, in both humans and rodents performing the stop signal task (Leventhal et al., 2012; Ray et al., 2012), as well as an earlier report showing beta increases for NoGo relative to Go trials recorded from STN during a Go/NoGo task (Kühn et al., 2004). In short, chapter 2 in the wider context of the literature shows that both STN and right IFG have similar activity patterns for similar tasks and are structurally connected to one another. This motivates

the hypothesis that successful stopping may depend on communication between these regions in the beta band.

Chapter 3 takes the results from chapter 2 a step further by testing if modulation of a subcortical node of the network (the STN) changes the overall network in a way that may be detectable as an amplitude change detected at the cortex. Here, patients with deep brain stimulation (DBS) as a treatment for Parkinson's Disease were tested on and off stimulation while performing a stop signal task. During each session EEG was recorded from the scalp. First, a behavioral improvement in stopping (SSRT reduction), but no change in go RT, was observed when patients were on stimulation compared to off, as has been reported elsewhere (van den Wildenberg et al., 2006; Mirabella et al., 2011). Thus, deep brain stimulation improved stopping, perhaps by improving the fidelity of information transfer in the brain network for response control. Second, for EEG there was a greater beta amplitude following the stop signal for the on vs. off stimulation sessions (Swann et al., 2011). Moreover, this effect was significant over right frontal electrodes, but not left frontal ones, and there was a significant difference between the two. This observation is in line with numerous reports suggesting that the response control network is predominantly right lateralized (Garavan et al., 1999; Aron et al., 2003; Chikazoe, 2010). These results support the hypothesis that communication between the STN and cortex during stopping may occur in the beta band, by showing that modulation of STN activity changed a behavioral index of stopping and beta amplitude at the cortex in an event-related manner.

Chapter 4 continues to examine the wider response control network, adding information from another node (the preSMA), by examining, in one rare patient, ECoG responses in right IFG and preSMA (after first validating the task in a group of healthy subject using fMRI). First preSMA electrodes were functionally identified using macrostimulation, (because macrostimulation is known to cause motor arrest when delivered over the area anterior to SMA (Luders et al., 1988; Fried et al., 1991)). Next a white matter tract connecting preSMA to rIFG was established in this patient, as has already been established in normative populations (Johansen-Berg et al., 2004; Aron et al., 2007a; Ford et al., 2010). This step also helped to identify electrodes that were good candidates for IFG activity in relation to stopping. Next, a functional connection was established between these two regions using cortico-cortical evoked potentials (CCEPs). Here stimulation at preSMA electrodes showed a strong and quick response in IFG, and particularly in the IFG electrode identified as a good candidate using DTI. These findings firmly established this connection in this individual patient, and motivated examination of functional connectivity. First we replicated the beta increase for the IFG electrode for successful stop trials. Next we showed a similar increase in preSMA. Again, this supports the idea that there may be communication between these areas in beta associated with stopping. We further investigated this by computing coherence between these two regions, a measure of functional connectivity (Fries, 2005). We found that indeed, there was significant coherence between these two regions in beta around the time of stopping for successful stopping, but not unsuccessful. This provides strong evidence, at least in one person, for the

involvement of beta in long distance communication between preSMA and IFG during stopping. Coherence can theoretically inform upon the directionality of an interaction, by investigating phase lag, however here the phase lag was near zero, suggesting either that both regions are driven by a 3rd region (perhaps the STN), or that successful stopping depends not on one region driving the other, but on overall interaction across regions (i.e. all regions 'synching up').

Chapter 4 also addressed the second goal of this thesis, i.e. what different cognitive processes are performed by the individual regions within the response control network? Here, in this same ECoG patient, we examined high gamma activity (thought to be an index of local neural activity) (Edwards et al., 2005; Miller et al., 2007; Ray et al., 2008; Conner et al., 2011; Scheeringa et al., 2011) in preSMA and right IFG during both preparing to stop and outright stopping. Besides being a potentially more ecologically valid model (see chapter 1 and Aron, 2011), preparing to stop can also be helpful for determining functional roles of regions since it effectively separates the response control process into preparation and outright stopping components. Such an approach can help determine if activity observed in a given region may reflect a functional role for that region in either the preparation or the outright stopping component. Using this approach we observed that for both preparing to stop (proactive control) and outright stopping (reactive control) preSMA activity preceded right IFG (Swann et al., 2012). However, for outright stopping, this finding was somewhat ambiguous because both regions became active in close temporal proximity, and, for both regions, activity preceded the stop signal. We interpret these

findings as suggesting that preSMA plays a role in converting the task rule into an action plan (task configuration) and setting up the rest of the network to prepare to stop (Rushworth et al., 2004). Meanwhile, right IFG performs the action control itself, perhaps by actively slowing (braking) the response (Jahfari et al., 2010).

Chapter 5 also addressed the question of what different cognitive processes are performed by individual regions within the response control network, but this time by comparing the right IFG (VLPFC more generally, for this chapter) with the right dorsolateral prefrontal cortex (DLPFC) in 5 ECoG patients who had grid coverage of both regions. We focused on go trials alone, specifically the contrast of 'Maybe Stop' and 'No Stop'. By doing so we could ask whether DLPFC and IFG have dissociable roles in preparing to stop, on trials where there is always a motor response. Again, we focused on high gamma activity as an index of local neural activity (Miller et al., 2007; Ray et al., 2008; Conner et al., 2011; Scheeringa et al., 2011). We showed that DLPFC activity, indexed by increases in high gamma amplitude relative to baseline, usually occurred after both the cue that instructs the subject whether or not stopping might be necessary and after the cue instructing subjects to go, while IFG was active usually only after the cue that instructs subjects to go, and mainly around the time of the response. Furthermore, in IFG there was significantly more activity around the response for trials where stopping was possible compared to trials where it was not, but only for subjects who showed proactive slowing (braking) of the motor response. We interpret our findings as suggesting that IFG plays a role in actively slowing ('braking') the motor response at the time of initiation, perhaps to allow for a late

cancelation of movement if necessary (Jahfari et al., 2010), while DLPFC, plays a role in working memory/task updating, as has previously been shown (Goldman-Rakic, 1990; Petrides, 2000; Muller and Knight, 2006).

Below we consider the findings of this thesis together and compared to other studies in terms of their contributions to the understanding of the individual roles of each region of the response control network and how they may work together to implement proactive and reactive control.

Reactive control

It has been well established by imaging studies that reactive control (outright stopping) recruits a network of brain areas including the preSMA, right IFG, and STN (reviewed by Garavan et al., 1999; Rubia et al., 2003; Aron et al., 2007a; Aron et al., 2007b; Li et al., 2008; Chikazoe, 2010; Levy and Wagner, 2011). Several questions remain though. For instance, what are the roles of each of these regions? Does the relative timing of neural events across these regions provide information about their different roles? And, does activity in any of these regions relate to the success of stopping? Electrophysiology has the temporal resolution to begin to answer these questions.

i. High frequency activity – local neural activity

First, we consider the relative timing of activations in different nodes of the network and how this may relate to different functional roles for each of these regions. Here,

we take high gamma activity as a proxy for local neural activity (because this frequency band correlates best with spiking, and also has the strongest relationship to the BOLD signal (Logothetis et al., 2001; Ray et al., 2008; Conner et al., 2011; Scheeringa et al., 2011). Using this approach, it becomes clear why it has been difficult to pull apart the timing of these regions using fMRI.

Chapters 4 and 5 along with a study which recorded LFPs from STN in human Parkinson's Disease patients (Ray et al., 2012) show that there are indeed high gamma increases in all three of these regions associated with reactive control (specifically, outright stopping). For the case study patient presented in chapter 4 it seems that the high gamma activity in preSMA preceded IFG but there was significant activity in each region before the stop signal, making it difficult to determine what activity was specifically related to outright stopping, and thus, difficult to determine whether outright stopping related effects occurred first in preSMA or IFG.. Likewise, Ray and colleagues show a similar pattern, with an increase in high gamma activity following the stop signal, but also above baseline activity preceding it (Ray et al., 2012). Moreover, since the study by Ray et al. 2002 used a different version of the stopping task, and was in a different group of patients, direct inferences about the temporal ordering of these regions are not straightforward. In brief, given the current data, it is difficult to pull apart the temporal ordering of activity because of the prominent prestimulus activity in each region making it difficult to determine what activity was specifically related to outright stopping, and because of the dearth of data recorded simultaneously from each region in the same subject(s). Rather, it seems that all three

regions rapidly boost their activity following the stop signal. It also suggests that in order for all these regions to simultaneously up-regulate activity, that there might be a way for all three to communicate rapidly.

Importantly, none of these regions seem to show greater high gamma for successful compared to failed stopping which suggests that it may not be simple activation (i.e. more metabolic activity) of any of these regions alone that determines the success of control. This observation is in line with fMRI observations that tend not to find a difference for this comparison (Aron and Poldrack, 2006; Aron et al., 2007b; Xue et al., 2008; Congdon et al., 2010), although not always (see Rubia et al., 2003; Li et al., 2006).

In summary, examining high gamma activity (or the BOLD signal) during reactive control is well suited to identify which areas are generally involved but may not be optimal to pull apart functional roles, at least using timing as a metric. Pulling apart activity by studying proactive control may be more useful here, and these functions may generalize to reactive control since often they are recruited in tandem (i.e. reactive control tasks usually contain both reactive and proactive control processes recruited in quick succession). See the later section for more discussion on this.

ii. Low frequency activity – communication between regions

The high frequency activity suggests that three regions of the response control network (preSMA, IFG, and STN), all show rapid boosts of activity during reactive

control. This suggests that there could be a communication mechanism between these regions. Low frequency activity in the beta band is a good candidate for this mechanism. Additionally, while it seems, according to the electrophysiology and fMRI evidence described above, that successful compared to failed stopping does not involve increased local neural/metabolic activity in any of these regions, it is possible that there may be differences in low frequency activity, reflecting changes in neural communication. This difference stems from the fact that fMRI and electrophysiology (local field potentials) are sensitive to different neural features, with electrophysiology being sensitive to quick temporal changes in *how* neurons are active (for example changes of synchrony in a population), while fMRI detects changes in metabolism (more or less activity, i.e. blood oxygen usage). Indeed it seems that there are beta amplitude increases in all three regions *following* the stop signal (chapters 2, 4, and (Leventhal et al., 2012; Ray et al., 2012)). In the IFG at least, this beta increase seems to be larger for successful compared to failed stopping (reported in chapter 2 and 4). However, this does not seem to be the case for preSMA (in one subject, chapter 4), and is somewhat ambiguous in the STN (Leventhal et al., 2012; Ray et al., 2012). There is also evidence that beta is a good candidate for communication between cortex and basal ganglia (Sharott et al., 2005; Lalo et al., 2008; Hirschmann et al., 2011; Litvak et al., 2011). Indeed, chapter 3 reports that modulations of STN affect cortical beta around the time of stopping. Moreover, chapter 4 reports significant coherence between preSMA and IFG when stopping is successful, but not when stopping is unsuccessful, supporting the notion that functional connectivity between these two

regions is associated with successful stopping. This is interesting since Parkinson's Disease patients who exhibit slowing and difficulty initiating movements also have pathologically high beta in their basal ganglia (Brown and Williams, 2005; Brown, 2007; Hammond et al., 2007; Jenkinson and Brown, 2011). This pathological beta correlates with the degree of slowing and rigidity (Kühn et al., 2009). Furthermore, it has been demonstrated that slowed movements can be produced by inducing beta in the cortex of healthy subjects (Pogosyan et al., 2009), and in the STN of Parkinson's patients (Chen et al., 2007; Eusebio et al., 2008; Chen et al., 2011). In short, cortico-basal ganglia communication in the beta frequency band may allow successful stopping during the stop signal task and coupling in this frequency band may have a specific inhibitory effect on the motor system (at least in certain contexts). Note also, that this interpretation is not out of line with broader functions recently ascribed to the beta band such as 'maintenance of the status quo' (Engel and Fries, 2010; and see Leventhal et al., 2012). Rather, the inhibitory effect of beta on the motor system can be considered a specific case of this maintenance typical for cognitive control tasks using the motor system as a model (response control).

An unanswered question is the directionality of the communication between these regions. Here we have a few pieces of evidence from different studies, which as of yet, do not form a fully clear story. The data presented in chapters 2 and 4 show that the beta amplitude increases in preSMA and IFG occur at the same time. (Note that the high gamma increase in IFG follows that in preSMA, though both occur before the stop signal. This suggests that preSMA may be active before IFG, but since this

activity precedes the stop signal, it may not be related to reactive control/outright stopping per se.). Chapter 4 reports coherence between IFG and preSMA, which in theory can provide directionality by examining phase-lag. However, here the phase-lag was near zero, suggesting that either 1) both regions are driven by a third, potentially subcortical source (such as the STN), or 2) that the coherence is driven not by one region influencing the others, but by all three regions influencing one another such that they eventually synch up (and perhaps in this synching up allow the STN to interrupt the motor command already in progress (see Mink, 1996; Nambu et al., 2002)). This later account fits with two monkey electrophysiology studies that suggest that the STN could be the last of these regions in the network since it is active later than preSMA on switch trials (Isoda and Hikosaka, 2007, 2008). Furthermore the STN is structurally well connected to interrupt an initiated motor response since it has direct excitatory connections to inhibitory motor output nuclei of the basal ganglia (Mink, 1996; Nambu et al., 2002). In either case (i.e. that the beta changes observed in cortical areas are driven by a subcortical source or that the three areas synching up allow the motor interruption to take place, perhaps via the STN), this interpretation fits well with the observation in chapter 3 that modulating STN affects cortical beta during stopping. Since this modulation was ongoing, and not event-related, it could be that there was general adaptation regarding STN-cortical communication as a result of the stimulation, which could result in bi-directional changes. (So changes in cortex as a result of STN stimulation do not necessarily imply that the cortex is downstream from STN in the stopping process, and in fact, this is not well-supported by structural

accounts (Mink, 1996; Nambu et al., 2002) or monkey electrophysiology (Isoda and Hikosaka, 2007, 2008).)

In summary, this thesis, in the context of other literature, tentatively supports a model of reactive control where three key regions of the cognitive control network (right IFG, preSMA, and STN), all show increases in beta activity during stopping, and that this beta activity could reflect all three of these regions synching up, resulting in effective communication of the need to stop, probably to the STN, which then interrupts the initiated motor response. An alternative account is that the STN triggers the beta activity which then 'reverberates' through the cognitive control network, resulting in beta amplitude increases (and phase synchronization), throughout the network, particularly the cortical regions. In this interpretation, the cortical beta is merely a 'fingerprint' of the STN activity, and does not play a causal role in stopping per se. However, because inducing cortical beta has been shown to result in slowing of movement (Pogosyan et al., 2009), this account seems less favorable then the former.

Overall, it is well established that the preSMA, IFG, and STN are all important for reactive control and there is mounting evidence to suggest that this reactive control relies on synchronization of these regions in the beta band. However, since the beta increases in each of these regions seems to occur at the same time, the cognitive contributions of each of these regions specific to reactive control remain unclear by this metric. There is some evidence from switching studies using a paired-pulse TMS study (Neubert et al., 2010) and monkey electrophysiology (Isoda and Hikosaka, 2007, 2008) that preSMA engagement precedes both IFG and STN. This combined with

structural studies (reviewed by Mink, 1996; Nambu et al., 2002) suggests that the order of activation of these three regions may be first preSMA, then IFG, and then STN. If this ordering is correct, it would imply specific roles for each of these regions, but overall, it seems as if all three regions are activated in close temporal proximity during reactive control, making functional differentiation a challenge. For this reason, and because it is a potentially more ecologically valid model (Aron, 2011), tasks which separately examine proactive and reactive control could help shed light on these questions.

Proactive control

In our daily lives it is probably rare that we have to outright cancel an initiated response to an external signal. Instead, it is probably more common that we exercise caution, or proactive control, in situations where we predict a potential need for control in the future (Aron, 2011). Recently, this approach of studying proactive control, often with the focus of how we prepare to stop, has gained favor in the literature (Jahfari et al., 2010; Zandbelt and Vink, 2010; Zandbelt et al., 2012). This method has the additional advantage in that it allows different components of the task to be pulled apart in time, so that the activity time-courses of different regions become more apparent.

Imaging studies show that a similar network of brain areas important for reactive control are also active in proactive control as shown in chapter 4 and in studies by other groups (Chikazoe et al., 2009; Zandbelt et al., 2012). These regions

include the right IFG, preSMA, STN, and DLPFC. This is usually determined by adding a condition where the probability of a stop signal is zero and comparing this condition to go trials where stopping is more likely to occur. Using this method with ECoG we showed in chapter 5 that DLPFC was active following both the cue indicating whether or not stopping was possible (task cue), and following the go cue. DLPFC has been consistently implicated in working memory (Goldman-Rakic, 1990; Petrides, 2000; Muller and Knight, 2006), and this activation pattern is consistent with that role, showing activity following task-relevant stimuli, perhaps reflecting general task updating. Chapter 4 reported in one subject, that preSMA became active later in the task-cue period, just a couple hundred milliseconds prior to the go cue, and remained active for the rest of the trial (with an additional increase near the stop signal if it occurred). Since preSMA has been implicated in configuring action sets (Rushworth et al., 2004), we suggest that its particular function in this context is to configure the action system for the possibility of a stop signal occurring, and the potential need to quickly switch action sets by converting the task goal into an action plan. This is also supported by the observation that when a single trial analysis is performed (like that presented in chapter 5, figure 6) activity in the preSMA scales with RT, not by tightly time locking to the response, as occurs in IFG shown in (chapter 5, figure 6), but by showing increased amplitude for longer RTs. So, on trials where there is greater slowing in anticipation of stopping, preSMA is more strongly engaged (unpublished observations). Chapters 4 and 5 also show that right IFG was active after both preSMA and DLPFC, not until well after the go signal, and typically

around the response itself. We suggest its activity, coincident with the response, is in line with a role in action control, perhaps slowing of the response as it is emitted ('braking'), as has been suggested previously (Jahfari et al., 2010), in order to allow for late cancelation of the response, if necessary and discussed in detail in chapter 5. While these accounts are derived from proactive control comparisons, these roles may generalize to reactive control as well.

There have so far been no recordings from STN during a proactive control task, so its role remains unclear. However, it likely does play a role given its importance in reactive control. Moreover, there is new evidence that STN stimulation with DBS in Parkinson's patients may modulate the degree of response preparation (Greenhouse et al. in preparation).

Agreement of these models with other studies

Overall, the findings above are consistent with those reported by Zandbelt and colleagues using fMRI (Zandbelt et al., 2012). They found that preSMA was active following the task cue, and IFG was active following the go cue. They interpret this result as suggesting that preSMA plays a role in preparing to stop, and the IFG in "violation of expectation" (because a stop signal did not occur). However, the ECoG findings shown in Chapter 5 have more precise temporal resolution, and link the IFG response more to the motor response itself instead of merely following the go cue. Therefore, a violation of expectation account would have to include a motor component to be viable, perhaps if the violation triggered the subsequent motor

response or the motor response triggered the expectancy violation. This order of activation is also consistent with the paired-pulse TMS study of (Neubert et al., 2010), which showed preSMA's influence over the motor output preceding that of IFG in a switching task, and that disruption of preSMA with repetitive TMS disrupted the inhibitory effects of IFG on M1, suggesting that IFG is downstream of preSMA in the switching process. The same may be true for stopping. This account of IFG's role in control also fits with a previous observation of active suppression of the motor system when stopping is anticipated where the degree of slowing correlated with BOLD signal activation in IFG (Jahfari et al., 2010). (And this is the case even when the stop signal is not consciously perceptible (van Gaal et al., 2010), arguing against a violation of expectation account).

However, other studies provide interpretations or results that are at odds with those discussed in this thesis. Particularly ones that posit that IFG activity is instead related to attention or detection (Hampshire et al., 2010; Sharp et al., 2010; Boehler et al., 2011; Chatham et al., 2012), either because right IFG shows activity even for a condition where stop signals required response continuation or an additional response, instead of inhibition (Hampshire et al., 2010; Chatham et al., 2012), but see (Boehler et al., 2011) which didn't show this difference, or for a similar task in an event related design (Sharp et al., 2010). (Note, though, that for most of these studies, the stop signal did cause response slowing which has been shown to recruit the response control network(Aron et al., 2007a)). Another paper using Granger causality methods with fMRI suggested an account where IFG played an attentional role in reactive

stopping and preSMA signaled for the actual inhibition to occur by communicating with STN (because the pattern of causal flow went from IFG to preSMA to STN) (Duann et al., 2009). It is likely however, that fMRI data is not meaningful for causal analysis when such quick changes are expected. Furthermore, the anatomically defined IFG region is relatively large and need not have only one functional role. Indeed, a recent TMS study was able to dissociate IFG into a dorsal region important for attention and a more ventral region (corresponding better with the location of the IFG electrodes presented in this thesis) important for 'action updating'(Verbruggen and Chambers, 2010).

Overall, it is not entirely clear yet what are the precise roles for each of these regions. This thesis presents results consistent with the notion that preSMA plays a role in task configuration and the role of IFG is in the actual action control, but other accounts suggest that preSMA performs action control and the role of IFG is in attentional monitoring. Because of the higher temporal precision of the methods used in the studies which support the former account, it may be the more viable alternative. However, the discrepancy in function could relate to imprecision in anatomical nomenclature, since IFG sub-regions have been shown to have separable roles in attention and action control (Verbruggen and Chambers, 2010).

Overall Model

Assuming that the roles of these regions may be generally similar for reactive and proactive control, the evidence presented in this thesis, along with other reports, begin to suggest tentative roles for each of these regions in response control.

When a cue is presented indicating a potential need to stop (or no need to stop) DLPFC encodes the presentation of this cue and holds it in working memory. This information is then conveyed to the preSMA (the mechanism of this communication is not yet clear), which plays a task configuration role by converting the goal into the action system, i.e. setting up the motor system to potentially stop (or be quickly reconfigured). This engagement of preSMA is maintained until the end of the trial. After the go signal is presented, DLPFC is again activated (signaling its presentation, i.e. updating working memory for the task set). PreSMA continues to be engaged, (particularly on trials where going is slowed in anticipation of stopping, i.e. braking occurs). When no stop signal occurs and a response is initiated, IFG is active around the onset of the response, perhaps related to proactive suppression that may facilitate the rapid termination of a response if necessary.

If, instead, a stop signal *does* occur, the beta band synchrony between preSMA, IFG, and STN, becomes strong, allowing the STN to quickly inhibit the motor system output. If the integrity of this signal is weak, reflected by less apparent synchrony between regions, stopping is more likely to be unsuccessful. After the stop signal, the potential roles of the preSMA and IFG may be generally similar to their roles in proactive control (preSMA playing a role in task configuration and IFG in action control), but now adjusted to bias the motor system towards stopping given the

presentation of the stop signal. While still extremely speculative and overly simplistic, this model helps lay a framework for possible mechanisms of action control in the human brain and motivates future studies (see Figure 6.1).

Wider implications

Besides contributing to the field of response control specifically, the findings presented in this thesis also have wider implications for cognitive psychology and cognitive neuroscience, as well as for clinical neuroscience.

Implications for cognitive psychology

Years of cognitive psychology research have led to the characterization of specific cognitive processes, such as 'inhibitory control' and 'attentional monitoring', thought to underlie behavioral performance in response control tasks. These processes could work in serial, with the output from each individual process contributing to the subsequent process, or they may work in parallel, with an integration of information occurring after each process is separately completed. This thesis provides novel insight into the mapping of such cognitive processes to brain regions, and specifically into whether these regions work in serial or in parallel.

The findings presented here suggest that, at times, the ordering of cognitive processes involved in response control fits with a *serial strategy*. Specifically, and as spelled out in Figure 6.1, when preparing to stop, the DLPFC may represent the stopping goal (in working memory), with this information then being conveyed to the

preSMA, which may translate the stopping goal into the action control system (task configuration), and prepare the rest of the response control network, including the IFG, for the potential need to stop. Subsequently, the IFG implements action control, for example by slowing or 'braking' the motor response as it is initiated. This prepared state could allow for rapid cancelation of the response if stopping becomes necessary. However, a different picture emerges at the time that outright stopping is needed. This perhaps points to a *parallel strategy* and/or integration of processing. Here success of stopping could depend on the preparedness of preSMA and IFG in terms of their contributions to the cognitive processes described above, and their ability to rapidly integrate information between one another and with the STN in order to cancel the response (via synchrony in the beta band). This grounding in biology does validate the cognitive psychological assumption of cognitive processes as separate entities, insofar as it shows they are associated with computations in separate neural regions. It also provides insight into which particular processing scheme may be used (i.e. serial vs. parallel) in which context, by shedding light on the timing of recruitment of these regions.

In considering how the data in this thesis elucidate how cognitive processes map onto the response control network, it is useful to consider analogous cases from a different research area, for instance, the language domain. One study, by Canolty and colleagues (2007), used ECoG to examine auditory processing of words and non-words and found evidence in support of a serial model of language processing where acoustic processing first takes place in auditory regions (specifically post and mid

superior temporal gyrus, STG) followed by word processing (in the more ventral superior temporal sulcus region, STS). A follow-up study by the same group sought to examine later stages of language processing, using a phoneme discrimination task, where subjects were instructed to respond to certain 'target' phonemes (Chang et al., 2011). They replicated the early activation of auditory regions and also showed that prefrontal areas became active next, followed by motor areas. Overall, the findings of both these studies together suggest that a serial processing model best explains the activity patterns observed across regions, since activity in areas sensitive to each of these processes occurred sequentially. Together, these example language studies, along with the response control studies of the thesis, point to a model of different regions performing different functions sequentially. The studies in this thesis differ from the language work in that they show that at certain times, when a fast interruption of behavior is required, a more parallel strategy is utilized. The observation of these processing schemes in the brain validates their use in cognitive psychology, and provide hypotheses about when serial vs. parallel processing may dominate (i.e. as a function of the urgency of the response). Thus, the addition of cognitive neuroscience approaches when considering cognitive processes makes it possible to validate and elaborate upon models developed by cognitive psychology.

Implications for cognitive neuroscience

This thesis also contributes to the field of cognitive neuroscience by providing insight into neural signatures for intra-regional and inter-regional processing and how

these signatures may relate to behavioral response control. In human cognitive neuroscience, by far the most popular approach to understanding how the brain produces behavior has focused on the one region/one cognitive process model. Yet the current thesis provides data suggesting that a particular cognitive process could be implemented via communication in a network of regions.

Here, we examined high gamma activity as a proxy for local neural activity. With this approach, we showed that, at least in the cortical areas we sampled, no high gamma activity differences were evident for successful stopping vs. unsuccessful stopping, despite an overt behavioral difference (i.e. the success of stopping). This result is also supported by no activation difference with fMRI for this same contrast of successful vs. unsuccessful stopping in regions known to be critical for stopping e.g. right IFG, preSMA, and STN (for meta-analysis see Congdon et al., 2010). These results together suggest that successful stopping may not rely only on metabolic activation of any particular region(s). Instead success of stopping seems to depend on communication within the stopping network. In particular, there is evidence that successful compared to unsuccessful stopping relates to increased frequency in the beta band in IFG (reported in chapter 2 and see Ray et al., 2012) and to increased communication between IFG and preSMA (presented in chapter 4), both of which may relate to network communication with the STN (see chapter 3). Thus, behavioral differences (i.e. successful vs. unsuccessful stopping) relate not only to activation of brain regions but also to proper communication between them.

Since the early observation by Gazzaniga and colleagues of the dramatic effects associated with severing the corpus callosum and, thus abolishing the communication between the two hemispheres of the brain, it has been clear to cognitive neuroscientists that communication between brain areas is an integral contributor to behavior (Gazzaniga et al., 1962; Gazzaniga, 1989, 2000). However, many of the cognitive neuroscientific methods typically used in humans are not well-suited to examine quick, task-relevant, communication changes in specific brain networks, either because of their low temporal resolution (fMRI) or their low spatial resolution (EEG). This thesis uses a method with high temporal and high spatial resolution to obtain data that suggest one example where task-relevant communication may contribute to behavior (i.e. that successful stopping relies on communication between IFG, preSMA, and STN in the beta band). This is an important finding because it suggests the best approach to understanding the neural underpinning of behavior is to use a combination of methods that allow examination of activity (such as fMRI), in conjunction with methods that examine indices of communication (such as electrophysiology).

Clinical implications

The results presented in chapter 3 provide insight into how DBS as a treatment of Parkinson's disease may work to improve cognitive function, specifically, by 'rectifying' abnormal activity in cortico-basal-ganglia circuits. It has been shown that there is pathologically high beta activity in the STN of Parkinson's disease patients,

which is reduced by DBS (Kühn et al., 2008; Ray et al., 2008a; Eusebio et al., 2011). This pathological synchrony may relate to "noise" in cortical-basal ganglia circuits (Brown, 2007; Litvak et al., 2011). Chapter 3 showed a cortical event-related beta amplitude increase at the time of stopping for Parkinson's patients ON DBS stimulation that was greater than that of patients OFF stimulation. These findings suggest that one way that DBS works is by reducing the 'noise' in the system (i.e. the pathologically high beta), thereby improving the fidelity of information transfer in the cortical-basal ganglia network, and restoring the healthy event-related coupling. This mechanistic insight fits recent theorizing that it is not the *amount* of activity, but rather the *kind* of activity (i.e. pathological beta coupling) that underlie symptoms in PD (Garcia-Munoz et al., 2010), and it also goes further by pointing to the link between a reduction of pathological noise and the 'freeing up' of a cognitive prefrontal-basal-ganglia circuit for stopping action; leading to improved behavioral performance. This insight could one day lead to improved treatment options. For example, since behavioral impairments observed in Parkinson's disease relate to "noise" in cortical-basal ganglia circuits, than perhaps treatment to reduce this noise could be targeted at the cortex instead of the basal ganglia, which would be less invasive. Indeed, recent work by Gardinaru and colleagues using optogenetics to modulate neural activity in a rodent model of Parkinson's showed that the benefits of STN stimulation may be specifically driven by stimulation of the afferents axons to STN. To further explore this possibility they used cortical stimulation (targeted to M1, an area known to have STN afferents), and showed improvements in Parkinson's symptoms similar to those

seen with STN as a stimulation target (Gradinaru et al., 2009). This provides proof of concept for the idea that a cortico-basal-ganglia circuit running through the STN could be modulated by cortical stimulation in a way that reduces the pathological noise. In short, it is becoming clear that Parkinson's disease is not a disease only of the basal ganglia, but also of cortico-basal ganglia communication. This insight could pave the way to approaches that modulate the relatively accessible cortex, rather than the deep basal ganglia, leading to less invasive treatments options.

Future Directions

Future experiments could help extend the findings presented in this thesis. For instance, paired-pulse TMS studies, which can elucidate functional connectivity, could help elaborate the functional roles of the preSMA and IFG in response control. Already this approach has been used to show that preSMA has an earlier facilatory effect on M1 during a switching task, while the influence of IFG on M1 is later and inhibitory (Mars et al., 2009; Buch et al., 2010; Neubert et al., 2010). The findings in this thesis predict that a similar temporal ordering, with preSMA influencing M1 before IFG, might be apparent for other response control tasks. It also predicts that when preparing to stop, the degree of slowing may be modulated by preSMA stimulation, whereas, stimulation of IFG might inhibit the cortico-spinal excitability as the response is emitted, and that the degree of this inhibition might relate to the likelihood that stopping will be successful should a stop signal occurs. Along the same lines, little research has investigated the possible role of STN in preparing to stop. It

remains an open question whether the slowing associated with preparation, and the associated cortico-spinal inhibition (Jahfari et al., 2010), is purely a cortical phenomena, or whether subcortical regions are recruited as well. Previous research suggests that cortical influences on M1 during response control can be either direct or through a subcortical routes (Neubert et al., 2010). Knowing how the STN behaves during preparation to stop might help reveal when each of these routes is relied upon most. Future studies can examine the STN more, perhaps with electrophysiology or stimulation approaches. Additionally, cortical stimulation studies, either in conjunction with ECoG, or in healthy populations using transcranial methods could also help establish causal roles for these regions, and for the network in general. For instance, to investigate whether the beta frequency increase in this putative brain network is causally necessary for successful stopping one could examine whether entraining beta frequency oscillations, e.g. with Transcranial Alternating Current Stimulation or TMS improves stopping at the behavioral level.

Overall, this thesis has made a unique contribution to the cognitive psychology and cognitive neuroscience of response control by using a method with high spatio-temporal resolution in humans. It also has clinical implications by providing insight into the functional mechanisms underlying DBS treatment in Parkinson's disease. Using a combination of electrophysiological methods and stimulation we were able to suggest specific roles for IFG, preSMA, and MFG and also identify a mechanisms by which IFG, preSMA, and STN may communicate as a network.

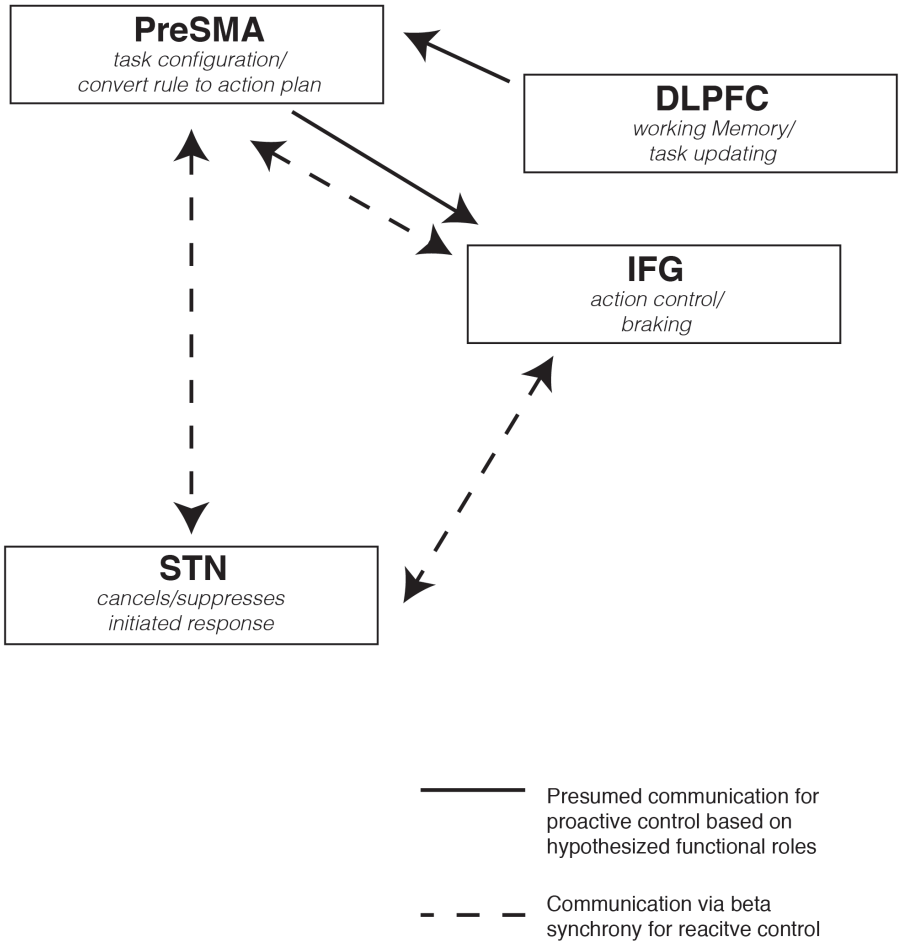


Figure 6.1: Network model for proactive and reactive control. A simplistic representation of preparing to stop is presented in solid arrows. Here information about task goals/working memory is maintained in DLPFC. This information is then conveyed to preSMA (by an unknown mechanism), where it is converted into an action plan in order to prepare the motor system to possible stop/or rapidly adapt a response. PreSMA then relays the information to IFG (by an unknown mechanism) which implements action control at the time of the response by 'braking' the response as it is initiated, perhaps in case it has to be rapidly canceled. It is currently less clear what the role of STN may be in preparing to stop, so it is not incorporated here. Reactive stopping is shown with dotted arrows, specifically reactive stopping involves the preSMA, STN, and IFG 'synching up' in the beta band, allowing for a response to be effectively canceled by the STN, once it is implemented.

REFERENCES

Aron AR (2011) From reactive to proactive and selective control: developing a richer model for stopping inappropriate responses. Biol Psychiatry 69:e55-68.

Aron AR, Poldrack RA (2006) Cortical and subcortical contributions to Stop signal response inhibition: role of the subthalamic nucleus. J Neurosci 26:2424-2433.

Aron AR, Fletcher PC, Bullmore ET, Sahakian BJ, Robbins TW (2003) Stop-signal inhibition disrupted by damage to right inferior frontal gyrus in humans. Nat Neurosci 6:115-116.

Aron AR, Behrens TE, Smith S, Frank MJ, Poldrack RA (2007a) Triangulating a cognitive control network using diffusion-weighted magnetic resonance imaging (MRI) and functional MRI. J Neurosci 27:3743-3752.

Aron AR, Durston S, Eagle DM, Logan GD, Stinear CM, Stuphorn V (2007b) Converging evidence for a fronto-basal-ganglia network for inhibitory control of action and cognition. J Neurosci 27:11860-11864.

Boehler CN, Appelbaum LG, Krebs RM, Chen L-C, Woldorff MG (2011) The role of stimulus salience and attentional capture across the neural hierarchy in a stop-signal task. PLoS ONE 6:e26386.

Brown P (2007) Abnormal oscillatory synchronisation in the motor system leads to impaired movement. Curr Opin Neurobiol 17:656-664.

Buch ER, Mars RB, Boorman ED, Rushworth MFS (2010) A network centered on ventral premotor cortex exerts both facilitatory and inhibitory control over primary motor cortex during action reprogramming. J Neurosci 30:1395-1401.

Canolty R, Soltani M, Dalal S, Edwards E, Dronkers N, Nagarajan S, Kirsch H, Barbaro N, Knight RT (2007) Spatiotemporal dynamics of word processing in the human brain. Front Neurosci 1.

Chang EF, Edwards E, Nagarajan SS, Fogelson N, Dalal SS, Canolty RT, Kirsch HE, Barbaro NM, Knight RT (2011) Cortical spatio-temporal dynamics underlying phonological target detection in humans. J Cogn Neurosci 23:1437-1446.

Chatham CH, Claus ED, Kim A, Curran T, Banich MT, Munakata Y (2012) Cognitive control reflects context monitoring, not motoric stopping, in response inhibition. PLoS One 7:e31546.

Chen CC, Lin WY, Chan HL, Hsu YT, Tu PH, Lee ST, Chiou SM, Tsai CH, Lu CS, Brown P (2011) Stimulation of the subthalamic region at 20 Hz slows the development of grip force in Parkinson's disease. Experimental Neurology 231:91-96.

Chen CC, Litvak V, Gilbertson T, Kühn A, Lu CS, Lee ST, Tsai CH, Tisch S, Limousin P, Hariz M, Brown P (2007) Excessive synchronization of basal ganglia neurons at 20 Hz slows movement in Parkinson's disease. Experimental Neurology 205:214-221.

Chikazoe J (2010) Localizing performance of go/no-go tasks to prefrontal cortical subregions. Curr Opin Psychiatry.

Chikazoe J, Jimura K, Hirose S, Yamashita K-i, Miyashita Y, Konishi S (2009) Preparation to Inhibit a Response Complements Response Inhibition during Performance of a Stop-Signal Task. J Neurosci 29:15870-15877.

Congdon E, Mumford JA, Cohen JR, Galvan A, Aron AR, Xue G, Miller E, Poldrack RA (2010) Engagement of large-scale networks is related to individual differences in inhibitory control. Neuroimage 53:653-663.

Conner C, Ellmore TM, Pieters TA, Disano M, Tandon N (2011) Variability of the Relationship between Electrophysiology and BOLD-fMRI across Cortical Regions in Humans. Journal of Neuroscience in press.

Coxon JP, Stinear CM, Byblow WD (2006) Intracortical inhibition during volitional inhibition of prepared action. J Neurophysiol.

Duann JR, Ide JS, Luo X, Li CS (2009) Functional connectivity delineates distinct roles of the inferior frontal cortex and presupplementary motor area in stop signal inhibition. J Neurosci 29:10171-10179.

Edwards E, Soltani M, Deouell LY, Berger MS, Knight RT (2005) High gamma activity in response to deviant auditory stimuli recorded directly from human cortex. J Neurophysiol 94:4269-4280.

Engel AK, Fries P (2010) Beta-band oscillations-signalling the status quo? Current Opinion in Neurobiology.

Eusebio A, Chen CC, Lu CS, Lee ST, Tsai CH, Limousin P, Hariz M, Brown P (2008) Effects of low-frequency stimulation of the subthalamic nucleus on movement in Parkinson's disease. Experimental Neurology 209:125-130.

Ford A, McGregor KM, Case K, Crosson B, White KD (2010) Structural connectivity of Broca's area and medial frontal cortex. Neuroimage 52:1230-1237.

Fried I, Katz A, McCarthy G, Sass KJ, Williamson P, Spencer SS, Spencer DD (1991) Functional organization of human supplementary motor cortex studied by electrical stimulation. J Neurosci 11:3656-3666.

Fries P (2005) A mechanism for cognitive dynamics: neuronal communication through neuronal coherence. Trends in Cognitive Sciences 9:474-480.

Garavan H, Ross TJ, Stein EA (1999) Right hemispheric dominance of inhibitory control: an event-related functional MRI study. Proc Natl Acad Sci U S A 96:8301-8306.

Garcia-Munoz M, Carrillo-Reid L, Arbuthnott GW (2010) Functional anatomy: dynamic States in Basal Ganglia circuits. Front Neuroanat 4:144.

Gazzaniga MS (1989) Organization of the human brain. Science 245:947-952.

Gazzaniga MS (2000) Cerebral specialization and interhemispheric communication: does the corpus callosum enable the human condition? Brain 123 (Pt 7):1293-1326.

Gazzaniga MS, Bogen JE, Sperry RW (1962) Some functional effects of sectioning the cerebral commissures in man. Proc Natl Acad Sci U S A 48:1765-1769.

Goldman-Rakic PS (1990) Cellular and circuit basis of working memory in prefrontal cortex of nonhuman primates. Prog Brain Res 85:325-335; discussion 335-326.

Gradinaru V, Mogri M, Thompson KR, Henderson JM, Deisseroth K (2009) Optical deconstruction of parkinsonian neural circuitry. Science 324:354-359.

Hampshire A, Chamberlain SR, Monti MM, Duncan J, OWEN AM (2010) The role of the right inferior frontal gyrus: inhibition and attentional control. NeuroImage.

Hirschmann J, Ozkurt TE, Butz M, Homburger M, Elben S, Hartmann CJ, Vesper J, Wojtecki L, Schnitzler A (2011) Distinct oscillatory STN-cortical loops revealed by simultaneous MEG and local field potential recordings in patients with Parkinson's disease. Neuroimage 55:1159-1168.

Isoda M, Hikosaka O (2007) Switching from automatic to controlled action by monkey medial frontal cortex. Nat Neurosci 10:240-248.

Isoda M, Hikosaka O (2008) Role for subthalamic nucleus neurons in switching from automatic to controlled eye movement. J Neurosci 28:7209-7218.

Jahfari S, Stinear CM, Claffey M, Verbruggen F, Aron AR (2010) Responding with restraint: what are the neurocognitive mechanisms? Journal of cognitive neuroscience 22:1479-1492.

Jensen O, Goel P, Kopell N, Pohja M, Hari R, Ermentrout B (2005) On the human sensorimotor-cortex beta rhythm: sources and modeling. Neuroimage 26:347-355.

Johansen-Berg H, Behrens TE, Robson MD, Drobnjak I, Rushworth MF, Brady JM, Smith SM, Higham DJ, Matthews PM (2004) Changes in connectivity profiles define functionally distinct regions in human medial frontal cortex. Proc Natl Acad Sci U S A 101:13335-13340.

Kopell N, Ermentrout GB, Whittington MA, Traub RD (2000) Gamma rhythms and beta rhythms have different synchronization properties. Proc Natl Acad Sci USA 97:1867-1872.

Kopell N, Kramer MA, Malerba P, Whittington MA (2010) Are different rhythms good for different functions? Front Hum Neurosci 4:187.

Kühn A, Tsui A, Aziz T, Ray N, Brücke C, Kupsch A, Schneider G, Brown P (2009) Pathological synchronisation in the subthalamic nucleus of patients with Parkinson's disease relates to both bradykinesia and rigidity. Experimental Neurology 215:380-387.

Lalo E, Thobois S, Sharott A, Polo G, Mertens P, Pogosyan A, Brown P (2008) Patterns of bidirectional communication between cortex and basal ganglia during movement in patients with Parkinson disease. J Neurosci 28:3008-3016.

Leventhal DK, Gage GJ, Schmidt R, Pettibone JR, Case AC, Berke JD (2012) Basal Ganglia Beta oscillations accompany cue utilization. Neuron 73:523-536.

Levy BJ, Wagner AD (2011) Cognitive control and right ventrolateral prefrontal cortex: reflexive reorienting, motor inhibition, and action updating. Ann N Y Acad Sci 1224:40-62.

Li CS, Huang C, Constable RT, Sinha R (2006) Imaging response inhibition in a stop-signal task: neural correlates independent of signal monitoring and post-response processing. J Neurosci 26:186-192.

Li CS, Yan P, Sinha R, Lee TW (2008) Subcortical processes of motor response inhibition during a stop signal task. Neuroimage 41:1352-1363.

Litvak V, Jha A, Eusebio A, Oostenveld R, Foltynie T, Limousin P, Zrinzo L, Hariz MI, Friston K, Brown P (2011) Resting oscillatory cortico-subthalamic connectivity in patients with Parkinson's disease. Brain 134:359-374.

Logothetis NK, Pauls J, Augath M, Trinath T, Oeltermann A (2001) Neurophysiological investigation of the basis of the fMRI signal. Nature 412:150-157.

Luders H, Lesser RP, Dinner DS, Morris HH, Wyllie E, Godoy J (1988) Localization of cortical function: new information from extraoperative monitoring of patients with epilepsy. Epilepsia 29 Suppl 2:S56-65.

Mars RB, Klein MC, Neubert F-X, Olivier E, Buch ER, Boorman ED, Rushworth MFS (2009) Short-latency influence of medial frontal cortex on primary motor cortex during action selection under conflict. J Neurosci 29:6926-6931.

Miller KJ, denNijs M, Shenoy P, Miller JW, Rao RPN, Ojemann JG (2007) Real-time functional brain mapping using electrocorticography. Neuroimage 37:504-507.

Mink JW (1996) The basal ganglia: focused selection and inhibition of competing motor programs. Prog Neurobiol 50:381-425.

Mirabella G, Iaconelli S, Romanelli P, Modugno N, Lena F, Manfredi M, Cantore G (2011) Deep Brain Stimulation of Subthalamic Nuclei Affects Arm Response Inhibition In Parkinson's Patients. Cereb Cortex.

Muller NG, Knight RT (2006) The functional neuroanatomy of working memory: Contributions of human brain lesion studies. In: Neuroscience, pp 51-58.

Nambu A, Tokuno H, Takada M (2002) Functional significance of the cortico-subthalamo-pallidal 'hyperdirect' pathway. Neurosci Res 43:111-117.

Neubert FX, Mars RB, Buch ER, Olivier E, Rushworth MF (2010) Cortical and subcortical interactions during action reprogramming and their related white matter pathways. Proc Natl Acad Sci U S A 107:13240-13245.

Petrides M (2000) The role of the mid-dorsolateral prefrontal cortex in working memory. Exp Brain Res 133:44-54.

Pfurtscheller G (1981) Central beta rhythm during sensorimotor activities in man. Electroencephalogr Clin Neurophysiol 51:253-264.

Pfurtscheller G, Graimann B, Huggins JE, Levine SP, Schuh LA (2003) Spatiotemporal patterns of beta desynchronization and gamma synchronization

in corticographic data during self-paced movement. Clin Neurophysiol 114:1226-1236.

Pogosyan A, Gaynor LD, Eusebio A, Brown P (2009) Boosting cortical activity at Beta-band frequencies slows movement in humans. Curr Biol 19:1637-1641.

Ray NJ, Brittain JS, Holland P, Joundi RA, Stein JF, Aziz TZ, Jenkinson N (2012) The role of the subthalamic nucleus in response inhibition: Evidence from local field potential recordings in the human subthalamic nucleus. Neuroimage 60:271-278.

Ray S, Crone NE, Niebur E, Franaszczuk PJ, Hsiao SS (2008) Neural correlates of high-gamma oscillations (60-200 Hz) in macaque local field potentials and their potential implications in electrocorticography. J Neurosci 28:11526-11536.

Rubia K, Smith AB, Brammer MJ, Taylor E (2003) Right inferior prefrontal cortex mediates response inhibition while mesial prefrontal cortex is responsible for error detection. Neuroimage 20:351-358.

Rushworth MF, Walton ME, Kennerley SW, Bannerman DM (2004) Action sets and decisions in the medial frontal cortex. Trends Cogn Sci 8:410-417.

Scheeringa R, Fries P, Petersson KM, Oostenveld R, Grothe I, Norris DG, Hagoort P, Bastiaansen MC (2011) Neuronal dynamics underlying high- and low-frequency EEG oscillations contribute independently to the human BOLD signal. Neuron 69:572-583.

Sharott A, Magill PJ, Bolam JP, Brown P (2005) Directional analysis of coherent oscillatory field potentials in the cerebral cortex and basal ganglia of the rat. The Journal of Physiology 562:951-963.

Sharp DJ, Bonnelle V, De Boissezon X, Beckmann CF, James SG, Patel MC, Mehta MA (2010) Distinct frontal systems for response inhibition, attentional capture, and error processing. Proceedings of the National Academy of Sciences:1-6.

Swann N, Tandon N, Canolty R, Ellmore TM, McEvoy LK, Dreyer S, DiSano M, Aron AR (2009) Intracranial EEG reveals a time- and frequency-specific role for the right inferior frontal gyrus and primary motor cortex in stopping initiated responses. J Neurosci 29:12675-12685.

Swann N, Poizner H, Houser M, Gould S, Greenhouse I, Cai W, Strunk J, George J, Aron AR (2011) Deep brain stimulation of the subthalamic nucleus alters the cortical profile of response inhibition in the beta frequency band: a scalp EEG study in Parkinson's disease. J Neurosci 31:5721-5729.

Swann NC, Cai W, Conner CR, Pieters TA, Claffey MP, George JS, Aron AR, Tandon N (2012) Roles for the pre-supplementary motor area and the right inferior frontal gyrus in stopping action: Electrophysiological responses and functional and structural connectivity. Neuroimage 59:2860-2870.

van den Wildenberg WPM, van Boxtel GJM, van der Molen MW, Bosch DA, Speelman JD, Brunia CHM (2006) Stimulation of the subthalamic region facilitates the selection and inhibition of motor responses in Parkinson's disease. Journal of cognitive neuroscience 18:626-636.

van Gaal S, Ridderinkhof KR, Scholte HS, Lamme VAF (2010) Unconscious activation of the prefrontal no-go network. J Neurosci 30:4143-4150.

Verbruggen F, Aron AR, Stevens MA, Chambers CD (2010) Theta burst stimulation dissociates attention and action updating in human inferior frontal cortex. Proc Natl Acad Sci U S A 107:13966-13971.

Xue G, Aron AR, Poldrack RA (2008) Common neural substrates for inhibition of spoken and manual responses. Cereb Cortex 18:1923-1932.

Zandbelt BB, Vink M (2010) On the role of the striatum in response inhibition. PLoS One 5:e13848.

Zandbelt BB, Bloemendaal M, Neggers SFW, Kahn RS, Vink M (2012) Expectations and violations: Delineating the neural network of proactive inhibitory control. Hum Brain Mapp.

APPENDIX

Supplementary Table 4.1: Preparing to stop fMRI values. Positive x-values correspond to right hemisphere and negative ones the left.

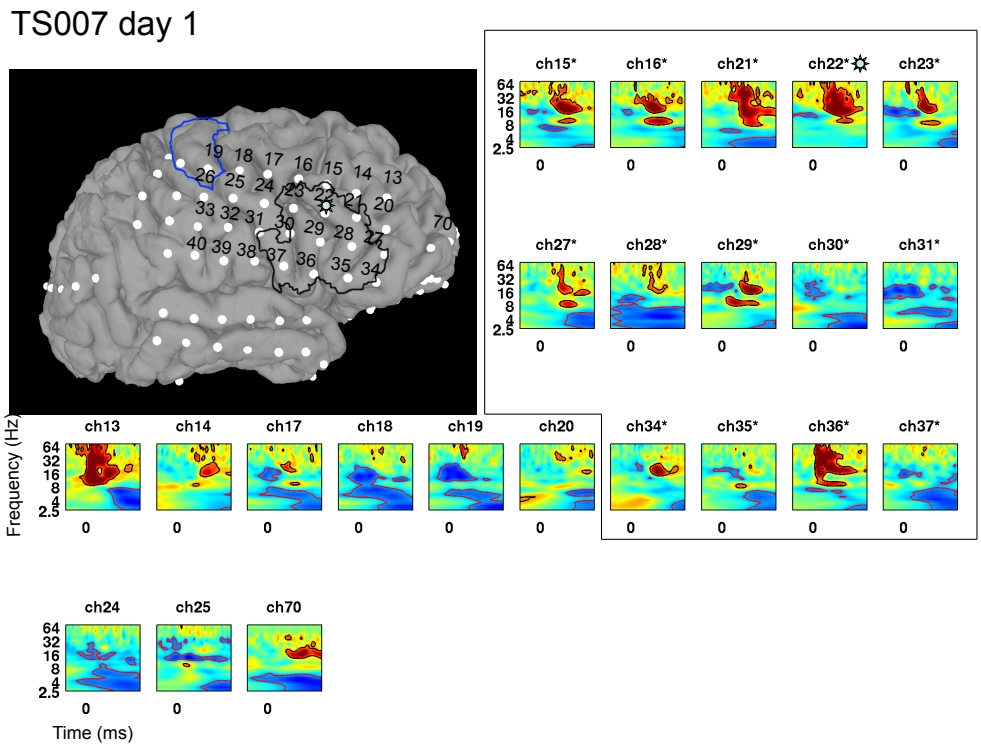
Contrast	Z	x	y	z	cluster size
MS-Go vs. NS-Go					
Frontal Pole	5.01	28	44	20	8844
Anterior cingulate gyrus	4.96	8	18	36	
Insular cortex	4.83	36	24	-2	
Frontal orbital cortex	4.81	40	22	-6	
Paracingulate gyrus	4.62	8	22	42	
Pre-supplementary motor area	4.33	6	24	54	
Inferior frontal gyrus, pars opercularis	4.51	48	18	2	
Angular gyrus	5.08	54	-54	38	3166
Angular gyrus	4.69	50	-50	30	
Supramarginal gyrus	4.51	60	-46	36	
Supramarginal gyrus	4.46	62	-42	36	
Supramarginal gyrus	4.31	50	-46	46	
Angular gyrus	4.21	56	-44	22	
Supramarginal gyrus	4.14	-56	-48	18	1895
Supramarginal gyrus	4.05	-58	-44	16	
Middle temporal gyrus	3.92	-56	-48	4	
Supramarginal gyrus	3.91	-58	-46	8	
Supramarginal gyrus	3.9	-54	-48	24	
Supramarginal gyrus	3.88	-58	-46	24	
Insular cortex	4.13	-32	22	0	843
Inferior frontal gyrus, pars opercularis	4.11	-40	14	2	
Frontal orbital cortex	4.03	-30	24	-8	
Insular cortex	3.97	-34	16	0	
Precentral gyrus	2.95	-52	4	10	
Frontal orbital cortex	2.91	-32	16	-16	
Middle frontal gyrus	3.93	-38	28	24	631
Middle frontal gyrus	3.67	-38	34	26	
Frontal Pole	3.23	-30	42	14	
Frontal Pole	3.16	-30	38	24	
Frontal Pole	2.54	-40	48	20	
Frontal Pole	2.52	-40	30	36	

Supplementary Table 4.2: Outright stopping fMRI values. Positive x-values correspond to right hemisphere and negative ones the left.

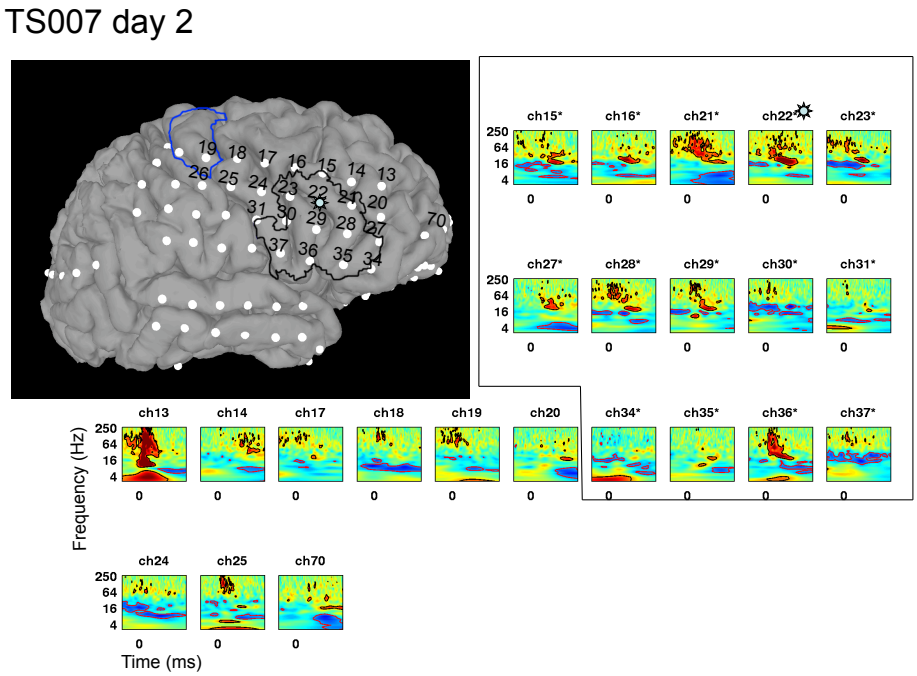
Contrast	Z	x	y	z	cluster size
MS-SS vs. MS-Go					
Superior temporal gyrus	5.08	56	-36	4	3946
Middle temporal gyrus	5.05	62	-34	0	
Middle temporal gyrus	4.8	50	-40	0	
Middle temporal gyrus	4.47	48	-36	-2	
Superior temporal gyrus	4.37	64	-18	-4	
Supramarginal gyrus	4.26	62	-44	20	
Supramarginal gyrus	3.95	-52	-50	14	1924
Supramarginal gyrus	3.87	-60	-42	40	
Supramarginal gyrus	3.85	-58	-42	36	
Middle temporal gyrus	3.85	-64	-56	0	
Angular gyrus	3.75	-62	-54	28	
Supramarginal gyrus	3.69	-64	-46	8	
Frontal orbital cortex	3.92	32	18	-16	829
Inferior frontal gyrus, pars triangularis	3.66	54	20	-6	
Insula cortex	3.58	36	16	-16	
Inferior frontal gyrus, pars opercularis	3.54	50	14	14	
Inferior frontal gyrus, pars triangularis	3.52	50	32	2	
Frontal orbital cortex	3.49	42	36	-8	

Supplementary Table 3: CCEPs and DTI results from the whole brain reveal functional/structural connections between the preSMA and the rIFG in particular. The table shows CCEP and DTI values for all the electrodes shown in Figure 6 (all electrodes over right lateral and medial cortex) that had structural (revealed by DTI) or functional (revealed by the CCEPs) connections to the preSMA (electrodes IH 11-12). Electrodes that show both a structural and functional connection to the preSMA (i.e. have both non-zero CCEP **and** non-zero DTI values) are shown in bold. Note that these electrodes are all in the rIFG region, with the exception being IH 1 (in the preSMA). Note also that electrodes LF 15 and 16 show the strongest connections with preSMA in terms of the 'path value' metric (see below) and the strongest CCEP responses of all the electrodes except IH 1 (in the preSMA). 'CCEP max' refers to maximum CCEP voltage following stimulation of electrodes IH 11-12. 'CCEP onset time' refers to the latency of voltage change after stimulation. 'Distance from stim' refers to the distance from the stimulation site (i.e. from electrodes IH 11-12). 'Number of tracts' refers to number of DTI fiber tracts. 'Tract Length' refers to length in mm of the path between electrodes IH 11-12 and each indicated electrode. 'Tract Average FA' refers to the average fractional anisotropy for each path connecting IH 11-12 to the indicated electrode. 'Path value' is a measure of connection strength, computed as a scalar cross-product of average FA (fractional anisotropy) along each streamline and mean length of the streamlines connecting electrode IH 11-12 to the indicated electrodes. See Supplementary Figure 4.2 for electrode locations not shown in Figure 4.2

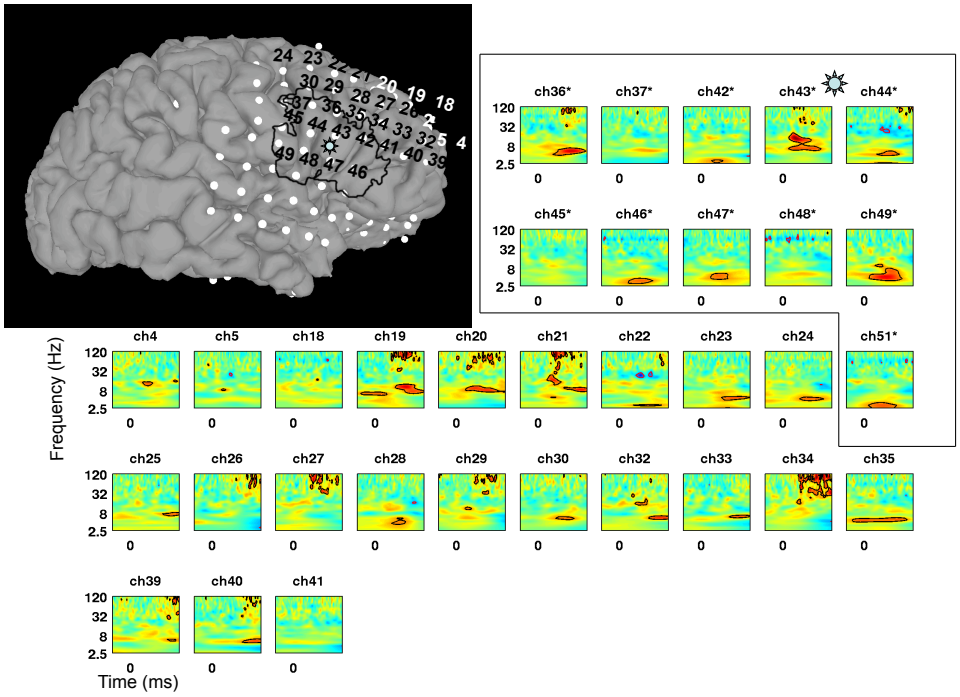
Electrode	CCEP max (mV)	CCEP onset time (ms)	Distance from stim. (mm)	Number of tracts	Tract Length (mm)	Tract Average FA	Path value (Avg. FA x length)
***IH1**	**966.75**	**11**	**9.65**	**1135**	**76.3**	**0.46**	**35.22**
*IH13	0	0	10.48	829	74.99	0.5	37.85
*IH14	0	0	20.56	83	67.59	0.47	31.94
*IH15	0	0	30.61	86	89.23	0.51	45.48
*IH16	0	0	40.27	72	92.63	0.51	47.44
*IH17	0	0	49.92	9	110.78	0.52	57.9
*IH18	0	0	60.42	8	112	0.54	61.03
*IH19	0	0	69.61	3	118.67	0.52	61.8
*IH2	0	0	9.23	905	67.16	0.47	31.72
*IH3	0	0	13.94	1243	86.62	0.52	44.96
*IH4	0	0	22.72	557	81.79	0.52	42.18
*IH5	0	0	31.84	92	89.07	0.51	45.7
*IH6	0	0	41.2	33	96.39	0.54	52.51
*IH7	0	0	50.85	27	97.78	0.56	54.39
*IH8	0	0	60.97	4	117	0.53	61.66
*LF1	139.81	29	55.25	0	0	0	0
*LF10	135.33	20	57.27	0	0	0	0
***LF14**	**46.29**	**32**	**65.68**	**16**	**173.13**	**0.53**	**91.44**
***LF15**	**141.77**	**21**	**65.79**	**16**	**176.94**	**0.54**	**95.16**
***LF16**	**169.91**	**19**	**66.67**	**15**	**176.4**	**0.54**	**94.89**
*LF17	30.43	21	68.15	0	0	0	0
***LF20**	**66.83**	**27**	**70.82**	**21**	**155.29**	**0.51**	**78.94**
***LF21**	**67.41**	**20**	**69.98**	**21**	**155.29**	**0.51**	**78.94**
*LF22	0	0	71.91	15	176.4	0.54	94.89
*LF3	230.22	31	51.62	0	0	0	0
*LF4	89.03	17	51.13	0	0	0	0
*LF5	64.86	20	53.47	0	0	0	0
*LF8	86.5	37	59.73	0	0	0	0
*LF9	141.57	27	58.95	0	0	0	0
*LP10	23.35	21	71.62	0	0	0	0
*LTO38	16.27	30	113.67	0	0	0	0
*SPC1	35.97	13	54.22	0	0	0	0
*SPC2	35.72	13	54.45	0	0	0	0
*SPC3	25.27	12	54.32	0	0	0	0
*SPC4	17.69	12	54.58	0	0	0	0
*SPC5	18.04	11	58.72	0	0	0	0



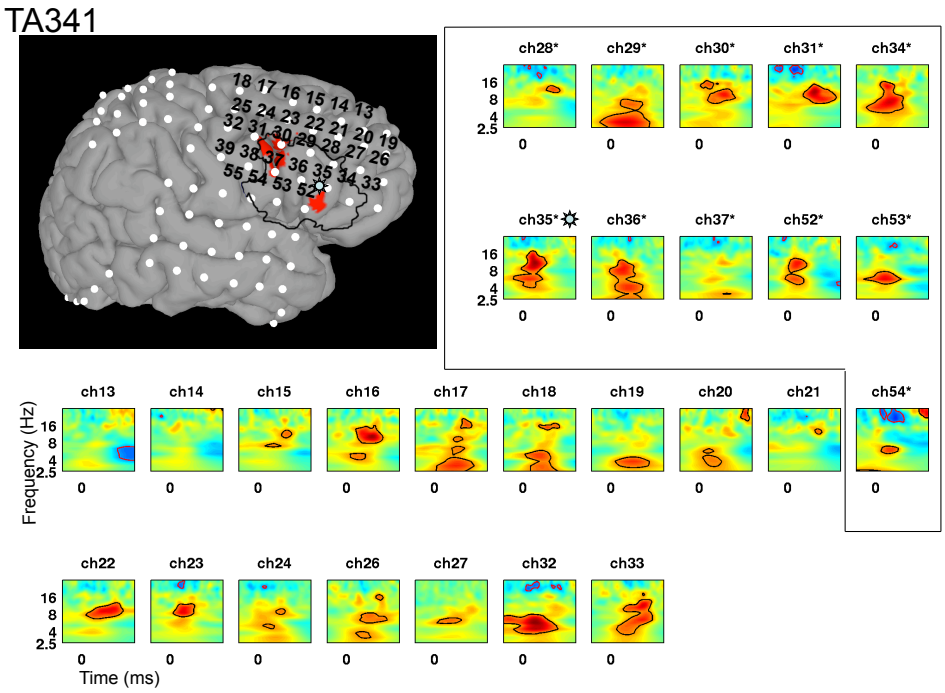
Supplementary Figure 2.1: The right IFG response to stopping is fairly specific within wider right lateral PFC – subject TS007 day 1. Data from all right lateral frontal electrodes for patients for which we present right IFG data are shown for completeness. Time frequency plots are shown for successful stop trials, where zero ms is the time of the stop signal. The channel number is derived from the patient's structural MRI. The MRI also has the probabilistic outlines of RIFG (and M1, when the left hand was used), and fMRI activations included when available (see Figure 2.2). The star denotes the electrode from which data are analyzed in detail (see Figure 2.5). The selection criteria for this electrode are within the main text. The channels which fall within the right IFG region are contained within the box.



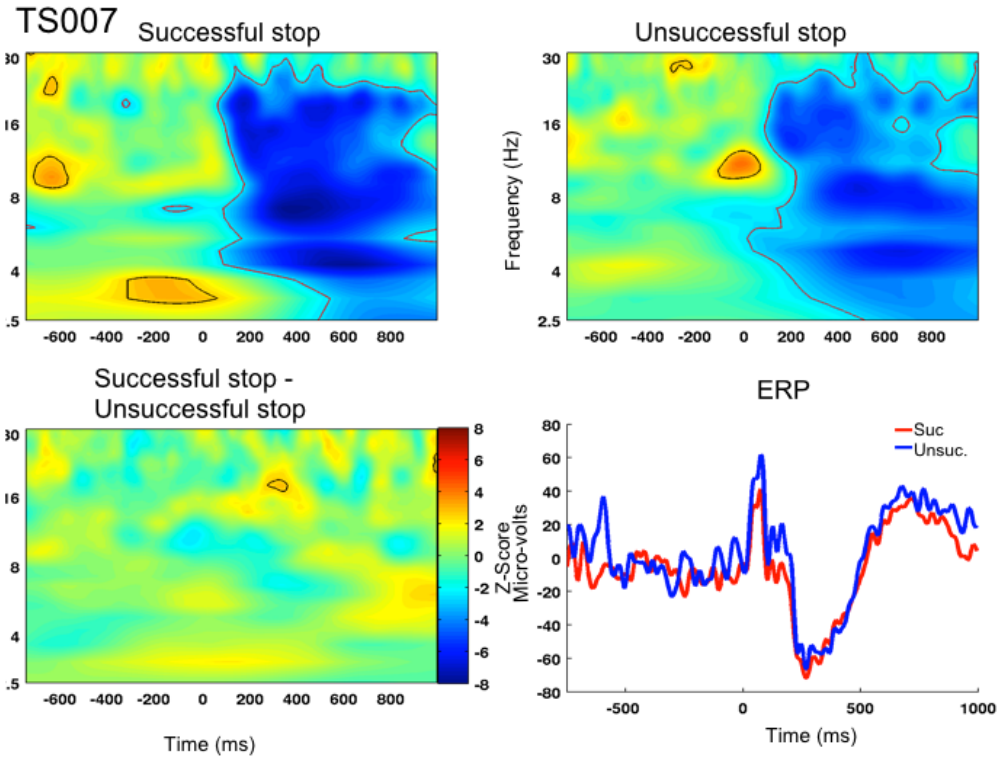
Supplementary Figure 2.2: The right IFG response to stopping is fairly specific within wider right lateral PFC – subject TS007 day 2. Details for this figure are the same as for Figure S2.1.



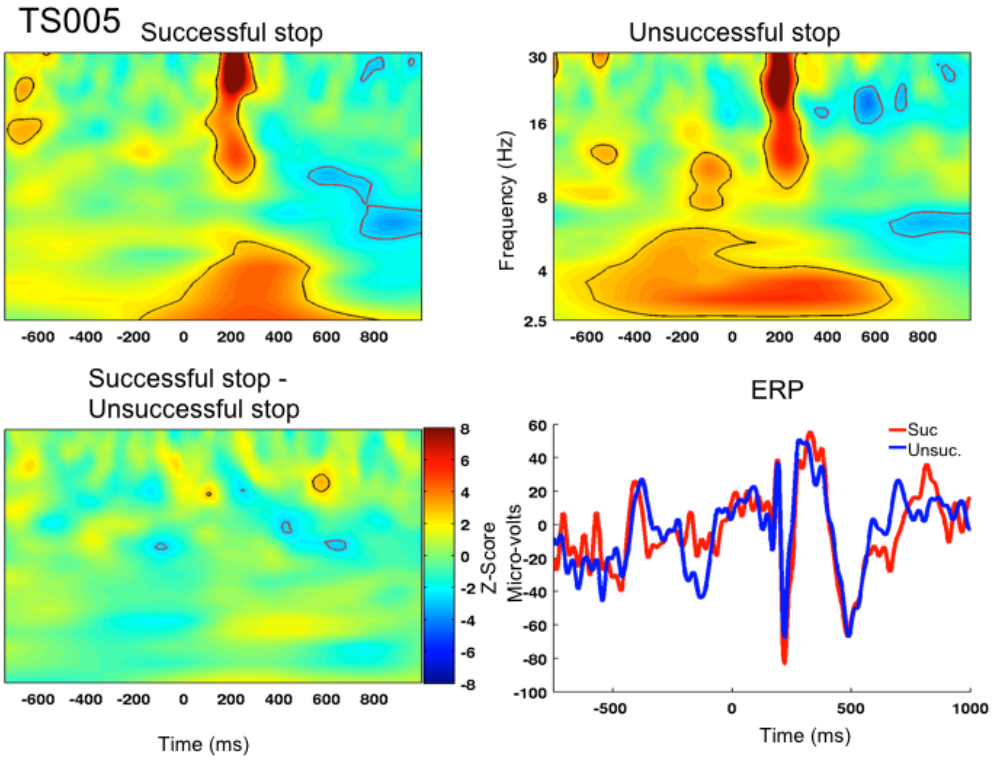
Supplementary Figure 2.3: The right IFG response to stopping is fairly specific within wider right lateral PFC – subject TS005. Details for this figure are the same as for Figure S2.1.



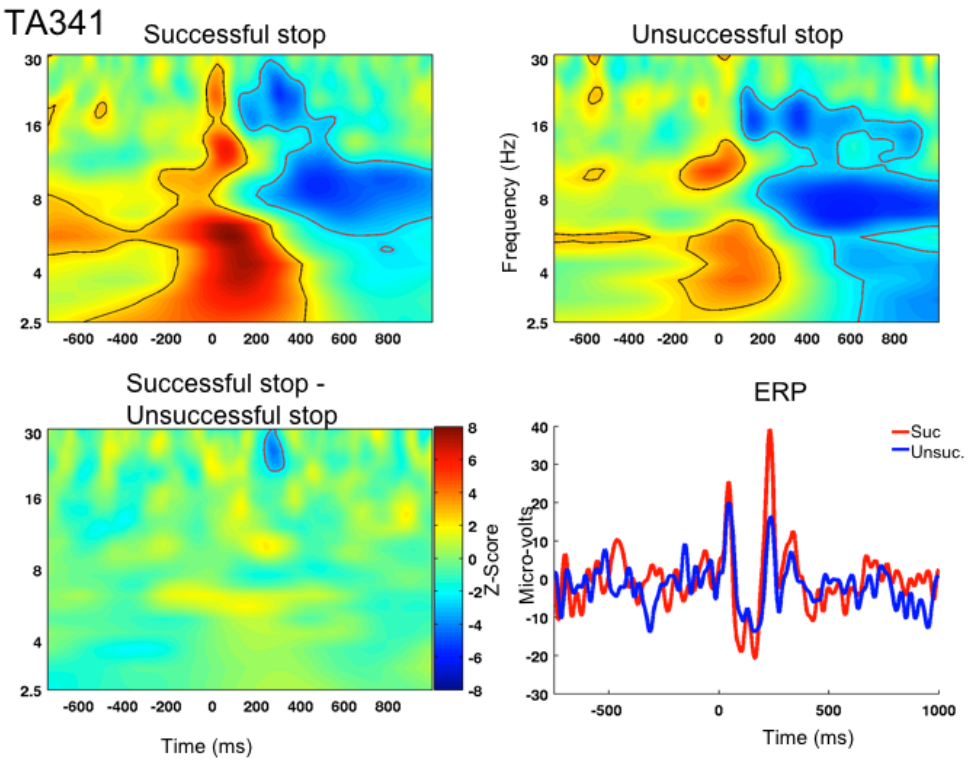
Supplementary Figure 2.4: The right IFG response to stopping is fairly specific within wider right lateral PFC – subject TA341. Details for this figure are the same as for Figure S2.1.



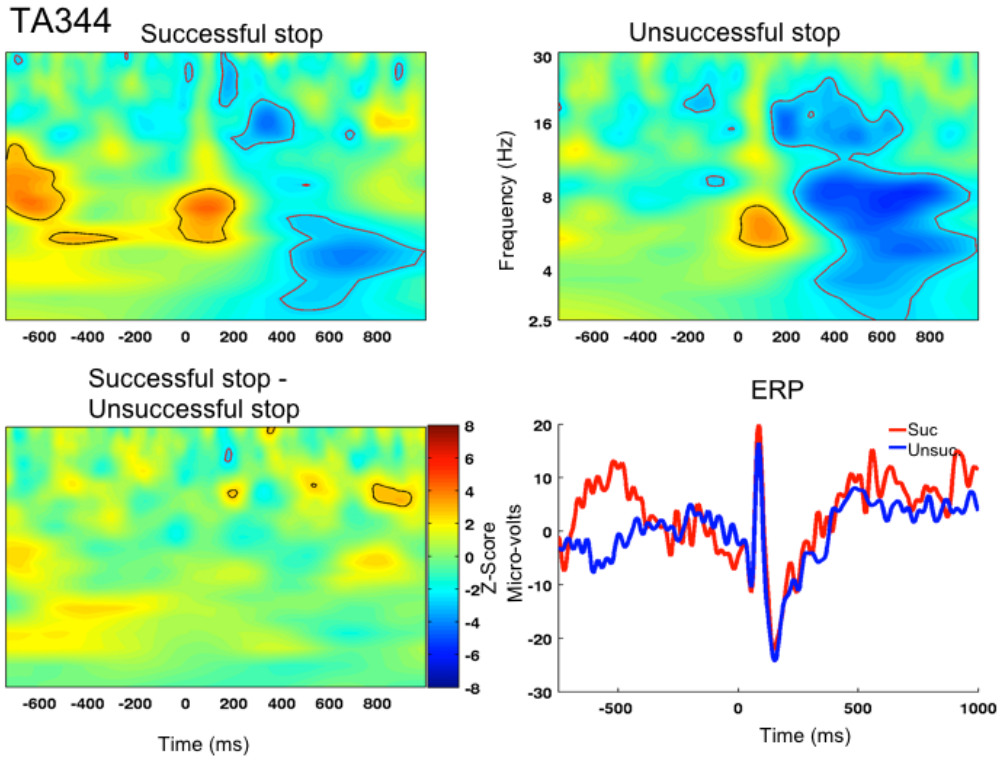
Supplementary Figure 2.5: Auditory electrode from subject TS007 day 1. Figure 2.6 shows data from a representative auditory cortex electrode from one subject. Here we show such an electrode for the other 4 subjects for completeness. Note no consistent differences between successful and unsuccessful stop trials across subjects.



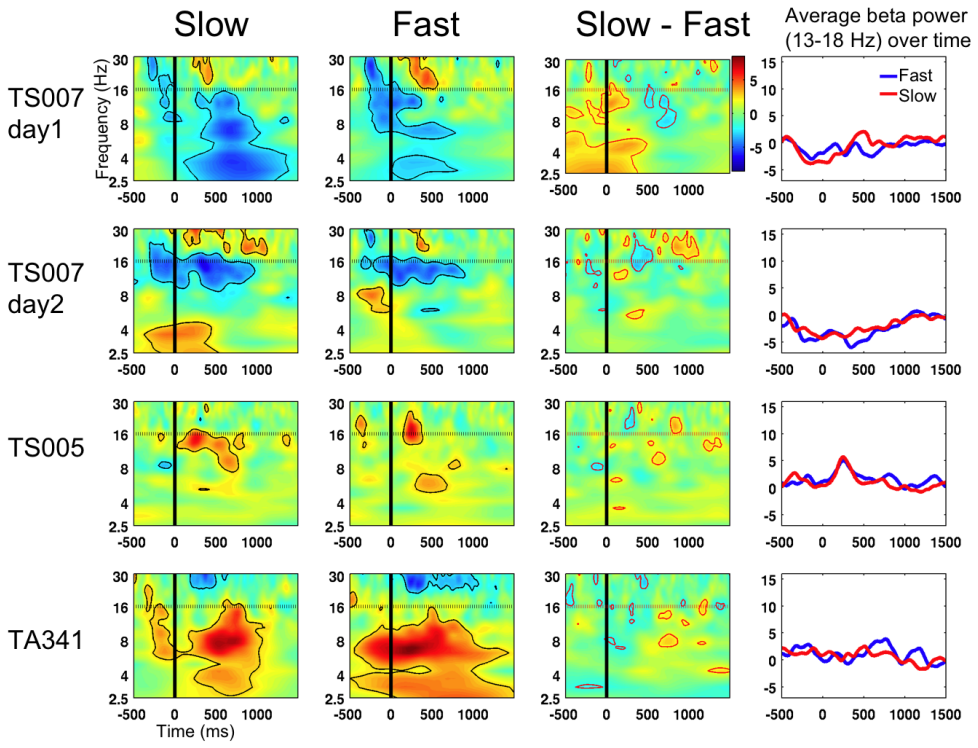
Supplementary Figure 2.6: Auditory electrode from subject TS005. Details for this figure are the same as for Figure 2S.5



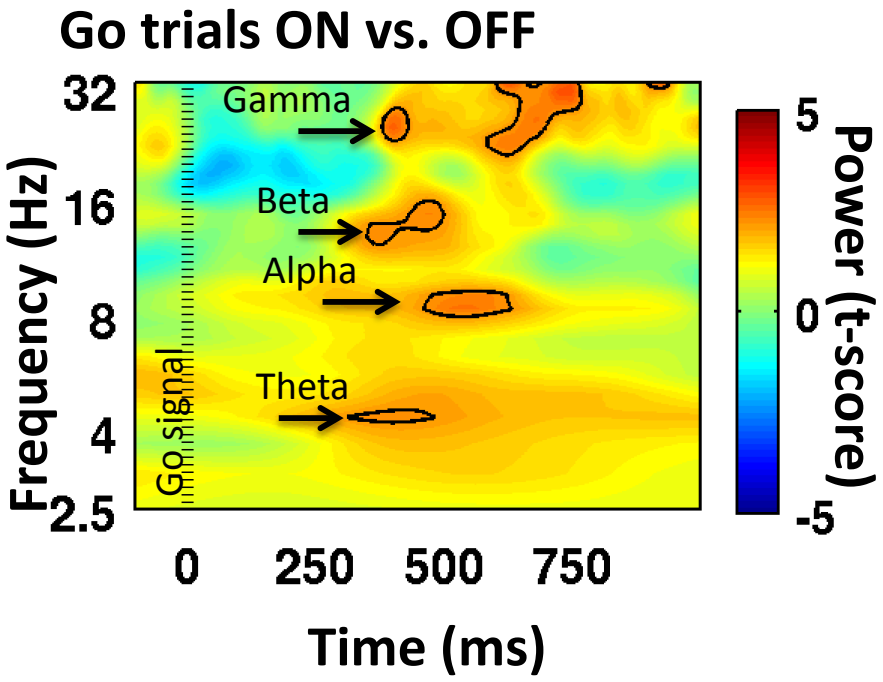
Supplementary Figure 2.7: Auditory electrode from subject TA341. Details for this figure are the same as for Figure 2S.5



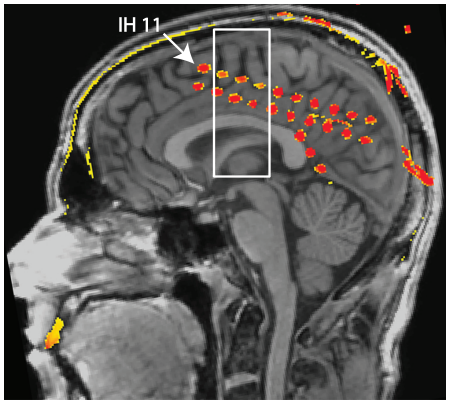
Supplementary Figure 2.8: Auditory electrode from subject TA344. Details for this figure are the same as for Figure 2S.5



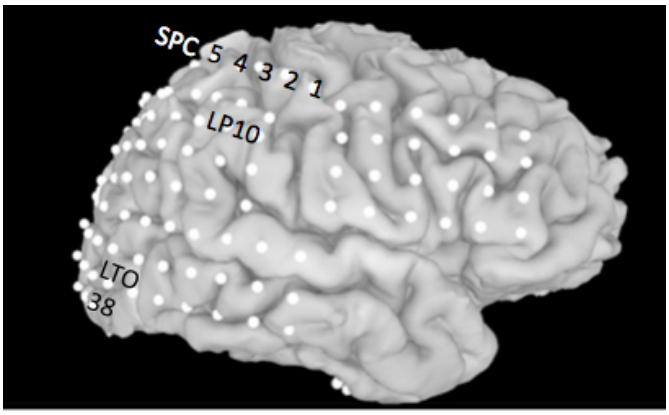
Supplementary Figure 2.9: Comparison of slow and fast go trials. The figure shows data from noncritical go trials (trials where subjects never have to stop) separated by a median split into trials with slower responses (first column) or fast ones (second column), expressed in z-scores. Zero ms is the time at which the go signal was presented. The first two columns show data from both conditions relative to baseline period (ITI) as a z-score. The third column shows the difference between conditions (relative to one another, not to the baseline), also as a z-score. The fourth column shows the same data with power averaged across only the beta band (13-18 Hz), plotted for both conditions over time (red line indicates successful stopping, blue line indicates unsuccessful stopping). As for Figure 2.5, thin black outlines indicate $p<.01$ FDR corrected, thin red outlines in the difference column indicate $p<.05$ uncorrected, dotted horizontal line marks 16 Hz for all subjects, the solid black vertical line denotes the time at which the go signal occurred.



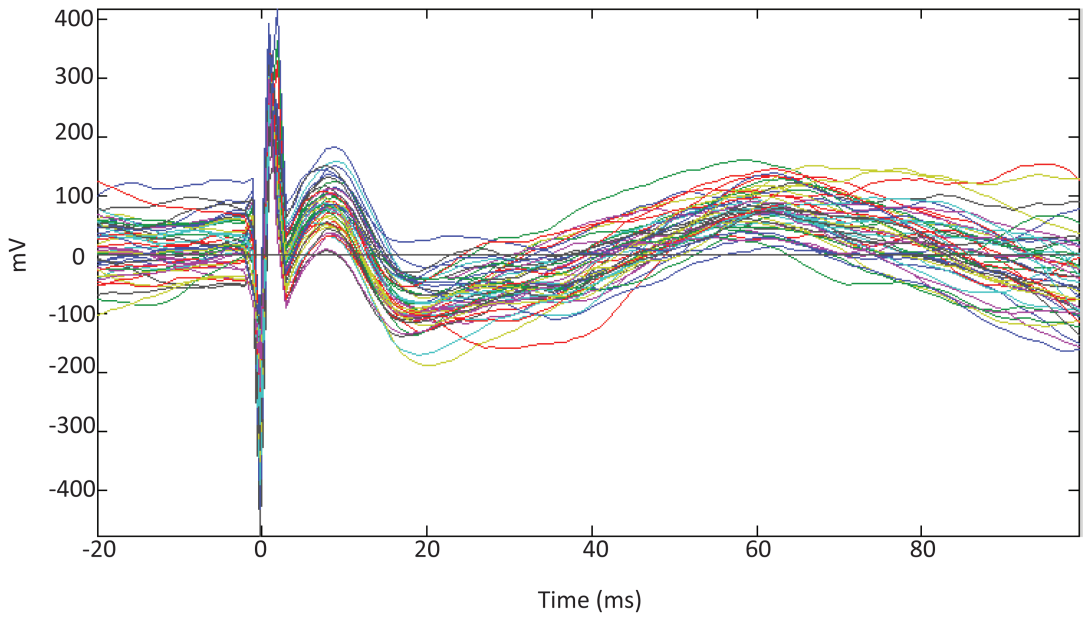
Supplementary Figure 3.1: Time-frequency plot of go trials for ON vs. OFF stimulation. Greater power around or just before the time of going is observed across many frequency bands, with significant effects in theta, alpha, beta, and gamma for a right frontal electrode cluster (F6, F8, FC6). Each condition is first normalized to its own baseline prior to making the ON vs. OFF comparison. Power is expressed with color as a t-score. Zero ms was the time of the go signal (indicated by the dotted line). Power changes significant at $p<0.05$ are encircled with either a black line (for ON > OFF) or a red line (for OFF > ON).



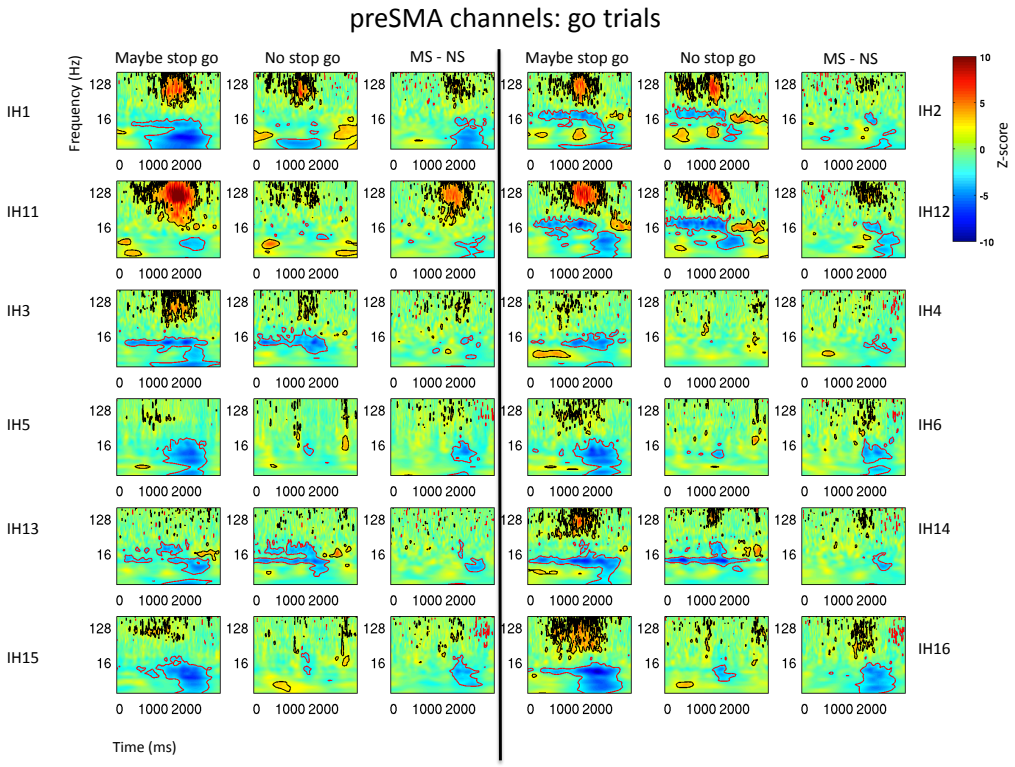
Supplementary Figure 4.1: preSMA location. Electrodes IH 11 and 1 are located in the posterior pre-SMA, with electrode IH 11 indicated with an arrow. The AC-PC line (indicating the locations of the anterior and posterior commissures) and perpendiculars from this line at the AC and the PC are shown. The AC line demarcates the junction between the pre-SMA and the SMA – this line passes posterior to the two electrodes (IH 11 and 1). Talairach co-ordinates of electrode IH11 are 0, 12, 51. Electrodes artifacts localized on CT scans are shown overlaid on the pre-implantation MRI.



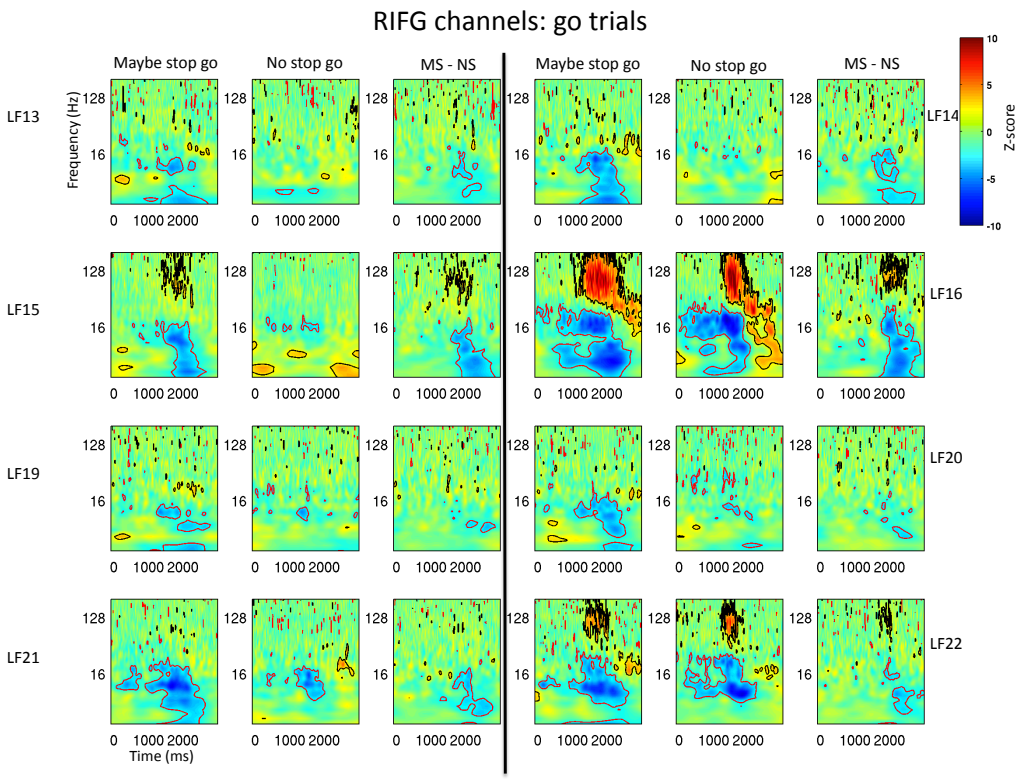
Supplementary Figure 4.2: Locations of electrodes with non-zero CCEP or DTI values (shown in Supplementary Table 4.3) which were not on the lateral frontal or inter-hemispheric grids (shown in Figure 4.2).



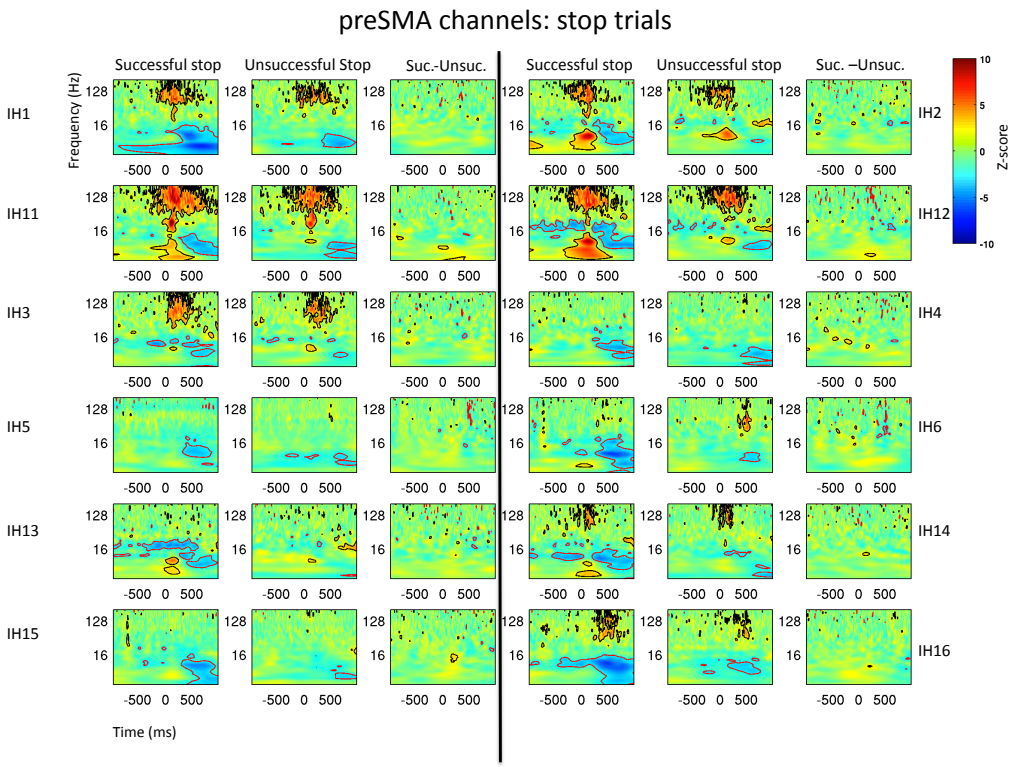
Supplementary Figure 4.3: Example CCEPs (cortico-cortical evoked potentials) from channel LF 16. Individual ECoG traces from 50 trials of 10mA stimulation at electrodes IH 11-12 are overlaid in different colors. Note the quick, large amplitude increases are remarkably consistent across trials.



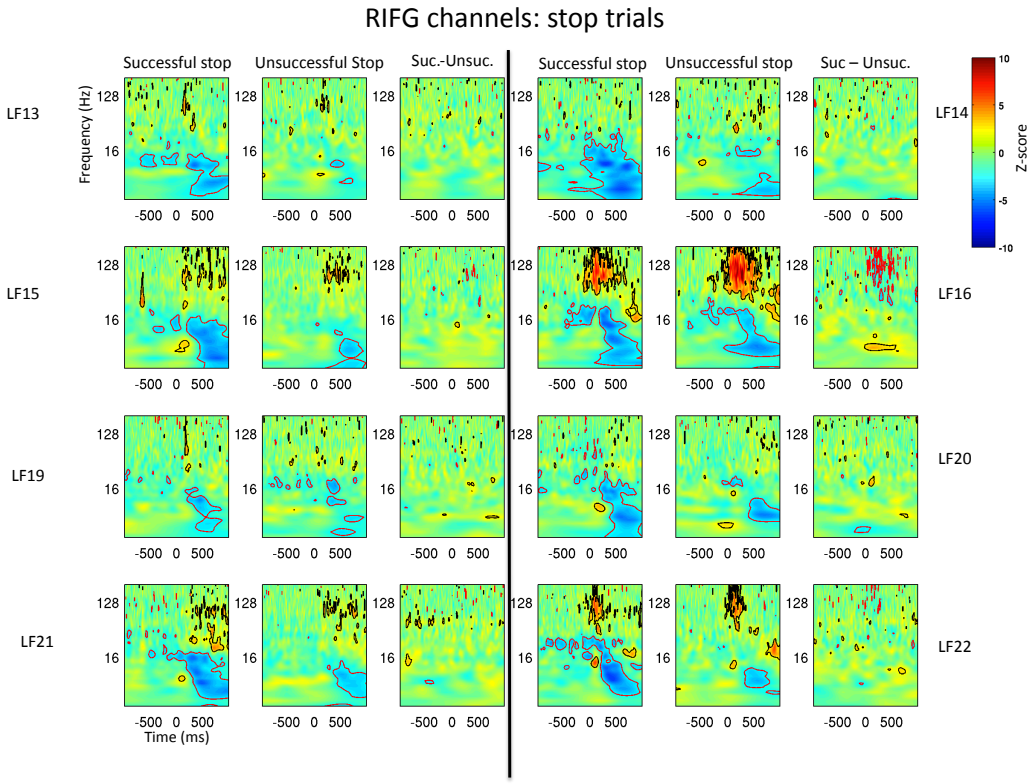
Supplementary Figure 4.4: Time-frequency responses for all preSMA electrodes for MS_Go and NS_Go trials and the difference between the two. Zero is the time of the MS/NS cue and 1000 ms is the time of the Go signal. Z-scored amplitude is expressed in color and significance at $p<0.01$ uncorrected is indicated with the black outline (for positive differences), or the red outline (for negative differences).



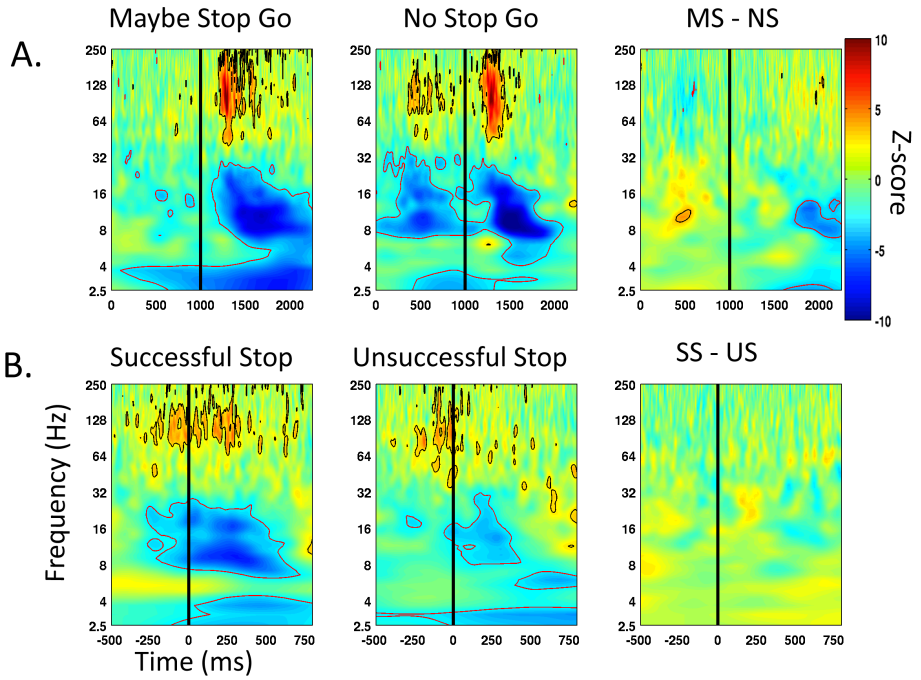
Supplementary Figure 4.5: Time-frequency responses for all rIFG electrodes for MS_Go and NS_Go trials and the difference between the two. Zero is the time of the MS/NS cue and 1000 ms is the time of the go signal. Z-scored amplitude is expressed in color and significance at $p<0.01$ uncorrected is indicated with the black outline (for positive differences), or the red outline (for negative differences).



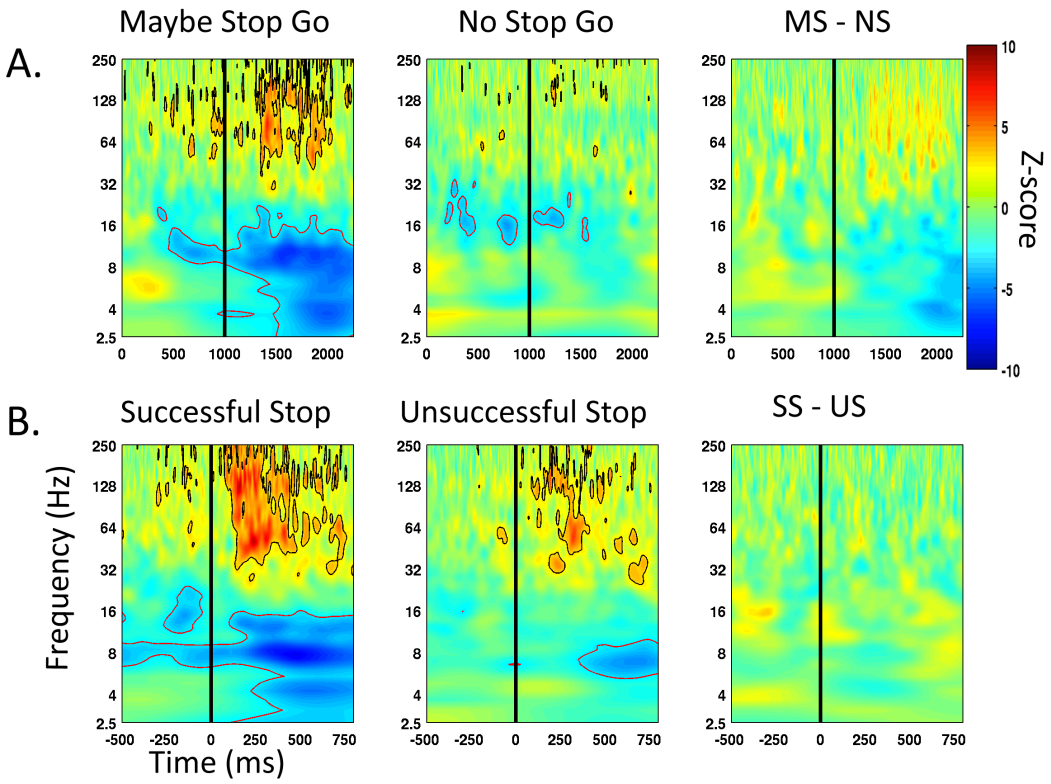
Supplementary Figure 4.6: Time-frequency responses for all preSMA electrodes MS_SS trials, MS_US trials, and the difference between the two. Zero is the time of the stop signal. Z-scored amplitude is expressed in color and significance at $p<0.01$ uncorrected is indicated with the black outline (for positive differences), or the red outline (for negative differences).



Supplementary Figure 4.7: Time-frequency responses for all rIFG electrodes MS_SS trials, MS_US trials, and the difference between the two. Zero is the time of the stop signal. Z-scored amplitude is expressed in color and significance at $p<0.01$ uncorrected is indicated with the black outline (for positive differences), or the red outline (for negative differences).



Supplementary Figure 4.8: Superior parietal ECoG from electrode indicated in Figure 4.6. A. Preparing to stop. High gamma amplitude increases for the superior parietal electrode began roughly 200 ms after the go signal for the MS_Go trials, and about 500 ms before the go signal for NS_Go trials. (However, this early activation was weaker). The high gamma amplitude increase in preSMA was also about 500 ms before the go signal, but only for the MS Go trials. In short, the superior parietal and preSMA electrodes show different activity patterns, but it is difficult to say that one precedes the other. Zero ms is the time of the MS/NS cue and 1000 ms is the time of the go signal (indicated by the solid black line). Z-scored amplitude is expressed in color. All results significant at $p<0.05$, FDR corrected are outlined (black indicates significance in positive direction, red indicates negative direction). B. Outright stopping. High gamma amplitude increases for the same electrode began roughly 250 ms before the stop signal for both MS_SS and MS_US trials. The high gamma amplitude increase in preSMA was also about 250 ms before the stop signal. Again, the timing of gamma amplitude onset for these two regions is difficult to distinguish. Zero ms is the time of the stop signal. Z-scored amplitude is expressed in color. All results significant at $p<0.05$, FDR corrected are outlined (black indicates significance in positive direction, red indicates negative direction).



Supplementary Figure 4.9: Temporal Parietal Junction (TPJ) ECoG from electrode indicated in Figure 4.6. A. Preparing to stop. High gamma amplitude increases for the TPJ electrode began roughly 350 ms after the go signal for the MS_Go trials. The high gamma amplitude increase in preSMA was about 500 ms before the go signal for the MS Go trials, preceding the TPJ high gamma increase by about 850 ms. Zero ms is the time of the MS/NS cue and 1000 ms is the time of the go signal (indicated by the solid black line). Z-scored amplitude is expressed in color. All results significant at $p<0.05$, FDR corrected are outlined (black indicates significance in positive direction, red indicates negative direction). B. Outright stopping. High gamma amplitude increases for the same electrode began roughly 75 ms after the stop signal for both MS_SS and MS_US trials. The high gamma amplitude increase in preSMA began about 250 ms before the stop signal, again, the timing of gamma amplitude onset in the preSMA seems to precede that of the TPJ. Zero ms is the time of the stop signal. Z-scored amplitude is expressed in color. All results significant at $p<0.05$, FDR corrected are outlined (black indicates significance in positive direction, red indicates negative direction).